Role of glucoside transporters in the biology of the heterocyst-forming cyanobacterium *Anabaena* sp.

Mercedes Nieves Morión

Sevilla 2017

Role of glucoside transporters in the biology of the heterocyst-forming cyanobacterium *Anabaena* sp.

Trabajo presentado para optar al grado
de Doctora en Biología por la Licenciada
Mercedes Nieves Morión

Sevilla, Noviembre de 2017

Director

Dr. Enrique Flores García
Profesor de Investigación del CSIC

Tutor

Dr. José María Romero Rodríguez
Catedrático de Bioquímica y Biología Molecular

A mis padres

Agradecimientos

Agradecimientos

Una vez concluida esta tesis dedico estas líneas de agradecimiento a las muchas personas que han hecho posible la elaboración de la misma. En primer lugar, tengo que agradecer a mi director de tesis, el Dr. Enrique Flores, por su incansable dedicación, esfuerzo y espíritu científico. Ha sido para mí un verdadero mentor y ha marcado una etapa muy importante de mi vida, por todo esto y más, GRACIAS. Gracias a la Dra. Antonia Herrero y al Dr. Ignacio Luque por sus consejos científicos, su organización y manera de trabajar, rigurosidad y capacidad científica. Todos esos detalles que marcan la diferencia.

Durante mi segundo año tuve la gran suerte de realizar una estancia con el Prof. Conrad W. Mullineaux en la Universidad Queen Mary de Londres al que, junto con el Dr. Enrique Flores, quiero agradecer esta oportunidad que me brindaron de desempeñar parte de esta tesis en el extranjero y vivir una experiencia inolvidable.

Estos dos últimos años he tenido que desempeñar horas de docencia. Agradecer a la Universidad de Sevilla y al Departamento de Bioquímica por hacer posible esta tarea que tanta ilusión me hacía.

Pasando ahora al laboratorio, mi sitio de trabajo, donde las horas vuelan entre tanto experimento, no puedo olvidarme de cada uno de mis compañeros durante estos cuatro años y dedicarles unas breves palabras de agradecimiento. Ana Valladares, gracias por cada uno de tus sabios consejos y mensajes que tanto me han ayudado y por haber compartido conmigo tantos momentos, sin olvidarme del día que nos presentaste a tus dos nuevos tesoros. A José Enrique Frías, gracias por tu gran ayuda con tanto plásmido y restricción sin pasar por alto tu rigurosidad en la investigación. Silvia Picossi, con la que he compartido charlas de todo tipo y risas que alegraban esos días interminables, gracias! A Vicente Mariscal, por las horas de microscopía. Mireia Burnat, gracias por estar ahí en mis inicios resolviendo cada una de mis dudas. A Leticia Escudero, Laura Corrales y Antonio López, compañeros en mis comienzos. Gracias Sergio Camargo por tu ayuda con los ensayos de RNA y mostrarme siempre algo nuevo en los programas informáticos. A Félix Ramos, gracias por ser compañero, y compartir conmigo esta etapa de doctorandos. Gracia Benítez, amiga y compañera, la técnico de laboratorio que muchos querrían tener, gracias por tu trabajo tan bien hecho y por tu disposición a ayudarnos en todo momento con una sonrisa. Javier Santamaría, Sergio Arévalo, Alexis, Francisco Lucena, Elvira Olmedo, gracias por ser compañeros en esta lucha diaria. En definitiva, gracias a todos, por haber hecho de mi estancia en el laboratorio una etapa especial en un ambiente inmejorable. Agradecer también a los Servicios Técnicos del IBVF, especialmente a la Dr. Alicia Orea (Servicio de Microscopía), y al Centro de

Investigación, Tecnología e Innovación de la Universidad de Sevilla (CITIUS) por su contribución a los resultados de esta tesis.

Gracias a mi "flatmate" Maialen Jauregi, y a mis doctoras y amigas Marta Sendra, Alejandra Guerra y Rocío Robles por escucharme cuando lo necesitaba y sus consejos tan acertados. Gracias a todos mis amigos, a los que han dedicado parte de su tiempo en escuchar mis largas historias incomprensibles de esos bichos con los que he trabajado. Cómo pasar por alto mi grupo de música, con los que he compartido cada fin de semana y me han llenado de alegría y buenas vibraciones.

Las últimas líneas se las dedico a mi familia, el gran pilar de mi vida. Los que me conocen saben de mis continuos viajes Sevilla-Jerez-Sevilla. Compartir con mi familia esta etapa ha sido mi gran fuente de motivación. A mis padres, hermanas y sobrinos, GRACIAS. Gracias por vuestra entrega, por creer en mí y estar siempre en cada momento de esta etapa de mi camino.

Index

Summary

The appearance of multicellular organisms is considered one of the major transitions during the course of early evolution, and multicellularity has been invented independently several times in all three domains of life. The cyanobacteria are a large group of oxygenic photosynthetic prokaryotes that represents a phylum with unicellular and multicellular (filamentous) forms. In many filamentous cyanobacteria, some cells can differentiate into specialized cells or groups of cells supporting different specialized functions, such as nitrogen fixation, survival and dispersion.

The heterocyst-forming cyanobacterium *Anabaena* sp. PCC 7120 represents a model organism to study multicellularity, cellular differentiation and N_2 fixation. *Anabaena* grows as chain of cells, termed trichomes or filaments, which under nitrogen deficiency contain two types of cells: vegetative cells that perform oxygenic photosynthesis and heterocysts that fix nitrogen gas. Vegetative cells transfer reduced carbon to heterocysts, which transfer fixed nitrogen to the vegetative cells. Intercellular molecular exchange is a very relevant aspect of the biology of *Anabaena* that has been addressed in this thesis. Two different pathways have been considered to explain the transfer of nutrients and regulators between the cells during heterocyst differentiation and diazotrophic growth in heterocyst-forming cyanobacteria: an indirect pathway via the continuous periplasm of the filament and a direct pathway via septal junction complexes. Intercellular molecular exchange in filamentous cyanobacteria has been studied using Fluorescent Recovery After Photobleaching (FRAP) analysis with different fluorescent markers: calcein, 5-carboxyfluorescein (5-CF) and the sucrose analog esculin. In Chapter 1, we analyzed the temperature-dependence of intercellular molecular exchange and found that it has properties of simple diffusion. This observation favors a direct pathway for intercellular communication. SepJ, FraC and FraD are septal proteins that have been proposed to be components of septal junction complexes. Septal junctions allow intercellular molecular exchange by simple diffusion and appear to be structures analogous to the connexons of the gap junctions of metazoans.

As mentioned above, the fluorescent sucrose analog esculin has been used to study intercellular molecular exchange. In the Experimental Preamble, we describe a specific assay that can be used to study the uptake of esculin into *Anabaena*. Using this assay, we could define that the transporters that mediate esculin uptake in *Anabaena* are α-glucoside transporters, since esculin uptake is inhibited by the α-glucosides sucrose and maltose. Chapter 2 and 3 describe the identification of components of ABC-type glucoside transporters. These components are GlsC and GlsD (nucleotide-binding domain proteins; NBDs), GlsP and GlsQ (transmembrane domain proteins; TMDs), and GlsR (a periplasmic solute-binding protein; SBP). Additionally, we found that HepP, a previously described Major Facilitator Superfamily (MFS) protein involved in the formation of the heterocyst-specific polysaccharide layer, also contributes to esculin uptake specifically in diazotrophic conditions.

Anabaena has been considered as a strict photoautotroph for a long time. Recent work has indicated however that *Anabaena* can grow heterotrophically with relatively high concentrations of fructose ($\geq$ 50 mM), although this cyanobacterium does not have any gene predicted to encode a fructose-specific transporter. In Chapter 3, we describe sucrose-, fructose- and glucose-stimulated growth of

Anabaena, showing that this cyanobacterium can grow mixotrophically with these sugars. To investigate whether the identified ABC components of glucoside transporters are involved in sugar-stimulated growth, we tested mixotrophic growth in their mutants. Whereas the *glsC* and *glsD* mutants were drastically impaired in sucrose-stimulated growth, the *glsP*, *glsQ* and *glsR* mutants were impaired at a lower level. All the mutants were also somewhat impaired in fructose- and glucose-stimulated growth suggesting that these sugars can taken up, at least in part, by the glucoside transporter(s). The *Anabaena* genome contains 12 genes encoding putative components of ABC glucoside transporters: four SBPs, six TMDs and two NBDs. This information and our results suggest the presence in *Anabaena* of at least three ABC glucoside transporters, one of which may be constituted by GlsR (SBP), GlsP-GlsQ (TMDs) and GlsC-GlsD (NBDs). Additional SBPs may be used by the membrane complex of this transporter, and the NBD proteins (GlsC and GlsD) appear to be shared by the three glucoside transporters, for which there are precedents in well-known ABC transporters. Bacterial Adenylate Cyclase Two Hybrid (BACTH) analysis has shown protein-protein interactions (GlsC-GlsD; GlsC-GlsQ; GlsD-GlsP) that are consistent with this proposal.

The effect of inactivation of some *gls* genes on the diazotrophic growth of *Anabaena* suggested the possibility of a limited transfer of sucrose to the heterocysts in some of these mutants. We found that the *glsC*, *glsP* and *hepP* mutants were impaired in the intercellular transfer of esculin, and we then extended our study to the intercellular transfer of calcein and 5–CF in all the *gls* mutants and the *hepP* mutant. All the glucoside transporter mutants are especially affected in the intercellular transfer of calcein, resembling the phenotype of *sepJ* mutants. As mentioned above, SepJ is a putative component of septal junctions, and we found that GlsP, GlsQ and HepP interact with SepJ in BACTH analysis, suggesting that GlsP, GlsQ and HepP are required for the correct function of septal junctions. On the other hand, GlsC influences the localization of SepJ and the number of septal peptidoglycan nanopores formed in *Anabaena*. These results suggest a specific role of GlsC influencing the formation of septal junctions.

In conclusion, the heterocyst-forming cyanobacterium *Anabaena* sp. PCC 7120 expresses glucoside transporters that have a role in sugar assimilation supporting mixotrophic growth. Additionally, these glucoside transporters influence intercellular communication mediated by the septal junction complexes.

Introduction

1.1. Multicellularity in bacteria

Multicellularity is a way of organization of outstanding importance in the biosphere, and the invention of multicellularity can be considered one of the major transitions during the course of early evolution (Bonner, 1998). Larger and more complex life forms have evolved from single unicellular ancestors (Carroll, 2001). Many studies suggest that the first step in the evolution of multicellularity is a size increase producing complex organisms that is followed by periods of high diversification; the larger the organism, the more cell types it presents (Carroll, 2001; Bonner, 2003). The transition to multicellularity has occurred independently several times in all three domains of life (Figure 1). These transitions may have happened for various ecological reasons, for example to mitigate predation risks and nutrient stress, and they have resulted in a broad range of phenotypes, involving or not involving cellular differentiation (Claessen et al., 2014). Aquatic organisms began their multicellularity by the products of cell division failing to separate, while most terrestrial microorganisms involve some form of motile aggregation of cells or nuclei in a multinucleate syncytium (Bonner 1998).
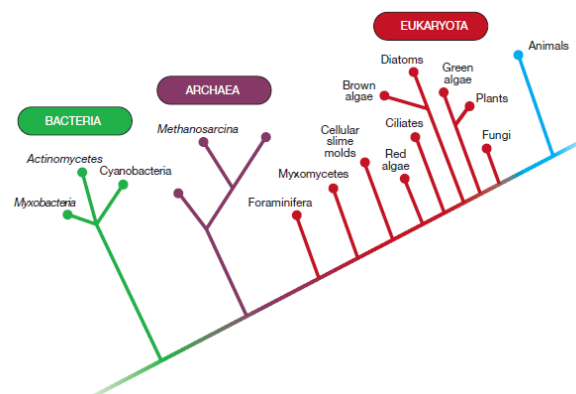
Figure 1. The phylogenetic relationships of multicellular taxa. Figure from Carroll (2001).

Bacteria have been considered as unicellular organisms over the years, but this idea started to change as the result of ecological observations. Studies from Beijerinck and Winogradsky elucidated the role of bacteria forming organized multicellular structures and living in groups in different habitats and ecosystems. The same particularity was observed under laboratory conditions, on petri dishes or adhered as organized populations to the walls of culture flasks (Shapiro, 1988).

There are recent studies that support the understanding of the origins and mechanisms of multicellularity in bacteria. These organisms use different strategies to grow in multicellular forms, which range from aggregation of individual cells to incomplete cell fission after cell division producing chains of cells and to the formation of syncytial filaments (Claessen et al., 2014). The different features of patterned multicellularity in bacteria can be explained using well-studied model organisms:

aggregative multicellularity in myxobacteria, differentiated multicellular growth in streptomycetes, and filamentous growth and cell differentiation in cyanobacteria.

Myxobacteria are a group of Gram-negative bacteria that are predominantly found in the soil. During starvation, growth is arrested and the bacteria initiate the formation of spore-bearing fruiting bodies. These structures form spherical spores that are metabolically inactive and partly resistant to desiccation and temperature. When nutrients become available, the spores germinate and complete the life cycle of the bacterium (Zusman et al., 2007).

Streptomyces, a genus of Gram-positive bacteria that belongs to the phylum Actinobacteria, grows as branching hyphae that form a mycelium, and aerial hyphae produce spores. When the spore of *Streptomyces* finds favorable conditions, it germinates and one or two tubes emerge to form new hyphae. This type of growth permits radial expansion and, producing mature spores, facilitates migration to an extended range of microenvironments. Production of secondary metabolites and morphological differentiation are initiated in response to nutrient depletion and other signals. The different polynucleated compartments in hyphae are connected by channels which transport nutrients and plasmids (Flärdh et al. 2009; Claessen et al., 2014).

Cyanobacteria are a large group of oxygenic photosynthetic prokaryotes. Whereas many cyanobacteria grow as single cells, many others can grow as chains of cells behaving as multicellular organisms. Multicellularity has been lost and regained several times in the course of evolution producing the current distribution of both unicellular and multicellular cyanobacterial forms. The filamentous cyanobacteria experience an incomplete separation of daughter cells after cell division, and in many cyanobacteria some cells can develop into differentiated cells or groups of cells supporting several distinct functions (Flores and Herrero, 2010; 2014; Claessen et al., 2014; Herrero et al., 2016).

1.2. Membrane transport

In bacteria, the cell envelope provides several functions, protecting the cells from damage, maintaining the cell shape, controlling the osmotic pressure, and mediating molecular exchange of the cell with the external medium. Gram-negative bacteria present a cell envelope that is composed of a cytoplasmic membrane (CM), a murein (peptidoglycan [PG]) sacculus, and an outer membrane (OM). The space between the CM and OM than contains the PG is called the periplasm. The OM is asymmetrical, its inner leaflet is rich in phospholipids and its outer leaflet is rich in lipopolysaccharide (LPS). The OM contains integral membrane proteins and lipoproteins (Bos et al., 2007), and its main function is to serve as a selective permeation barrier. Porins, with a β-barrel fold, are the characteristic OM proteins that permit low-specificity diffusion of small ions and hydrophilic molecules of a size of up to 600 Da, such as amino acids and sugars (Nikaido, 2003). This facilitated diffusion involves the movement of molecules downhill as determined by their relative concentrations inside (in the periplasm) and outside of the cell. The murein sacculus is porous permitting the movement of molecules smaller than 25-50 kDa. The CM is a phospholipid bilayer that forms a barrier which impedes the exchange of hydrophilic molecules between the cytoplasm and the periplasm, maintaining the internal composition of the cell. Hence, to regulate the composition of the cytoplasm, allow incorporation of nutrients and exclude byproducts of metabolism, specific mechanisms are needed for different compounds to traverse the CM.

The simplest mechanism by which molecules can traverse the CM is passive diffusion. The molecule dissolves in the phospholipid bilayer, diffuses across it and enters inside the cytoplasm. In this type of transport proteins are not needed. The relative concentrations of the molecule inside and outside of the cell determine the direction of the transport. The transport is always down the molecule's concentration gradient. Only gases, relatively hydrophobic molecules, and small polar but uncharged molecules can diffuse across the membrane (Cooper, 2000). To be transferred across the CM, other types of molecules need specific CM transporters.

Between 3 and 16% of the open reading frames in bacterial genomes are predicted to encode transport proteins, and the average percentage (9%) is higher than that in archaeal (7%) or eukaryotic (4%) genomes (Ren and Paulsen, 2005). Two families of transporters have been found to occur ubiquitously and abundantly in all types of living organisms. These are the ATP-binding cassette (ABC) superfamily and the major facilitator superfamily (MFS), the latter also called the uniporter-symporter-antiporter superfamily.

1.2.1. ABC transporters

The ABC (ATP binding cassette) transporter superfamily is one of the largest families among transport proteins, widely distributed in all the three domains of life. ABC transporters can recognize almost any solute of biological interest, and they can be divided into importers and exporters. ABC exporters are found in both eukaryotes and prokaryotes being involved in diverse roles, including drug resistance mediated by the

export of certain toxic substances. ABC importers appear to be present exclusively in prokaryotes and are crucial in mediating uptake of nutrients.

ABC transporters have a characteristic structure. The ABC importers generally comprise one periplasmic solute-binding protein (SBP), two integral membrane proteins (transmembrane domains [TMDs] or permeases) that form the solute-translocation pathway, and two nucleotide-binding domains (NBD) that hydrolyze ATP in the cytoplasm (Cui and Davidson, 2011). NBDs present conserved motifs; in contrast, the sequences of SBPs and the sequences and architectures of the TMDs are quite variable, reflecting the chemical diversity of the translocated substrates.

In Gram-negative bacteria, SBPs are most frequently soluble proteins located in the periplasmic space between the inner and outer membranes. In Gram-positive bacteria, SBPs are either tethered to the cytoplasmic membrane as lipoproteins or fused to the TMDs (van der Heide and Poolman, 2002; Cui and Davidson, 2011). Some SBPs associated in these ways to the CM are also found in cyanobacteria (Flores et al., 2005; Pernil et al., 2008). SBPs function as high affinity binding proteins that specifically associate with the ligand in the periplasm for delivery to the appropriate ABC transporter (Ress et al., 2009). SBPs adopt a similar folding pattern made of two globular domains which are connected by one or more polypeptide chains, and the substrate binds between them. Some SBPs are versatile, having a wide substrate specificity as illustrated by the multiple-sugar transporter Msm of *Streptococcus mutans*, which recognizes melibiose, sucrose, raffinose, isomaltotriose, and isomaltotetraose (Russell et al., 1992; Tapia et al., 1999). Alternatively, multiple SBPs with different binding specificities can interact with a single transporter, as illustrated by the histidine, lysine, and arginine transport system in *Enterobacteriaceae* (Higgins and Ames, 1981) and the oligopeptide/muramyl peptide transport system of *Escherichia coli* (Park et al., 1998; Davidson et al., 2008). On the other hand, although most of the bacterial importers require an SBP, there are exceptions; most notably, a novel class of ABC transporters termed ECF (energy-coupling factor) transporters (Rice et al., 2014). Whereas these transporters contain a canonical NBD dimer, the TMDs are thought to differentiate into a substrate-specific subunit that binds substrate with high affinity and an energy-coupling subunit. ECF ABC transporters are relatively abundant in Gram-positive bacteria, but are rare in Gram-negative bacteria.

TMDs of typical ABC transporters contain a total of 12 TM helices (6 per domain), but the membrane spanning subunits are structurally heterogeneous, with three distinct sets of folds currently recognized (Ress et al., 2009; Rice et al. 2014). Regarding bacterial ABC importers, TMDs are expressed as separate protein subunits that belong to either type I or type II, depending on whether the fold is similar to that first observed in *Archaeoglobus fulgidus* ModBC (type I) or *E.coli* BtuCD (type II). Another fold has been found in ECF-type transporters that belong to the ABC-importer family. Only one ABC exporter fold has been defined (type III), referred to as the B-family ABC-export fold (Locher, 2016). TMDs have a final cytoplasmic loop containing an EAA amino acid motif that is highly conserved and makes contact with the Q-loop of the NBD at the NBD-TMD interface. The EAA motif plays an important role in coupling the NBDs to the TMDs (Cui and Davidson, 2011).

NBDs contain two subdomains: a RecA-like domain common in many ATPases, which contains the nucleotide-binding Walker A and Walker B motifs, and a helical subdomain specific to ABC proteins, which contains the ABC family signature motif LSGGQ. Because the NBDs are dimeric, there are two ATP-binding sites in the NBDs, which are located between the Walker A motif of one subunit and the LSGGQ motif of the opposite subunit (Cui and Davidson, 2011; Rees et al., 2009; Wilkens 2015). Many prokaryote NBDs, such as *E. coli* MalK, have an extra C-terminal domain involved in regulation. Some NBD proteins serving different permease complexes in ABC transporters —the so-called multitask ABC ATPases— are well known, and classical examples are MalK and similar proteins that energize di- an oligo-saccharide uptake in several bacteria (Schlösser et al., 1997; Webb et al., 2008; Ferreira and de Sá-Nogueira, 2010). The type I transporter MalEFGK$_2$ from *E. coli* is shown in Figure 2 as a model ABC importer.
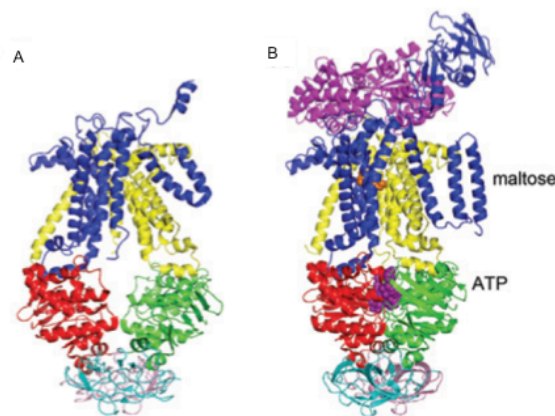
Figure 2. The maltose/maltodextrin ABC importer from *E. coli*. Different domains are shown: blue and yellow, TMDs (MalF, MalG); red and green, NBDs (MalK); pink and cyan, C-terminal regulatory domains of NBDs (MalK); magenta, SBP (MalE). The conserved EAA motif is shown as short horizontal blue and yellow helices at the TMD-NBD interface. (A) The maltose/maltodextrin MalFGK$_2$ complex. (B) The MalE-MalFGK$_2$ complex, with maltose (orange spheres) bound to MalF and ATP (purple spheres) sandwiched by NBDs. Figure from Cui and Davidson (2011).

TMDs and NBDs can form homodimeric or heterodimeric complexes and can exist as separate subunits or be fused together in different ways. In addition, genes encoding the SBP, TMD and NBD for a specific transporter are often organized in one locus that frequently behaves as an operon in which the gene encoding the SBP is 5' to the others. However, there are exceptions, for instance in transporters which share the same NBDs.

1.2.2. MFS transporters

The MFS proteins represent the largest family of secondary transporters and play a crucial role in a multitude of physiological processes. MFS proteins transport a large

variety of ions and solutes across membranes. They comprise facilitators, symporters, and antiporters, which move substrates across membranes via facilitated diffusion, cotransport or exchange respectively (Yan, 2015). Whereas facilitators mediate substrate transfer across the membrane down its concentrations gradient, symporters or antiporters use the energy released from the downhill translocation of one substrate to drive the uphill translocation of another substrate either in the same direction (symporters) or in the opposite direction (antiporters). As a general principle, if charged molecules are unidirectionally pumped as a consequence of the consumption of a primary cellular energy source, electrochemical potentials result (Mitchell, 1967). The consequential chemiosmotic energy generated can then be used to drive the active transport of additional solutes via secondary carriers, such as MFS transporters, that facilitate the transport of one or more molecular species across the membrane (Maloney, 1990, 1992; reviewed in Pao et al.,1998).

The structures of seven distinct prokaryotic MFS transporters have been elucidated sharing a common fold known as MFS fold. These include, for instance, the lactose:H$^+$ symporter LacY and the glycerol-3-phosphate:phosphate antiporter GlpT. The core MFS fold contains 12 TM segments (TMSs), which are organized into N- and C-domains. An MFS fold contains four structural repeats, each comprising three consecutive TMSs. In addition to the core MFS fold, some MFS transporters may contain extra TMSs that help to stabilize the overall structure (Figure 3) (Shi, 2013; Yan, 2015).

Regarding the general transport mechanism, the prevailing model was proposed more than four decades ago by Jardetzki (1966). This model, now known as the alternating-access mechanism, predicts that the transporter must switch between at least two conformations, an outward-facing conformation and an inward-facing one, in order to allow alternating access to the substrate binding site from either side of the membrane (Shi, 2013). Of note, in the MFS transporters, a single substrate binding cavity is located in a position corresponding to the center of the membrane and enclosed by the N and C domains (Figure 3).

The MFS comprises different families. The largest family, family 1, corresponds to the sugar porter (SP) family. These transporters are present in all of the major groups of living organisms: bacteria, archaea, eukaryotic protists, fungi (mostly yeast), animals and plants. They can function by uniport, solute:solute antiport, and/or solute:cation symport, depending on the system and/or conditions. Substrates transported by SP family members include hexoses, pentoses, disaccharides, quinate, inositols and organic cations. The glucose transporters GLUT1-GLUT4 represent some of the physiologically most important and best characterized transporters. They are responsible for the cellular uptake of glucose and other monosaccharides or disaccharides in all kingdoms of life. Among the bacterial homologs is XylE from *E. coli.* Another representative well-characterized example of the SP family protein is the arabinose:H$^+$ symport permease (AraE) of *E. coli* (Pao et al., 1998; Maiden et al., 1988).
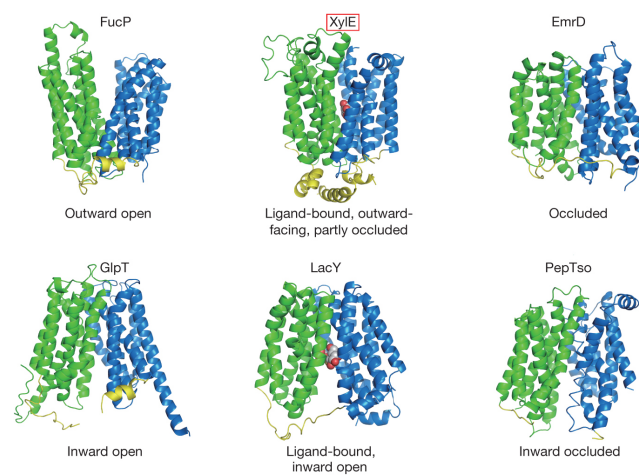
Figure 3. MFS structures display distinct conformations. FucP, the L-fucose:H$^+$ symporter; XylE, the D-xylose:H$^+$ symporter; EmrD, the multidrug transporter; GlpT, the glycerol-3-phosphate:phosphate antiporter; LacY, lactose:H$^+$ symporter; PepTso, the peptide transporter. For instance, XylE contains an intracellular helix domain (yellow) that is not seen in the other structures. The distinct N and C domains are colored green and blue, respectively, in all the structures. From Sun et al. (2012).

1.3. Cyanobacteria

The cyanobacteria are a group of prokaryotes that perform oxygenic photosynthesis. These organisms are widely distributed in aquatic and terrestrial environments, including extreme habitats such as deserts, hot springs and polar regions (Whitton, 2000). Also, some cyanobacteria establish symbiotic associations with plants, fungi and other organisms (Meeks and Elhai, 2002). Cyanobacteria play an important role in the carbon and nitrogen cycles in the biosphere, contributing greatly to global primary production and the global nitrogen budget (Capone et al., 1997; Montoya et al., 2004). In Earth's history, the cyanobacteria were key players in the oxygenation of the Earth's atmosphere during the so-called Great Oxygenation Event (GOE) and are generally accepted to be the precursors of chloroplasts of plants and algae. Finally, their potential for providing renewable chemicals and biofuels is currently attracting increased attention (Dismukes et al., 2008).

1.3.1. Morphology and phylogeny of cyanobacteria

Morphologically, cyanobacteria show an impressive diversity. Rippka et al. (1979) distinguished five sections by their particular patterns of structure and development. These sections correspond to taxonomic orders (Castenholz, 2001). Section I (Chroococcales) is composed of unicellular organisms whose reproduction is by binary fission or by budding, showing spherical, cylindrical or oval cells. In Section II (Pleurocapsales), unicellular organisms are grouped that show multiple fission producing baeocytes, small cells enclosed in a fibrous wall layer that are subsequently released by breakage of such layer. Section III to Section V comprise cyanobacteria that grow as chains of cells termed filaments or trichomes. Section III (Oscillatoriales) is composed of filamentous non-heterocyst-forming cyanobacteria. (Heterocysts are cells specialized for N_2 fixation that will be described in detail below.) Cell division occurs regularly in one plane at a right angle to the long axis of the trichome. Section IV (Nostocales) comprises filamentous cyanobacteria that, unlike Section III cyanobacteria, exhibit a wide capability of cellular differentiation including the production of heterocysts. And finally, Section V (Stigonematales) is composed of filamentous, heterocyst-forming cyanobacteria whose cells can divide in more than one plane, producing branched filaments. Some Section IV and V cyanobacteria can produce akinetes, a type of spores that resist cold and desiccation and germinate when conditions favorable for growth are met. In addition, many Section IV and V cyanobacteria, as well as some Section III cyanobacteria, undergo a developmental cycle forming hormogonia, which are short motile filaments with a dispersal function (Rippka et al., 1979; Flores and Herrero, 2010).

Different molecular studies have now introduced new ideas about the phylogeny of cyanobacteria supporting only partially Rippka's classification. Giovannoni et al. (1988) performed phylogenetic analysis based on 16S RNA sequences and found that cyanobacteria are a monophyletic group of organisms that includes algal and plant plastids. They also found that cyanobacteria of Section II and, on the other hand, those of Sections IV and V together appear to be monophyletic.

There is some controversy about the phylogeny of strains from Sections I and III, which in any case appear to be spread in the phylogenetic tree of cyanobacteria (Tomitani et al., 2006; Shih et al., 2013). Figure 4 shows a phylogenetic analysis from Shih et al. (2013) in which the wide spreading of unicellular and filamentous cyanobacteria in the tree is evident. In contrast, note that all heterocyst-forming cyanobacteria analyzed are clustered in group B1.

The origin of cyanobacteria can be dated in relation to the oxygenation of the Earth's atmosphere, GOE, which took place about 2.4 to 2.2 billion years ago, in the Precambrian. This event was produced by oxygenic photosynthesis carried out by cyanobacterial ancestors, which therefore had evolved before that time (Knoll, 2008). Studies based on 16S RNA sequences and on the Precambrian fossil record have suggested the origin of cyanobacteria in the Archean and a transition to multicellularity early in cyanobacterial evolution, before the GOE (Schirrmeister et al., 2011). Moreover, cyanobacterial fossils attributed to Sections IV and V cyanobacteria have suggested the idea that heterocyst formation evolved after the GOE (Tomitani et al. 2006).

As mentioned earlier, cyanobacteria are considered to be the progenitors of the chloroplast, the photosynthetic organelle found in eukaryotes. Although most studies support the monophyly of primary plastids (Giovannoni et al., 1988; Chan et al., 2011), others have reported a polyphyletic origin (Nozaki et al., 2009; Baurain et al., 2010). Shih et al. (2013) found strong support for the monophyletic placement of plastids near the base of the cyanobacterial tree but did not identify which lineage was most closely related to the original plastid endosymbiont. Ochoa de Alda et al. (2014) placed the origin of plastids among the members of one of the major cyanobacterial lineages that includes filamentous N_2-fixing cyanobacteria. The topic of the origin of plastids (and mitochondria) is currently the subject of intense research (Zimorski et al., 2014).

DNA transfer by means of two processes, horizontal gene transfer or vertically inherited genes, contributes to bacterial diversification and evolution (Novichkov et al., 2004). Laboratory work in molecular genetics has settled the basis for DNA transfer in cyanobacteria, which includes natural transformation in some unicellular cyanobacteria and transfer promoted by promiscuous conjugative plasmids to cyanobacteria of the order Nostocales (Flores et al., 2008). Conjugal transfer of plasmid DNA from *E. coli* to *Anabaena* followed by establishment of replicating plasmids in the recipient (Wolk et al., 1984) or by recombination of the incoming material with genomic DNA (discussed in Flores et al., 2008) have permitted the development of the genetics of several strains of Nostocales. This is the basis of mutant construction presented in this thesis.

Figure 4. Cyanobacterial maximum-likelihood phylogenetic tree. The 126 genomes sequenced by 2013 are presented in the tree, which was generated with a sequence resulting from concatenating 31 conserved proteins. Branches are colored according to morphological subsection. Nodes supported with a bootstrap of at least 70% are indicated by a black dot. Morphological transitions are denoted by blue triangles. Phylogenetic subclades are grouped into seven major subclases (A-G), some of which are made up of smaller subgroups. Figure from Shih et al. (2013).

1.3.2. Assimilation of carbon and nitrogen in cyanobacteria

Cyanobacteria have very simple nutritional requirements, being able to grow in media containing only a few mineral salts (including a source of nitrogen, which is a macronutrient) and exposed to air as a source of carbon. Those cyanobacteria that can also fix atmospheric nitrogen can literally be said to grow "on air and water".

1.3.2.1. Carbon assimilation

Almost all cyanobacteria are photoautotrophic organisms, performing oxygenic photosynthesis and carbon dioxide fixation (Figure 5). Ribulose 1,5-bisphosphate carboxylase/oxygenase (Rubisco) is the enzyme that catalyzes the fixation of CO_2 in photosynthetic organisms. The affinity of Rubisco for CO_2 is low relative to the concentration of ambient CO_2. This problem is solved in cyanobacteria by expressing an efficient inorganic carbon concentration mechanism (CCM). CCM includes CO_2 and bicarbonate transporters, carbonic anhydrase to interconvert CO_2 and HCO_3^-, and the core component, the carboxysome. This is an intracellular microcompartment in which Rubisco is confined to enhance its CO_2-fixing activity and to depress reaction of 1,5-bisphosphate with O_2 (Kaplan and Reinhold, 1999; Cameron et al, 2014). The fact that CCM activity is modulated by environmental factors provides an ecological advantage, conferring the ability to acclimate to a wide range of CO_2 concentrations (Kaplan and Reinhold, 1999). Most cyanobacteria possess active uptake systems for both CO_2 and HCO_3^- species. However, based on genomic data, the oceanic *Prochlorococcus* spp. seem to be an exception since they only have identifiable genes for HCO_3^- uptake (Badger *et al.,* 2002; Price, 2008). Active uptake and accumulation of Ci species requires the input of metabolic energy, and several different mechanisms of energization have been putatively identified (Price, 2008).

In spite of the dominant trophic mode of cyanobacteria, which is protoautotrophy performing oxygenic photosynthesis, a large number of cyanobacterial strains have the ability to grow on exogenous organic substrates as the carbon source (Rippka, 1972, 1979). Some cyanobacteria can take up and use sugars either only in the light, growing mixotrophically, or in the dark, growing heterotrophically (Wolk and Shaffer, 1976; Bottomley and van Baalen, 1978; Smith, 1983; Schmetterer and Flores, 1988). The unicellular cyanobacterium *Synechocystis* sp. strain PCC 6803 can grow in the dark using glucose as long as a short, regular exposure to light is provided (Anderson and McIntosh, 1991). Consistently, some sugar transporters that mediate sugar uptake supporting some kind of heterotrophic growth have been identified in cyanobacteria. Well-known examples include a major facilitator superfamily (MFS) glucose transporter, GlcP, that has been characterized in *Synechocystis* sp. strain PCC 6803 (Zhang et al., 1989; Schmetterer, 1990) and in the heterocyst-forming cyanobacterium *Nostoc punctiforme* ATCC 29133 (Ekman et al., 2013). An MFS transporter for glucose is also expressed in some marine unicellular cyanobacteria (Muñoz-Marín et al., 2013), which seems to be phylogenetically distant to the *Synechocystis* transporter (Picossi et al., 2013). Another example is the ABC-type fructose transporter, Frt, that has been characterized in the heterocyst-forming

cyanobacteria *Anabaena variabilis* (Ungerer et al., 2008) and *N. punctiforme* (Ekman et al., 2013). *A. variabilis* can grow heterotrophically with fructose (Wolk and Shaffer, 1976a) and *N. punctiforme* does so with glucose or fructose (Summers et al. 1995).

The model heterocyst-forming cyanobacterium *Anabaena* sp. strain PCC 7120 (hereafter *Anabaena*) has been considered for a long time to be a strict photoautotroph. Recent work has shown however that *Anabaena* can grow heterotrophically using fructose as long as this sugar is provided at relatively high concentrations (≥ 50 mM) (Stebegg et al., 2012). Incorporation of the genes encoding the Frt transporter from *A. variabilis* permits growth of *Anabaena* dependent on 5 mM fructose concentration (Ungerer et al., 2008). Thus, *Anabaena* has the metabolic capability to use fructose as a carbon and energy source, but lacks a high affinity transporter for this sugar. Additionally, Malatinszky et al. (2017) have described mixotrophic growth of *Anabaena* with different carbon sources including sugars (fructose, glucose, maltose, sucrose), amino acids (glutamate, glutamine, proline) and other simple organic compounds (acetate, glycerol, pyruvate) in molar equivalency to carbon contained in 5 mM glucose. Whereas ABC transporters for amino acids (Pernil et al., 2008, 2015) and a TRAP transporter that can take up pyruvate (Pernil et al., 2010) are known to be expressed in *Anabaena*, transporters that mediate the uptake of sugars are less known.

1.3.2.2. Nitrogen assimilation

Cyanobacteria are able to utilize various inorganic and organic nitrogen sources. These compounds have to be taken up from the environment and converted intracellularly to ammonium, which is assimilated into carbon skeletons (Figure 5) (Luque and Forchhammer, 2008). The various sources of nitrogen that can be assimilated by different cyanobacteria include: ammonium, nitrate, nitrite, urea, some amino acids and dinitrogen.

Ammonium is the preferred source of combined nitrogen for cyanobacteria, since it is directly incorporated into carbon skeletons. Ammonia diffuse through biological membranes, whereas the ammonium ion cannot. Cyanobacteria bear transporters which mediate the uptake of ammonium when it is found in low concentrations in the external medium (Boussiba et al., 1984). These transporters belong to the Amt protein family and have been identified in *Synechocystis* sp. strain PCC 6803 (Montesinos et al., 1998), *Synechoccocus elongatus* (Vázquez-Bermúdez et al., 2002b; Paz-Yepes et al., 2007) and *Anabaena* (Paz-Yepes et al., 2008). Ammonium is incorporated into organic compounds through the glutamine synthetase/glutamate synthase (GS/GOGAT) pathway, which generates glutamate from 2-oxoglutarate (2-OG) and ammonium in a two-step reaction: first, glutamine is synthetized from ammonium and glutamate in an ATP-dependent reaction catalyzed by GS; second, the synthesis of two molecules of glutamate takes place from glutamine and 2-OG catalyzed GOGAT, which requires reductant provided in many cyanobacteria by ferredoxin (Luque and Forchhammer, 2008). Thus, the GS/GOGAT pathway generates glutamate and glutamine, the main nitrogen distributing compounds in the cell, and incorporates 2-OG, which derives from CO_2 fixation and

serves as a carbon backbone. Additionally, because cyanobacteria lack 2-oxoglutarate dehydrogenase in the Krebs cycle (Stanier and Cohen-Bazire, 1977), the GS/GOGAT pathway efficiently links the carbon and nitrogen metabolisms. Interestingly, 2-OG is the compound that senses the C-to-N balance in cyanobacteria (Muro-Pastor et al., 2001). Nonetheless, it has been recently reported that cyanobacteria can close the tricarboxylic acid cycle (Zhang and Bryant, 2011; Xiong et al., 2014).
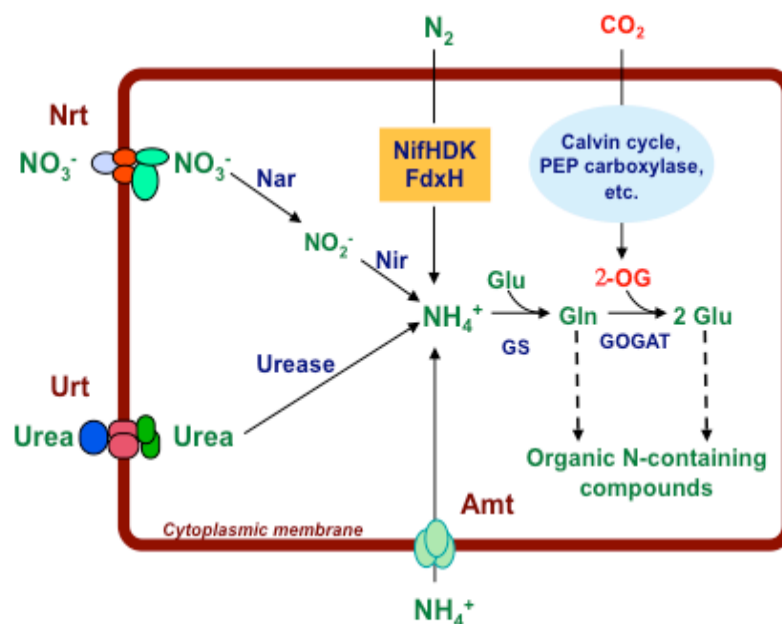
Figure 5. Summary scheme of the carbon and nitrogen metabolism in cyanobacteria (Flores and Herrero, 2005). Uptake of nitrate, urea and ammonium by the Nrt, Urt and Amt transporters, respectively, are shown. Reduction of nitrate and nitrite by nitrate reductase and nitrite reductase, respectively, is also shown, as is urea hydrolysis by urease. Reduction of N_2 to ammonium by nitrogenase (the *nifHDK* product) and heterocyst-specific ferredoxin is also indicated. Ammonium is incorporated into carbon skeletons through the GS/GOGAT pathway producing organic nitrogen-containing compounds. CO_2 fixation by the Calvin cycle and phosphoenol-pyruvate (PEP) carboxylase is indicated too. Stoichiometry of reactions not indicated.

The assimilatory reduction of nitrate to ammonium is a key step of the nitrogen cycle in the biosphere. Nitrate reduction to ammonium is carried out by many bacteria, fungi, algae and plants. In cyanobacteria, incorporation of nitrate (and nitrite) takes place through a nitrate/nitrite transporter, which can be either an ABC-type uptake transporter or a MFS permease that concentrates the substrate inside the cell, where nitrate and nitrite reductases sequentially act to produce ammonium that is incorporated into carbon skeletons through the GS/GOGAT pathway (Flores et al., 2005). Genes involved in nitrate/nitrite assimilation are commonly found in a gene cluster that behaves as an operon, including the genes encoding nitrite reductase (*nirA*), the ABC-type uptake transporter (*nrtABCD*) or permease (*nrtP*), and nitrate reductase (*narB*). In addition, located close to the *nirA* operon, a set of genes are

found encoding proteins that influence the expression of the operon (Flores et al., 2005; Luque and Forchhammer, 2008).

Urea is one of the most abundant simple forms of organic nitrogen in nature. In the oceans urea is the dominant component of dissolved organic nitrogen (Luque and Forchhammer, 2008). Urea can diffuse through the cytoplasmic membrane readily but transporters with a very high affinity for urea have been physiologically characterized in yeast, fungi, algae and a few bacteria. The urea transporter of *Anabaena*, Urt, is an ABC-type transporter encoded by the *urtABCDE* operon. Once inside the cell, urea is hydrolyzed to CO_2 and ammonium by urease (Valladares et al., 2002).

Energetically, the most expensive source of nitrogen is molecular nitrogen or dinitrogen (Luque and Forchhammer, 2008). N_2 fixation is the process of reduction of N_2 to ammonium, which is carried out exclusively by prokaryotes including many cyanobacteria. Nitrogenase is the enzyme that catalyzes the ATP-dependent reduction of N_2 (Fay, 1992). This enzyme is constituted by two components: dinitrogenase (comprised by NifD and NifK proteins) and dinitrogenase reductase (NifH) (Rubio and Ludden, 2008), and it is extremely sensitive to oxygen. Thus, bacteria fix N_2 under anoxic conditions or have developed diverse strategies to protect nitrogenase from O_2. In diazotrophic cyanobacteria, oxygenic photosynthesis and N_2 fixation are separated temporally or spatially. For instance, in some unicellular and filamentous cyanobacteria the fixation of N_2 takes place in the dark, when photosynthesis is not operative (Rippka and Waterbury, 1977; Bergman et al., 1997; Stal and Zehr, 2008). In other cases, some filamentous cyanobacteria separate spatially both process, taking place the N_2 fixation in specific cells named heterocysts that keep a micro-oxic environment in which the *nif* genes are expressed and the N_2 fixation machinery can operate (Figure 6) (Fay, 1992; Flores and Herrero, 2014).

The control of nitrogen metabolism in cyanobacteria is orchestrated by the NtcA protein, a transcription factor of the CRP (or CAP) family of bacterial transcriptional regulators that is generally conserved in cyanobacteria (Herrero et al., 2001, 2004). This transcriptional regulator influences the expression of many genes whose products are involved in nitrogen assimilation and related functions. NtcA activates transcription by binding to the promoter region of the regulated genes at a DNA-binding site with the consensus sequence $GTAN_8TAC$, which is frequently found about 22 bp upstream of a canonical -10 promoter box of sequence TAN_3T (Luque et al., 1994; Herrero et al., 2001). NtcA-dependent transcription activation can take place when the cells are in the absence of ammonium, the preferred N source. In addition to being autoregulated at the level of gene expression, NtcA is modulated at the activity level as a function of the C-to-N balance of the cells. Thus, NtcA-dependent genes are activated only under conditions that lead to high C-to-N ratios (Luque et al., 2004; Olmedo-Verd et al., 2008). As mentioned above, 2-oxoglutarate (2-OG) levels indicate the C-to-N ratio in cyanobacterial cells (Muro-Pastor et al., 2001; Luque and Forchhammer, 2008). Nitrogen-limiting conditions result in an increase in the cellular levels of 2-OG, which binds to NtcA leading to a positive effect on the expression of NtcA-activated genes (Vázquez-Bermúdez et al., 2002a; Valladares et al., 2008). On the other hand, in some gene promoters, NtcA can act as a repressor (Luque and Forchhammer, 2008). Finally, NtcA also plays a principal role in transcriptional

regulation for the triggering of heterocyst differentiation and for subsequent steps of heterocyst development and function (Herrero et al., 2004), and it appears to represent the largest bacterial regulon characterized to date (Picossi et al., 2014).

1.3.3. Heterocysts

Heterocysts are differentiated cells where N_2 fixation takes place under conditions of nitrogen deprivation. As mentioned above, cyanobacteria from Sections IV and V of Rippka's classification (Rippka et al., 1979) perform N_2 fixation in this type of cells. Thus, these organisms separate spatially oxygenic photosynthesis (that takes place in vegetative cells) from nitrogen fixation. Differentiating cells undergo many morphological and metabolic changes (Golden and Yoon, 1998), and differentiated heterocysts are distinguished from vegetative cells by their larger and rounder shape, diminished pigmentation, the deposition of two additional cell wall layers resulting in a thicker cell envelope, and usually prominent cyanophycin granules at the cell poles adjacent to vegetative cells (Kumar et al., 2010; Herrero et al., 2016). Oxygen-producing photosystem II (PSII) is dismantled during differentiation, and the heterocysts show an increased rate of respiration (Wolk et al., 1994).
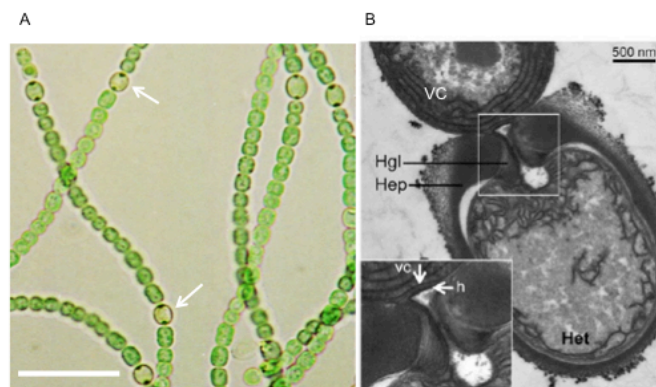
Figure 6. Micrographs of *Anabaena* sp. strain PCC 7120 observed by optical and transmission electron microscopy. (A) Light micrograph of diazotrophic filaments showing vegetative cells and heterocyst (indicated by arrows). Scale bar, 20 μm. (B) Transmission electron micrograph of septa between a terminal heterocyst (Het) and the neighbouring vegetative cell (VC). Hep, heterocyst-specific polysaccharide envelope; Hgl, heterocyst-specific glycolipid envelope. A larger magnification is shown (vc, vegetative cell CM; h, heterocyst CM). Image from Merino-Puerto et al. (2011b).

1.3.3.1. Structure of the heterocyst

Morphological changes include the deposition of two additional envelope layers around the heterocyst (Figure 6): an inner laminated layer composed of heterocyst-specific glycolipids (HGL) and a homogenous outer polysaccharide layer (HEP) (Cardemil and Wolk 1979; Cardemil and Wolk 1981). The HGL layer is a permeability barrier for gases, specially O_2 (Fay, 1992), and the HEP layer protects the glycolipid layer from physical damage (Xu et al., 2008). Defects in the structure of the envelope

can result in an inability to fix dinitrogen under oxic conditions and, thus, in the inability to grow fixing nitrogen under these conditions (the Fox⁻ phenotype) (Wolk et al. 1988; Fan et al. 2005; Huang et al. 2005; Nicolaisen et al. 2009a).

Most of the genes involved in heterocyst envelope formation, encoding both regulatory proteins and enzymes for the synthesis and export of envelope material, are induced after 6-12 h of nitrogen deprivation. Deposition of the external polysaccharide layer is one of the earliest morphological changes during heterocyst differentiation. In the time course of differentiation, the homogeneous layer (HEP) is formed before the laminated layer (HGL) appears (Wilcox et al., 1973). However, the formation of the HEP layer is not a prerequisite for HGL formation as seen in mutants defective in HEP layer formation, e.g., the *hepA* mutant (Zhu et al., 1998). Many genes involved in HEP biosynthesis in *Anabaena* are clustered in the so-called "HEP island" (Huang et al., 2005). Zhu et al. (1998) identified the essential role of *hepA* from *Anabaena* in the deposition of the HEP layer. The encoded protein is a member of the ABC transporter family, more precisely an ABC exporter. Another gene, *hepC* encoding a UDP-galactose-lipid carrier transferase, is located upstream of *hepA*. Additional *hep* genes are located in other regions of the *Anabaena* chromosome and include genes encoding glycosyl transferases (Maldener et al., 2003; Wang et al., 2007), a polysaccharide export protein (Maldener et al., 2003; Lechno-Yossef et al., 2011), and HepP, a predicted membrane protein that belongs to the major facilitator superfamily (MFS) and could function as a glycoside exporter (López-Igual et al., 2012). Regulation of HEP deposition depends upon signal transduction systems that comprise, at least, the histidine kinase HepN (Fan et al., 2006; Ning et al. 2004), the response regulator HenR (Fan et al., 2006), the serine/threonine kinase HepS (Fan et al., 2006), and the interacting two-component regulatory proteins HepK and DevR (Zhou and Wolk 2003; Zhu et al., 1998). All these proteins are required for the normal maturation of heterocysts (Fan et al., 2006; Lechno-Yossef et al., 2006; Wang et al., 2007).

The heterocyst glycolipid layer is assembled beneath the polysaccharide layer and is composed of fatty alcohols glycosidically linked to sugar residues. The *hglB*, *hglC*, *hglD* and *hglE* genes along with a cluster of nearby genes are required for the synthesis of these glycolipids (Campbell et al., 1997; Fan et al. 2005; Maldener et al., 2014). ORF all5341, named *hglT*, has been described to be necessary for glycosylation of the aglycone hexacosane-1,3,25-triol (Awai and Wolk, 2007). DevH, a trans-acting regulatory protein, is required for the formation of the glycolipid layer, either by direct regulation of the expression of the genes or indirectly through other gene products (Ramírez et al., 2005). The *hglK* gene (encoding a pentapeptide repeat-containing protein that bears four transmembrane segments) is required for the localization of the glycolipids, and HglK may be involved in their deposition (Black et al. 1995). However, it is now known that differentiation and maturation of heterocysts are dependent on *devBCA*, which encodes an ABC-type exporter (Fiedler *et al.*, 1998), and HgdD, which encodes an outer membrane TolC-like protein (Moslavac *et al.*, 2007a) that together form an ATP-driven efflux pump for the export of HGLs across the cell wall (Staron *et al.*, 2011). Hence, the role of HglK in this process is unclear.

Profound changes in the nature and distribution of the intracellular membrane system (photosynthetic membranes or thylakoids) occur during heterocyst differentiation. Intracellular membranes are reorganized in the heterocyst to form the so-called honeycomb membrane system (Figure 6), which is localized near the polar regions, close to the heterocyst necks (Lang and Fay, 1971). These honeycomb membranes harbor the enzymes for respiration (Fay, 1992; Wolk, 2000; Wilcox et al., 1973). Also, the FraH protein, which may be involved in intermolecular interactions, has been shown to be needed for the formation of the honeycomb system (Merino-Puerto et al., 2011a).

Among the intracellular structures present in vegetative cells that disintegrate during heterocyst formation are the carboxysomes and glycogen granules. However, the structured granules of cyanophycin (a polymer made of aspartate and arginine that functions as a nitrogen reserve material), which are present in different locations in the vegetative cells, are specifically located at each heterocyst neck (Lang *et al.*, 1972).

1.3.3.2. Heterocyst metabolism

Besides the structural changes, heterocysts also exhibit metabolic differences with regard to vegetative cells. It has been known for some time that heterocysts maintain a highly reducing environment. Strong reducing conditions in the heterocyst, essential for the maintenance of N_2-fixing activity, appear to result partly from the absence of O_2-evolving activity. Additionally, respiratory metabolism in heterocysts fulfills two functions: (i) to provide ATP for the nitrogenase-catalyzed reduction of N_2, and (ii) to protect the enzyme from O_2-inactivation by maintaining an anoxic or micro-oxic microenvironment at the site of enzyme function (Wolk et al., 1994).

In the genome of the heterocyst-forming cyanobacterium *Anabaena*, three gene clusters putatively encoding cytochrome *c* oxidases (*cox*) have been identified and characterized (Valladares et al., 2003). Among these, *cox1* is expressed in vegetative cells irrespective of the nitrogen regime and is involved in vegetative growth or maintenance in this cyanobacterium (Jones and Haselkorn, 2002; Valladares et al., 2003; Stebegg et al., 2012), whereas *cox2* and *cox3* are expressed in developing and mature heterocysts, and at least one of them must be present to support diazotrophic growth (Valladares et al., 2003). Interestingly, *cox2* and *cox3* not only have a role in the protection of nitrogenase, but also play a role in the formation of the honeycomb membranes, since a double *cox2 cox3* mutant lacks this structure (Valladares et al., 2007). Other O_2-removing enzymes, such as specific flavodiiron proteins expressed in the heterocyst have also been characterized (Ermakova et al., 2014).

In developing heterocysts, the oxygenic PSII is inactivated accompanied by degradation of light harvesting phycobilisomes and the dissolution of enzymes associated with photosynthetic CO_2 fixation (Fay, 1992). Degradation of phycobiliproteins, accounting for up to 50 % of the soluble protein in the cyanobacterial cell, may serve as a source of nitrogen during differentiation (Meeks and Elhai, 2002). In contrast, PSI is operative in the heterocyst carrying out non-cyclic

electron transport and photophosphorylation that generate ATP and reductant needed for N_2 fixation (Wolk et al., 1994). On the other hand, due to the lack Rubisco, reduced carbon needed as a source of energy and reductant for N_2 fixation, and as a hydrocarbon backbone for assimilation of the newly fixed N, is mainly received from the neighboring vegetative cells (Wolk, 1968) in the form of sucrose, glutamate and alanine (described in detail below).

1.3.3.3. Regulation of heterocyst differentiation

As mentioned above, the process of heterocyst differentiation takes place under conditions of nitrogen deprivation. Heterocyst differentiation involves regulation of gene expression and establishment of the spatial pattern of heterocysts (Flores and Herrero, 2010). Two transcription factors act early in differentiation promoting gene expression: NtcA and HetR (Figure 7). As described above, NtcA is a global transcriptional regulator found in cyanobacteria that regulates gene expression in response to the cellular C-to-N balance signaled by 2-oxoglutarate (Herrero et al., 2001, 2004; Valladares et al., 2008). HetR plays a key role in heterocyst formation (Buikema and Haselkorn, 1991), being *hetR* one of the earliest genes induced in differentiating cells, 2 h following nitrogen deprivation (Black et al., 1993; Buikema and Haselkorn, 2001). HetR also has DNA-binding activity (Huang et al., 2004), which was thought to require the formation of a HetR homodimer (Kim et al., 2011) but appears to involve tetramers (Valladares et al., 2016). During the initial steps of differentiation, *ntcA* and *hetR* are auto- and mutually regulated and induced in the cells differentiating into heterocysts (Black et al., 1993; Frías et al., 1994; Muro-Pastor et al., 2002), leading to an increase of both proteins to the levels that are required for the establishment of the path to heterocyst differentiation (Black et al., 1993; Olmedo-Verd et al., 2008; Flores and Herrero 2010). NrrA, a response regulator, has been identified as a regulatory link between NtcA and HetR. NtcA upregulates the expression of *nrrA*, and then NrrA upregulates the expression of *hetR* during heterocyst differentiation (Elhira and Ohmori, 2006), although its specific role in heterocyst differentiation has been questioned (Flores and Herrero, 2010). PipX, a protein found only in cyanobacteria, is expressed mainly in an NtcA- and HetR-dependent manner at intermediate to late stages of the differentiation process (Valladares et al., 2011). When heterocyst differentiation has been completed, the expression of many of the genes that have increased expression upon combined nitrogen deprivation return to initial levels. It is interesting to note that other proteins, such as PatA and HetF, could influence the levels of HetR. The inactivation of *patA* leads to heterocyst differentiation mostly at the end of the filament, and *hetF* is required for differentiation and for activation of several HetR-dependent promoters (Herrero et al., 2016).
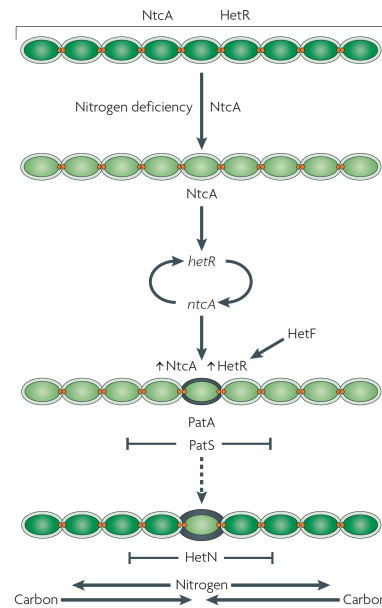
Figure 7. Process of heterocyst differentiation in the filament of a N$_2$-fixing cyanobacterium. Under nitrogen deprivation the two transcription factors, NtcA and HetR, are auto- and mutually regulated and induced in the cells differentiating into heterocysts, leading to an increase of both proteins that act early in differentiation. HetF influences positively the HetR activity. The production of PatS by differentiating heterocysts inhibits the differentiation in neighboring cells, and PatA counteracts the action of inhibitors in the differentiating cell. When the differentiation is finished, HetN contributes to control the maintenance of the pattern of heterocysts. Finally, heterocysts fixing nitrogen and vegetative cells performing oxygenic photosynthesis exchange nitrogen and carbon compounds. Figure from Flores and Herrero (2010).

In cyanobacteria such as those of the genera *Anabaena* and *Nostoc*, heterocysts are found at semiregular intervals along the filament, with 10-15 vegetative cells separating two heterocysts. Several genes are involved in the formation of the spatial pattern of heterocysts. Among these, *patS*, the heterocyst inhibition-signaling peptide gene, is needed to establish the spatial pattern of heterocyst distribution, since its inactivation leads to a Multiple contiguous heterocyst (Mch) phenotype and its overexpression abolishes differentiation. This gene is induced in the cells undergoing differentiation (Yoon and Golden, 1998, 2001), and genes homologous to *patS* are widespread among filamentous cyanobacteria, both heterocyst- and non-heterocyst-forming strains (Zhang et al., 2009). PatS is a peptide of 17 amino acids that is processed in the producing cells to render a morphogen made of a C-terminal peptide which likely contains the ERGSGR sequence (Feldmann et al., 2012; Corrales-Guerrero et al., 2013; Zhang et al., 2017). This morphogen is transferred to neighboring cells inhibiting their differentiation, likely by acting on the transcription factor HetR (Khudyakov and Golden 2004; Risser and Callahan, 2009). A PatS concentration gradient in vegetative cells decreases from source differentiating cells as observed by immunofluorescene with antibodies against the C-terminal pentapeptide of PatS (Corrales-Guerrero et al., 2013).

Another gene involved in pattern formation is *hetN* (Black and Wolk, 1994; Callahan and Buikema, 2001). Expression of *hetN* is activated later than *patS* during differentiation. HetN bears an internal ERGSGR sequence and, as in the case of PatS, mutation of this sequence leads to a Mch phenotype and the overexpression of *hetN* suppresses heterocyst formation. Whereas PatS is involved in the early steps of pattern formation, HetN participates in the maintenance of the pattern of heterocyst distribution once it has been established (reviewed in Flores and Herrero, 2010). The HetN protein is associated with cellular membranes (Li et al., 2002; Higa et al., 2012), and it has been shown specifically localized in the thylakoids at the heterocyst periphery and poles, being the N terminal part of HetN required for localization (Corrales-Guerrero et al., 2014).

1.4. Multicellularity in cyanobacteria

In the presence of a source of combined nitrogen including nitrate or ammonium, heterocyst-forming cyanobacteria such as *Nostoc* sp. and *Anabaena* sp. grow as long filaments containing hundreds of photosynthetic vegetative cells. In the absence of combined nitrogen, heterocysts are produced at semiregular intervals between vegetative cells as described above. Intercellular relations take place between vegetative cells and between vegetative cells and heterocysts, and these relations are at the basis of the multicellular behavior of these organisms. We will address now some key aspects of the intercellular relations that take place in heterocyst-forming cyanobacteria and of the cellular structures that support them.
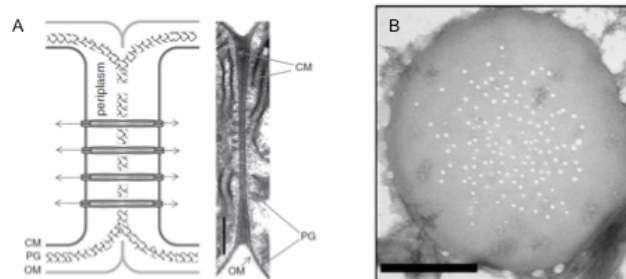
1.4.1. Filament structure

Cyanobacteria bear a Gram-negative type of cell envelope in which the periplasm contains a peptidoglycan (PG) layer that is thicker than in most other well characterized Gram-negative bacteria (Hoiczyk and Hansel, 2000). Regarding the outer membrane (OM), the *Anabaena* genome contains some genes encoding proteins that have been assigned as porins (Nicolaisen et al., 2009a), and four of them (Alr4550, All4499, Alr0834 and Alr3608) could be identified in an OM proteomic analysis (Moslavac et al., 2005). Five of the putative *Anabaena* porins have been described as OprB-like porins (Nicolaisen et al., 2009a). OprB is a well-characterized porin from *Pseudomonas aeruginosa* with specificity for monosaccharides (Wylie and Worobec, 1995), although it can also transport sucrose with low activity (van den Berg, 2012). Two of the *Anabaena* OprB-like porins, All4499 and Alr4550, have been identified as the most abundant proteins in the outer membrane of both vegetative cells and heterocysts (Moslavac et al., 2005, 2007b). Ekman et al. (2013) have inactivated a homologue of OprB in *N. punctiforme* and have shown that it facilitates uptake of fructose and glucose.

     The cytoplasmic membrane proteome of *Anabaena* contains many different proteins involved in the transport of solutes (Hahn and Schleiff, 2014). Among them, as mentioned above, transporters involved in the uptake of nitrate, bicarbonate, urea, ammonium and amino acids have been described. The genome of *Anabaena* contains 249 ORFs that encode predicted ABC transporter components and 19 ORFs that encode predicted MFS proteins (Paulsen, 2016). In addition, in filamentous cyanobacteria, different proteins localized in the septum, likely constituting septal junction complexes, have been shown to have an essential role in the exchange of metabolites and regulators along the filament. These proteins are described below.

     Regarding cell division, filamentous cyanobacteria show distinct characteristics as compared to unicellular bacteria. Instead of terminating cell division with daughter cell separation by amidase-catalyzed PG splitting and invagination of the OM mediated by a Pal-Tol complex (Vollmer et al., 2008; Typas et al., 2012), cell division in filamentous cyanobacteria does not involve PG splitting and OM invagination (Herrero et al., 2016). This results in the presence of a continuous OM and periplasm

along the filament (Flores et al., 2006; Schneider et al., 2007; Mariscal et al., 2007; Wilk et al., 2011), as illustrated in Figure 8A. The individual cells in the filament share the periplasm and are joined by protein complexes located at the intercellular septa. These complexes traverse the septal PG layer(s) and are postulated to form septal junctions (Figure 8A), which will be described in detail below.

Figure 8. Structure of the septa in filamentous heterocyst-forming cyanobacteria. (A) Electron micrograph of a septal region between vegetative cells of *Nostoc puntiforme* (right panel), and scheme of the septal region showing the structures that join the cells and the composition of the envelope (left panel). CM, cytoplasm membrane; PG, peptidoglycan; OM, outer membrane. Image from Lehner et al. (2013). (B) Transmission electron micrograph of purified septal peptidoglycan disks from *Anabaena* showing nanopores. Scale bar, 500 nm. Image from Bornikoel et al. (2017).

1.4.2. Intercellular molecular exchange

A central question in multicellularity is whether the different cells that comprise an organism communicate with each other and, if so, how this communication takes place. Intercellular molecular exchange of nutrients (Wolk et al., 1994) and regulatory factors, such as the C-terminal fragment of PatS discussed above (Yoon and Golden, 1998; Corrales-Guerrero et al., 2013), takes place between the cells of the filament in heterocyst-forming cyanobacteria during heterocyst differentiation and diazotrophic growth. Vegetative cells provide products of CO_2 fixation to the heterocysts (Wolk, 1968), and heterocysts provide N_2 fixation products to the vegetative cells (Wolk et al., 1974). The importance of the C compounds transferred from vegetative cells to heterocysts resides in that they should support the differentiation process –including the provision of building blocks for the heterocyst envelope–, and the metabolism of the mature heterocyst –providing a source of electrons for the N_2 reduction reaction and the C skeleton for the incorporation of the ammonium resulting from N_2 fixation.

1.4.2.1. Physiological substrates

Different physiological substrates are subjected to intercellular molecular exchange. Regarding reduced carbon compounds, based on experiments performed with radiolabeled $^{14}CO_2$, Jüttner (1983) suggested that alanine, glutamate and glucose-6-

phosphate could function as carbon vehicles from vegetative cells to heterocysts. In *Anabaena*, the catabolic enzyme alanine dehydrogenase (Ald) is expressed in the heterocyst, and an *ald* mutant is impaired both in diazotrophic growth and nitrogenase activity (Pernil et al., 2010), which is consistent with the suggested transfer of alanine to the heterocysts (Jüttner, 1983). Concerning glutamate, because heterocysts lack GOGAT but have high levels of GS (Thomas et al., 1977; Martin-Figueroa et al., 2000), glutamate has to be transferred from vegetative cells to heterocysts to provide a substrate for incorporation of ammonia resulting from N_2 fixation to produce glutamine. Finally, a key sugar in carbon metabolism in the cyanobacteria is sucrose, which is also an important vehicle of reduced carbon in plants. Sucrose was first proposed to be transferred from vegetative cells to heterocysts because diazotrophic cultures from some heterocyst-forming cyanobacteria have a high activity of sucrose metabolism enzymes (Schilling and Ehrnsperger, 1985; Wolk et al., 1994). In *Anabaena*, two sucrose-phosphate synthases (encoded by *spsA* and *spsB*) and a sucrose-phosphate phosphatase (*sspA*) are involved in sucrose biosynthesis (Porchia and Salerno, 1996; Cumino et al., 2002), whereas three proteins, sucrose synthase (SusA) and alkaline/neutral invertases InvA and InvB have a role in sucrose degradation (Figure 9) (Schilling and Ehrnsperger, 1985; Curatti et al., 2002). Diazotrophic growth was impaired in a *susA* overexpressing strain, suggesting a role for sucrose in diazotrophic metabolism and the involvement of SusA in the control of carbon flux in the N_2-fixing filament (Curatti et al., 2002). InvA has likely a role in carbon flux in vegetative cells, and InvB is crucial for sucrose catabolism in heterocysts and diazotrophic growth (López-Igual et al., 2010; Vargas et al., 2011). Sucrose is a more important carbon vehicle to heterocysts than alanine because inactivation of *invB* has a stronger negative effect on diazotrophic growth that inactivation of *ald* (López-Igual et al., 2010; Pernil et al., 2010; Vargas et al., 2011).

Concerning vehicles of fixed N, glutamine has been identified as a putatively important amino acid transferred from heterocysts to vegetative cells, as suggested by $^{13}N_2$ radiolabeling experiments (Wolk et al., 1974, 1976b; Thomas et al., 1977). GOGAT activity in vegetative cells converts the glutamine imported from heterocysts into glutamate. As mentioned above, the GS-GOGAT pathway is not operative in the heterocysts, and hence glutamate must be transferred from the adjacent vegetative cells to sustain GS activity (Thomas et al., 1977; Martin-Figueroa et al., 2000). On the other hand, cyanophycin (multi-L-arginyl-poly [L-aspartic acid]) accumulates in heterocysts. Cyanophycin is synthesized by cyanophycin synthetase and degraded by the concerted action of cyanophycinase (that releases β-aspartyl-arginine) and isoaspartyl dipeptidase (that produces aspartate and arginine). Cyanophycin synthetase and cyanophycinase are present at high levels in the heterocysts, whereas isoaspartyl dipeptidase is present at high levels only in vegetative cells (Picossi et al., 2004; Burnat *et al.*, 2014). This makes isolated heterocysts to release substantial amounts of β-aspartyl-arginine, suggesting that β-aspartyl-arginine produced from cyanophycin in the heterocysts is transferred intercellularly to be hydrolyzed, producing aspartate and arginine, in the vegetative cells (Burnat *et al.*, 2014).
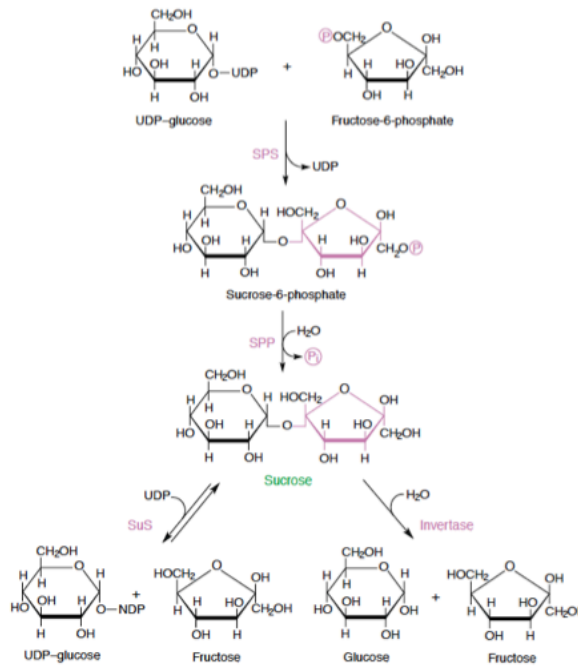
Figure 9. Reactions and enzymes in sucrose metabolism. The principal sucrose-biosynthesis route involves the action of sucrose-phosphate synthase (SPS) and sucrose-phosphate phosphatase (SPP) producing sucrose and inorganic phosphate (P_i). This pathway is irreversible providing an efficient production of sucrose even at low substrate concentrations. Sucrose synthase (SuS, also known as SusA) catalyze a reversible reaction and could be involved in both the synthesis and cleavage of sucrose, being the cleavage of sucrose the main function of this enzyme *in vivo*. However, invertases act hydrolyzing sucrose producing hexoses in an irreversible reaction. From Salerno and Curatti (2003).

1.4.2.2. FRAP analysis

Fluorescence Recovery After Photobleaching (FRAP) analysis, using calcein (622-Da) or 5-carboxyfluorescein (5-CF, 376-Da) as fluorescent markers, has permitted to study the communication between cells in filamentous cyanobacteria and to investigate proteins related to septal junction complexes (Mullineaux et al., 2008; Mariscal et al., 2011; Merino-Puerto et al., 2011b). Calcein acetoxymethyl ester and 5-carboxyfluorescein diacetate acetoxymethyl ester are sufficiently hydrophobic to traverse cell membranes. In the cytoplasm, they are hydrolyzed by cytoplasmic esterases producing highly fluorescent, hydrophilic substances. Calcein and 5-CF thus loaded into de cytoplasm of the cells are stably retained so that FRAP experiments can be performed (Mullineaux et al., 2008; Merino-Puerto et al., 2011b). In these experiments, filaments containing the markers are visualized with a laser-scanning confocal microscope. Fluorescence is excited and detected at specific wavelengths. After capturing a pre-bleach image, the fluorescence of the cell of interest is bleached out by scanning this area with a high laser intensity, and recovery is then recorded in a sequence of full-frame images (Figure 10). The recovery of

fluorescence in the bleached cell is calculated by analysis of the images, and recovery or exchange constants are calculated with specific equations for FRAP analysis (Mullineaux et al., 2008; Merino-Puerto et al., 2011b). Importantly, the fluorescence recovered in the bleached cell corresponds to fluorescence lost from adjacent cells, implying intercellular movement of the marker.
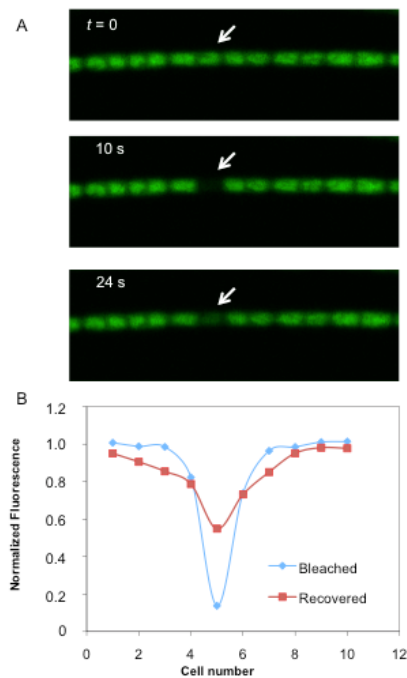
Figure 10. Fluorescence Recovery After Photobleaching (FRAP) analysis in a filament of *Anabaena*. (A) Confocal microscopy images of a filament labeled with 5-carboxyfluorescein (5-CF) at time 0 (before photobleaching) and 10 and 24 s after photobleaching. The arrows point the bleached cell. (B) Normalized fluorescence present in each cell (the bleached cell and the neighboring cells) of the filament after bleaching (blue) and recovery (red).

1.4.3. Structures for intercellular molecular exchange

Two possible pathways have been considered for intercellular molecular exchange in *Anabaena*: the continuous periplasm and a direct intercellular pathway via septal junction complexes.

1.4.3.1. A continuous periplasm

The filament structure of heterocyst-forming cyanobacteria implies the existence of a continuous periplasm which could constitute a communication conduit for the transfer of compounds in the filaments. An engineered green fluorescent protein (GFP) that was exported to the periplasm of the proheterocysts of *Anabaena* was observed also in the periphery of neighboring vegetative cells implying that the GFP moves through the periplasm; in contrast, if the GFP was anchored to the cytoplasmic membrane, it

was not observed in adjacent vegetative cells (Mariscal *et al*., 2007). Nonetheless, barriers for the diffusion of the 27-kDa GFP appear to exist, which could correspond to the PG present in the intercellular septa that may have a size exclusion limit of 25-50 kDa (Mariscal et al., 2007; Zhang et al., 2008, 2013). Transfer of metabolites through the periplasm would therefore be possible and, for intercellular communication, transport into and out of the cytoplasm of the different cell types should take place. As mentioned above, a cyanobacterium such as *Anabaena* contains many specific cytoplasmic membrane transporters that could be involved in intercellular molecular exchange (Picossi et al., 2005; Nicolaisen et al., 2009b; Hahn and Schleiff, 2014). Mutants of some outer membrane components of *Anabaena* exhibit increased permeability for sucrose and glutamate, implying that the outer membrane represents a permeability barrier for these metabolites (Nicolaisen *et al*. 2009b). This feature could avoid the leakage to the external medium of metabolites transferred through the periplasm.

1.4.3.2. Septal junctions

The other possible pathway of intercellular communication is related to the cell-cell joining structures, septal junctions, which traverse the septal peptidoglycan (Figure 8A). These structures were observed by electron microscopy in the septum in the form of thin strands perpendicular to the cytoplasmic membranes and were termed "microplasmodesmata", since they were thought to be reminiscent of the plasmodesmata of plant cells (Lang and Fay, 1971). These strand-like structures were identified as the pits and protrusions seen in electron micrographs of freeze-fracture preparations of cells of *Anabaena cylindrica* (Giddings and Staehelin, 1978). Vegetative cells are connected by 200 to 300 microplasmodesmata, while about 50 are found between heterocysts and vegetative cells. However, microplasmodesmata are now thought to represent structures that could be analogous to the connexons of the gap junctions of metazoans. Hence, these structures are now termed septal junctions (Mariscal 2014; Mullineaux and Nürnberg, 2014; Flores et al., 2016). Nonetheless, BLAST searches of the sequenced cyanobacterial genomes reveal no homologs of the gap junction protein connexin, indicating that the animal and cyanobacterial systems have no evolutionary relationship (Flores et al., 2006). A study using electron tomography after chemical fixation emphasized the proteinaceous nature of the septal junctions and showed that septal junctions between vegetative cells occur in a structured manner in the center of the septum (Wilk et al., 2011). They have been reported to be 12 nm long and 12 nm in diameter in the septa between vegetative cells, and 21 nm long and 14 nm in diameter in the septa between vegetative cells and heterocysts (summarized in Herrero et al., 2016). Therefore, septal junctions may form channels that allow small molecules to move from cytoplasm to cytoplasm. These "channels" have also been shown in the septa between vegetative cells and heterocysts by cryo-electron tomography (Omairi-Nasser et al., 2014). Nanopores (Figure 8B) are the cell wall perforations reported to be present in septal peptidoglycan disks (Lehner et al., 2013; Nürnberg et al., 2015), which may be the sites that accommodate septal junction complexes linking the

cytoplasms of adjacent cells (Mariscal et al., 2011; Wilk et al., 2011). Formation of the nanopores in the septa requires N-acetylmuramyl-L-alanine amidases, enzymes that hydrolyze the septal PG (Lehner et al., 2013). There are five subgroups of these enzymes in *E. coli*: periplasmic AmiA, AmiB, AmiC, AmiD, and cytoplasmic AmpD. AmiA, AmiB and AmiC are important for septation and cell separation, since the triple mutant *amiABC* results in a filamentous *E. coli* strain (Heidrich et al., 2002).

As in other heterocyst-forming cyanobacteria, the *amiC2* gene of *Anabaena* is located downstream of a very similar gene, *amiC1*. Büttner et al. (2016) have described the structural features of AmiC2, which shows a mechanism of action and regulation distinct from other amidases. Whereas inactivation of *amiC1* in *Nostoc punctifo*rme was not achieved (Lehner et al., 2011), the genes homologous to *amiC1* and *amiC2* have been functionally characterized in *Anabaena* (Zhu et al., 2001; Berendt et al., 2012; Bornikoel et al., 2017). The two amidases have related functions in *Anabaena* and one of the two enzymes, *amiC1* or *amiC2* (*hcwA* in Zhu et al., 2001), is required for remodeling of the septal peptidoglycan, which is essential for intercellular molecular exchange and necessary for the development of a heterocyst-containing filament. In addition, since inactivation of *amiC1* delocalizes SepJ and counteracts the fragmentation phenotypes of *sepJ* and *fraC-fraD* mutants (see below), a functional relation between AmiC1 and SepJ on one hand, and of AmiC1 and FraCD on the other, is evident (Bornikoel et al., 2017). SepJ and FraCD might determine where nanopores will be built and direct AmiC proteins to digest the nanopores at specific sites, in order for septal junctions to occupy available nanopores. Zheng et al. (2016) have characterized an additional amidase in *Anabaena*, AmiC3, which is required for the expandability of the septal wall, allowing proper channel formation, intercellular molecular exchange and the differentiation of heterocysts. Finally, *sjcF1* encodes a protein involved in structuring the peptidoglycan layer (Rudolf et al., 2015). Whereas AmiC appears to be involved in the formation of perforations in the septal PG, SjcF1 influences their dimension and may bridge the septal junction complexes with the PG layer in multicellular cyanobacteria.
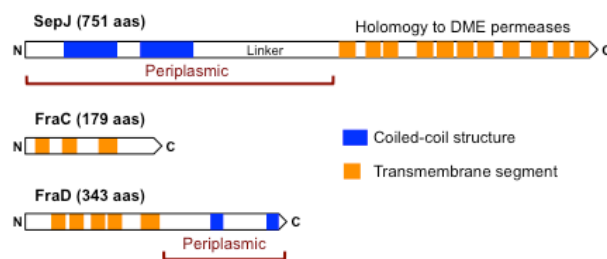
1.4.4. Septal proteins

Proteins that are putative components of the septal junctions were identified as the products of genes whose mutation results in a filament fragmentation phenotype. Inactivation of *sepJ* results in filament fragmentation in the absence as well as in the presence of combined nitrogen, although fragmentation is stronger in the former case (Flores et al., 2007; Nayar et al, 2007). Inactivation of each gene in the *fraC-fraD-fraE* operon results in filament fragmentation mainly under nitrogen deprivation (Bauer et al., 1995; Merino-Puerto et al., 2010). Using GFP fusions, it has been shown that SepJ, FraC and FraD are located at the cell poles in the intercellular septa (Flores et al., 2007; Merino-Puerto et al., 2010). Such location has been confirmed by immunogold-electron microscopy for FraD (Merino-Puerto et al., 2011b) and SepJ (Omairi-Nasser et al., 2015).

1.4.4.1. SepJ

SepJ has three well-defined domains (Figure 11): (i) an N-terminal coiled-coil domain; (ii) a central linker rich in proline and serine which shows sequence similarity to plant extensins and to the human titin protein, an elastic protein also known as connectin; and (iii) a C-terminal protein membrane domain that shows homology to permeases of the drug/metabolite exporter (DME) family (Flores et al., 2007). Topology predictions and a GFP fusion to the C-terminus of the protein indicate that SepJ bears a large extra-cytoplasmic domain (coiled-coil and linker domains), which could be involved in bridging the gap between adjacent cells in the filament, and that the C-terminus of the protein is cytoplasmic (Flores et al., 2007; Mariscal and Flores, 2010). Whereas the cytoplasmic location of the C-terminus of SepJ has been confirmed by Bacterial Adenylate Cyclase Two-Hybrid (BACTH) analysis (Ramos-León et al., 2015), the periplasmic location of the N-terminal section of the protein has been questioned (Omairi-Naser et al., 2015). Nonetheless, binding of the protein to peptidoglycan (Ramos-León et al., 2017) and its interactions with periplasmic proteins (discussed in Flores et al., 2016) are consistent with a periplasmic location of the section of SepJ containing the coiled-coil and linker domains.

GFP fusion to SepJ shows that it is localized not only to the cell poles in the intercellular septa but also to a position similar to a Z ring, in the middle of the cells where cell division starts (Flores et al., 2007). SepJ self-interaction and a specific interaction with cell-division protein FtsQ, confirmed by co-purification and involving parts of the SepJ and FtsQ periplasmic sections, has been shown by BACTH analysis (Ramos-León et al., 2015). Thus, SepJ can form multimers, and in *Anabaena*, the divisome has a role beyond cell division, localizing at the septa a protein essential for multicellularity. Formation of SepJ multimers has been recently confirmed by Blue-Native electrophoresis analysis (Ramos-León et al., 2017).

Figure 11. Schematic of septal proteins SepJ, FraC and FraD. SepJ is composed of three well-differentiated structures: an N-terminal region with two long coiled-coil domains, a central linker domain and a C-terminal permease domain. The binding of SepJ to peptidoglycan and its interactions with periplasmic proteins are consistent with a periplasmic location of the SepJ coiled-coil and linker domains. FraC has a predicted periplasmic N-terminus, three transmembrane segments and a predicted cytoplasmic C-terminus. FraD has a predicted cytoplasmic N-terminus, five transmembrane segments and a predicted long periplasmic C-terminal section that bears two short coiled-coil domains.

Using FRAP analysis, it has been shown that mutants lacking SepJ are severely impaired in calcein transfer, both after growth in the presence of nitrate and after incubation in the absence of combined nitrogen (Mullineaux et al., 2008). Intercellular transfer of 5-CF is also affected in *sepJ* deletion mutants grown with nitrate, but clearly to a lesser extent than calcein transfer (Mariscal et al., 2011). Inactivation of *sepJ* also decreases the number of nanopores to about 15 % of the wild-type value (Nürnberg et al., 2015). These results showed that SepJ is needed for formation of fully active septal junctions, but that SepJ-independent intercellular molecular exchange is still possible.

1.4.4.2. Fra proteins

FraC, FraD and FraE are the products of an operon that shows low expression both in the presence and absence of combined nitrogen (Merino-Puerto et al., 2010). The *fraC* operon is conserved in the heterocyst-forming cyanobacteria whose genomic sequence is available, as well as in many filamentous non-heterocyst formers. Single mutants of these genes do not grow diazotrophically but, in contrast to *sepJ* mutants, form heterocysts (Merino-Puerto et al., 2010). The three proteins are integral membrane proteins (see schemes of FraC and FraD in Figure 11). Whereas FraC and FraD have no homologues outside of the cyanobacteria, FraE is homologous to permeases of type II ABC transporters. Mutants with double inactivation of *fraC* and *fraD* show the same phenotype as that of the single mutants (Merino-Puerto et al., 2011b). This observation together with gene clustering suggest that these proteins can participate in the same process or contribute to the same structure relevant for filamentation in *Anabaena*.

Single *fraC* and *fraD* mutants and the double mutant are impaired in the intercellular transfer of calcein and 5-CF (Merino-Puerto et al., 2010; 2011b). The double mutant has been shown to form about 10 % of the nanopores formed by the wild type (Nürnberg et al., 2015). It has been considered that the impairment of calcein transfer in the *fra* mutants could be an indirect effect, since *fraC* and *fraD* mutants show an alteration of the SepJ localization and SepJ is required for calcein transfer. Therefore, FraC and FraD could together be involved in a separate pathway for the transfer of 5-CF independently of SepJ (Merino-Puerto et al., 2011b).

A triple *sepJ fraC fraD* mutant shows an altered septum structure with thinner septa but a denser peptidoglycan layer (Nürnberg et al., 2015). The number of nanopores is about 7 % that in the wild type. In conclusion, SepJ, FraC and FraD are important for the formation of functional septal junctions in *Anabaena*.

1.5. Objectives of this study

The main goals of this study were to contribute to the knowledge of the mechanism of intercellular molecular exchange in the filament of heterocyst-forming cyanobacteria and to characterize transporters that mediate the incorporation into the cyanobacterial cells of sucrose, an important vehicle of reduced carbon in cyanobacteria and plants. These general goals were addressed through the following objectives:

1. To study by FRAP analysis the mechanism for intercellular molecular exchange through cyanobacterial septal junctions.
2. To study, using the fluorescent sucrose analog esculin, some *Anabaena* genes that are predicted to encode sugar transporters.
3. The study of the possible role of the identified components of ABC glucoside transporters in a response of *Anabaena* to sugars.
4. To study the relationship between some glucoside transporters and the septal junctions that join the cells in the *Anabaena* filament.

These studies have been performed with the heterocyst-forming cyanobacterium *Anabaena* sp. strain PCC 7120, which is a model organism to study N_2 fixation, cellular differentiation and multicellularity in cyanobacteria.

Experimental Preamble

Esculin uptake

Intercellular molecular exchange in filamentous cyanobacteria has previously been studied using the fluorescent markers calcein and 5-carboxyfluorescein (5-CF), which do not resemble any natural substance (see Introduction, 1.4.2.2). To investigate intercellular molecular transfer with a compound more similar to a physiological substrate, we centered our attention on esculin that is an analog of sucrose. Esculin (6,7-dihydroxycoumarin 6-β-D-glucoside; Figure 1) is a fluorescent compound that has been used to study plant sucrose uptake transporters (Reinders et al., 2012; Sivitz et al., 2007). Indeed, it has been shown to be taken up by transgenic *Saccharomyces cerevisiae* cells expressing plant sucrose transporters (Gora et al., 2012).
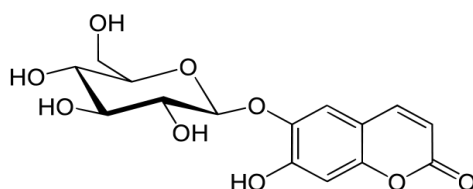

Figure 1. Chemical structure of esculin.

Table 1 shows a comparison of the molecular properties of sucrose, esculin, calcein and 5-CF. These properties make it evident that esculin is a more appropriate probe than calcein or 5-CF to study physiological activities related to sucrose.

Parameter	sucrose	esculin	calcein	5-CF
Molecular mass (Da)	342.3	340.3	622.5	376.3
Polar surface area (Å^2)	189.5	145.9	231.7	113.3
Solvent-accessible molecular surface area (Å^2)	456.5	414.6	794.8	448.4
Van der Waals volume (Å^3)	289	278.0	510.4	299.1
Minimal projection area (Å^2)	57.1	45.8	67.0	59.2
Length perpendicular to minimal projection area (Å)	11.5	14.8	19.7	13.1
Maximal projection area (Å^2)	78.0	90.1	139.1	91.0
Length perpendicular to maximal projection area (Å)	9.2	7.0	10.4	9.7
Charge (s) of different species at pH 7.0 (% abundance [s])	0 (100)	0 (93), -1 (7)	-3 (48), -2 (25), -4 (25), -5 (2)	-1 (98), -2 (2)

Table 1. Predicted physico-chemical properties of sucrose, esculin and the hydrolyzed intracellular forms of calcein and 5-CF used to probe intercellular communication in *Anabaena* (taken from Nürnberg et al., 2015).

Regarding spectroscopic properties of esculin, we tested the fluorescence excitation and emission spectra of a solution of esculin at 0.1 µM in 10 mM HEPES-NaOH (pH 7.2) using a Varian Cary Eclipse Fluorescence Spectrophotometer. The

excitation peak was found at 357 nm and the emission peak at 458 nm (Figure 2). Fluorescence intensity was directly proportional to concentration between at least 0.01 and 0.4 µM esculin.
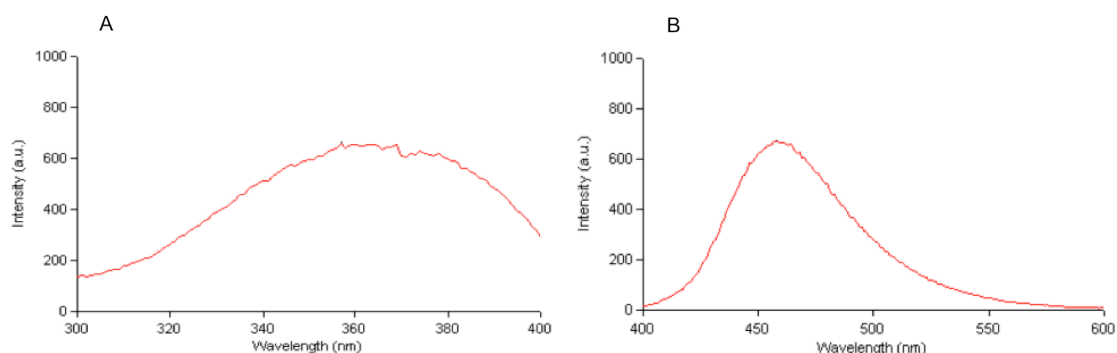
Figure 2. Excitation and emission spectra of esculin (at 0.1 µM) in 10 mM HEPES-NaOH (pH 7.2). (A) Excitation spectrum showing a wide peak with a maximum at 357 nm (emission recorded at 462 ± 10 nm). (B) Emission spectrum with a peak at 458 nm (excitation at 360 ± 10 nm).

When filaments of *Anabaena* sp. strain PCC 7120 (hereafter *Anabaena*) were incubated with esculin for periods of less than one hour, the cells showed efficient esculin fluorescence (Figure 3).
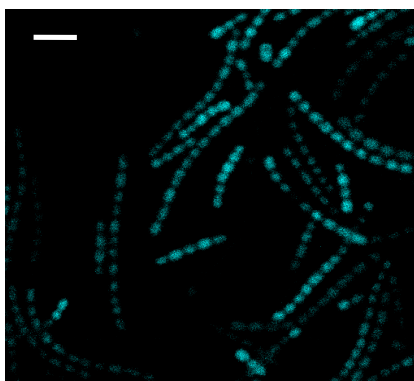
Figure 3. Confocal microscopy image of *Anabaena* cells incubated with esculin. BG11-grown filaments were incubated for 30 min with 100 µM esculin in BG11 medium, washed with the same medium and spotted on BG11 medium plates. Filaments visualized with a confocal microscope are shown. Excitation, 355 nm; fluorescence detection, 443 to 490 nm. Size bar, 10 µm.

Anabaena expresses sucrose transport activity (Nicolaisen et al., 2009b). To study the incorporation of esculin into the cells of *Anabaena*, we developed a fluorometric assay for esculin uptake. For this assay, filaments of *Anabaena* were grown in BG11 medium (containing nitrate as the nitrogen source) or incubated in

$BG11_0$ medium (lacking any source of combined nitrogen) to study the uptake in the two conditions. *Anabaena* filaments grown in BG11 medium were harvested by centrifugation, washed three times with BG11 or $BG11_0$ medium and incubated for 18 h in the same medium under culture conditions. Filaments were then harvested, washed and resuspended in the corresponding growth medium supplemented with 10 mM HEPES-NaOH buffer (pH 7). Assays of esculin uptake were started by addition of esculin hydrate (Sigma-Aldrich) at 100 µM (final concentration), and suspensions were incubated at 30 ºC in the light ($\sim$170 µmol photons m^{-2} s^{-1}) for up to 70 min. One-ml samples were withdrawn and filtered at different times. Cells on the filters were washed with 10 mM HEPES-NaOH buffer (pH 7) and resuspended in 2 ml of the same buffer. Fluorescence of the resulting cell suspension was measured in a Varian Cary Eclipse Fluorescence Spectrophotometer with excitation at 360 ± 10 nm and emission at 462 ± 10 nm. Fluorescent data were standardized by subtracting fluorescence at time zero, determined from the straight line obtained representing fluorescence versus time of incubation. Esculin was taken up linearly for at least 70 min, and it was higher in $BG11_0$ medium than in BG11 medium (Figure 4). This demonstrated to be a reliable assay that could be used to determine the esculin uptake activity of *Anabaena* under different conditions and in different *Anabaena* mutants, as will be illustrated in Chapters 1, 2 and 3 of this work.
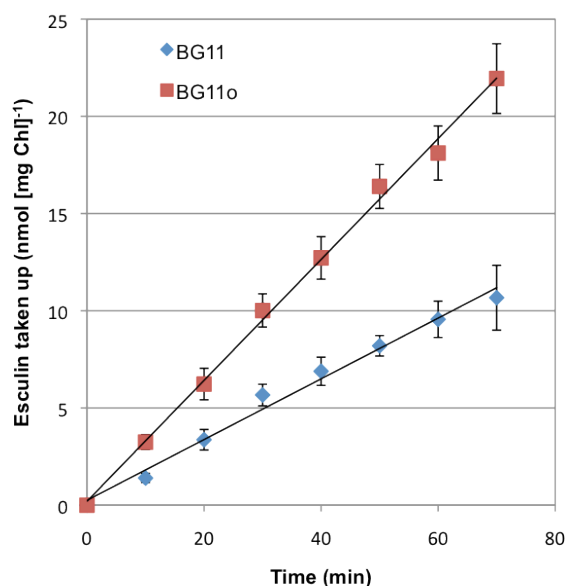
Figure 4. Time course of esculin uptake in *Anabaena* cells. Cells were grown in BG11 medium and incubated for 18 h in BG11 or $BG11_0$ medium. Uptake of esculin (100 µM) was measured as described in the text. Error bars represent SEM (n = 21 and 16 for BG11 and $BG11_0$ medium, respectively). Rates of uptake differed significantly between BG11 and $BG11_0$ (Student's *t* test, *p* = 0.0002).

Because esculin fluorescence is pH sensitive (Nürnberg et al., 2015), a note of clarification regarding pH is necessary. In uptake assays performed at different pH values, the washing of the filaments in the filter was done at the same pH of the assay

to avoid changing the uptake conditions. However, because the cytoplasmic pH of cyanobacterial cells grown in BG11 medium is about 7 (Blanco-Rivero et al., 2005), to diminish possible effects on esculin determination, all esculin determinations were made in filaments finally re-suspended in a buffer at pH 7 (see Figure 2 in Chapter 2).

The method of esculin uptake described here was included in the following article published in the journal mBio:

RESEARCH ARTICLE

CrossMark
← click for updates

Intercellular Diffusion of a Fluorescent Sucrose Analog via the Septal Junctions in a Filamentous Cyanobacterium

Dennis J. Nürnberg,[a] Vicente Mariscal,[b] Jan Bornikoel,[c] Mercedes Nieves-Morión,[b] Norbert Krauß,[a] Antonia Herrero,[b] Iris Maldener,[c] Enrique Flores,[b] Conrad W. Mullineaux[a]

School of Biological and Chemical Sciences, Queen Mary University of London, London, United Kingdom[a]; Instituto de Bioquímica Vegetal y Fotosíntesis, Consejo Superior de Investigaciones Científicas and Universidad de Sevilla, Seville, Spain[b]; Department of Microbiology/Organismic Interactions, University of Tübingen, Tübingen, Germany[c]

D.J.N. and V.M. contributed equally to this work.

Chapter 1: Molecular diffusion through cyanobacterial sepal junctions

Molecular Diffusion through Cyanobacterial Septal Junctions

Mercedes Nieves-Morión,[a] Conrad W. Mullineaux,[b] Enrique Flores[a]

Instituto de Bioquímica Vegetal y Fotosíntesis, Consejo Superior de Investigaciones Científicas and Universidad de Sevilla, Seville, Spain[a]; School of Biological and Chemical Sciences, Queen Mary University of London, London, United Kingdom[b]

ABSTRACT Heterocyst-forming cyanobacteria grow as filaments in which intercellular molecular exchange takes place. During the differentiation of N_2-fixing heterocysts, regulators are transferred between cells. In the diazotrophic filament, vegetative cells that fix CO_2 through oxygenic photosynthesis provide the heterocysts with reduced carbon and heterocysts provide the vegetative cells with fixed nitrogen. Intercellular molecular transfer has been traced with fluorescent markers, including calcein, 5-carboxyfluorescein, and the sucrose analogue esculin, which are observed to move down their concentration gradient. In this work, we used fluorescence recovery after photobleaching (FRAP) assays in the model heterocyst-forming cyanobacterium *Anabaena* sp. strain PCC 7120 to measure the temperature dependence of intercellular transfer of fluorescent markers. We find that the transfer rate constants are directly proportional to the absolute temperature. This indicates that the "septal junctions" (formerly known as "microplasmodesmata") linking the cells in the filament allow molecular exchange by simple diffusion, without any activated intermediate state. This constitutes a novel mechanism for molecular transfer across the bacterial cytoplasmic membrane, in addition to previously characterized mechanisms for active transport and facilitated diffusion. Cyanobacterial septal junctions are functionally analogous to the gap junctions of metazoans.

IMPORTANCE Although bacteria are frequently considered just as unicellular organisms, there are bacteria that behave as true multicellular organisms. The heterocyst-forming cyanobacteria grow as filaments in which cells communicate. Intercellular molecular exchange is thought to be mediated by septal junctions. Here, we show that intercellular transfer of fluorescent markers in the cyanobacterial filament has the physical properties of simple diffusion. Thus, cyanobacterial septal junctions are functionally analogous to metazoan gap junctions, although their molecular components appear unrelated. Like metazoan gap junctions, the septal junctions of cyanobacteria allow the rapid intercellular exchange of small molecules, without stringent selectivity. Our finding expands the repertoire of mechanisms for molecular transfer across the plasma membrane in prokaryotes.

Address correspondence to Conrad W. Mullineaux, c.mullineaux@qmul.ac.uk, or Enrique Flores, eflores@ibvf.csic.es.

Heterocyst-forming cyanobacteria grow as chains of cells—filaments—that can be hundreds of cells long, and the cells in the filament communicate with each other. Under deprivation of combined nitrogen, two cell types are found in the filament: vegetative cells that fix CO_2 through oxygenic photosynthesis and heterocysts that fix N_2 (1, 2). The process of heterocyst differentiation from vegetative cells involves intercellular molecular exchange, since differentiating heterocysts inhibit the differentiation of nearby cells (3), and this phenomenon involves the intercellular transfer of a regulator, such as the PatS morphogen (4, 5). In the diazotrophic cyanobacterial filament, heterocysts represent a low percentage of cells (about 5 to 10% in the model heterocyst-forming cyanobacterium *Anabaena* sp. strain PCC 7120 [hereinafter *Anabaena*]). For the filament to grow diazotrophically, an intercellular exchange of

Nieves-Morión et al.

nutrients is necessary. The vegetative cells provide the heterocysts with photosynthate, mainly in the form of sucrose (see reference 6 and references therein), and the heterocysts provide the vegetative cells with fixed nitrogen, mainly in the form of glutamine and β-aspartyl-arginine dipeptide (see reference 7 and references therein). Because one heterocyst feeds about 5 to 10 vegetative cells with nitrogen, intercellular molecular exchange must also occur between vegetative cells. Indeed, as evidenced by the use of fluorescent markers, including calcein (8), 5-carboxyfluorescein (5-CF) (9), and the sucrose analogue esculin (6), intercellular molecular exchange takes place between the vegetative cells not only of diazotrophic filaments but also of filaments grown in the presence of combined nitrogen.

Intercellular molecular transfer appears to take place through conduits joining adjacent cells in the filament. Structures previously known as "microplasmodesmata" and now as "septal junctions" (10–12) may provide such conduits (8, 9). Proteins that are likely components of septal junctions have been identified. SepJ (13; also known as FraG [14]), FraC, and FraD (9, 15, 16) are integral membrane proteins located at the cell poles in the intercellular septa (13, 16). The integral membrane section of SepJ is homologous to permeases of the drug and metabolite exporter (DME) family (13). SepJ and FraD also have long extramembrane domains that, as discussed previously (12), may reside in the periplasmic area of the intercellular septa. These proteins are necessary for the formation of septal peptidoglycan nanopores (6), through which septal junctions appear to traverse the septal peptidoglycan (17). Structures observed by electron tomography of *Anabaena* that have been termed "channels" (18, 19) likely correspond to the nanopores.

Fluorescence recovery after photobleaching (FRAP) experiments with several fluorescent markers demonstrate the movement of molecules from cytoplasm to cytoplasm (6, 8, 9, 16). Net movement always occurs down the concentration gradient, and the kinetics appear to be independent of direction. For example, the rate constant for movement of the sucrose analog esculin from vegetative cells to heterocysts is similar to the rate constant for the reverse movement from heterocysts to vegetative cells (6). The fact that a range of dyes can be exchanged on rapid timescales, including fluorescein derivatives with no resemblance to any known *Anabaena* metabolite, suggests that the mechanism has low selectivity. Nonetheless, the participation of proteins (with homology to permeases in the case of SepJ) in the process of intercellular transfer led us to inquire further into its physical nature. Temperature dependence provides a way to distinguish simple diffusion from carrier-mediated facilitated diffusion. In a facilitated diffusion mechanism, the substrate interacts strongly with the membrane transporter protein, forming a bound intermediate state. Such a mechanism confers specificity but also introduces an activation energy barrier. This makes the transport strongly temperature dependent, with a Q_{10} (the factor by which the rate increases with a 10°C increase in temperature) typically of at least 2 (20, 21). In contrast, the rate of simple diffusion will be proportional to the absolute temperature, giving a Q_{10} of about 1.035 in the physiological temperature range. Here, we report the observation that intercellular transfer of the fluorescent markers in *Anabaena* exhibits a dependence on temperature that denotes a process of simple diffusion.

Temperature dependence. Intercellular molecular transfer was investigated with the fluorescent markers calcein, 5-CF, and esculin. Calcein and 5-CF are loaded into the cells as hydrophobic acetoxymethyl esters, which are hydrolyzed by cytoplasmic esterases, producing hydrophilic, fluorescent compounds that are stably retained within the cells (8, 9). Esculin is taken up into the *Anabaena* cells by permeases that build up an intercellular pool appropriate for analysis (6). FRAP assays were carried out at different temperatures, from 10 to 37°C, in *Anabaena* filaments that had been grown at 30°C. The constant, R, of the rate of fluorescence recovery in the bleached cells was calculated (9). Figure 1 (red squares) shows the results of the FRAP analysis with the three markers. We found Q_{10} values of 1.078, 1.045, and 1.015 for calcein, 5-CF, and esculin, respectively. For comparison, the expected values calculated assuming a
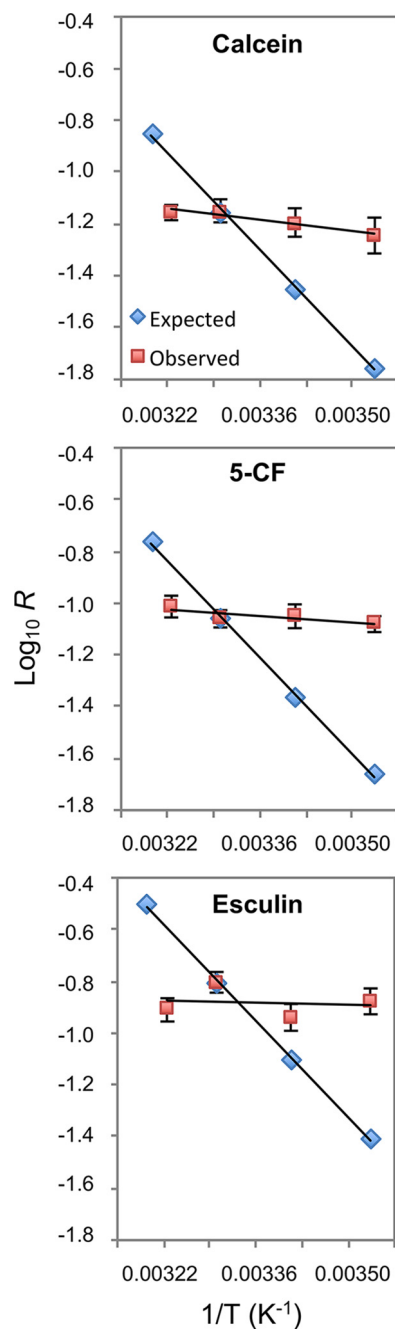
FIG 1 Effect of temperature on the intercellular transfer of calcein, 5-CF, and esculin in *Anabaena* (Arrhenius plots). BG11-grown filaments were used in FRAP assays as described in "Methods." The assay temperature was set at 10, 20, 30, or 37°C. Observed, experimental data (mean and standard deviation of 26 to 43 filaments subjected to FRAP analysis for each marker and temperature, except that 43 to 126 filaments were tested at 30°C); Expected, values calculated assuming a Q_{10} of 2, taking as reference the experimental value at 30°C. FRAP data are presented as the recovery rate constant, R (s^{-1}).

Q_{10} of 2 (taking as reference the experimental value at 30°C) are also shown for the three markers (Fig. 1, blue rhombi). The observed Q_{10} values are fully consistent with a mechanism of simple diffusion but not with active transport or carrier-mediated facilitated diffusion.

Concluding remarks. Cells in the filaments of heterocyst-forming cyanobacteria are joined by septal junctions that functionally resemble metazoan gap junctions (10–12, 17). The observation that intercellular molecular transfer in *Anabaena* is proportional to

Nieves-Morión et al.

mBio®

the absolute temperature, presented here, strongly supports that septal junctions allow simple diffusion of small molecules, as gap junctions do (22, 23). The proteins that are putative components of septal junctions bear no homology, however, with connexins, which are the constituents of the connections that form the gap junctions (24). In gap junctions, the plasma membranes of the two cells are in close proximity. It should be noted that linking two cells in a cyanobacterial filament requires a larger and more complex structure, since the intercellular channel must span the periplasm and the intervening peptidoglycan layer. A major task for future research is to explore whether septal junctions can, like gap junctions (22, 23), be regulated by gating.

Methods. *Anabaena* sp. strain PCC 7120 was grown in BG11 medium modified to contain ferric citrate instead of ferric ammonium citrate (25) at 30°C in the light (ca. 25 to 30 μmol photons m^{-2} s^{-1}) in shaken (100 rpm) liquid cultures. For esculin transfer assays, filaments from 1 ml of culture were harvested, resuspended in 500 μl of fresh growth medium, mixed with 15 μl of saturated (~5 mM) aqueous esculin hydrate solution (Sigma-Aldrich), and incubated for 1 h in the dark with gentle shaking at 30°C prior to washing 3× in growth medium, followed by dark incubation for 15 min in 1 ml medium at 30°C with gentle shaking. Cells were then washed, concentrated about 20×, and spotted onto BG11 medium solidified with 1% (wt/vol) Difco Bacto agar. Small blocks of agar with cells adsorbed on the surface were placed in custom-built, temperature-controlled sample holders under glass coverslips and at the different assay temperatures. Cells were visualized with a laser-scanning confocal microscope (Leica TCS SP5) using a 63× oil immersion objective (1.4 numerical aperture [NA]). Fluorescence was excited at 355 nm, with detection of esculin at 443 to 490 nm. High-resolution imaging used a 6× line average with an optical section of ~0.7 μm. FRAP measurements were performed without line averaging and with a wide pinhole that gave an optical section of ~4 μm. After capturing a prebleach image, the fluorescence of a defined region of interest was bleached out by scanning this region at ~6-times-higher laser intensity, and the recovery was then recorded in a sequence of full-frame images.

For calcein and 5-CF transfer assays, calcein and 5-CF staining and FRAP analysis were performed as previously reported (8, 9). Cell suspensions were spotted onto agar and placed in a custom-built, temperature-controlled sample holder as described above, and measurements were carried out at the temperatures indicated in the legend to Fig. 1. For both calcein and 5-CF, cells were imaged with a Leica HCX Plan-Apo 63×, 1.4 NA oil immersion objective attached to a Leica TCS SP5 confocal laser-scanning microscope with a 488-nm line argon laser as the excitation source. Fluorescence emission was monitored by collection across windows of 500 to 525 nm with a 150-μm pinhole. After an initial image was recorded, bleaching was carried out by an automated FRAP routine which switched the microscope to X-scanning mode, increased the laser intensity by a factor of 10, and scanned a line across 1 cell for 0.137 s before reducing the laser intensity, switching back to XY-imaging mode and recording a sequence of images typically at 1-s intervals.

For FRAP data analysis, the kinetics of fluorescent marker transfer between vegetative cells located in the middle of filaments (hence, with 2 cell junctions) was quantified by measuring the recovery rate constant R from the formula $C_B = C_0 + C_R (1 - e^{-2Rt})$, where C_B is fluorescence in the bleached cell, C_0 is fluorescence immediately after the bleach and tending towards ($C_0 + C_R$) after fluorescence recovery, t is time, and R is the recovery rate constant due to transfer of the marker from one neighbor cell (9).

REFERENCES

1. Flores E, Herrero A. 2010. Compartmentalized function through cell differentiation in filamentous cyanobacteria. Nat Rev Microbiol 8:39–50. https://doi.org/10.1038/nrmicro2242.
2. Kumar K, Mella-Herrera RA, Golden JW. 2010. Cyanobacterial heterocysts. Cold Spring Harb Perspect Biol 2:a000315. https://doi.org/10.1101/cshperspect.a000315.
3. Wolk CP. 1996. Heterocyst formation. Annu Rev Genet 30:59–78. https://doi.org/10.1146/annurev.genet.30.1.59.
4. Yoon HS, Golden JW. 1998. Heterocyst pattern formation controlled by a diffusible peptide. Science 282:935–938. https://doi.org/10.1126/science.282.5390.935.
5. Corrales-Guerrero L, Mariscal V, Flores E, Herrero A. 2013. Functional dissection and evidence for intercellular transfer of the heterocyst-differentiation PatS morphogen. Mol Microbiol 88:1093–1105. https://doi.org/10.1111/mmi.12244.
6. Nürnberg DJ, Mariscal V, Bornikoel J, Nieves-Morión M, Krauß N, Herrero A, Maldener I, Flores E, Mullineaux CW. 2015. Intercellular diffusion of a fluorescent sucrose analog via the septal junctions in a filamentous cyanobacterium. mBio 6:e02109-14. https://doi.org/10.1128/mBio.02109-14.
7. Burnat M, Herrero A, Flores E. 2014. Compartmentalized cyanophycin metabolism in the diazotrophic filaments of a heterocyst-forming cyanobacterium. Proc Natl Acad Sci U S A 111:3823–3828. https://doi.org/10.1073/pnas.1318564111.
8. Mullineaux CW, Mariscal V, Nenninger A, Khanum H, Herrero A, Flores E, Adams DG. 2008. Mechanism of intercellular molecular exchange in heterocyst-forming cyanobacteria. EMBO J 27:1299–1308. https://doi.org/10.1038/emboj.2008.66.
9. Merino-Puerto V, Schwarz H, Maldener I, Mariscal V, Mullineaux CW, Herrero A, Flores E. 2011. FraC/FraD-dependent intercellular molecular exchange in the filaments of a heterocyst-forming cyanobacterium, *Anabaena* sp. Mol Microbiol 82:87–98. https://doi.org/10.1111/j.1365-2958.2011.07797.x.
10. Mariscal V. 2014. Cell-cell joining proteins in heterocyst-forming cyanobacteria, p 293–304. *In* Flores E, Herrero A (ed), The cell biology of Cyanobacteria. Caister Academic Press, Norfolk, United Kingdom.
11. Mullineaux CW, Nürnberg DJ. 2014. Tracing the path of a prokaryotic paracrine signal. Mol Microbiol 94:1208–1212. https://doi.org/10.1111/mmi.12851.
12. Flores E, Herrero A, Forchhammer K, Maldener I. 2016. Septal junctions in filamentous heterocyst-forming cyanobacteria. Trends Microbiol 24:79–82. https://doi.org/10.1016/j.tim.2015.11.011.
13. Flores E, Pernil R, Muro-Pastor AM, Mariscal V, Maldener I, Lechno-Yossef S, Fan Q, Wolk CP, Herrero A. 2007. Septum-localized protein required for filament integrity and diazotrophy in the heterocyst-forming cyanobacterium *Anabaena* sp. strain PCC 7120. J Bacteriol 189:3884–3890. https://doi.org/10.1128/JB.00085-07.
14. Nayar AS, Yamaura H, Rajagopalan R, Risser DD, Callahan SM. 2007. FraG is necessary for filament integrity and heterocyst maturation in the cyanobacterium *Anabaena* sp. strain PCC 7120. Microbiology 153:601–607. https://doi.org/10.1099/mic.0.2006/002535-0.
15. Bauer CC, Buikema WJ, Black K, Haselkorn R. 1995. A short-filament mutant of *Anabaena* sp. strain PCC 7120 that fragments in nitrogen-deficient medium. J Bacteriol 177:1520–1526. https://doi.org/10.1128/jb.177.6.1520-1526.1995.
16. Merino-Puerto V, Mariscal V, Mullineaux CW, Herrero A, Flores E. 2010. Fra proteins influencing filament integrity, diazotrophy and localization of septal protein SepJ in the heterocyst-forming cyanobacterium *Anabaena* sp. Mol Microbiol 75:1159–1170. https://doi.org/10.1111/j.1365-2958.2009.07031.x.
17. Lehner J, Berendt S, Dörsam B, Pérez R, Forchhammer K, Maldener I. 2013. Prokaryotic multicellularity: a nanopore array for bacterial cell communication. FASEB J 27:2293–2300. https://doi.org/10.1096/fj.12-225854.
18. Omairi-Nasser A, Haselkorn R, Austin J II. 2014. Visualization of channels connecting cells in filamentous nitrogen-fixing cyanobacteria. FASEB J 28:3016–3022. https://doi.org/10.1096/fj.14-252007.
19. Omairi-Nasser A, Mariscal V, Austin JR, II, Haselkorn R. 2015. Requirement of Fra proteins for communication channels between cells in the filamentous nitrogen-fixing cyanobacterium *Anabaena* sp. PCC 7120. Proc Natl Acad Sci U S A 112:E4458–E4464. https://doi.org/10.1073/pnas.1512232112.
20. Docherty K, Brenchley GV, Hales CN. 1979. The permeability of rat liver lysosomes to sugars. Evidence for carrier-mediated facilitated diffusion. Biochem J 178:361–366. https://doi.org/10.1042/bj1780361.
21. Friedman MH. 2008. Principles and models of biological transport. Springer, Berlin, Germany. https://doi.org/10.1007/978-0-387-79240-8.
22. Ek-Vitorin JF, Burt JM. 2013. Structural basis for the selective permeability of channels made of communicating junction proteins. Biochim Biophys Acta 1828:51–68. https://doi.org/10.1016/j.bbamem.2012.02.003.
23. Hervé JC, Derangeon M. 2013. Gap-junction-mediated cell-to-cell communication. Cell Tissue Res 352:21–31. https://doi.org/10.1007/s00441-012-1485-6.
24. Yeager M, Harris AL. 2007. Gap junction channel structure in the early 21st century: facts and fantasies. Curr Opin Cell Biol 19:521–528. https://doi.org/10.1016/j.ceb.2007.09.001.
25. Stanier RY, Deruelles J, Rippka R, Herdman M, Waterbury JB. 1979. Generic assignments, strain histories and properties of pure cultures of cyanobacteria. Microbiology 111:1–61. https://doi.org/10.1099/00221287-111-1-1.

Chapter 2: Specific glucoside transporters influence septal structures and function in the filamentous, heterocyst-forming cyanobacterium *Anabaena* sp. strain PCC 7120

Check for updates
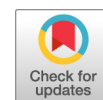
Specific Glucoside Transporters Influence Septal Structure and Function in the Filamentous, Heterocyst-Forming Cyanobacterium *Anabaena* sp. Strain PCC 7120

Mercedes Nieves-Morión,[a] Sigal Lechno-Yossef,[b] Rocío López-Igual,[a*]
José E. Frías,[a] Vicente Mariscal,[a] Dennis J. Nürnberg,[c] Conrad W. Mullineaux,[d]
C. Peter Wolk,[b] Enrique Flores[a]

Instituto de Bioquímica Vegetal y Fotosíntesis, CSIC and Universidad de Sevilla, Seville, Spain[a]; MSU-DOE Plant Research Laboratory, Michigan State University, East Lansing, Michigan, USA[b]; Department of Life Sciences, Imperial College London, London, United Kingdom[c]; School of Biological and Chemical Sciences, Queen Mary University of London, London, United Kingdom[d]

ABSTRACT When deprived of combined nitrogen, some filamentous cyanobacteria contain two cell types: vegetative cells that fix CO_2 through oxygenic photosynthesis and heterocysts that are specialized in N_2 fixation. In the diazotrophic filament, the vegetative cells provide the heterocysts with reduced carbon (mainly in the form of sucrose) and heterocysts provide the vegetative cells with combined nitrogen. Septal junctions traverse peptidoglycan through structures known as nanopores and appear to mediate intercellular molecular transfer that can be traced with fluorescent markers, including the sucrose analog esculin (a coumarin glucoside) that is incorporated into the cells. Uptake of esculin by the model heterocyst-forming cyanobacterium *Anabaena* sp. strain PCC 7120 was inhibited by the α-glucosides sucrose and maltose. Analysis of *Anabaena* mutants identified components of three glucoside transporters that move esculin into the cells: GlsC (Alr4781) and GlsP (All0261) are an ATP-binding subunit and a permease subunit of two different ABC transporters, respectively, and HepP (All1711) is a major facilitator superfamily (MFS) protein that was shown previously to be involved in formation of the heterocyst envelope. Transfer of fluorescent markers (especially calcein) between vegetative cells of *Anabaena* was impaired by mutation of glucoside transporter genes. GlsP and HepP interact in bacterial two-hybrid assays with the septal junction-related protein SepJ, and GlsC was found to be necessary for the formation of a normal number of septal peptidoglycan nanopores and for normal subcellular localization of SepJ. Therefore, beyond their possible role in nutrient uptake in *Anabaena*, glucoside transporters influence the structure and function of septal junctions.

IMPORTANCE Heterocyst-forming cyanobacteria have the ability to perform oxygenic photosynthesis and to assimilate atmospheric CO_2 and N_2. These organisms grow as filaments that fix these gases specifically in vegetative cells and heterocysts, respectively. For the filaments to grow, these types of cells exchange nutrients, including sucrose, which serves as a source of reducing power and of carbon skeletons for the heterocysts. Movement of sucrose between cells in the filament takes place through septal junctions and has been traced with a fluorescent sucrose analog, esculin, that can be taken up by the cells. Here, we identified α-glucoside transporters of *Anabaena* that mediate uptake of esculin and, notably, influence septal structure and the function of septal junctions.

Filamentous cyanobacteria of the orders *Nostocales* and *Stigonematales* fix atmospheric nitrogen in specialized cells called heterocysts (1). Heterocysts are formed from vegetative cells when the filaments of those cyanobacteria lack a source of combined nitrogen (2). The heterocysts provide the vegetative cells with fixed nitrogen, and the vegetative cells, which fix carbon dioxide through oxygenic photosynthesis, provide the heterocysts with reduced carbon (3). Substances exchanged between the two cell types include regulators, such as PatS- and HetN-derived peptides, and nutrients, including amino acids and sugars (4). In the model heterocyst-forming cyanobacterium *Anabaena* sp. strain PCC 7120 (here called *Anabaena*) grown in the absence of combined nitrogen, heterocysts constitute about 10% of the cells and are distributed with a semiregular pattern along the filament (2). This implies that one heterocyst feeds more than one vegetative cell with fixed nitrogen. Two routes have been considered for intercellular molecular transfer, the continuous periplasm of the filament (5, 6) and cell-cell joining structures (7), now termed septal junctions (8–10). The latter would represent a kind of symplasmic route (11) implying intercellular transfer between vegetative cells as well as between heterocysts and vegetative cells.

Proteins SepJ, FraC, and FraD, which are located at the cell poles in the intercellular septa of the filaments of *Anabaena*, are integral membrane proteins (12, 13). SepJ and FraD have predicted extramembrane domains that appear to reside in the periplasm (10, 14–16). Intercellular molecular exchange in the cyanobacterial filament can be traced with fluorescent markers, including calcein, 5-carboxyfluorescein (5-CF), and esculin, and transfer has been found to be impaired in inactivated mutants of *sepJ*, *fraC*, and *fraD* (7, 14, 17, 18). Additionally, perforations (termed nanopores) that have been observed in septal peptidoglycan disks from heterocyst-forming cyanobacteria (19) are present at decreased numbers in those mutants (18). Structures observed by electron tomography of *Anabaena* that have been termed channels (20) likely correspond to the nanopores. SepJ, FraC, and FraD appear to contribute to the formation of cell-cell joining structures (septal junctions) that traverse the septal peptidoglycan through the nanopores. Differential impairment in the transfer of calcein and 5-CF in the *sepJ* and *fraC-fraD* mutants has suggested that two types of septal junction complexes exist, one related to SepJ and another related to FraCD (14).

Sucrose appears to be a quantitatively important metabolite transferred from vegetative cells to heterocysts (21–25). Intercellular transfer of sucrose has been probed in *Anabaena* using esculin (6,7-dihydroxycoumarin β-D-glucoside), a fluorescent analog of this sugar (18). Esculin is taken up into the cells by a mechanism that can be inhibited by the presence of sucrose. Once inside the cells, esculin can be transferred cell to cell in the filament by diffusion through the septal junctions (18, 26). Thus, septal junctions are functionally analogous to the gap junctions of metazoans (18, 26).

In this work, we addressed the transporters that are involved in esculin uptake in *Anabaena* and their role, if any, in intercellular molecular transfer. The genome of *Anabaena* contains several open reading frames (ORFs) predicted to encode components of sugar transporters (27). We have identified three genes that are involved in uptake of esculin, two that encode components of two different ABC uptake transporters and one that encodes a major facilitator superfamily (MFS) transporter. We also found that the three identified glucoside transporters influence intercellular molecular exchange in *Anabaena*. One of the ABC transporter components, an ATP-binding subunit, is needed for the correct subcellular localization of SepJ, and the two other transporters appear to affect SepJ function.

RESULTS

Esculin uptake through α-glucoside transporters. We have previously shown that esculin can be taken up by *Anabaena* filaments grown in BG11 medium (containing
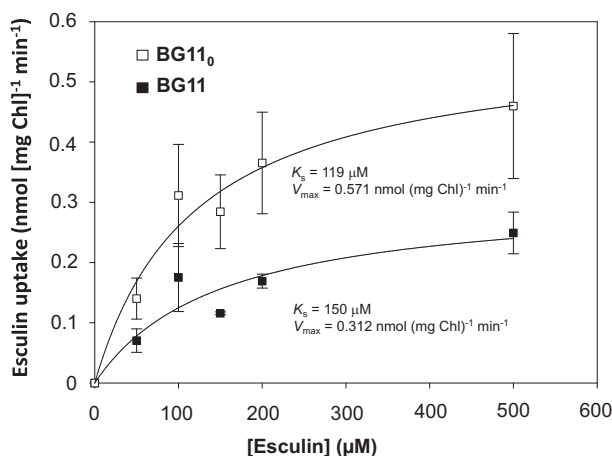
FIG 1 Effect of concentration of esculin on the uptake of esculin by *Anabaena*. BG11-grown filaments or filaments grown in BG11 medium and incubated for 18 h in BG11$_0$ medium were resuspended in the same medium supplemented with 10 mM HEPES-NaOH (pH 7) and used in uptake assays with the indicated concentrations of esculin as described in Materials and Methods. Error bars refer to standard deviations (SD); $n = 3$.

nitrate as the nitrogen source) or grown in BG11 medium and incubated for 18 h in BG11$_0$ medium (lacking any source of combined nitrogen), and that uptake is linear for at least 70 min and takes place at higher levels in the filaments incubated in BG11$_0$ medium (18). To understand better the process of esculin uptake, we determined the dependence of esculin uptake on esculin concentration. Esculin uptake was faster in cells that had been incubated in the absence of nitrate compared to nitrate-grown cultures, with V_{max} values of about 0.31 and 0.57 nmol (mg chlorophyll a [Chl])$^{-1}$ min^{-1} for BG11-grown filaments and filaments incubated in BG11$_0$ medium, respectively (Fig. 1). Esculin concentrations giving half-maximal uptake rates (K_s) were 150 and 119 μM in BG11 and BG11$_0$, respectively. Because a concentration somewhat lower than the K_s would permit observation of effects such as competitive or noncompetitive inhibition, we have used 100 μM esculin as a standard concentration in our uptake assays.

The pH dependence of uptake of esculin was investigated. As shown in Fig. 2, the

FIG 2 Effect of pH on the uptake of esculin by *Anabaena*. Filaments were grown in BG11 medium and then either were resuspended in BG11 medium or were incubated for 18 h in BG11$_0$ medium and then resuspended in BG11$_0$ medium. Both media were supplemented with 10 mM HEPES-NaOH at the indicated pH values and were used in assays of uptake with 100 μM esculin as described in Materials and Methods. The differences in the mean values of uptake of esculin between filaments resuspended in BG11$_0$ and BG11 at the different pH values tested were represented as BG11$_0$-BG11. Error bars indicate SD. For pH 7, $n = 25$ (BG11) or 20 (BG11$_0$); for all other pH values, $n = 3$.
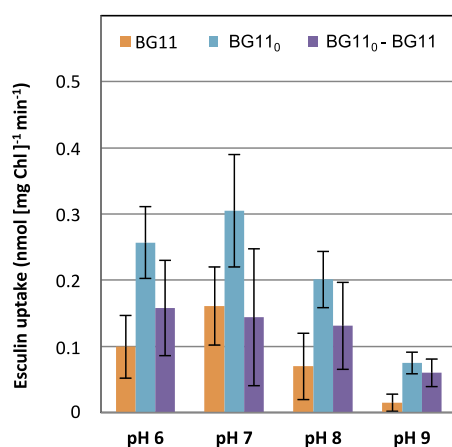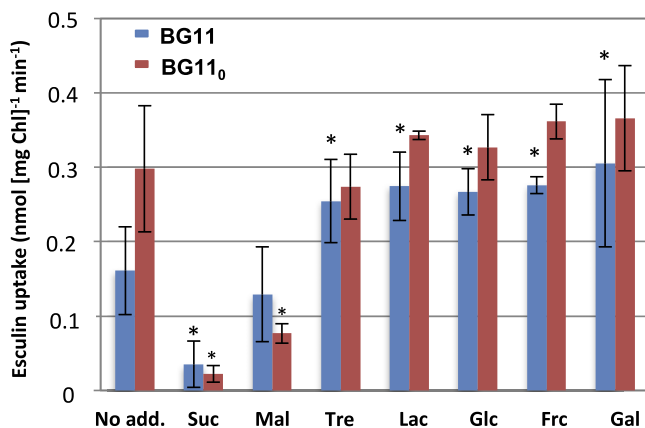
FIG 3 Effect of sugars on the uptake of esculin by *Anabaena*. BG11-grown filaments or filaments grown in BG11 medium and incubated for 18 h in $BG11_0$ medium were resuspended in the same medium supplemented with 10 mM HEPES-NaOH (pH 7) and the indicated sugar at 1 mM. No add., no sugar added; Suc, sucrose; Mal, maltose; Tre, trehalose; Lac, lactose; Glc, glucose; Frc, fructose; Gal, galactose. The assays were performed with 100 μM esculin as described in Materials and Methods. Error bars indicate SD; n = 2 to 3, except for the No add. group (n = 25 [BG11] or 20 [$BG11_0$]). Asterisks denote significant differences compared to the assays without added sugars in BG11 or $BG11_0$ medium ($P <$ 0.05 by Student's *t* test).

rate of uptake was higher at pH 7 than at lower or higher pH values and was, in every case, higher in filaments incubated in $BG11_0$ medium than in filaments from BG11 medium. The difference in the rate of uptake between filaments from $BG11_0$ and BG11 media decreased as the pH of the assay buffer was increased, suggesting that a H^+-dependent transporter is induced in filaments incubated in $BG11_0$ medium.

Esculin has been used to test the activity of some higher plant sucrose transporters (28) and, consistent with the possibility of uptake through a sucrose transporter(s), inhibition of uptake of esculin by sucrose has been observed in *Anabaena* (18). To characterize further the transporters involved, we tested whether uptake of esculin would be inhibited by various monosaccharides (glucose, fructose, and galactose) and disaccharides (sucrose, maltose, trehalose, and lactose). The results depicted in Fig. 3 show that, in BG11-grown filaments, uptake of esculin was inhibited mainly by sucrose and, to a lesser extent, by maltose. Other sugars tested appear to have stimulated uptake of esculin. In filaments that were incubated in $BG11_0$ medium, inhibition of uptake by sucrose and maltose again was evident. Our results suggest that although esculin is a β-glucoside, its uptake is inhibited mainly by some α-glucosides, sucrose (glucose 1$\alpha\rightarrow$2 fructose) and maltose (glucose 1$\alpha\rightarrow$4 glucose), whereas neither lactose (a β-galactoside; galactose 1$\beta\rightarrow$4 glucose) nor trehalose (a different α-glucoside; glucose 1$\alpha\rightarrow$1α glucose) inhibits uptake of esculin.

Identification of three transporters mediating esculin uptake. Two genes, Ava_2050 and Ava_2748, that encode possible components of ABC uptake transporters for disaccharides or oligosaccharides, are induced in the heterocysts of *Anabaena variabilis* ATCC 29413 (29). BLAST analysis with the genomic sequence of *Anabaena* (30) identified Alr4781 and All0261, with 97% and 99% amino acid identity, respectively, as the products of the *Anabaena* orthologs of those *A. variabilis* genes. Among characterized proteins included in the Transporter Classification Database (TCDB; http://www.tcdb.org), Alr4781 is most similar (45.4% identity, 59.6% similarity; expect, 3.2 $\times$ 10^{-111}) to MalK1, an ATP-binding subunit shared by the glucose/mannose (TCDB no. 3.A.1.1.24) and the trehalose/maltose/sucrose/palatinose (TCDB no. 3.A.1.1.25) transporters from *Thermus thermophilus*, and All0261 is most similar (36.4% identity, 58.9% similarity; expect, 3.3 $\times$ 10^{-51}) to the AraQ permease component of the arabinosaccharide transporter AraNPQ-MsmX from *Bacillus subtilis* (TCDB no. 3.A.1.1.34). We denote *alr4781* as *glsC* and *all0261* as *glsP* (*gls* standing for glucoside). Neither *glsC* nor *glsP* is clustered with other ABC transporter-encoding genes in the *Anabaena* genome.

**TABLE 1** Esculin uptake in *Anabaena* and some mutant strains[a]

| | | | Esculin uptake[a] (nmol [mg Chl]$^{-1}$ min^{-1}) in: | | | |
| | | | BG11 | | BG11$_0$ | |
Strain	Genotype	Product(s) of the mutated gene(s)	Mean ± SD (n)	% of WT (P)	Mean ± SD (n)	% of WT (P)
PCC 7120	WT		0.161 ± 0.059 (25)		0.298 ± 0.085 (20)	
DR3912a	alr4781::C.S3	GlsC	0.079 ± 0.037 (10)	49 (0.0003)	0.220 ± 0.065 (9)	74 (0.021)
DR3915	all0261::C.S3	GlsP	0.095 ± 0.041 (10)	59 (0.003)	0.217 ± 0.089 (9)	73 (0.027)
DR3912a DR3985a	alr4781::C.S3 all0261::C.CE	GlsC, GlsP	0.041 ± 0.020 (10)	25 (10^{-6})	0.149 ± 0.024 (5)	50 (0.007)
CSRL15	alr3705::pCSRL49	MFS permease	0.181 ± 0.067 (3)	112 (0.591)	0.339 ± 0.073 (4)	113 (0.383)
FQ163	all1711::Tn5-1063	HepP	0.174 ± 0.076 (4)	108 (0.703)	0.206 ± 0.020 (4)	69 (0.046)
CSMN3	alr3705::pCSRL49 all1711::Tn5-1063	MFS permease, HepP	0.139 ± 0.058 (3)	86 (0.553)	0.200 ± 0.042 (4)	67 (0.037)

[a]Filaments grown in BG11 medium (in the presence of antibiotics for the mutants) were washed and resuspended in BG11 or BG11$_0$ medium without antibiotics and incubated for 18 h under culture conditions. Filaments were then resuspended in the same medium supplemented with 10 mM HEPES-NaOH (pH 7) and used in assays of uptake of 100 μM esculin as described in Materials and Methods. Data are means and SD from the indicated number of assays performed with independent cultures. The significance of the difference between each mutant and the wild type (P) was assessed by Student's *t* test.

To test whether the transporters encoded by these *Anabaena* genes can be involved in uptake of esculin, *glsC* was inactivated by insertion of gene cassette C.S3 (31), resulting in *Anabaena* strains that bear the DR3912a mutation (see Fig. S1 in the supplemental material), and *glsP* was inactivated by insertion of C.S3, resulting in *Anabaena* strains that bear the DR3915 mutation, or of C.CE1 (31), resulting in *Anabaena* strains that bear the DR3985a mutation (Fig. S1). BG11-grown filaments of the *glsC* and *glsP* mutants showed esculin uptake activities that were 49% and 59%, respectively, of the wild-type activity (Table 1), and filaments of the *glsC* and *glsP* mutants that had been incubated in BG11$_0$ medium showed 74% and 73%, respectively, of the wild-type activity. Thus, the products of both genes contribute to esculin uptake by *Anabaena* in medium containing nitrate (BG11) and after incubation in medium lacking combined nitrogen (BG11$_0$).

ABC uptake transporters typically comprise one periplasmic solute-binding protein, two integral membrane proteins (transmembrane domains or permeases), and two nucleotide-binding domains that hydrolyze ATP in the cytoplasm (32). If the GlsC ATP-binding subunit and the GlsP permease belong to the same ABC transporter, we would expect that mutation of the two genes would not increase the effect on the uptake of esculin over that of the single mutations. If, on the other hand, GlsC and GlsP belong to two different transporters, we would expect an additive effect of the mutations. A double *glsC glsP* mutant, i.e., an *Anabaena* strain bearing the DR3912a and DR3985a mutations (Fig. S1), showed 25% of the wild-type activity of esculin uptake in BG11-grown filaments and 50% in filaments incubated in BG11$_0$ medium (Table 1), percentages that represent decreased values compared to the effects of the single mutations (49% and 59% for BG11 and 74% and 73% for BG11$_0$). These results suggest that GlsC and GlsP are components of different ABC transporters that can mediate esculin uptake. Notably, significant uptake activity remains in the double mutant, especially in filaments that had been incubated in medium lacking combined nitrogen (BG11$_0$).

Genes *all1711* (*hepP*) and *alr3705* encode predicted MFS proteins that would facilitate movement of disaccharides or oligosaccharides across cell membranes. As shown by results with *all1711*::Tn5-1063 mutant strain FQ163 (33), HepP may be a glucoside transporter that is involved in production of the heterocyst-specific polysaccharide layer and may also mediate sucrose transport. According to BLAST analysis, Alr3705 is the predicted *Anabaena* genomic product most similar to higher plant sucrose transporters. *alr3705* was mutated by insertion of C.S3-containing plasmid pCSRL49, producing strain CSRL15, and insertion of pCSRL49 was also combined with *all1711*::Tn5-1063 to produce a double mutant, strain CSMN3 (Fig. S2). None of the strains FQ163, CSRL15, or CSMN3, when grown in BG11 medium, was significantly affected in uptake of esculin (P values of 0.553 to 0.703 by Student's *t* test), and CSRL15 was not significantly affected when incubated in BG11$_0$ medium (Table 1). In contrast, filaments
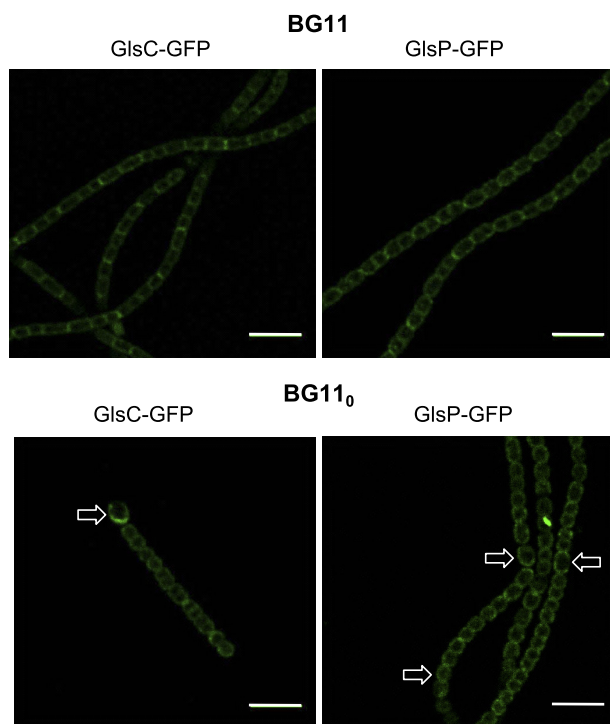
FIG 4 Subcellular localization of GlsC-GFP and GlsP-GFP. Filaments of strains CSMN13 (*glsC::gfp*) and CSMN15 (*glsP::gfp*) grown in BG11 medium in the presence of antibiotics were incubated in BG11 or $BG11_0$ medium without antibiotics for 24 h. GFP fluorescence was visualized by confocal microscopy as described in Materials and Methods. Brightness and contrast were enhanced to improve visibility. Arrows point to heterocysts. Size bars, 10 μm.

of mutants FQ163 and CSMN3 incubated in $BG11_0$ medium showed similarly decreased activities, 69% and 67% of the wild-type activity, respectively (Table 1). These results indicate that HepP, but not Alr3705, contributed to uptake of esculin in filaments deprived of combined nitrogen.

In conclusion, two ABC transporters, of which GlsC and GlsP are independent components, together are responsible for about 75% and 50% of uptake of esculin in BG11 and $BG11_0$ filaments, respectively, and HepP is responsible for about 30% of uptake of esculin in $BG11_0$ filaments when tested at pH 7. Other transporters therefore should contribute to uptake of esculin in both BG11 and $BG11_0$ media.

Subcellular localization of GlsC and GlsP. To understand better the role of the transporters identified in this work in the physiology of *Anabaena*, we investigated their subcellular localization. The localization of HepP in the cytoplasmic membrane of both vegetative cells and heterocysts has been described previously (33). To study the subcellular localization of GlsC and GlsP, strains producing GlsC-GFP and GlsP-GFP fusion proteins were constructed. As a putative nucleotide-binding domain of an ABC transporter, GlsC is expected to reside in the cytoplasmic face of the cytoplasmic membrane. GlsP is a predicted integral membrane protein that bears six putative transmembrane segments with both the N and C termini in the cytoplasm. Because GFP folds efficiently in the cytoplasm (34), the *gfp-mut2* gene was added to the 3' end of the *glsC* and *glsP* genes, and the corresponding constructs were transferred to *Anabaena* (Fig. S3). Visualization of filaments of the corresponding strains, CSMN13 (*glsC-gfp*) and CSMN15 (*glsP-gfp*), incubated in BG11 or $BG11_0$ medium showed a relatively low GFP signal that was spread through the periphery of the cells, including the septal regions, where the signal was increased (Fig. 4). Quantification of GFP fluorescence was performed as described in Materials and Methods and is summarized in Fig. S4. The data show that fluorescence was roughly 2-fold higher in the septa than in lateral areas for both GlsC-GFP and GlsP-GFP in cells grown in BG11 medium as well as in cells
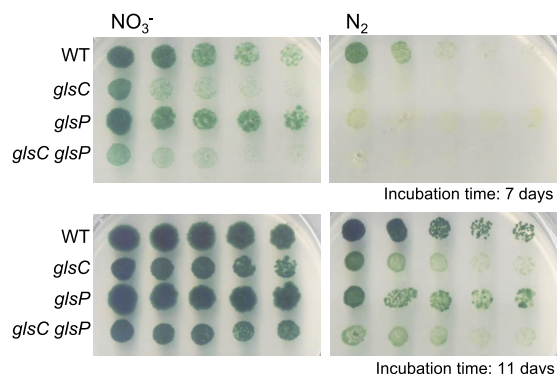
FIG 5 Tests of growth on solid medium of wild-type *Anabaena* and the *glsC* (DR3912a), *glsP* (DR3915), and *glsC glsP* (DR3912a DR3985a) mutants. Filaments grown in BG11 medium (in the presence of antibiotics for the mutants) were resuspended in $BG11_0$ medium, dilutions were prepared, and a 10-μl portion of each dilution (from left to right, 1, 0.5, 0.25, 0.125, and 0.0625 μg Chl ml^{-1}) was spotted on BG11 (NO_3^-) or $BG11_0$ (N_2) medium. The plates were incubated under culture conditions, and photographs taken after 7 and 11 days of incubation are shown to help appreciate the growth defect phenotypes.

incubated in $BG11_0$ medium, indicating that the increased fluorescence from the septa corresponds to the combination of the fluorescence from the adjacent cytoplasmic membranes. Nonetheless, somewhat higher-level GFP fluorescence was observed in septal areas of cells grown in BG11 medium than of cells incubated in $BG11_0$ medium. In filaments incubated in $BG11_0$ medium, the GFP signal was present at similar levels in heterocysts and vegetative cells. These results indicate that GlsC and GlsP are located throughout the cytoplasmic membrane of both vegetative cells and heterocysts. Our results also indicate that levels of GlsC-GFP or GlsP-GFP are generally similar in cells incubated in BG11 and $BG11_0$ media (Fig. S4).

Fox phenotype of the *glsC* and *glsP* mutants. The Fox$^-$ phenotype denotes inability to grow fixing N_2 under oxic conditions, and it is frequently associated with malformation of the heterocyst envelope, as in the case of the *hepP* mutant (33). The growth phenotype was investigated here for the *glsC* and *glsP* mutants. On solid medium, the *glsC* and *glsP* single mutants and the *glsC glsP* double mutant could grow using nitrate or N_2 as the nitrogen source, but the *glsP* mutant showed poorer diazotrophic growth than the wild type, and the *glsC* and *glsC glsP* mutants showed poorer growth in both media (Fig. 5). To determine growth rate constants, growth tests were carried out in liquid medium. In the presence of nitrate (BG11 medium), the growth rate of the single mutants was identical to that of the wild type, whereas the growth rate of the double mutant was 75% of that of the wild type (Table 2). In the absence of combined nitrogen ($BG11_0$ medium), the growth rate of the three mutants was lower than that of the wild type, being especially low in the case of the double mutant (Table 2). Thus, the *glsC*, *glsP*, and *glsC glsP* mutants cannot grow normally fixing N_2 under oxic conditions and therefore show, at best, a weak Fox$^+$ phenotype. The phenotype of diminished growth of the single mutants could be complemented by introducing in the corresponding mutant a replicative plasmid bearing the wild-type gene, *glsC* or *glsP*; however, when tested on solid medium, complementation was incomplete (Fig. S5). To investigate whether incomplete complementation could result from insufficient expression of the genes in the complemented strains, reverse transcription-quantitative PCR (RT-qPCR) analysis was performed as described in Materials and Methods. Rather than low expression, this analysis indicated 6-fold and 11-fold higher expression of the *glsC* and *glsP* genes, respectively, in the complemented mutants than in the wild type. Therefore, it is possible that overexpression of these genes is deleterious for *Anabaena*.

Production of heterocysts and nitrogenase activity were determined in filaments grown in BG11 medium and incubated for 48 h in $BG11_0$ medium. The *glsC*, *glsP*, and *glsC glsP*

TABLE 2 Growth rates, heterocyst level, and nitrogenase activity in *Anabaena* and ABC transporter mutant strains

| Strain (mutated gene[s]) | Growth rate constant[a] (day^{-1}) [mean $\pm$ SD]) (n) in: | | Heterocysts[b] (%) | Nitrogenase activity[c] (nmol ethylene produced [μg Chl]$^{-1}$ h^{-1} [mean $\pm$ SD]) (n) | |
	BG11	BG11$_0$		Oxic	Anoxic
PCC 7120 (WT)	0.67 $\pm$ 0.07 (5)	0.49 $\pm$ 0.09 (5)	9.33	23.37 $\pm$ 5.17 (4)	10.54 $\pm$ 3.05 (3)
DR3912a (*glsC*)	0.67 $\pm$ 0.14 (5)	0.28 $\pm$ 0.15 (5)	5.58	2.52 $\pm$ 1.89 (3)	2.47 $\pm$ 0.15 (2)
DR3915 (*glsP*)	0.67 $\pm$ 0.07 (5)	0.36 $\pm$ 0.08 (5)	7.93	2.13 $\pm$ 0.63 (3)	3.00 $\pm$ 1.48 (2)
DR3912a DR3985a[d] (*glsC, glsP*)	0.50 $\pm$ 0.10 (5)	0.06 $\pm$ 0.07 (5)	2.22	1.53 $\pm$ 1.61 (8)	2.08 $\pm$ 1.70 (6)

[a]Growth rate constants (μ) were determined in BG11 or BG11$_0$ liquid medium as described in Materials and Methods for the number of independent cultures shown in parentheses. The difference between the *glsC glsP* mutant and the WT was significant in BG11 ($P = 0.014$ by Student's t test) and BG11$_0$ ($P < 0.001$) media; the differences were also significant between *glsC* and WT strains ($P = 0.029$) and between *glsP* and WT strains ($P = 0.045$) in BG11$_0$ medium.

[b]Filaments of the indicated strains grown in BG11 medium (with antibiotics for the mutants) and incubated in BG11$_0$ medium without antibiotics for 48 h were used to determine the percentage of heterocysts (about 1,500 cells were counted for each strain).

[c]Filaments of the indicated strains grown in BG11 medium (with antibiotics for the mutants) and incubated in BG11$_0$ medium without antibiotics for 48 h were used to determine nitrogenase activity. Acetylene reduction was assayed under oxic and anoxic conditions (see Materials and Methods); the differences were significant for all of the mutants versus the WT (P values were <0.002 [oxic conditions] and ≤0.05 [anoxic conditions] by Student's t test). The number of determinations done with independent cultures is indicated in parentheses.

[d]After 48 h of incubation in BG11$_0$ medium, the filaments of this strain were extensively fragmented (see the text). Those filaments containing heterocysts also contained a mean of 5.4 vegetative cells per filament.

mutants showed about 60%, 85%, and 24%, respectively, of the number of heterocysts observed in the wild type (Table 2). Under oxic conditions, nitrogenase activity was about 10% of the wild-type activity in the two single mutants and about 6.5% in the double mutant (Table 2). Thus, the heterocysts produced in the mutants exhibited low nitrogenase activity. Assay under anoxic conditions showed little or no increase in activity, in contrast to what is normally observed in mutants that bear a defect in the heterocyst envelope (see, for instance, reference 33). The heterocyst envelope-specific polysaccharide layer can be stained with alcian blue, a stain useful to detect bacterial polysaccharides (35). Microscopic inspection of filaments of the *glsC glsP* double mutant stained with alcian blue showed the presence of stained heterocysts, indicating the existence of a polysaccharide layer in the double mutant (Fig. 6). Microscopic inspection also showed that the filaments of the double mutant were very short (Fig. 6). Inspection of cultures of the three mutants showed
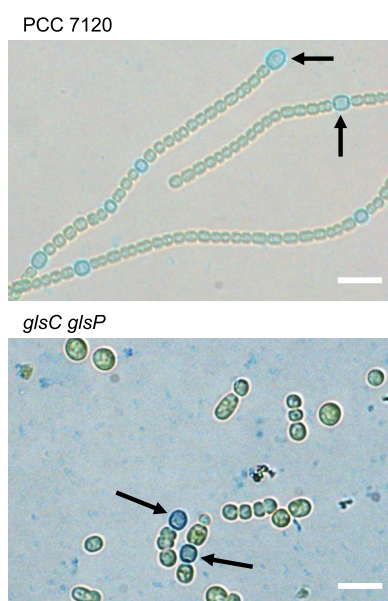
FIG 6 Heterocysts in the *glsC glsP* double mutant. Filaments of the wild type (PCC 7120) and of the double mutant grown in BG11 medium (in the presence of antibiotics for the mutant) were inoculated in liquid BG11$_0$ medium without antibiotics and incubated for 4 days under culture conditions. Staining with alcian blue was done as described in Materials and Methods, and the filament suspensions were observed by light microscopy. Arrows point to some stained heterocysts. Scale bars, 10 μm.

TABLE 3 Transfer of esculin between vegetative cells or from vegetative cells to heterocysts in *Anabaena* and glucoside transporter mutant strains

	Esculin transfer[a] (R [s^{-1}])					
	Vegetative cells in BG11-grown filaments		Filaments incubated in $BG11_0$ medium			
			Vegetative cells		Heterocysts	
Strain (mutated gene[s])	Mean ± SD (n)	% of WT (P)	Mean ± SD (n)	% of WT (P)	Mean ± SD (n)	% of WT (P)
PCC 7120 (WT)	0.157 ± 0.052 (49)		0.162 ± 0.062 (60)		0.060 ± 0.067 (82)	
DR3912a (*glsC*)	0.122 ± 0.051 (77)	78 ($<10^{-3}$)	0.047 ± 0.048 (28)	29 ($<10^{-12}$)	0.074 ± 0.081 (55)	123 (0.277)
DR3915 (*glsP*)	0.144 ± 0.054 (43)	92 (0.200)	0.094 ± 0.077 (25)	58 ($<10^{-4}$)	0.091 ± 0.084 (33)	152 (0.060)
DR3912a DR3985a (*glsC, glsP*)	0.105 ± 0.042 (55)	67 ($<10^{-6}$)	0.094 ± 0.070 (37)	58 ($<10^{-5}$)	0.088 ± 0.057 (25)	147 (0.070)
FQ163 (*hepP*)	0.090 ± 0.058 (56)	57 ($<10^{-4}$)	0.068 ± 0.051 (17)	42 ($<10^{-10}$)	0.156 ± 0.082 (27)	260 (10^{-8})

[a]Filaments of the wild type and the indicated mutants grown in BG11 medium (with antibiotics for the mutants) and incubated in BG11 medium without antibiotics for 18 to 24 h or in $BG11_0$ medium without antibiotics for 48 h were used in FRAP analysis as described in Materials and Methods. Data are means ± SD from the results obtained with the indicated number of filaments (n) subjected to FRAP analysis. Filaments from two to six independent cultures were used. The P value, determined by Student's t test (mutant versus wild type), is indicated in each case.

the presence of short filaments in the *glsC glsP* double mutant in both BG11 and $BG11_0$ media, but filament fragmentation was strongest in $BG11_0$ medium (Fig. S6). Such short filaments were not observed in the *glsC* or *glsP* single mutants. Thus, the phenotypic alterations were stronger in the *glsC glsP* double mutant than in the *glsC* or *glsP* single mutants, which is consistent with independent action of the GlsC and GlsP proteins as concluded above from the esculin uptake data.

Intercellular exchange of fluorescent markers. Because the *glsC*, *glsP*, and *hepP* mutants are impaired in glucoside transport and diazotrophic growth, the proteins encoded by these genes could influence intercellular transfer of sucrose. We therefore tested intercellular exchange of esculin in the *glsC*, *glsP*, and *hepP* mutants by means of FRAP (fluorescence recovery after photobleaching) analysis. The results of these tests were analyzed to determine the recovery constant (R) of fluorescence in the cells in which esculin had been bleached (see Materials and Methods and Text S1). To attain adequate labeling of esculin to carry out the FRAP analysis, filaments were incubated for 1 h with 150 μM esculin. Transfer of esculin between vegetative cells of BG11-grown filaments was decreased in a limited way (by about 22%) in the *glsC* mutant but not in the *glsP* mutant (Table 3). However, the effect was larger in the *glsC glsP* double mutant (about 33% inhibition). In the *hepP* mutant, esculin transfer was 43% lower than that in the wild type.

In filaments of the wild type that had been incubated for 48 h in $BG11_0$ medium, esculin transfer between vegetative cells was similar to transfer between BG11-grown vegetative cells, but transfer from vegetative cells to heterocysts was decreased to about 38% of the value between vegetative cells (Table 3). These results are consistent with previously reported data (18). In the mutants, esculin transfer was lower in the $BG11_0$-incubated than in the BG11-grown vegetative cells, and it was especially decreased in the *glsC* mutant (Table 3). In contrast, esculin transfer from vegetative cells to heterocysts was increased in all of the mutants compared to the wild type, and this increase was particularly significant in the *hepP* mutant. In summary, esculin transfer was impaired between vegetative cells of heterocyst-containing filaments but not from vegetative cells to heterocysts.

To assess how specific the effect on intercellular transfer could be, transfer of calcein and 5-CF between nitrate-grown vegetative cells was also tested in the mutants. Calcein transfer was significantly impaired in the three single mutants, and it was lowest (21% of the wild-type activity) in the *glsC glsP* double mutant (Table 4). Transfer of 5-CF was also significantly impaired in the *glsC* and *glsP* mutants, although the effect of the mutations was lower in this case than on calcein transfer, and it was not impaired in the *hepP* mutant. These studies showed that GlsC, GlsP, and HepP are required for normal intercellular molecular exchange in *Anabaena*, but this requirement is more evident when the exchange is tested with calcein than with 5-CF or, as shown above, esculin (compared to BG11-grown filaments).

TABLE 4 Transfer of calcein and 5-CF between nitrate-grown vegetative cells in *Anabaena* and glucoside transporter mutant strains[a]

	Transfer (R [s^{-1}]) of:				
	Calcein		5-CF		
Strain (mutated gene[s])	Mean ± SD (n)	% of WT (P)	Mean ± SD (n)	% of WT (P)
PCC 7120 (WT)	0.070 ± 0.053 (50)		0.087 ± 0.045 (136)	
DR3912a (*glsC*)	0.039 ± 0.033 (47)	55 ($<10^{-3}$)	0.069 ± 0.060 (105)	79 (0.009)
DR3915 (*glsP*)	0.028 ± 0.041 (68)	39 ($<10^{-5}$)	0.059 ± 0.059 (96)	68 ($<10^{-4}$)
DR3912a DR3985a (*glsC, glsP*)	0.015 ± 0.020 (43)	21 ($<10^{-8}$)	0.064 ± 0.054 (48)	74 (0.004)
FQ163 (*hepP*)	0.022 ± 0.027 (33)	31 ($<10^{-5}$)	0.082 ± 0.044 (27)	94 (0.604)

[a]Filaments of the wild type and the indicated mutants grown in BG11 medium (with antibiotics for the mutants) and incubated in BG11 medium without antibiotics for 18 to 24 h were used in FRAP analysis as described in Materials and Methods. Data are means ± SD from the results obtained with the indicated number of filaments (n) subjected to FRAP analysis. Filaments from two to six (calcein) or up to 9 (5-CF) independent cultures were used. The P value, determined by Student's t test (mutant versus wild type), is indicated in each case.

SepJ localization and nanopores in the *glsC*, *glsP*, and *hepP* mutants. The fragmentation of filaments observed in the *glsC glsP* double mutant and the effect of the mutation of the glucoside transporters on calcein exchange described above are reminiscent of effects of inactivation of *sepJ* in *Anabaena* (12, 18). We therefore investigated the effect of the inactivation of *glsC*, *glsP*, and *hepP* on the subcellular localization of SepJ. For this investigation, plasmids bearing a *sepJ-gfp* fusion gene were transferred to mutants of those genes, producing strains CSMN9 (*glsC sepJ-gfp*), CSMN10 (*glsP sepJ-gfp*), and CSMN16 (*hepP sepJ-gfp*) (for PCR analysis of the genomic structure of each strain, see Fig. S7). Confocal microscopic inspection of filaments of strains producing SepJ-GFP showed that whereas the *glsP* and *hepP* mutations did not impair SepJ-GFP localization at the intercellular septa, the *glsC* mutation had a strong effect on localization (Fig. 7; for SepJ-GFP localization in four independent clones inspected by fluorescence microscopy, see Fig. S8). In the *glsC sepJ-gfp* strain, spots of
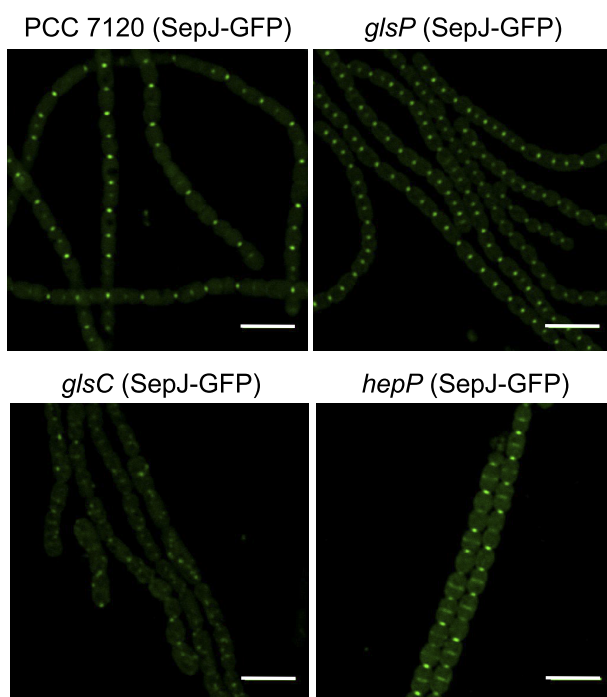
FIG 7 Subcellular localization of SepJ-GFP in the wild-type and transporter mutant genetic backgrounds. Filaments of strains CSAM137 (PCC 7120 [*sepJ*::pCSAM137]), CSMN9 (*glsC*::C.S3 *sepJ*::pCSVT22), CSMN10 (*glsP*::C.S3 *sepJ*::pCSVT22), and CSMN16 (*hepP*::Tn5-1063 *sepJ*::pCSAM137) were grown in BG11 medium in the presence of antibiotics and visualized by confocal microscopy as described in Materials and Methods. Size bars, 10 μm. In the *hepP* mutant, SepJ is seen localized in the middle of many cells; these cells are likely starting cell division, and SepJ is known to localize to the cell division site when cell division starts (12, 15).
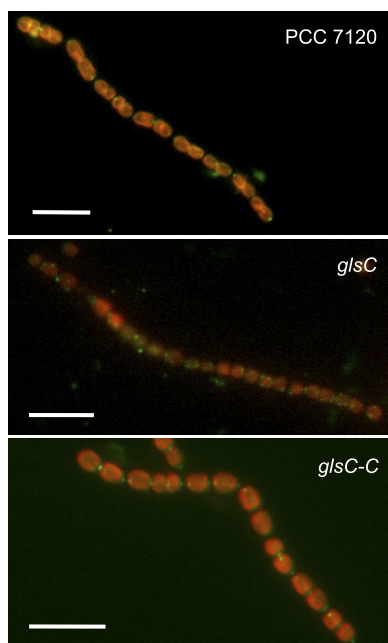
FIG 8 Immunofluorescence localization of SepJ in *Anabaena* (PCC 7120) and the *glsC* and *glsC-C* strains. Filaments of strains PCC 7120, DR3912a (*glsC*::C.S3), and DR3912a(pCSMN22) (*glsC*::C.S3 *glsC*) were grown in BG11 medium in the presence of antibiotics for the mutants and subjected to immunofluorescence analysis with anti-SepJ coiled-coil antibodies as described in Materials and Methods. Overlay images of antibody green fluorescence and cyanobacterial autofluorescence are shown. Size bars, 10 μm.

GFP were only sporadically observed in the center of the septa, and the GFP signal was frequently found throughout the periphery of the cells, including the intercellular septa. Thus, GlsC, but not GlsP or HepP, appears necessary for proper subcellular localization of SepJ.

To corroborate delocalization of SepJ as a result of inactivation of *glsC*, immunolocalization of SepJ was performed using antibodies raised against its coiled-coil domain (17). The antibodies localized SepJ at the cell poles of *Anabaena* (Fig. 8), as previously described (15). In the *glsC* mutant, the signal was largely delocalized, being observed at the cell poles only sporadically. In the complemented *glsC-C* strain [DR3912a(pCSMN22)], SepJ was observed clearly at the cell poles (Fig. 8). These results are fully consistent with the observation that the SepJ-GFP fusion protein shows delocalization of SepJ as the result of inactivation of *glsC* (Fig. 7 and Fig. S8).

Because SepJ is necessary for *Anabaena* to make a normal number of septal peptidoglycan nanopores (18), the number of nanopores was counted in septal peptidoglycan disks observed in murein sacculi isolated from the wild type and the *glsC*, *glsP*, and *hepP* mutants (Fig. 9). Whereas the *glsP* and *hepP* mutants contained a number of nanopores per septum similar to that of the wild type, the septa of the *glsC* mutant contained about 48% of the nanopores found in the wild-type septa.

Protein-protein interactions. The results in the previous section, showing that GlsC is necessary for proper localization of SepJ and formation of septal peptidoglycan nanopores, provides a rationale for understanding the effect of inactivation of *glsC* on the intercellular transfer of calcein, but no effect of inactivation of *glsP* or *hepP* was found. We then studied possible protein-protein interactions involving the glucoside transporters and SepJ using the bacterial adenylate cyclase two-hybrid (BACTH) assay, in which adenylate cyclase activity is reconstituted from two fragments, T25 and T18, of an adenylate cyclase from *Bordetella pertussis* brought together by interacting proteins fused to each of those fragments (36). Reconstituted adenylate cyclase in *Escherichia coli* produces cyclic AMP (cAMP) that promotes induction of *lacZ* encoding
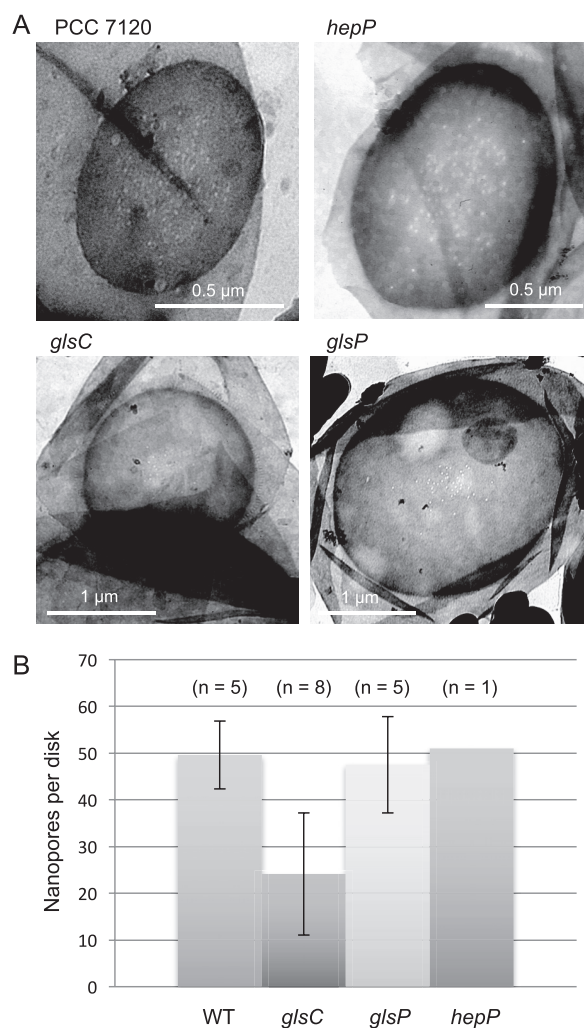
FIG 9 Septal peptidoglycan disk nanopores in wild-type *Anabaena* and mutants. (A) Murein sacculi were isolated from strains PCC 7120 (WT), DR3912a (*glsC*::C.S3), DR3915 (*glsP*::C.S3), and FQ163 (*hepP*::Tn*5*-1063) grown in BG11 medium and visualized by transmission electron microscopy. (B) Quantification of nanopores in disks from the indicated strains (means and SD; *n*, number of disks counted). *P* = 0.002 by Student's *t* test for WT versus *glsC* strains.

β-galactosidase. We have previously shown that SepJ-T25 and SepJ-T18 fusions (where the order of protein names denotes N-terminal to C-terminal orientation) are functional in SepJ self-interactions that produce high *β*-galactosidase activity (15, 16). As is the case for GlsP, HepP is a predicted integral membrane protein with both the N and C termini in the cytoplasm (33). Because of possible copy number or steric hindrance problems (37, 38), here we tested possible interactions of SepJ-T25 and SepJ-T18 with both N-terminal and C-terminal fusions to T18 and T25, respectively, of each of the glucoside transporter components investigated in this work, GlsC, GlsP, and HepP. The negative control in this analysis was an *E. coli* strain carrying plasmids that produce nonfused T25 and T18 fragments, and additional negative controls producing nonfused T25 or T18 and some of the tested fusions were used. None of these controls produced *β*-galactosidase activity significantly different from that of the T25/T18 control (Table 5). Combinations of protein fusions involving SepJ that produced *β*-galactosidase activity significantly higher than the controls included SepJ-T25/SepJ-T18 (positive control), SepJ-T25/T18-HepP, SepJ-T18/T25-HepP, and SepJ-T18/T25-GlsP, but no fusion involving GlsC. These results suggest significant interactions between SepJ and GlsP and, more strongly, between SepJ and HepP. On the other hand, significant interactions were also observed between HepP and GlsP. Finally, HepP self-interactions and GlsC

TABLE 5 Bacterial two-hybrid analysis of protein-protein interactions[a]

Fragment or fusion protein	β-Galactosidase activity (no. of independent transformants) with:							
	T18	SepJ-T18	GlsC-T18	T18-GlsC	GlsP-T18	T18-GlsP	HepP-T18	T18-HepP
T25	12.66 ± 2.34 (9)	10.88 ± 1.06 (6)	13.01 ± 3.49 (4)	12.34 ± 0.80 (4)	12.11 ± 4.10 (4)	10.95 ± 3.37 (4)	12.12 ± 1.33 (4)	11.99 ± 2.69 (4)
SepJ-T25	11.22 ± 2.04 (2)	**80.12 ± 37.03** (9)**	13.25 ± 2.91 (5)	15.75 ± 11.31 (3)	11.74 ± 3.68 (5)	14.66 ± 2.12 (4)	11.42 ± 1.36 (4)	**28.35 ± 5.93** (4)**
GlsC-T25	ND	11.66 ± 1.99 (6)	12.52 ± 3.32 (4)	**20.52 ± 4.90* (4)**	12.36 ± 0.95 (3)	13 ± 5.72 (3)	12.27 ± 3.61 (3)	12.11 ± 1.48 (4)
T25-GlsC	ND	13.09 ± 3.06 (6)	**25.98 ± 5.46** (4)**	15.93 ± 6.35 (6)	12.72 ± 3.11 (4)	12.79 ± 3.73 (3)	13.57 ± 1.92 (4)	11.98 ± 0.86 (4)
GlsP-T25	ND	14.34 ± 2.22 (7)	12.32 ± 3.11 (5)	14.19 ± 7.44 (4)	12.16 ± 2.11 (4)	11.64 ± 4.06 (3)	13.13 ± 2.23 (4)	17.44 ± 4.70 (4)
T25-GlsP	ND	**29.12 ± 9.36** (7)**	11.80 ± 2.27 (5)	15.48 ± 8.28 (4)	11.85 ± 0.55 (3)	12.04 ± 6.11 (3)	13.63 ± 1.47 (4)	**23.08 ± 7.03* (4)**
HepP-T25	10.58 ± 4.35 (4)	12.96 ± 3.26 (4)	12.83 ± 1.50 (4)	12.08 ± 1.12 (4)	13.94 ± 2.29 (4)	13.65 ± 2.48 (4)	13.86 ± 1.37 (4)	16.73 ± 8.38 (4)
T25-HepP	13.60 ± 2.01 (4)	**75.31 ± 6.74** (4)**	14.56 ± 2.47 (4)	13.06 ± 2.81 (4)	18.33 ± 2.50 (4)	**34.16 ± 7.18** (4)**	13.77 ± 0.99 (4)	**79.97 ± 22.12** (4)**

[a]Interactions of T25 and T18 fusion proteins produced in *E. coli* were measured as β-galactosidase activity in liquid cultures. Activity corresponds to nanomoles *o*-nitrophenol (milligrams protein)$^{-1}$ minute^{-1}. The protein fused to the N or the C terminus of T18 or T25 is indicated in each case (N terminus, protein-T18 or protein-T25; C terminus, T18-protein or protein-T25). The means and standard deviations of the results obtained with the indicated number of independent transformants are presented. The difference between each fusion protein combination and the T18/T25 pair was assessed by Student's *t* test; boldface type denotes significant differences

(*, $P \leq 0.005$; **, $P \leq 0.001$). All other combinations gave activities not significantly different from the T25/T18 control ($P > 0.05$). ND, not determined.

self-interactions were also observed, suggesting that HepP and GlsC can form homo-oligomers.

DISCUSSION

Glucoside transporters. Esculin has been successfully used as a fluorescent analog of sucrose to study intercellular molecular exchange in the filaments of *Anabaena* by means of FRAP analysis (18). This analysis requires esculin to be taken up by the cells in the filament, and we have now identified three genes, *glsC*, *glsP*, and *hepP*, that encode components of transporters that mediate esculin uptake in *Anabaena*. The *glsC* (*alr4781*) gene encodes an ATP-binding subunit of an ABC transporter, and the *glsP* (*all0261*) gene encodes an integral membrane (permease) subunit of a different ABC transporter. These genes were investigated because they are the possible *Anabaena* orthologs of genes highly expressed in the heterocysts of a closely related cyanobacterium, *A. variabilis* (29). In *Anabaena*, because the effect of inactivating *glsC* and *glsP* is evident in filaments grown in the presence of nitrate (Table 1), GlsC and GlsP appear to be active in vegetative cells. Additionally, as observed with GFP fusions, GlsC and GlsP are present in heterocysts as well as in vegetative cells (Fig. 4; see also Fig. S4 in the supplemental material). In transcriptomic analysis of *Anabaena*, these genes appear to have low expression, and their expression is not affected by nitrogen deprivation (39). According to the results of inhibition of uptake of esculin by sugars (Fig. 3), the natural substrate of these transporters can be sucrose or an α-glucoside. Sucrose uptake by vegetative cells of *Anabaena* has previously been reported (40), and sucrose transporters that can also transport maltose are frequently found in plants (41). The *Anabaena* glucoside transporters could have a role in the recovery of glucosides from extracellular polysaccharides produced under certain physiological conditions, as has been shown to occur in cyanobacterial mats (42). Consistent with this, biomass of the *glsC* and *glsP* mutants in old BG11 plates is shiny (not shown), which may be indicative of exopolysaccharide accumulation (33). It is also of interest that although *Anabaena* has been considered an obligatory photoautotroph (43), recent data suggest that it can grow using fructose, although this sugar has to be provided at a high concentration unless *Anabaena* is engineered to express a fructose transporter (27, 44). On the other hand, trehalose, lactose, glucose, fructose, and galactose could stimulate esculin uptake (Fig. 3), suggesting that *Anabaena* can use these sugars to support physiological activities such as active transport. As noted earlier, the *Anabaena* genome bears several genes putatively encoding sugar transporters (27), some of which could be involved in the uptake of those sugars.

The third gene that encodes an esculin transporter is *hepP* (*all1711*), which encodes an MFS protein that is also necessary for production of the heterocyst-specific polysaccharide layer (33). We have previously shown that HepP is present at higher levels in developing heterocysts (proheterocysts) and heterocysts than in vegetative cells, and that HepP could mediate sucrose uptake specifically in (pro)heterocysts (33). Because the contribution of HepP to uptake of esculin is evident only in filaments that had been incubated in the absence of combined nitrogen, and because uptake of esculin in these filaments is inhibited by sucrose, HepP may be involved in uptake of sucrose/esculin by (pro)heterocysts. MFS proteins, including sucrose transporters, frequently act as secondary transporters that mediate symport with protons (45). Uptake of esculin that is associated with incubation in $BG11_0$ medium minus uptake in BG11 medium decreases with increasing pH beyond pH 6 (Fig. 2). This observation suggests that a H^+-dependent transporter is induced in filaments incubated in $BG11_0$ medium. Because HepP contributes to esculin uptake associated with incubation in $BG11_0$ medium, our results are consistent with the idea that HepP is a sucrose-H^+ or α-glucoside-H^+ symporter.

Glucoside transporter mutant phenotypes. Inactivation of *hepP* leads to a Fox$^-$ phenotype that has been described in detail (33). We have found that the *glsC* and *glsP* mutants exhibit a weak Fox$^+$ phenotype: they grow slowly without a source of combined nitrogen under oxic conditions and express low levels of nitrogenase activity

(Table 2). Combination in the same strain of the two mutations, *glsC* and *glsP*, resulted in a greater impairment of diazotrophic growth, very low nitrogenase activity, and a low percentage of heterocysts. Nonetheless, these heterocysts bore an envelope polysaccharide layer (Fig. 6) and their nitrogenase activity was not substantially increased in anoxic assays, suggesting that they do not have a cell envelope problem. To explore the possibility of a limited sucrose supply to the heterocysts, we investigated whether the *glsC* and *glsP* mutations affect intercellular molecular exchange tested with the fluorescent sucrose analog esculin. We have observed that the transfer of esculin in filaments of strains mutated in *glsC*, *glsP*, or *hepP* is impaired between vegetative cells but not from vegetative cells to heterocysts (Table 3). Impairment of sucrose transfer between vegetative cells might eventually limit sucrose supply to heterocysts, and a low supply of reductant would explain the low nitrogenase activities detected in *glsC*, *glsP*, and *glsC glsP* mutants. In the case of the *glsC glsP* double mutant, the small number of vegetative cells in heterocyst-containing filaments, which are short (Fig. 6 and Fig. S6), may further limit the supply of reductant for nitrogenase. On the other hand, esculin transfer to heterocysts was substantially increased in the *hepP* mutant (Table 3). At least some sucrose transporters of the MFS family can function bidirectionally (45), and this could be the case for HepP, which appears to export saccharides from the heterocysts (33). Therefore, the apparently increased transfer of esculin to heterocysts in the *hepP* mutant might reflect increased retention of esculin in the heterocysts of this strain.

Influence of the glucoside transporters on septal junctions. Starting from the observation that the *glsC*, *glsP*, and *hepP* mutants characterized in this work are impaired in the transfer of esculin between vegetative cells, we found that intercellular transfer of fluorescent markers is in general affected in these mutants, with the highest effect being observed on the transfer of calcein. A greater effect on transfer of calcein than of 5-CF or esculin is reminiscent of the effect of inactivation of *sepJ* (14, 17, 18). Hence, these observations suggest a role of the glucoside transporters in proper function of the SepJ-related septal junctions. GFP fusions indicate that GlsC, GlsP, and HepP are located in the periphery of the cells, including the intercellular septa (Fig. 4 and Fig. S4) (33), where they could interact with the septal junction complexes. To investigate whether such interactions are feasible, BACTH analysis was carried out with the glucoside transporter proteins and SepJ. This analysis showed that GlsP and, most strongly, HepP can interact with SepJ, whereas no interaction was observed between SepJ and GlsC. Hence, GlsP and HepP may affect SepJ function by means of protein-protein interactions. A functional dependence between SepJ and an ABC transporter for polar amino acids has also been described (46). These observations suggest that proper operation of SepJ and, hence, of the SepJ-related septal junctions requires interaction with other cytoplasmic membrane proteins.

GlsC is instead required for proper location of SepJ and maturation of the intercellular septa, as illustrated by the presence of a lower number of nanopores in the *glsC* mutant than in the wild type. How GlsC influences SepJ localization and nanopore formation is unknown, but we note (i) that an N-acetylmuramoyl-L-alanine amidase, AmiC, is required for drilling the septal peptidoglycan nanopores (19), and (ii) that the presence of septal proteins, including SepJ, is needed for the amidase to make the nanopores (18). In other bacteria, the ABC transporter-like FtsEX complex, in which FtsE is an ATP-binding subunit, is required for activation of amidases that split the septal peptidoglycan during cell division (47, 48) and of endopeptidases that function in cell elongation (49, 50). An appealing hypothesis is that GlsC participates in an ABC transporter-like complex that regulates amidases involved in nanopore formation with an effect on localization of SepJ.

The different effects of inactivation of *glsC*, i.e., impairment of esculin uptake and alteration of septal structure, indicate that GlsC has multiple functions. Multitask ATP-binding subunits that serve different ABC transporters have been described, e.g., in *Streptomyces lividans* (51), *Streptococcus mutans* (52), *Bacillus subtilis* (53), and *Co-*

Nieves-Morión et al.

rynebacterium alkanolyticum (54), as well as in Anabaena (55). As checked at the Integrated Microbial Genomes webpage (https://img.jgi.doe.gov/cgi-bin/m/main.cgi), the glsC gene is not clustered with any other gene encoding an ABC transporter component in any cyanobacterium whose genome sequence is available. Therefore, no preferential association of GlsC to any particular ABC transporter can be established based on genomic data. Nonetheless, in a few cases the neighboring genes are related to cell wall biosynthesis, including an N-acetylmuramoyl-L-alanine amidase-encoding gene in Spirulina major PCC 6313, consistent with the idea of a relationship between GlsC and cell wall maturation.

In summary, we have identified three genes encoding components of transporters that mediate α-glucoside uptake, including sucrose uptake, in Anabaena. These transporters appear to influence septal junction maturation in the case of glsC or function in the case of glsP and hepP. As a consequence, inactivation of these genes impairs molecular transfer between vegetative cells, negatively affecting diazotrophy. A major task for future research is to explore whether the interplay between these transporters and SepJ has a function regulating the activity of septal junctions.

MATERIALS AND METHODS

Strains and growth conditions. Anabaena sp. strain PCC 7120 and derivative strains (described in Table S1 in the supplemental material) were grown in BG11 medium modified to contain ferric citrate instead of ferric ammonium citrate (43) or BG11$_0$ medium (BG11 further modified by omission of NaNO$_3$) at 30°C in the light (ca. 25 to 30 μmol photons m^{-2} s^{-1}) in shaken (100 rpm) liquid cultures. For tests on solid medium, medium BG11 or BG11$_0$ was solidified with 1% (wt/vol) Difco Bacto agar. For isolation of the glsC (alr4781), glsP (all0261), and glsC glsP mutants, Anabaena was grown, with shaking, in flask cultures of AA/8 liquid medium with nitrate (56) or in medium AA with nitrate solidified with 1.2% (wt/vol) purified (Difco) Bacto agar (56) at 30°C and illuminated as described above. When appropriate, antibiotics were added to the cyanobacterial cultures at the following concentrations: in liquid cultures, streptomycin sulfate (Sm), 2 to 5 μg ml^{-1}; spectinomycin dihydrochloride pentahydrate (Sp), 2 to 5 μg ml^{-1}; erythromycin (Em), 5 μg ml^{-1}; and neomycin sulfate (Nm), 5 to 25 μg ml^{-1}; in solid media, Sm, 5 to 10 μg ml^{-1}; Sp, 5 to 10 μg ml^{-1}; Em, 5 to 10 μg ml^{-1}; and Nm, 30 to 40 μg ml^{-1}. Chlorophyll a (Chl) content of cultures was determined by the method of Mackinney (57).

E. coli strains were grown in LB medium, supplemented when appropriate with antibiotics at standard concentrations (58). E. coli strain DH5α or DH5αMCR was used for plasmid constructions. E. coli strain DH5α or ED8654, bearing a conjugative plasmid, and strain HB101 or DH5αMCR, bearing a methylase-encoding helper plasmid and the cargo plasmid, were used for conjugation with Anabaena, unless stated otherwise (59).

Construction of Anabaena mutant strains. The alr4781 (glsC) mutant, DR3912a, was generated by a diparental mating between Anabaena and DH5αMCR carrying pRL443, pRL3857a, and pRL3912a (plasmids described in Table S1). The single recombinant was selected on Em, tested for sucrose sensitivity, and then went through a sucrose selection cycle, as described by Cai and Wolk (60), for selection of the double recombinant (Fig. S1). Similarly, an all0261 (glsP) double recombinant deletion mutant, DR3915 (Fig. S1), was generated by mating between Anabaena and DH5αMCR carrying pRL443, pRL3857a, and pRL3915. Because DR3912a and DR3915 carry the same antibiotic resistance marker (Sm^r Sp^r), a new plasmid, pRL3985a, was constructed for creation of the glsC glsP double mutant (Fig. S1). In this case, pRL3985a was introduced into DR3912a by conjugation, and the mutant was selected as described above.

For complementation of the glsC mutant (DR3912a), a fragment containing ORF alr4781 and 202 bp of upstream and 49 bp of downstream DNA was amplified using Anabaena DNA as the template and primers alr4781-3 and alr4781-4 (oligodeoxynucleotide primers are described in Table S1). The PCR product was cloned into vector pSpark I, producing pCSMN21. This construct was verified by sequencing and transferred as a BamHI fragment to pRL25C (61) digested with the same enzyme, producing pCSMN22. This plasmid was transferred to DR3912a by conjugation. Clones resistant to Sm, Sp, and Nm were isolated and their genetic structure verified by PCR with primers alr4781-3 and alr4781-4 (Fig. S5). This strain was named CSMN11. For complementation of the glsP mutant (DR3915), a fragment containing ORF all0261 and 103 bp of upstream and 40 bp of downstream DNA was amplified using Anabaena DNA as the template and primers all0261-3 and all0261-4. The PCR product was cloned into pSpark I, producing pCSMN19, which was confirmed by sequencing and transferred as a BamHI fragment to pRL25C digested with BamHI, producing pCSMN20. This plasmid was transferred to DR3915 by conjugation. Clones resistant to Sm, Sp, and Nm were insolated and their genetic structure was verified by PCR with primers all0261-3 and all0261-4 (Fig. S5). This strain was named CSMN12.

For inactivation of alr3705, an internal fragment of 560 bp was amplified by PCR using Anabaena DNA as the template and primers alr3705-1 (bearing a BamHI site in its 5' end) and alr3705-2. The amplified fragment was cloned into pMBL-T (http://www.molbiolab.es/uploads/phpgSgmue.pdf; Dominion MBL, Spain) and transferred as a BamHI-ended fragment (the second BamHI site is from the vector multiple-cloning site) to BamHI-digested pCSV3 (62), producing pCSRL49. This plasmid was transformed into E. coli HB101 carrying pRL623 and transferred to Anabaena and to hepP (all1711) mutant strain FQ163 (33) by

conjugation with selection for Sm^r and Sp^r (because FQ163 is itself Nm^r, Sm^r, and bleomycin resistant, in this case effective selection is only for Sp^r). Clones that had incorporated pCSRL49 by single recombination were selected for further study and named strain CSRL15 (wild-type background) and CSMN3 (*hepP* background) (Fig. S2).

To prepare an *Anabaena* strain producing a fusion of GFP to GlsC, a 950-bp DNA fragment from the 3′ region of *glsC* (*alr4781*) was amplified using *Anabaena* DNA as the template and primers alr4781-5 and alr4781-6. The 950-bp PCR product was cloned into pSpark I, producing pCSMN23. This construct was validated by sequencing and transferred to SacI-XhoI-digested pRL277 (63) as a SacI-NheI fragment together with NheI-SalI-digested *gfp-mut2* (64), producing pCSMN24, in which the *gfp-mut2* gene is fused to *glsC*. pCSMN24 was transferred to *Anabaena* by conjugation. Clones resistant to Sm and Sp were selected and their genetic structure was verified by PCR with primer pairs alr4781-3/gfp-5 and alr4781-3/alr4781-4. This strain was named CSMN13 (Fig. S3). To prepare an *Anabaena* strain producing a fusion of GFP to GlsP, a 482-bp DNA fragment from the 3′ region of *glsP* (*all0261*) was amplified using *Anabaena* DNA as the template and primers all0261-6 and all0261-5. The PCR product, a SacI-NheI fragment, was inserted together with NheI-SalI-digested *gfp-mut2* into SacI-XhoI-digested pRL277 (63), producing pCSMN25, which bears a fusion of the *all0261* coding sequence to the *gfp-mut2* gene. This construct was verified by sequencing and transferred to *Anabaena* by conjugation. Clones resistant to Sm and Sp were isolated, and integration of the *glsP-gfp* construct was verified by PCR using primer pairs all0261-4/gfp-5 and all0261-3/all0261-4. This strain was named CSMN15 (Fig. S3).

To study the effect of inactivation of transporter genes on the localization of SepJ-GFP, Nm^r plasmid pCSVT22, bearing *sepJ-gfp* (13), was transferred to strains DR3912a (*alr4781*::C.S3) and DR3915 (*all0261*::C.S3) by conjugation. Similarly, the Sm^r Sp^r plasmid pCSAM137, bearing *sepJ-gfp* (12), was transferred to FQ163 (*hepP*::Tn5-1063) (33). The genetic structure of selected clones bearing *sepJ-gfp* fusions was studied by PCR with DNA from those clones and primer pair alr2338-3/gfp-5 to test recombination in the correct genomic location (*sepJ*). We also verified the mutant background in the exconjugants using the following primer pairs: for *alr4781*, alr4781-3/alr4781-4; for *all0261*, all0261-3/all0261-4; and for *hepP*, all1711-3/all1711-4 (Fig. S7). Clones bearing the *sepJ-gfp* fusion were named strain CSMN9 (*alr4781* background), CSMN10 (*all0261* background), and CSMN16 (*hepP* background).

RT-qPCR. For RT-qPCR, RNA was isolated as described previously (33) from 50 to 100 ml of shaken *Anabaena* cultures. RNA was treated with Ambion TURBO DNA-free DNase according to the manufacturer's protocol. Three independent RNA samples were analyzed from each strain (the wild type and the complemented *glsC* and *glsP* strains), and three technical replicates were carried out for each sample. RNA (200 ng) was reverse transcribed using a QuantiTect reverse transcription kit (Qiagen) with random primers as indicated by standard protocols of the manufacturer. Quantitative real-time PCR was performed on an iCycler iQ real-time PCR detection system equipped with the iCycler iQ v 3.0 software from Bio-Rad. PCR amplification was performed in a 20-μl reaction mix according to standard protocols of the SensiFAST SYBR and fluorescein kit (Bioline). qPCR conditions were the following: 1 cycle at 95°C for 2 min, followed by 30 cycles of 95°C for 15 s, 67.5°C for 20 s, and 72°C for 30 s. PCR products were checked by a single-peak melting curve. The threshold cycle (C_T) of each gene was determined and normalized to those of reference genes *ispD* (*all5167*) and *dxs* (*alr0599*) to obtain ΔC_T values from each sample. Relative gene expression was calculated using the $2^{-\Delta\Delta CT}$ method (65), and the data presented correspond to the average of data obtained with each reference gene. The following primer pairs were used: all0261-11/all0261-12, alr4781-9/alr4781-10, all5167-1/all5167-2, and alr0599-1/alr0599-2 (Table S1).

Uptake of esculin. *Anabaena* strains grown in BG11 medium, with antibiotics for the mutants, were harvested by centrifugation, washed three times with BG11 or BG11$_0$ medium without antibiotics, and incubated for 18 h in the same medium under culture conditions. Cells were harvested, washed, and resuspended in the corresponding growth medium supplemented with 10 mM HEPES-NaOH buffer (pH 7, unless indicated otherwise), and 1 mM the indicated sugar in the experiment depicted in Fig. 3. Assays of uptake were started by addition of esculin hydrate (Sigma-Aldrich) at 100 μM, and suspensions were incubated at 30°C in the light (~170 μmol photons m^{-2} s^{-1}) for up to 70 min. One-ml samples were withdrawn and filtered. Cells on the filters were washed with 10 mM HEPES-NaOH buffer of the same pH used in the assay and were resuspended in 2 ml of 10 mM HEPES-NaOH buffer (pH 7). Fluorescence of the resulting cell suspension was measured in a Varian Cary eclipse fluorescence spectrophotometer (excitation, 360 $\pm$ 10 nm; emission, 462 $\pm$ 10 nm). Esculin solutions in the same buffer (pH 7) were used as standards. Significance in the differences of uptake between strains (as well as in other parameters investigated in this work) was assessed by unpaired Student's *t* tests, assuming a normal distribution of the data. Data sets with *P* values of <0.05 are considered significant.

Growth curves and nitrogenase activity. The growth rate constant ($\mu = [\ln2]/t_d$, where t_d is the doubling time) was calculated from the increase in the optical density at 750 nm (OD$_{750}$) of shaken liquid cultures. Cultures were inoculated with an amount of cells giving an OD$_{750}$ of about 0.05 (light path, 1 cm) and grew logarithmically until reaching an OD$_{750}$ of about 0.8 to 0.9. The suspensions of filaments were carefully homogenized with a pipette before taking the samples.

For determination of nitrogenase activity, filaments grown in BG11 medium were harvested, washed with BG11$_0$ medium, and resuspended in BG11$_0$ medium. After 48 h of incubation under growth conditions, the filaments were used in acetylene reduction assays performed under oxic or anoxic conditions at 30°C in the light (ca. 150 μmol photons m^{-2} s^{-1}). For these assays, the cell suspensions (2 ml; ca. 10 μg Chl ml^{-1}) were placed in flasks sealed with rubber stoppers (total volume, 12 to 14 ml). For the anoxic assays, the cell suspensions were supplemented with 10 μM 3-(3,4-dichlorophenyl)-1,1-dimethylurea (DCMU), bubbled thoroughly with argon for 3 min, and incubated for 60 min under assay conditions before starting the reaction. Production of ethylene, determined by gas chromatography in

1-ml samples from the gas phase, was monitored for up to 3 h after starting the reaction by addition of acetylene (2 ml).

Light, confocal, and fluorescence microscopy. Cultures were routinely observed by light micros-copy. To stain the polysaccharide layer of heterocysts, cell suspensions were mixed (1:2) with a filtered 1% (wt/vol) alcian blue (Sigma) solution.

For visualization by confocal microscopy of filaments of strains producing genetic fusions to GFP, small blocks of agar-solidified BG11 or $BG11_0$ medium bearing the filaments were excised and placed in a sample holder with a glass coverslip on top. GFP fluorescence was visualized using a Leica HCX Plan Apo 63× 1.4-numeric-aperture (NA) oil immersion objective attached to a Leica TCS SP2 confocal laser-scanning microscope. GFP was excited using 488-nm irradiation from an argon ion laser. Fluores-cent emission was monitored by collection across windows of 498 to 541 nm (GFP imaging) and 630 to 700 nm (cyanobacterial autofluorescence). GFP fluorescence intensity was analyzed using ImageJ 1.45s software. To determine the relative fluorescence intensity in different cell zones, integrated density was recorded in squares of 0.2 to 0.8 μm^2. About 80 to 190 measurements were made for each of the lateral walls and septal areas of vegetative cells from BG11 or $BG11_0$ medium, and 50 to 60 measurements were made for lateral walls of heterocysts. We could not accurately quantify GFP fluorescence from heterocyst-vegetative cell septa, which are thinner than the septa between vegetative cells. Because fluorescence did not follow a normal distribution, data are presented as median and interquartile ranges (66).

For fluorescence microscopy, filaments of cells were imaged using a Leica DM6000B fluorescence microscope and an ORCA-ER camera (Hamamatsu). GFP fluorescence was monitored using a fluorescein isothiocyanate (FITC) L5 filter (excitation band pass [BP], 480/40 nm; emission BP, 527/30 nm), and red autofluorescence was monitored using a Texas red TX2 filter (excitation BP, 560/40 nm; emission BP, 645/75 nm).

Immunolocalization of SepJ. Cells from 1.5 ml of liquid cultures were collected by centrifugation, placed atop a poly-L-lysine-precoated microscope slide, and covered with a 45-μm-pore-size Millipore filter. The filter was removed and the slide was left to dry at room temperature, immersed in 70% ethanol at −20°C for 30 min, and dried for 15 min at room temperature. The cells were washed twice (2 min each time, room temperature) by covering the slide with PBS-T (PBS supplemented with 0.05% Tween 20). Subsequently, the slides were treated with a blocking buffer (5% milk powder in PBS-T) for 15 min. Cells on the slides were then incubated for 90 min with anti-SepJ-CC antibodies (17) diluted in blocking buffer (1:250), washed three times with PBS-T, incubated for 45 min in the dark with anti-rabbit antibody conjugated to FITC (1:500 dilution in PBS-T; Sigma), and washed three times with PBS-T. After being dried, several drops of FluorSave (Calbiochem) were added atop, covered with a coverslip, and sealed with nail lacquer. Fluorescence was monitored as described above, and images were analyzed with ImageJ software (http://imagej.nih.gov/ij).

Visualization of nanopores by electron microscopy. The murein sacculi (which are made of peptidoglycan) were isolated from filaments grown in BG11 medium and analyzed as described previously (18, 19). The purified sacculi were deposited on Formvar/carbon film-coated copper grids and stained with 1% (wt/vol) uranyl acetate. All of the samples were examined with a Zeiss Libra 120 Plus electron microscope at 120 kV.

FRAP analysis. For assays of intercellular transfer of esculin, filaments were harvested, resuspended in 500 μl of fresh growth medium, mixed with 15 μl of saturated (~5 mM) aqueous esculin hydrate solution, incubated for 1 h in the dark with gentle shaking at 30°C, and then washed three times with growth medium, followed by incubation in the dark for 15 min in 1 ml medium at 30°C with gentle shaking. Cells were then washed and spotted onto a BG11 or $BG11_0$ agar plate (1%, wt/vol), and excess medium was removed. Small blocks of agar with cells adsorbed on the surface were placed in a custom-built temperature-controlled sample holder under a glass coverslip at 30°C. Cells were visualized with a laser-scanning confocal microscope (Leica TCS SP5) using a Leica HCX Plan Apo 63× 1.4-NA oil-immersion objective. Fluorescence was excited at 355 nm, with detection of esculin at 443 to 490 nm and detection of Chl at 670 to 720 nm. High-resolution imaging used a 6× line average with an optical section of ~0.7 μm. FRAP measurements were without line averaging and with a wide pinhole, giving an optical section of ~4 μm. After capturing a prebleach image, the fluorescence of a defined region of interest was bleached out by scanning this region at ~6× higher laser intensity, and recovery was then recorded in a sequence of full-frame images.

For calcein and 5-CF transfer assays, calcein and 5-CF staining and FRAP analysis were performed as previously reported (7, 14). Cell suspensions were spotted onto agar and placed in a custom-built temperature-controlled sample holder with a glass coverslip on top. All measurements were carried out at 30°C. For both calcein and 5-CF, cells were imaged with a Leica HCX Plan Apo 63×, 1.4-NA oil immersion objective attached to a Leica TCS SP5 confocal laser-scanning microscope as previously described for calcein (7), with a 488-nm line argon laser as the excitation source. Fluorescent emission was monitored by collection across windows of 500 to 520 nm or 500 to 527 nm in different experiments and a 150-μm pinhole. After an initial image was recorded, the bleach was carried out by an automated FRAP routine which switched the microscope to X scanning mode, increased the laser intensity by a factor of 10, and scanned a line across one cell for 0.137 s before reducing the laser intensity, switching back to XY imaging mode, and recording a sequence of images typically at 1-s intervals.

For FRAP data analysis, we quantified kinetics of transfer of the fluorescent tracer to either (i) a terminal cell (with one cell junction) or (ii) a cell somewhere in the middle of a filament (i.e., with two cell junctions). For the first option, the recovery rate constant, R, was calculated from the formula $C_B = C_0 + C_R (1 − e^{−Rt})$, where C_B is fluorescence in the bleached cell, C_0 is fluorescence immediately after the bleach and tending toward $(C_0 + C_R)$ after fluorescence recovery, t is time, and R is the recovery rate

constant due to transfer of the tracer from one neighbor cell (14). For the second option, the formula $C_B = C_0 + C_R (1 - e^{-2Rt})$ was used. Development of equations for FRAP analysis is described in the supplemental material (Text S1).

BACTH strain construction and assays. The possible interaction of the different glucoside transporters with SepJ was tested using bacterial adenylate cyclase two-hybrid (BACTH) analysis. For this analysis, all tested genes were amplified using *Anabaena* DNA as the template. The following primers were used: alr4781-7 and alr4781-8 to amplify *glsC*, all0261-7 and all0261-8 to amplify *glsP*, and all1711-9 and all1711-10 to amplify *hepP*. The PCR products were cloned in vector pSpark I, transformed into *E. coli* DH5α, and sequenced. Inserts with the correct sequence were transferred as XbaI- and KpnI-digested fragments to pUT18, pUT18C, pKNT25, and pKT25 (37), producing fusions to the 5′ and 3′ ends of the genes encoding the adenylate cyclase T18 and T25 fragments, respectively. The resulting plasmids were transformed into *E. coli* XL1-Blue to amplify the plasmids. Fusions of the *sepJ* gene to the 5′ end of T18 or T25 were as previously described (15). Isolated plasmids were cotransformed into *E. coli* BTH101 (*cya-99*). Transformants were plated onto LB medium containing selective antibiotics and 1% glucose. Efficiencies of interactions between different hybrid proteins were quantified by measurement of β-galactosidase activity in cells from liquid cultures.

To determine β-galactosidase activity, bacteria were grown in LB medium in the presence of 0.5 mM isopropyl-β-D-thiogalactopyranoside (IPTG) and appropriate antibiotics at 30°C for 16 h. Before the assays, cultures were diluted 1:5 into buffer Z (60 mM Na_2HPO_4, 40 mM NaH_2PO_4, 10 mM KCl, and 1 mM $MgSO_4$). To permeabilize cells, 30 μl of toluene and 35 μl of a 0.1% SDS solution were added to 2.5 ml of bacterial suspension. The tubes were vortexed for 10 s and incubated with shaking at 37°C for 30 min for evaporation of toluene. For the enzymatic reaction, 875 μl of permeabilized cells was added to buffer Z supplemented with β-mercaptoethanol (25 mM final concentration) to a final volume of 3.375 ml. The tubes were incubated at 30°C in a water bath for at least 5 min. The reaction was started by adding 875 μl of 0.4 mg ml^{-1} *o*-nitrophenol-β-galactoside (ONPG) in buffer Z. Samples of 1 ml, taken at different times (up to 12 min), were added to 0.5 ml of 1 M Na_2CO_3 to stop the reaction. A_{420} was recorded, and the amount of *o*-nitrophenol produced was calculated using an extinction coefficient, ε_{420}, of 4.5 mM^{-1} cm^{-1} and referred to the amount of total protein, determined by a modified Lowry procedure.

SUPPLEMENTAL MATERIAL

Supplemental material for this article may be found at https://dx.doi.org/10.1128/JB.00876-16.

TEXT S1, PDF file, 8.4 MB.

REFERENCES

1. Flores E, Herrero A. 2014. The cyanobacteria: morphological diversity in a photoautotrophic lifestyle. Perspect Phycol 1:63–72. https://doi.org/10.1127/pip/2014/0008.
2. Wolk CP. 1996. Heterocyst formation. Annu Rev Genet 30:59–78. https://doi.org/10.1146/annurev.genet.30.1.59.
3. Wolk CP, Ernst A, Elhai J. 1994. Heterocyst metabolism and development, p 769–823. *In* Bryant DA (ed), The molecular biology of cyanobacteria. Kluwer Academic Publishers, Dordrecht, the Netherlands.
4. Herrero A, Stavans J, Flores E. 2016. The multicellular nature of filamentous heterocyst-forming cyanobacteria. FEMS Microbiol Rev 40:831–854. https://doi.org/10.1093/femsre/fuw029.
5. Flores E, Herrero A, Wolk CP, Maldener I. 2006. Is the periplasm continuous in filamentous multicellular cyanobacteria? Trends Microbiol 14:439–443. https://doi.org/10.1016/j.tim.2006.08.007.
6. Mariscal V, Herrero A, Flores E. 2007. Continuous periplasm in a filamentous, heterocyst-forming cyanobacterium. Mol Microbiol 65:1139–1145. https://doi.org/10.1111/j.1365-2958.2007.05856.x.
7. Mullineaux CW, Mariscal V, Nenninger A, Khanum H, Herrero A, Flores E, Adams DG. 2008. Mechanism of intercellular molecular exchange in heterocyst-forming cyanobacteria. EMBO J 27:1299–1308. https://doi.org/10.1038/emboj.2008.66.
8. Mariscal V. 2014. Cell-cell joining proteins in heterocyst-forming cyanobacteria, p 293–304. *In* Flores E, Herrero A (ed), The cell biology of cyanobacteria. Caister Academic Press, Norfolk, United Kingdom.
9. Mullineaux CW, Nürnberg DJ. 2014. Tracing the path of a prokaryotic paracrine signal. Mol Microbiol 94:1208–1212. https://doi.org/10.1111/mmi.12851.
10. Flores E, Herrero A, Forchhammer K, Maldener I. 2016. Septal junctions in filamentous heterocyst-forming cyanobacteria. Trends Microbiol 24:79–82. https://doi.org/10.1016/j.tim.2015.11.011.
11. Erickson RO. 1986. Symplastic growth and symplasmic transport. Plant Physiol 82:1153. https://doi.org/10.1104/pp.82.4.1153.
12. Flores E, Pernil R, Muro-Pastor AM, Mariscal V, Maldener I, Lechno-Yossef S, Fan Q, Wolk CP, Herrero A. 2007. Septum-localized protein required

for filament integrity and diazotrophy in the heterocyst-forming cyanobacterium *Anabaena* sp. strain PCC 7120. J Bacteriol 189:3884–3890. https://doi.org/10.1128/JB.00085-07.

13. Merino-Puerto V, Mariscal V, Mullineaux CW, Herrero A, Flores E. 2010. Fra proteins influencing filament integrity, diazotrophy and localization of septal protein SepJ in the heterocyst-forming cyanobacterium *Anabaena* sp. Mol Microbiol 75:1159–1170. https://doi.org/10.1111/j.1365-2958.2009.07031.x.

14. Merino-Puerto V, Schwarz H, Maldener I, Mariscal V, Mullineaux CW, Herrero A, Flores E. 2011. FraC/FraD-dependent intercellular molecular exchange in the filaments of a heterocyst-forming cyanobacterium, Anabaena sp. Mol Microbiol 82:87–98. https://doi.org/10.1111/j.1365-2958.2011.07797.x.

15. Ramos-León F, Mariscal V, Frías JE, Flores E, Herrero A. 2015. Divisome-dependent subcellular localization of cell-cell joining protein SepJ in the filamentous cyanobacterium *Anabaena*. Mol Microbiol 96:566–580. https://doi.org/10.1111/mmi.12956.

16. Rudolf M, Tetik N, Ramos-León F, Flinner N, Ngo G, Stevanovic M, Burnat M, Pernil R, Flores E, Schleiff E. 2015. The peptidoglycan-binding protein SjcF1 influences septal junction function and channel formation in the filamentous cyanobacterium *Anabaena*. mBio 6(4):e00376-15.

17. Mariscal V, Herrero A, Nenninger A, Mullineaux CW, Flores E. 2011. Functional dissection of the three-domain SepJ protein joining the cells in cyanobacterial trichomes. Mol Microbiol 79:1077–1088. https://doi.org/10.1111/j.1365-2958.2010.07508.x.

18. Nürnberg DJ, Mariscal V, Bornikoel J, Nieves-Morión M, Krauß N, Herrero A, Maldener I, Flores E, Mullineaux CW. 2015. Intercellular diffusion of a fluorescent sucrose analog via the septal junctions in a filamentous cyanobacterium. mBio 6(2):e02109.

19. Lehner J, Berendt S, Dörsam B, Pérez R, Forchhammer K, Maldener I. 2013. Prokaryotic multicellularity: a nanopore array for bacterial cell communication. FASEB J 27:2293–2230. https://doi.org/10.1096/fj.12-225854.

20. Omairi-Nasser A, Mariscal V, Austin JR, II, Haselkorn R. 2015. Requirement of Fra proteins for communication channels between cells in the filamentous nitrogen-fixing cyanobacterium *Anabaena* sp. PCC 7120. Proc Natl Acad Sci U S A 112(32):E4458–E4464.

21. Schilling N, Ehrnsperger K. 1985. Cellular differentiation of sucrose metabolism in *Anabaena variabilis*. Z Naturforsch 40c:776–779.

22. Curatti L, Flores E, Salerno G. 2002. Sucrose is involved in the diazotrophic metabolism of the heterocyst-forming cyanobacterium *Anabaena* sp. FEBS Lett 513:175–178. https://doi.org/10.1016/S0014-5793(02)02283-4.

23. López-Igual R, Flores E, Herrero A. 2010. Inactivation of a heterocyst-specific invertase indicates a principal role of sucrose catabolism in the heterocysts of *Anabaena* sp. J Bacteriol 192:5526–5533. https://doi.org/10.1128/JB.00776-10.

24. Vargas WA, Nishi CN, Giarrocco LE, Salerno GL. 2011. Differential roles of alkaline/neutral invertases in *Nostoc* sp. PCC 7120: Inv-B isoform is essential for diazotrophic growth. Planta 233:153–162.

25. Kolman MA, Nishi CN, Perez-Cenci M, Salerno GL. 2015. Sucrose in cyanobacteria: from a salt-response molecule to play a key role in nitrogen fixation. Life (Basel) 5:102–126.

26. Nieves-Morión M, Mullineaux CW, Flores E. 2017. Molecular diffusion through cyanobacterial septal junctions. mBio 8:e01756-16.

27. Stebegg R, Wurzinger B, Mikulic M, Schmetterer G. 2012. Chemoheterotrophic growth of the cyanobacterium *Anabaena* sp. strain PCC 7120 dependent on a functional cytochrome *c* oxidase. J Bacteriol 194:4601–4607. https://doi.org/10.1128/JB.00687-12.

28. Gora PJ, Reinders A, Ward JM. 2012. A novel fluorescent assay for sucrose transporters. Plant Methods 8:13. https://doi.org/10.1186/1746-4811-8-13.

29. Park J-J, Lechno-Yossef S, Wolk CP, Vieille C. 2013. Cell-specific gene expression in *Anabaena variabilis* grown phototrophically, mixotrophically and heterotrophically. BMC Genomics 14:759. https://doi.org/10.1186/1471-2164-14-759.

30. Kaneko T, Nakamura Y, Wolk CP, Kuritz T, Sasamoto S, Watanabe A, Iriguchi M, Ishikawa A, Kawashima K, Kimura T, Kishida Y, Kohara M, Matsumoto M, Matsuno A, Muraki A, Nakazaki N, Shimpo S, Sugimoto M, Takazawa M, Yamada M, Yasuda M, Tabata S. 2001. Complete genomic sequence of the filamentous nitrogen-fixing cyanobacterium *Anabaena* sp. strain PCC 7120. DNA Res 8:205–213. https://doi.org/10.1093/dnares/8.5.205.

31. Elhai J, Wolk CP. 1988. A versatile class of positive-selection vectors based on the nonviability of palindrome-containing plasmids that allows cloning into long polylinkers. Gene 68:119–138. https://doi.org/10.1016/0378-1119(88)90605-1.

32. Cui J, Davidson AL. 2011. ABC solute importers in bacteria. Essays Biochem 50:85–99. https://doi.org/10.1042/bse0500085.

33. López-Igual R, Lechno-Yossef S, Fan Q, Herrero A, Flores E, Wolk CP. 2012. A major facilitator superfamily protein, HepP, is involved in formation of the heterocyst envelope polysaccharide in the cyanobacterium Anabaena sp. strain PCC 7120. J Bacteriol 194:4677–4687. https://doi.org/10.1128/JB.00489-12.

34. Drew D, Sjöstrand D, Nilsson J, Urbig T, Chin CN, de Gier JW, von Heijne G. 2002. Rapid topology mapping of *Escherichia coli* inner-membrane proteins by prediction and PhoA/GFP fusion analysis. Proc Natl Acad Sci U S A 99:2690–2695. https://doi.org/10.1073/pnas.052018199.

35. McKinney RE. 1953. Staining bacterial polysaccharides. J Bacteriol 66:453–454.

36. Karimova G, Pidoux J, Ullmann A, Ladant D. 1998. A bacterial two-hybrid system based on a reconstituted signal transduction pathway. Proc Natl Acad Sci U S A 95:5752–5756. https://doi.org/10.1073/pnas.95.10.5752.

37. Battesti A, Bouveret E. 2012. The bacterial two-hybrid system based on adenylate cyclase reconstitution in Escherichia coli. Methods 58:325–334. https://doi.org/10.1016/j.ymeth.2012.07.018.

38. Stynen B, Tournu H, Tavernier J, Van Dijck P. 2012. Diversity in genetic in vivo methods for protein-protein interaction studies: from the yeast two-hybrid system to the mammalian split-luciferase system. Microbiol Mol Biol Rev 76:331–382. https://doi.org/10.1128/MMBR.05021-11.

39. Flaherty BL, van Nieuwerburgh F, Head SR, Golden JW. 2011. Directional RNA deep sequencing sheds new light on the transcriptional response of *Anabaena* sp. strain PCC 7120 to combined-nitrogen deprivation. BMC Genomics 12:332. https://doi.org/10.1186/1471-2164-12-332.

40. Nicolaisen K, Mariscal V, Bredemeier R, Pernil R, Moslavac S, López-Igual R, Maldener I, Herrero A, Schleiff E, Flores E. 2009. The outer membrane is a permeability barrier for intercellularly exchanged metabolites in a heterocyst-forming cyanobacterium. Mol Microbiol 74:58–70. https://doi.org/10.1111/j.1365-2958.2009.06850.x.

41. Reinders A, Sivitz AB, Ward JM. 2012. Evolution of plant sucrose uptake transporters. Front Plant Sci 3:22.

42. Stuart RK, Mayali X, Lee JZ, Craig Everroad R, Hwang M, Bebout BM, Weber PK, Pett-Ridge J, Thelen MP. 2015. Cyanobacterial reuse of extracellular organic carbon in microbial mats. ISME J 10:1240–1251.

43. Rippka R, Deruelles J, Waterbury JB, Herdman M, Stanier RY. 1979. Generic assignments, strain histories and properties of pure cultures of cyanobacteria. J Gen Microbiol 111:1–61.

44. Ungerer JL, Pratte BS, Thiel T. 2008. Regulation of fructose transport and its effect on fructose toxicity in *Anabaena* spp. J Bacteriol 190:8115–8125. https://doi.org/10.1128/JB.00886-08.

45. Ayre BG. 2011. Membrane-transport systems for sucrose in relation to whole-plant carbon partitioning. Mol Plant 4:377–394. https://doi.org/10.1093/mp/ssr014.

46. Escudero L, Mariscal V, Flores E. 2015. Functional dependence between septal protein SepJ from *Anabaena* sp. strain PCC 7120 and an amino acid ABC-type uptake transporter. J Bacteriol 197:2721–2730. https://doi.org/10.1128/JB.00289-15.

47. Yang DC, Peters NT, Parzych KR, Uehara T, Markovski M, Bernhardt TG. 2011. An ATP-binding cassette transporter-like complex governs cell-wall hydrolysis at the bacterial cytokinetic ring. Proc Natl Acad Sci U S A 108:E1052–E1060. https://doi.org/10.1073/pnas.1107780108.

48. Bartual SG, Straume D, Stamsås GA, Muñoz IG, Alfonso C, Martínez-Ripoll M, Håvarstein LS, Hermoso JA. 2014. Structural basis of PcsB-mediated cell separation in *Streptococcus pneumoniae*. Nat Commun 5:3842.

49. Domínguez-Cuevas P, Porcelli I, Daniel RA, Errington J. 2013. Differentiated roles for MreB-actin isologues and autolytic enzymes in *Bacillus subtilis* morphogenesis. Mol Microbiol 89:1084–1098. https://doi.org/10.1111/mmi.12335.

50. Meisner J, Montero Llopis P, Sham LT, Garner E, Bernhardt TG, Rudner DZ. 2013. FtsEX is required for CwlO peptidoglycan hydrolase activity during cell wall elongation in *Bacillus subtilis*. Mol Microbiol 89:1069–1083. https://doi.org/10.1111/mmi.12330.

51. Schlösser A, Kampers T, Schrempf H. 1997. The *Streptomyces* ATP-binding component MsiK assists in cellobiose and maltose transport. J Bacteriol 179:2092–2095. https://doi.org/10.1128/jb.179.6.2092-2095.1997.

52. Webb AJ, Homer KA, Hosie AH. 2008. Two closely related ABC transporters in *Streptococcus mutans* are involved in disaccharide and/or oligo-

saccharide uptake. J Bacteriol 190:168–178. https://doi.org/10.1128/JB.01509-07.

53. Ferreira MJ, de Sá-Nogueira I. 2010. A multitask ATPase serving different ABC-type sugar importers in *Bacillus subtilis*. J Bacteriol 192:5312–5318. https://doi.org/10.1128/JB.00832-10.

54. Watanabe A, Hiraga K, Suda M, Yukawa H, Inui M. 2015. Functional characterization of *Corynebacterium alkanolyticum* β-xylosidase and xyloside ABC transporter in *Corynebacterium glutamicum*. Appl Environ Microbiol 81:4173–4183. https://doi.org/10.1128/AEM.00792-15.

55. Pernil R, Picossi S, Mariscal V, Herrero A, Flores E. 2008. ABC-type amino acid uptake transporters Bgt and N-II of *Anabaena* sp. strain PCC 7120 share an ATPase subunit and are expressed in vegetative cells and heterocysts. Mol Microbiol 67:1067–1080. https://doi.org/10.1111/j.1365-2958.2008.06107.x.

56. Hu N-T, Thiel T, Giddings TH, Wolk CP. 1981. New *Anabaena* and *Nostoc* cyanophages from sewage settling ponds. Virology 114:236–246. https://doi.org/10.1016/0042-6822(81)90269-5.

57. Mackinney G. 1941. Absorption of light by chlorophyll solutions. J Biol Chem 140:315–322.

58. Ausubel FM, Brent R, Kingston RE, Moore DD, Seidman JG, Smith JA, Struhl K. 2014. Current protocols in molecular biology. Greene Publishing and Wiley-Interscience, New York, NY.

59. Elhai J, Vepritskiy A, Muro-Pastor AM, Flores E, Wolk CP. 1997. Reduction of conjugal transfer efficiency by three restriction activities of *Anabaena* sp. strain PCC 7120. J Bacteriol 179:1998–2005. https://doi.org/10.1128/jb.179.6.1998-2005.1997.

60. Cai Y, Wolk CP. 1990. Use of a conditionally lethal gene in *Anabaena* sp. strain PCC 7120 to select for double recombinants and to entrap insertion sequences. J Bacteriol 172:3138–3145. https://doi.org/10.1128/jb.172.6.3138-3145.1990.

61. Wolk CP, Cai Y, Cardemil L, Flores E, Hohn B, Murry M, Schmetterer G, Schrautemeier B, Wilson R. 1988. Isolation and complementation of mutants of *Anabaena* sp. strain PCC 7120 unable to grow aerobically on dinitrogen. J Bacteriol 170:1239–1244. https://doi.org/10.1128/jb.170.3.1239-1244.1988.

62. Valladares A, Rodríguez V, Camargo S, Martínez-Noël GM, Herrero A, Luque I. 2011. Specific role of the cyanobacterial PipX factor in the heterocysts of *Anabaena* sp. strain PCC 7120. J Bacteriol 193:1172–1182. https://doi.org/10.1128/JB.01202-10.

63. Black TA, Cai Y, Wolk CP. 1993. Spatial expression and autoregulation of *hetR*, a gene involved in the control of heterocyst development in *Anabaena*. Mol Microbiol 9:77–84. (Erratum, **10:**1153, 1993).

64. Cormack BP, Valdivia RH, Falkow S. 1996. FACS-optimized mutants of the green fluorescent protein (GFP). Gene 173:33–38. https://doi.org/10.1016/0378-1119(95)00685-0.

65. Livak KJ, Schmittgen TD. 2001. Analysis of relative gene expression data using real-time quantitative PCR and the 2(-Delta Delta C(T)) method. Methods 25:402–408. https://doi.org/10.1006/meth.2001.1262.

66. Krzywinski M, Altman N. 2014. Visualizing samples with box plots. Nat Methods 11:119–120. https://doi.org/10.1038/nmeth.2813.
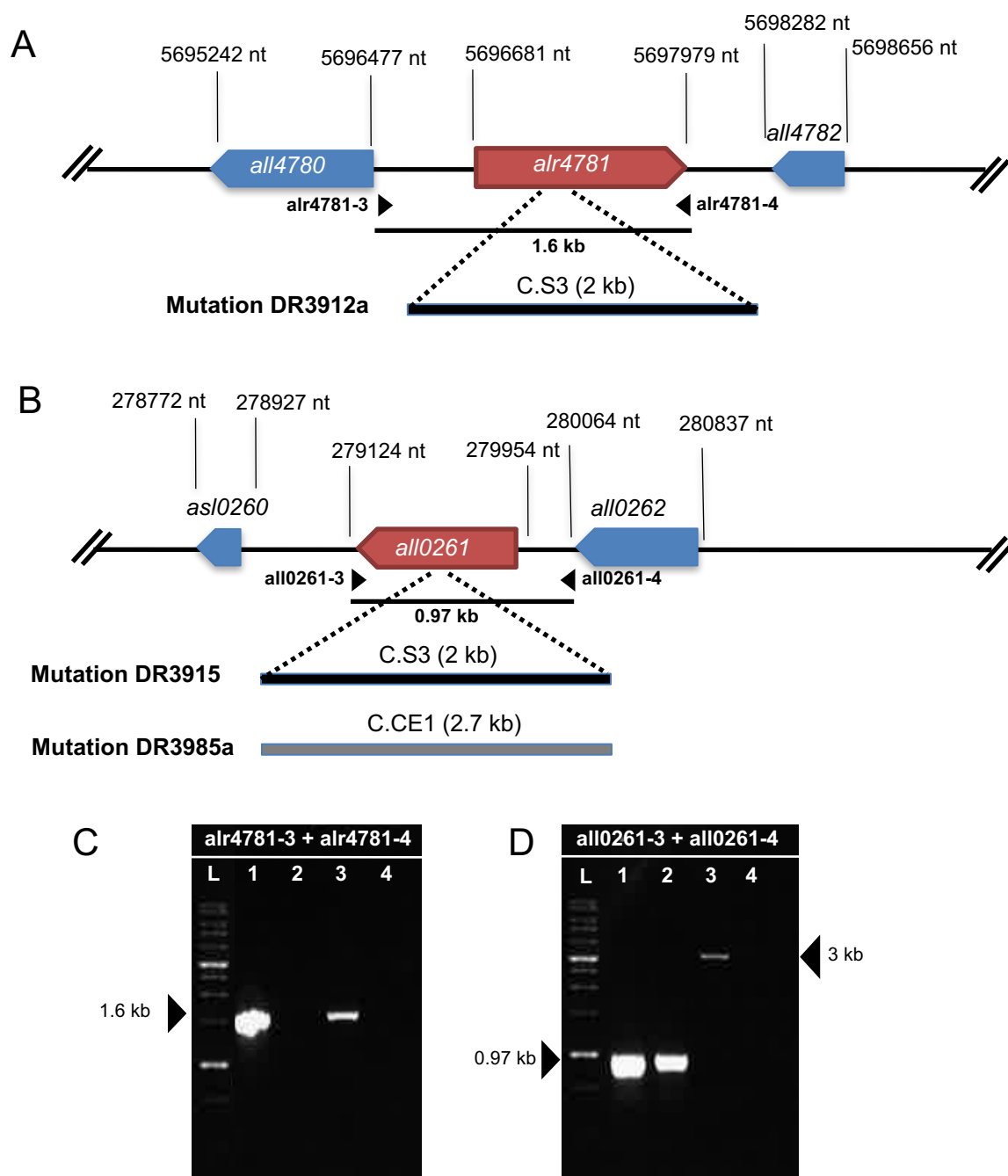
Figure S1. Construction and verification of mutants *glsC*, *glsP* and *glsC glsP*. Schematic of the insertional mutation of (A) the *alr4781* (*glsC*) and (B) *all0261* (*glsP*) genes, with indication of their genomic regions and the inserted gene-cassettes. (C, D) Verification of strains by colony PCR. L, 1-kb DNA ladder (Biotools). Primer pairs are indicated on top. Templates: 1, wild-type DNA; 2, *glsC* mutant DNA; 3, *glsP* mutant DNA; 4, *glsC glsP* mutant DNA.
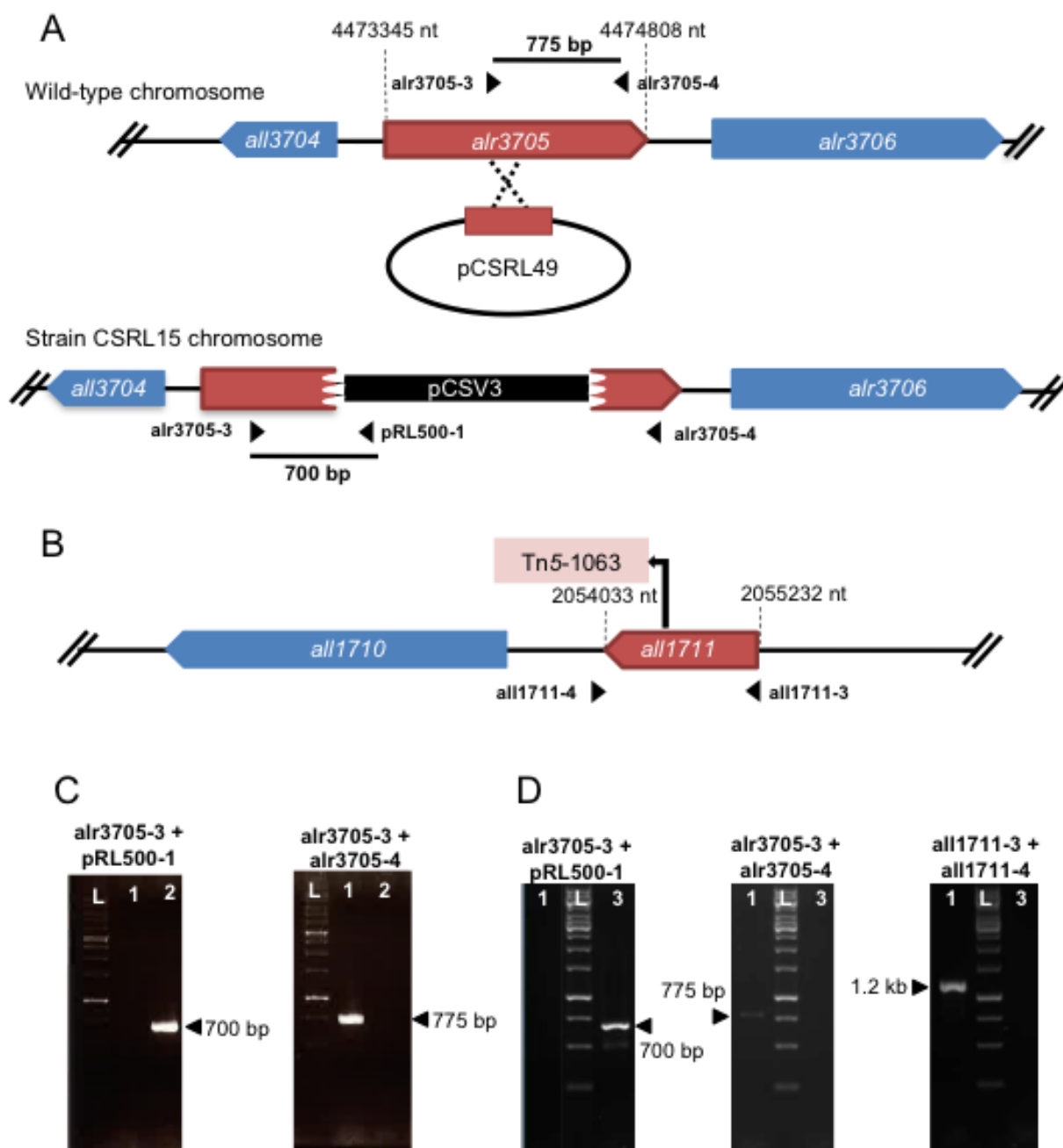
Figure S2. Schematic of the insertional mutations of (A) *alr3705* in strain CSRL15 and (B) *all1711* (*hepP*) in strain FQ163 (36), with indication of their genomic regions, the inserted DNA and approximate positions of primers (arrowheads). Plasmid pCSRL49 is pCSV3 bearing an internal fragment of *alr3705*. The strain bearing both mutations is called CSMN3. (C) Colony PCR analysis of mutant CSRL15. (D) Colony PCR analysis of mutant CSMN3. Primers shown on top. Template: 1, wild-type DNA; 2, DNA from mutant CSRL15 (panel C); 3, DNA from mutant CSMN3 (panel D). L,1-kb DNA ladder (Biotools).
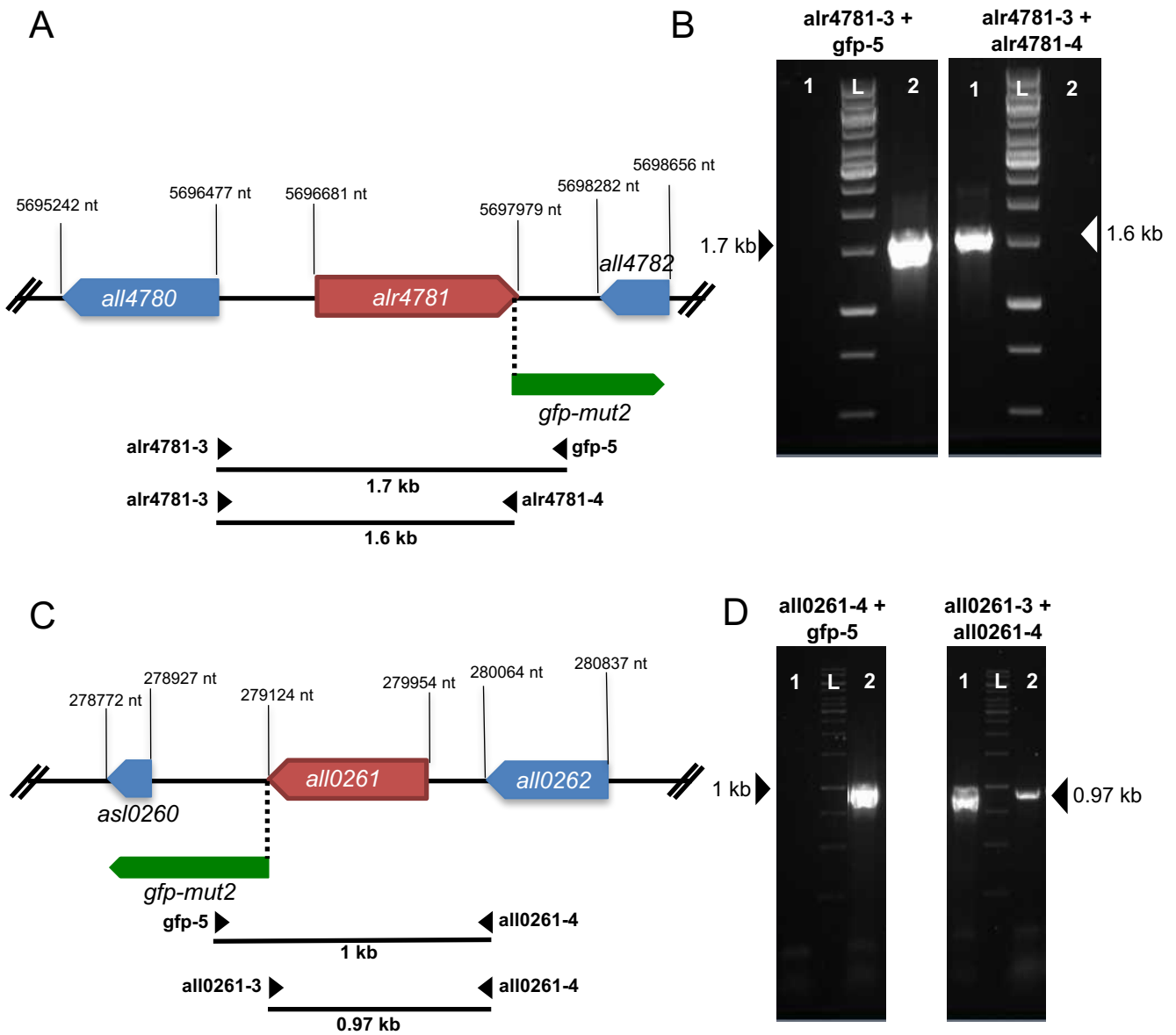
Figure S3. Genomic structure and verification by PCR of strains CSMN13 (*glsC-gfp*) and CSMN15 (*glsP-gfp*). Schematic of the *alr4781-gfp* gene fusion (A) and of the *all0261-gfp* gene fusion (C). The approximate positions of the primers used are indicated (black arrowheads). Verification by colony PCR of strains CSMN13 (B) and CSMN15 (D). L,1-kb DNA ladder (Biotools). Template: 1, wild-type DNA; 2, DNA from strain CSMN13 (B) or CSMN15 (D).
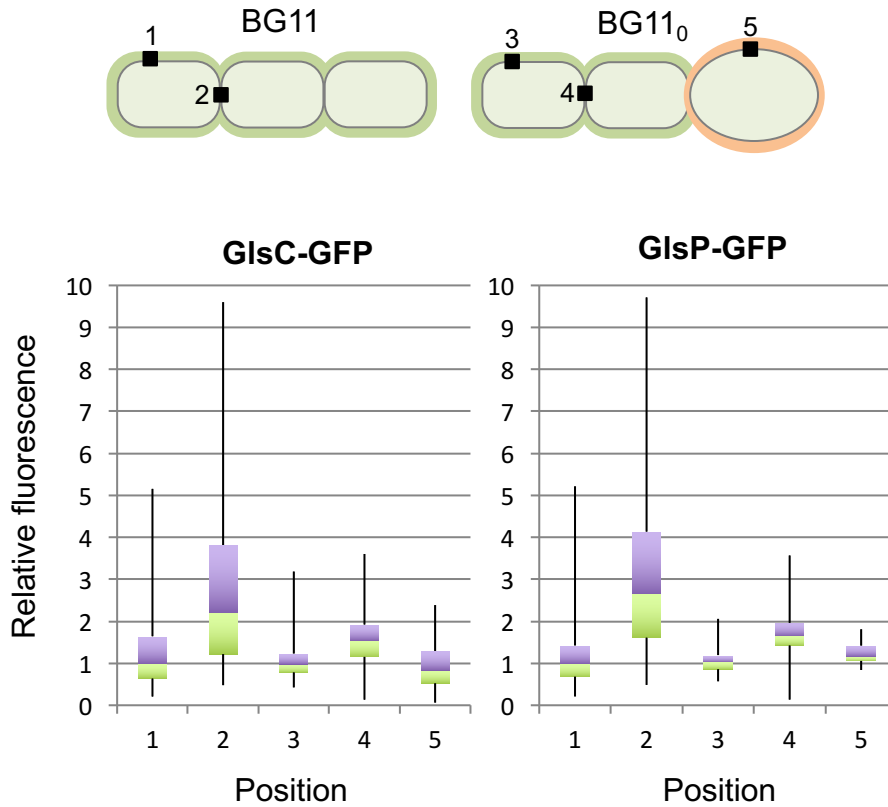
Figure S4. Box plot representation of the GFP fluorescence from GlsC-GFP and GlsP-GFP fusions. Filaments of strains CSMN13 (*glsC*::*gfp*) and CSMN15 (*glsP*::*gfp*) grown in BG11 medium in the presence of antibiotics were incubated in BG11 or $BG11_0$ medium without antibiotics for 24 h. GFP fluorescence was visualized by confocal microscopy and quantified as described in Materials and Methods at the positions indicated in the schemes (top; the cell to the right end in $BG11_0$ represents a heterocyst). Fluorescence was normalized to the median of lateral walls of vegetative cells from filaments incubated in BG11 medium (position 1). The table summarizes the median (*m*) and interquartile ranges (IQR) at the indicated positions.
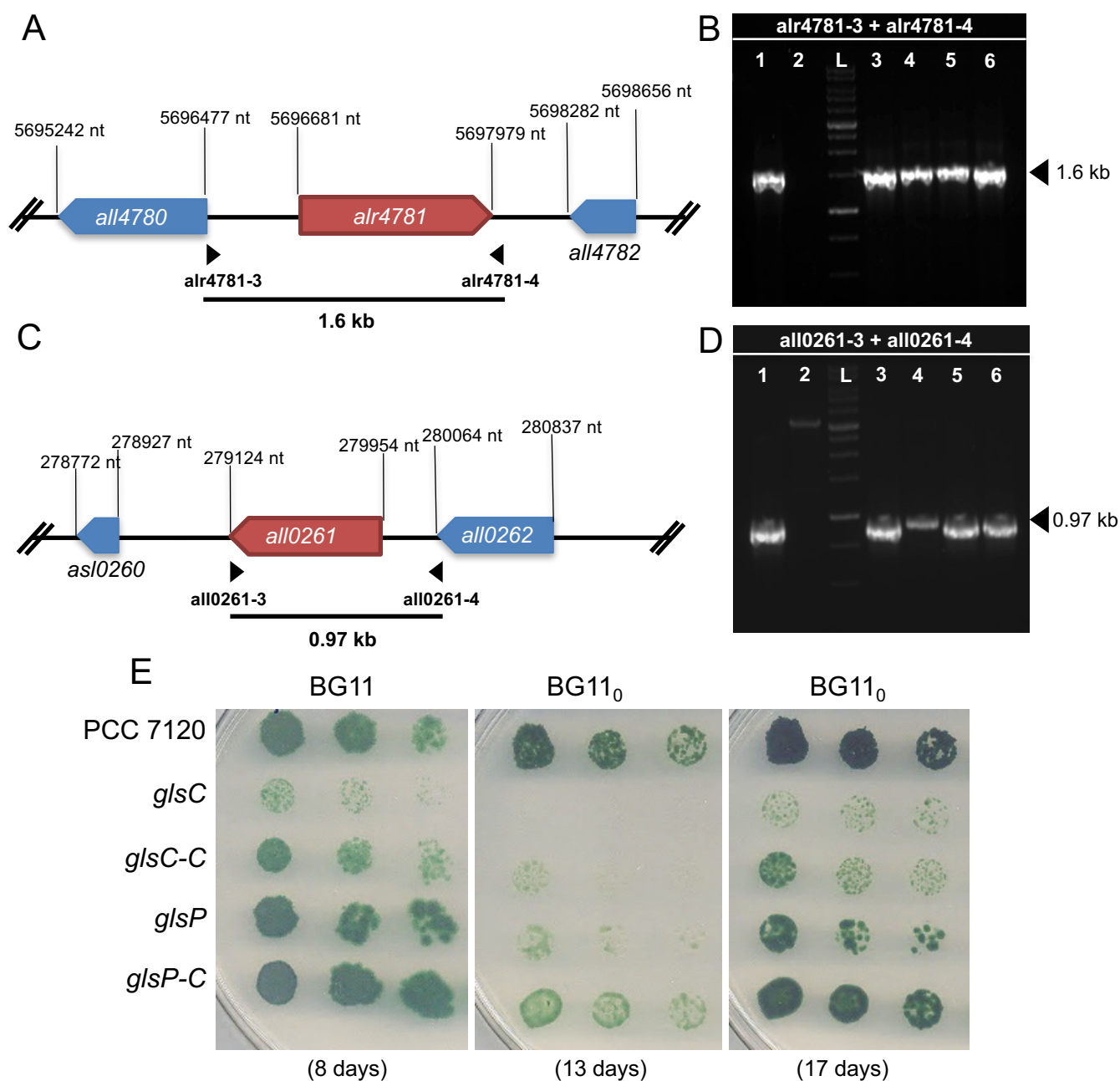
Figure S5. Complementation of the *glsC* and *glsP* mutants. Schemes of the *alr4781* (*glsC*) (A) and *all0261* (*glsP)* (B) genomic regions in *Anabaena*. Arrowheads represent primers used to amplify these regions by PCR. PCR products were transferred to BamHI-digested pRL25C (Nm^R), producing pCSMN22 (*alr4781*) and pCSMN20 (*all0261*), which were transferred to the corresponding *Anabaena* mutant (see Materials and Methods). (B, D) Verification of exconjugants by PCR. Primer pairs are indicated on top. Templates: 1, wild-type DNA; 2, *glsC* (B) or *glsP* (D) mutant DNA; 3 to 6, DNA from four Nm-resistant clones, showing that they bear wild-type copies of the corresponding genes, *glsC* (B) or *glsP* (D). (E) Growth tests of wild-type *Anabaena* (PCC 7120), the *glsC* and *glsP* mutants, and their complemented derivatives (*glsC-C* and *glsP-C*) in BG11 and $BG11_0$ media without antibiotics. Two incubation times are shown for $BG11_0$ medium to help appreciate complementation.

WT, NO$_3^-$ 　　　　WT, N$_2$

glsC, NO$_3^-$ 　　　　glsC, N$_2$

glsP, NO$_3^-$ 　　　　glsP, N$_2$

glsC glsP, NO$_3^-$ 　　　　glsC glsP, N$_2$
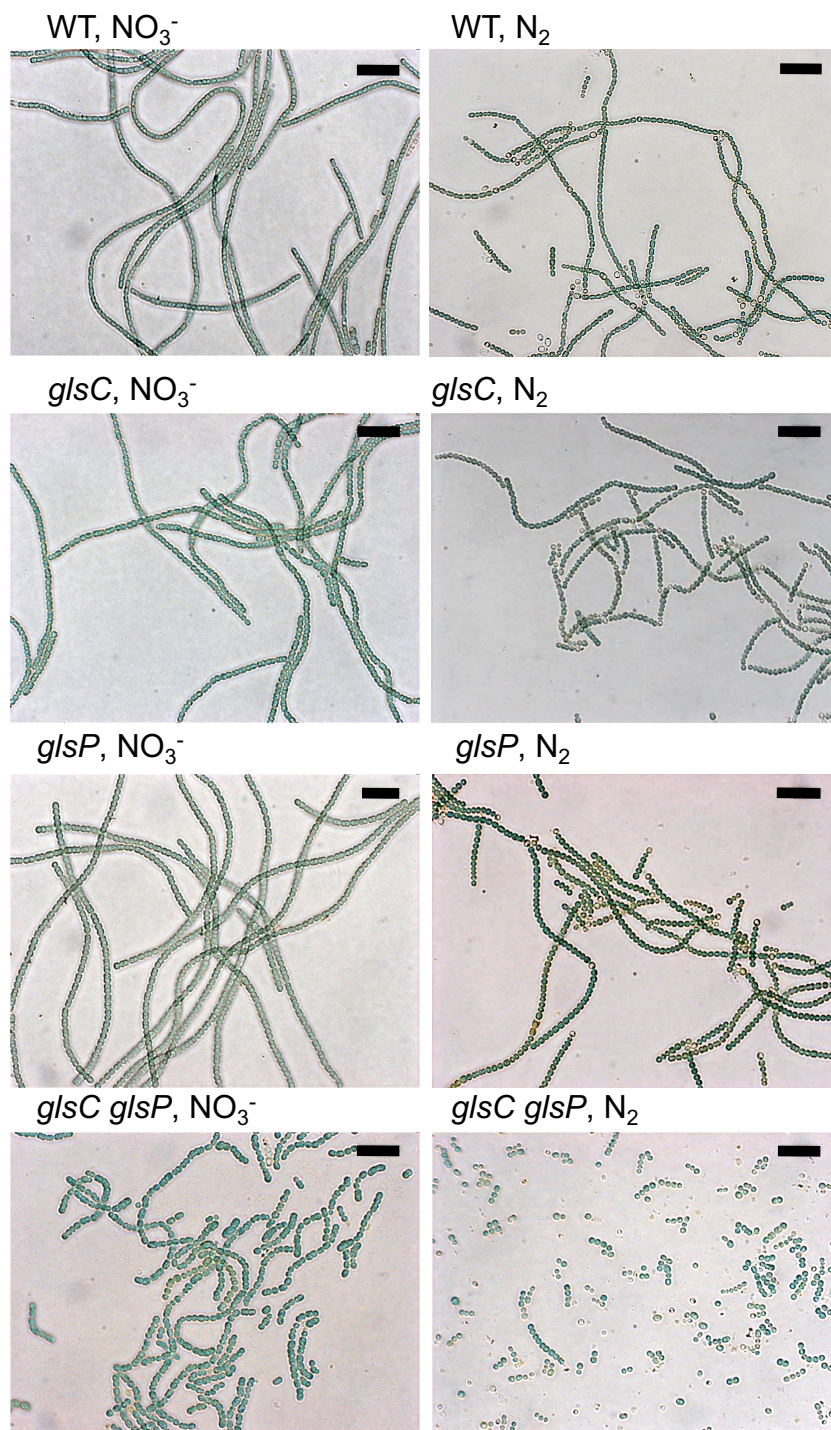
Figure S6. Microscopic images of the ABC transporter mutants. Filaments of *Anabaena* (WT), the *glsC, glsP* and double mutants grown in BG11 medium—in the presence of antibiotics for the mutants—were transferred to liquid BG11 (NO$_3^-$) or BG11$_0$ (N$_2$) medium without antibiotics, incubated five days under culture conditions, and observed by light microscopy. Scale bars, 25 μm.
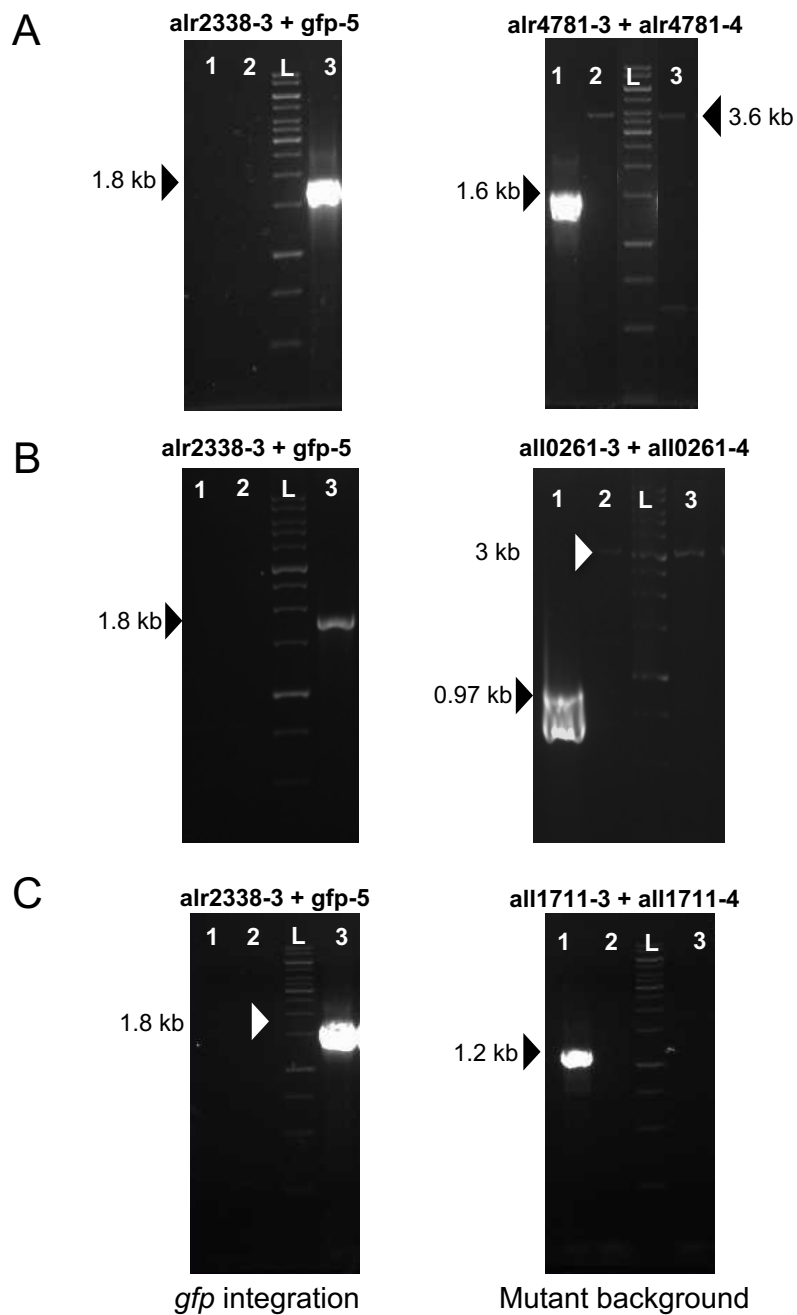
Figure S7. PCR analysis of the *sepJ-gfp* fusion in the *glsC, glsP* and *hepP* mutant backgrounds. Strains CSMN9 (*glsC sepJ-gfp*) and CSMN10 (*glsP sepJ-gfp*) were constructed with plasmid pCSVT22 (Nm^R), and strain CSMN16 (*hepP sepJ-gfp*) with plasmid pCSAM137. Verification by PCR of strain CSMN9 (A), CSMN10 (B), and CSMN16 (C). Primers are indicated atop each panel. Template: 1, wild-type DNA; 2, DNA from *glsC* (A), *glsP* (B) or *hepP* (FQ163) mutant; 3, DNA from CSMN9 (A), CSMN10 (B) or CSMN16 (C). L, 1-kb DNA ladder (Biotools). The column at left illustrates integration of *gfp* into the *sepJ* locus. The column at right illustrates that each strain, CSMN9 (A), CSMN10 (B) and CSMN16 (C), keeps its inactivated gene (*glsC, glsP*, and *hepP*, respectively).

CSAM137 (*sepJ-gfp)*

CSMN9 (*glsC sepJ-gfp*) clone 1

CSMN9 (*glsC sepJ-gfp*) clone 2

CSMN9 (*glsC sepJ-gfp*) clone 3

CSMN9 (*glsC sepJ-gfp*) clone 4
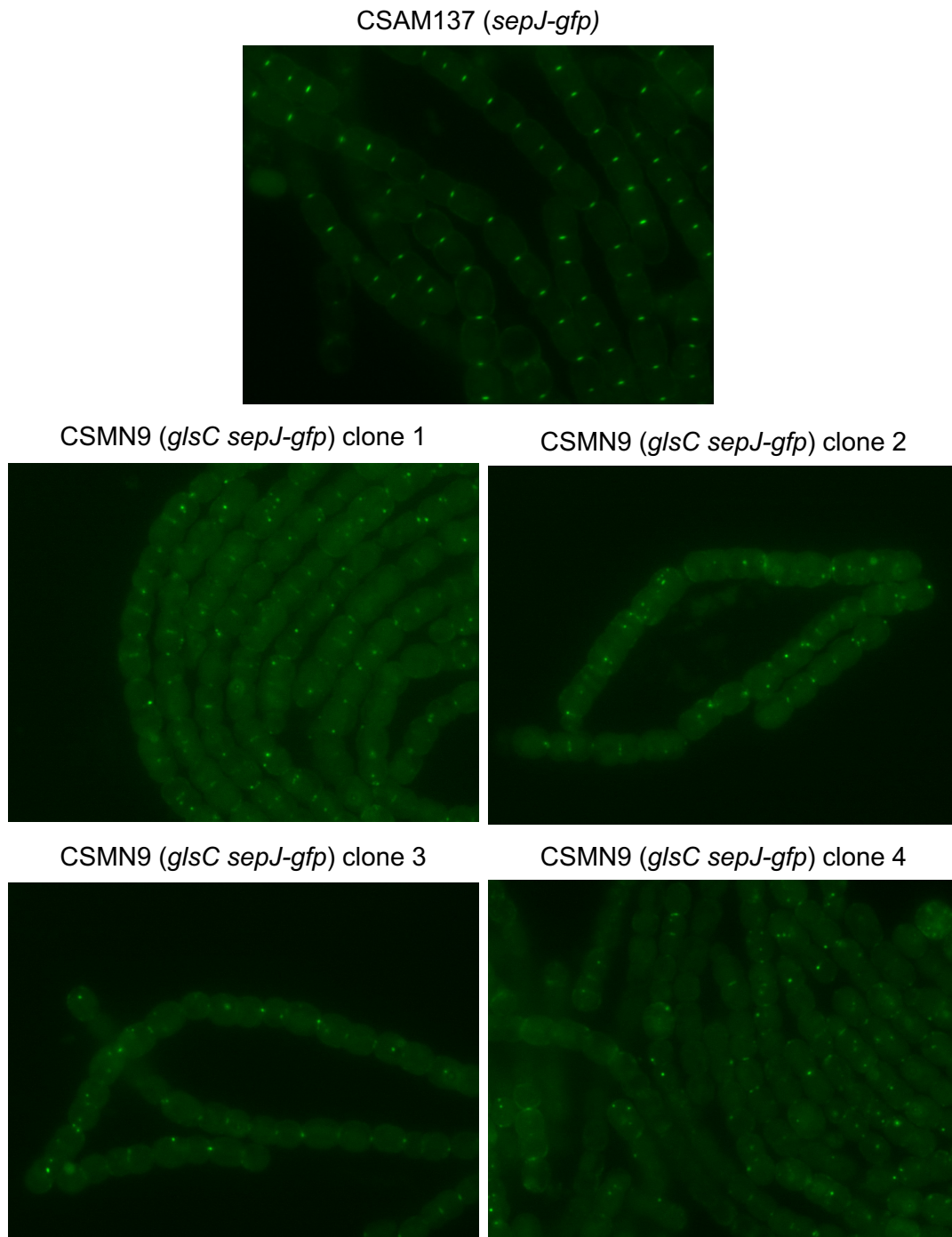
Figure S8. Subcellular localization of SepJ-GFP in the wild-type and *glsC* genetic backgrounds visualized by fluorescence microscopy. Filaments of strains CSAM137 (PCC 7120 [*sepJ*::pCSAM137]) and four independently isolated clones of CSMN9 (*glsC*::C.S3 *sepJ*::pCSVT22) were grown in BG11 medium in the presence of antibiotics and visualized by fluorescence microscopy as described in Materials and Methods.

Table S1. Strains, plasmids and oligodeoxynucleotide primers used in this work.

Strain, plasmid or primer	Relevant characteristic(s)[a]	Source or reference
Strains		
Anabaena sp. PCC 7120	Wild-type strain	1
CSMN3	Sm^R Sp^R Nm^R derivative of strain FQ163; *alr3705*::pCSRL49	This study
CSMN9	Sm^R Sp^R Nm^R derivative of strain DR3912a; *alr4781*::pCSVT22	This study
CSMN10	Sm^R Sp^R Nm^R derivative of strain DR3915; *all0261*::pCSVT22	This study
CSMN11	Sm^R Sp^R Nm^R derivative of strain DR3912a; pRL25C::*alr4781*	This study
CSMN12	Sm^R Sp^R Nm^R derivative of strain DR3915; pRL25C::*all0261*	This study
CSMN13	Sm^R Sp^R derivative of strain PCC 7120; *alr4781*::pCSMN24	This study
CSMN15	Sm^R Sp^R derivative of strain PCC 7120; *all0261*::pCSMN25	This study
CSMN16	Sm^R Sp^R Nm^R derivative of strain FQ163; *all1711*::pCSAM137	This study
CSRL15	Sm^R Sp^R derivative of strain PCC 7120; *alr3705*::pCSRL49	This study
DR3912a	Sm^R Sp^R derivative of strain PCC 7120; *alr4781*::C.S3	This study
DR3915	Sm^R Sp^R derivative of strain PCC 7120; *all0261*::C.S3	This study
DR3912a/DR3985a	Sm^R Sp^R Em^R derivative of strain PCC 7120; *alr4781*::C.S3, *all0261*::C.CE1	This study
FQ163	Bm^R Nm^R Sm^R derivative of strain PCC 7120: *all1711*::Tn5-1063	2
Plasmids		
anp05647	*Anabaena* sp. chromosomal DNA from bp 5692388 to 5699787 in the *Bam*HI site of pUC18. Contains *alr4781;* Ap^R	3
anp07443	*Anabaena* sp. chromosomal DNA from bp 275318 to 283470 in the *Bam*HI site of pUC18. Contains *all0261*; Ap^R.	3
pCSAM135	Promoterless *gfp* gene (EcoRV-ApaI fragment) introduced into EcoRV- and ApaI-digested pCSAM134 (C-terminal portion of *sepJ* cloned into the pGEM-T Easy plasmid), Ap^R.	4
pCSAM137	PstI fragment from pCSAM135, containing the translational fusion between the C-terminal region of the *sepJ* and the *gfp* gene, cloned into pCSV3; Sm^R Sp^R	4
pCSMN19	PCR-amplified *all0261* cloned in pSpark I; Ap^R	This study
pCSMN20	*all0261* from pCSMN19 cloned in pRL25C; Nm^R	This study
pCSMN21	PCR-amplified *alr4781* cloned in pSpark I; Ap^R	This study
pCSMN22	*alr4781* from pCSMN21 cloned in pRL25C; Nm^R	This study
pCSMN23	SacI-NheI *alr4781* fragment cloned in pSpark I; Ap^R	This study
pCSMN24	SacI-NheI fragment from pCSMN23 and NheI-SalI *gfp-mut2* cloned in SacI-XhoI-digested pRL277; Sm^R Sp^R	This study

pCSMN25	SacI-NheI *all0261* fragment and NheI-SalI *gfp-mut2* cloned in SacI-XhoI-digested pRL277; Sm^R Sp^R	This study
pCSMN26	XbaI-KpnI *all0261* fragment cloned in pSpark I; Ap^R	This study
pCSMN27	XbaI-KpnI *alr4781* fragment cloned in pSpark I; Ap^R	This study
pCSMN28	XbaI-KpnI *all0261* fragment from pCSMN26 cloned in pUT18	This study[b]
pCSMN29	XbaI-KpnI *all0261* fragment from pCSMN26 cloned in pUT18C	This study[b]
pCSMN30	XbaI-KpnI *all0261* fragment from pCSMN26 cloned in pKT25	This study[b]
pCSMN31	XbaI-KpnI *all0261* fragment from pCSMN26 cloned in pKNT25	This study[b]
pCSMN32	XbaI-KpnI *alr4781* fragment from pCSMN27 cloned in pUT18	This study[b]
pCSMN33	XbaI-KpnI *alr4781* fragment from pCSMN27 cloned in pUT18C	This study[b]
pCSMN34	XbaI-KpnI *alr4781* fragment from pCSMN27 cloned in pKT25	This study[b]
pCSMN35	XbaI-KpnI *alr4781* fragment from pCSMN27 cloned in pKNT25	This study[b]
pCSMN42	XbaI-KpnI all1711 fragment from pCSMN50 cloned in pUT18	This study[b]
pCSMN43	XbaI-KpnI all1711 fragment from pCSMN50 cloned in pUT18C	This study[b]
pCSMN44	XbaI-KpnI all1711 fragment from pCSMN50 cloned in pKT25	This study[b]
pCSMN45	XbaI-KpnI all1711 fragment from pCSMN50 cloned in pKNT25	This study[b]
pCSMN50	XbaI-KpnI *all1711* fragment cloned in pSpark I; Ap^R	This study
pCSRL48	PCR-amplified *alr3705* cloned in pMBL-T; Ap^R	This study
pCSRL49	BamHI fragment from pCSRL48 inserted into BamHI-digested pCSV3; Sm^S Sp^R	This study
pCSV3	Mobilizable vector; Sm^R Sp^R	5
pCSVT22	*sepJ-gfp* from pCSAM135 cloned in pRL424; Nm^R.	6
pPS854	Cloning vector for introduction of a removable marker between *FRT* recognition sequences; Ap^R	7
pRL25C	pRL25 containing 403-bp cos site; cyanobacterial replicon; Nm^R.	8
pRL44	Source of C.S3 between symmetrical polylinkers; Km^R Sm^R Sp^R	9
pRL277	*sacB*-containing mobilizable plasmid; Sm^R Sp^R	10
pRL278	*sacB*-containg mobilizable plasmid; Nm^R	10
pRL149a	Source of C.CE1 between symmetrical polylinkers; Ap^R Cm^R Em^R	11
pRL424	S.K3 containing L.HEH2 and C.C1; Cm^R Km^R	11
pRL443	Conjugative plasmid; Ap^R Tc^R	12
pRL623	Helper plasmid; carries *mob* and DNA methylases; Cm^R	13
pRL1075	Source of OriT, SacB and a selection marker; Cm^R Em^R.	9
pRL3332	Omega cassette was excised from pRL44 with *Hind*III (blunt) and cloned into pPS854 digested with *Eco*RI (blunt); Ap^r Sm^r Sp^R.	This study
pRL3798a	*FRT*-flanked C.S3 digested from pRL3332 with *Eco*53KI and cloned into anp07443 digested with *Nhe*I (blunt); Ap^R Sm^R Sp^R,	This study
pRL3857a	Helper plasmid (Gm^R); carries *mob* and DNA methylases; Gm^R gene was inserted in pRL623, and Cm^R gene was removed from the resulting plasmid.	This study

pRL3907a	*FRT*-flanked C.S3 digested from pRL3332 with *Bam*HI and cloned into anp05647 digested with *Bcl*I; Ap^{R}Sm^{R}Sp^R	This study
pRL3912a	*Fsp*I fragment of pRL1075 cloned in SalI-digested (blunt) pRL3907a; Ap^{R}Cm^{R}Em^{R}Sm^{R}Sp^R	This study
pRL3915	*Sac*I-*Sal*I fragment of pRL3798a cloned into pRL278 digested with *Sac*I-*Xho*I; Km^{R}Nm^{R}Sm^{R}Sp^R	This study
pRL3985a	C.CE1 digested from pRL149a with *Sma*I and cloned into pRL3915 digested with *Eco*47III; Km^{R}Nm^{R}Cm^{R}Em^R	This study
pSpark I	Cloning vector; Ap^R	Canvax, Biotech SL
Primer name	**Sequence (5´ to 3´)^c**	
all0261-3	AGATCTACTGGAGAATGACTTTTGA	
all0261-4	GGATCCTAGTAAGTTTTTATACTGTGGC	
all0261-5^d	AAAGCTAGC*ACCTCCACCGCC*TCCTTTACCGCCTGTAAAAG	
all0261-6	AAAGAGCTCTAACTAGCCGTACCAGCCCA	
all0261-7	TCTCTAGACCGTTCTTTACCGTTG	
all0261-8	TAATGGTACCCCTTTACCGCCTGTAAAAG	
all0261-11	GCCAGACTCAGCTTTGTAGGTAA	
all0261-12	ACAATCATGCCCTGGTAAGAAT	
alr4781-3	GGATCCACACCTCCAGACAGCCCT	
alr4781-4	AGATCTCAATCGGATTCATAGAAAAACT	
alr4781-5	GAGCTCTAAGGATCGGAAGAACACAG	
alr4781-6^d	GCTAGC*ACCTCCACCGCC*ATTTTTAGGAAATATTGCTAAATCAG	
alr4781-7	GACTAAACTCTAGAGCAAGTTGTTTTAGAAAACG	
alr4781-8	AAGGTACCTTTTTAGGAAATATTGCTAAATCAG	
alr4781-9	TTCCCCATCCCAACTCC	
alr4781-10	TAACAAATGCGCTACAGACC	
all1711-3	TTATTAGCTGCCATCATCTTCA	
all1711-4	GACATTGCCCACTCTACTCATA	
all1711-9	GACTAAACTCTAGATAACTCTGTCAATACCCGC	
all1711-10	TAATGGTACCTAAGGCAATATACGAAATCTTCT	
alr2338-3	CGAATGTATAACCAACAGCAGC	
alr3705-1	GGATCCCGATCGCCAGCAACAGT	
alr3705-2	TCAATCACATCGGGAATCAT	
alr3705-3	CTATTGGTGGCAGCATTTTA	
alr3705-4	CTGGTTGTATTGGTAGAGTA	
gfp-5	GTATGTTGCATCACCTTCAC	
pRL500-1	ATAGGCGTATCACGAGGC	
alr0599-1	CCAAATAGCTGGGCCAGTGTTAGT	
alr0599-2	GGAATTGCTTTGCCAGTTGTCAG	
all5167-1	GCTCAAGCAATTCGTCACTGTTCC	
all5167-2	AAAGATTGCGTCGGTCTGGTGT	

^{a} Resistance to the indicated antibiotic (denoted by ^{R}): Ap: ampicillin; Bm, bleomycin; Cm: chloramphenicol; Em, erythromycin; Gm, gentamycin; Km, kanamycin; Nm: neomycin; Sm: streptomycin; and Sp: spectinomycin.
^{b} See main text.
^{c} Introduced restriction enzyme cutting sites are underlined.
^{d} The nucleotide sequence that, inverted, encodes the four-Glycine linker is italicized.

References

1. Rippka R, Deruelles J, Waterbury JB, Herdman M, Stanier RY. 1979. Generic assignments, strain histories and properties of pure cultures of cyanobacteria. J Gen Microbiol **111:**1-61.

2. López-Igual R, Lechno-Yossef S, Fan Q, Herrero A, Flores E, Wolk CP. 2012. A major facilitator superfamily protein, HepP, is involved in formation of the heterocyst envelope polysaccharide in the cyanobacterium *Anabaena* sp. strain PCC 7120. J Bacteriol **194:**4677-4687.

3. Kaneko T, Nakamura, Y, Wolk CP, Kuritz T, Sasamoto S, Watanabe A, Iriguchi M, Ishikawa A, Kawashima K, Kimura T, Kishida Y, Kohara M, Matsumoto M, Matsuno A, Muraki A, Nakazaki N, Shimpo S, Sugimoto M, Takazawa M, Yamada M, Yasuda M, Tabata S. 2001. Complete genomic sequence of the filamentous nitrogen-fixing cyanobacterium *Anabaena* sp. strain PCC 7120. DNA Res **8**:205-213.

4. Flores, E., Pernil, R., Muro-Pastor, A.M., Mariscal, V., Maldener, I., Lechno-Yossef, S., Fan, Q., Wolk, C.P., and Herrero, A. 2007. Septum-localized protein for filament integrity and diazotrophy in the heterocyst-forming cyanobacterium *Anabaena* sp. strain PCC 7120. J Bacteriol **189:**3884-3890.

5. Valladares A, Rodríguez V, Camargo S, Martínez-Noël GMA, Herrero A, Luque I. 2011. Specific role of the cyanobacterial PipX factor in the heterocysts of *Anabaena* sp. PCC 7120. J Bacteriol **193:**1172-1182.

6. Merino-Puerto, V., Mariscal, V., Mullineaux, C.W., Herrero, A., and Flores, E. 2010. Fra proteins influencing filament integrity, diazotrophy and localization of septal protein SepJ in the heterocyst-forming cyanobacterium *Anabaena* sp. Mol Microbiol **75**:1159-11707.

7. Hoang TT, Karkhoff-Schweizer RR, Kutchma AJ, Schweizer HP. 1998. A broad-host-range Flp-FRT recombination system for site-specific excision of chromosomally-located DNA sequences: application for isolation of unmarked *Pseudomonas aeruginosa* mutants. Gene **212:**77-86.

8. Wolk CP, Cai Y, Cardemil L, Flores E, Hohn B, Murry M, Schmetterer G, Schrautemeier B, Wilson R. 1988. Isolation and complementation of mutants of *Anabaena* sp. strain PCC 7120 unable to grow aerobically on dinitrogen. J Bacteriol **170:**1239-1244.

9. Cai Y, Wolk CP. 1990. Use of a conditionally lethal gene in *Anabaena* sp. strain PCC 7120 to select for double recombinants and to entrap insertion sequences. J Bacteriol **172**:3138-3145.

10. Black TA, Cai Y, Wolk CP. 1993. Spatial expression and autoregulation of *hetR*, a gene involved in the control of heterocyst development in *Anabaena*. Mol Microbiol **9**:77-84 Publisher's correction (1993): Mol Microbiol **10**:1153.

11. Elhai J, Wolk CP. 1988. A versatile class of positive-selection vectors based on the nonviability of palindrome-containing plasmids that allows cloning into long polylinkers. Gene **68:**119-138.

12. Elhai J, Wolk CP. 1988. Conjugal transfer of DNA to cyanobacteria. Methods Enzymol **167**:747-754.

13. Elhai J, Vepritskiy A, Muro-Pastor AM, Flores E, Wolk CP. 1997. Reduction of conjugal transfer efficiency by three restriction activities of *Anabaena* sp. strain PCC 7120. J Bacteriol **179**:1998-2005.

Text S1

Development of equations for FRAP analysis

Recovery of fluorescence, C_B, of a bleached cell is expected to have the form $C_B = C_0 + C_R (1 - e^{-Et})$ if the bleached cell is the terminal cell in a filament and to have the form $C_B = C_0 + C_R (1 - e^{-2Et})$ if the bleached cell is between vegetative cells on both sides. In these models, C_0 is the fluorescence of the bleached cell immediately after the bleach; $C_0 + C_R$ stands for full recovery of fluorescence; E is the exchange coefficient at the junction between the bleached cell and its contiguous neighboring cell or cells; and C_0, C_R, and E are considered constants. A similar expression can be written substituting E by R, a recovery rate constant. Here, we provide a validation of the exponentials e^{-Et} and e^{-2Et} in those expressions.

If the fluorescence of a *terminal* bleached cell approximates the fluorescence of that cell during recovery, one could write that $dC_B/dt = E(C_0 + C_R - C_B)$, and if the bleached cell is *between* vegetative cells within a filament, one could write that $dC_B/dt = 2E(C_0 + C_R - C_B)$. We let "K" stand for either "1" (for the first case) or "2" (for the second case) so $dC_B/dt = KE (C_0 + C_R - C_B)$.

Because C_0 and C_R are constants, and a derivative d/dt of a constant is 0, it is legitimate to state that

$dC_B/dt = - d(C_0 + C_R - C_B)/dt$.

According to the last two equations, $- d(C_0 + C_R - C_B)/dt = KE (C_0 + C_R - C_B)$, or

$d(C_0 + C_R - C_B)/dt = - KE (C_0 + C_R - C_B)$

Dividing by $(C_0 + C_R - C_B)$ and multiplying by dt, one obtains

$[d(C_0 + C_R - C_B)]/(C_0 + C_R - C_B) = - KE$ dt.

ln is the logarithm of base e, and d(function)/(function) = d ln(function), so

$[d(C_0 + C_R - C_B)]/(C_0 + C_R - C_B) = d \ln (C_0 + C_R - C_B)$ which, in turn, $= - KE$ dt.

Integrating from time 0 to time t,

$\ln (C_0 + C_R - C_B)_{time\ t} - \ln (C_0 + C_R - C_B)_{time\ 0} = - KEt - (- KE0) = - KEt$

At time t = 0, $C_B = C_0$, so that $\ln (C_0 + C_R - C_B)_{time\ 0} = \ln (C_R)$.

In general, ln x - ln y = ln (x/y).

Therefore, $\ln (C_0 + C_R - C_B)_{time\ t} - \ln (C_R)_{time\ 0} = \ln [(C_0 + C_R - C_B)/C_R] = - KEt$.

In general, $e^{\ln Z} = Z$. Therefore, converting to exponentials, i.e., raising each side of the last equation to a power of e,

$e^{\ln [(C_0 + C_R - C_B)/C_R]} = (C_0 + C_R - C_B)/C_R = e^{-KEt}$.

Multiplying both sides of the equation by C_R,

$C_0 + C_R - C_B = C_R e^{-KEt}$,

Subtracting $C_0 + C_R$ from both sides of the equation,

$- C_B = - C_0 - C_R + C_R e^{-KEt}$

and multiplying both sides of the equation by -1, one obtains

$C_B = C_0 + C_R - C_R e^{-KEt} = C_0 + C_R (1 - e^{-KEt})$, validating the expressions, above, for K = 1 and K = 2.

Chapter 3: Multiple ABC glucoside transporters mediate sugar-stimulated growth in the heterocyst-forming cyanobacterium *Anabaena* sp. strain PCC 7120

Multiple ABC glucoside transporters mediate sugar-stimulated growth in the heterocyst-forming cyanobacterium *Anabaena* sp. strain PCC 7120

Mercedes Nieves-Morión and Enrique Flores*
Instituto de Bioquímica Vegetal y Fotosíntesis, CSIC and Universidad de Sevilla, Américo Vespucio 49, 41092 Seville, Spain.

Summary

Cyanobacteria are generally capable of photoautotrophic growth and are widely distributed on Earth. The model filamentous, heterocyst-forming strain *Anabaena* sp. PCC 7120 has long been considered as a strict photoautotroph but is now known to be able to assimilate fructose. We have previously described two components of ABC glucoside uptake transporters from *Anabaena* that are involved in uptake of the sucrose analog esculin: GlsC [a nucleotide-binding domain subunit (NBD)] and GlsP [a transmembrane component (TMD)]. Here, we created *Anabaena* mutants of genes encoding three further ABC transporter components needed for esculin uptake: GlsD (NBD), GlsQ (TMD) and GlsR (periplasmic substrate-binding protein). Phototrophic growth of *Anabaena* was significantly stimulated by sucrose, fructose and glucose. Whereas the *glsC* and *glsD* mutants were drastically hampered in sucrose-stimulated growth, the different *gls* mutants were generally impaired in sugar-dependent growth. Our results suggest the participation of Gls and other ABC transporters encoded in the *Anabaena* genome in sugar-stimulated growth. Additionally, Gls transporter components influence the function of septal junctions in the *Anabaena* filament. We suggest that mixotrophic growth is important in cyanobacterial physiology and may be relevant for the wide success of these organisms in diverse environments.

Introduction

Cyanobacteria are an ecologically important group of organisms that significantly impact the carbon and nitrogen cycles in the biosphere (Whitton and Potts, 2000).

They are characterized by their ability to perform oxygenic photosynthesis, and they are generally capable of photoautotrophic growth (Rippka *et al.*, 1979). Although many cyanobacteria are strict photoautotrophs, some are capable of photoheterotrophic growth assimilating sugars (Rippka *et al.*, 1979). Additionally, some heterocyst-forming cyanobacteria are capable of sugar-dependent chemoheterotrophic growth in the dark (Wolk and Shaffer, 1976; Bottomley and van Baalen, 1978; Schmetterer and Flores, 1988). Consistently, some sugar transporters that mediate sugar uptake supporting some kind of heterotrophic growth have been identified in cyanobacteria. Well-known examples include a major facilitator superfamily (MFS) glucose transporter, GlcP, that has been characterized in the unicellular cyanobacterium *Synechocystis* sp. strain PCC 6803 (Zhang *et al.*, 1989; Schmetterer, 1990) and in the heterocyst-forming cyanobacterium *Nostoc punctiforme* (Ekman *et al.*, 2013), and an ABC fructose transporter, Frt, that has been characterized in the heterocyst-forming cyanobacteria *Anabaena variabilis* (Ungerer *et al.*, 2008) and *N. punctiforme* (Ekman *et al.*, 2013).

Heterocyst-forming cyanobacteria are filamentous organisms that, in the absence of a source of combined nitrogen, contain two cell types: vegetative cells that fix CO_2 performing oxygenic photosynthesis and heterocysts that are specialized for the fixation of N_2 (Flores and Herrero, 2010). In the diazotrophic filament, an exchange of nutrients takes place that results in the transfer of reduced carbon from vegetative cells to heterocysts and of fixed nitrogen from heterocysts to vegetative cells (Wolk, 1968; Wolk *et al.*, 1974; Jüttner, 1983). Intercellular molecular exchange has been traced with fluorescent markers (including calcein and 5-carboxyfluorescein) and shown to take place by simple diffusion (Mullineaux *et al.*, 2008; Nieves-Morión *et al.*, 2017a). The cyanobacterial filament consists of individual cells surrounded by their cytoplasmic membrane and peptidoglycan layer(s) but sharing the outer membrane, which is continuous along the filament determining the presence of a continuous periplasmic space, and the cells in the filament are joined by proteinaceous structures termed septal junctions (Wilk *et al.*, 2011; Flores

2   *M. Nieves-Morión and E. Flores*

et al., 2016; Herrero *et al.*, 2016). Proteins SepJ (also known as FraG), FraC and FraD that are located at the intercellular septa have been identified as putative components of the septal junctions (reviewed in Flores *et al.*, 2016; Herrero *et al.*, 2016).

In the heterocyst-forming cyanobacterium *Anabaena* sp. strain PCC 7120 (hereafter *Anabaena*), sucrose appears to be a quantitatively important metabolite transferred from vegetative cells to heterocysts (Curatti *et al.*, 2002; Cumino *et al.*, 2007), where it is hydrolyzed by invertase InvB producing fructose and glucose to support heterocyst metabolism (López-Igual *et al.*, 2010; Vargas *et al.*, 2011). A fluorescent analog of sucrose, esculin (Gora *et al.*, 2012), has also been used as a marker to trace intercellular molecular transfer, and it has additionally been used to test uptake from the outer medium into *Anabaena* cells (Nürnberg *et al.*, 2015). Three glucoside transporters (or components of transporters) that are involved in uptake of esculin have been identified in *Anabaena* (Nieves-Morión *et al.*, 2017b). HepP (*Anabaena* ORF product All1711) is an MFS transporter that was previously shown to be needed for deposition of the polysaccharide layer of the heterocyst envelope (López-Igual *et al.*, 2012), GlsC (Alr4781) is a nucleotide-binding subunit of an ABC transporter and GlsP (All0261) is a transmembrane (permease) subunit of an ABC transporter. In addition to mediating esculin uptake, these proteins were shown to influence the septal junctions. Thus, whereas GlsC is needed for proper localization of SepJ at the intercellular septa, HepP and GlsP influence septal function in a process that may involve interactions with septal protein SepJ (Nieves-Morión *et al.*, 2017b).

Anabaena is an important model in studies of N_2 fixation, heterocyst differentiation and bacterial multicellularity that has been considered for a long time to be a strict photoautotroph. Recent work has shown however that *Anabaena* can grow heterotrophically using fructose as long as this sugar is provided at relatively high concentrations ($\geq$ 50 mM) (Stebegg *et al.*, 2012). Incorporation of the genes encoding the Frt transporter from *A. variabilis* into the *Anabaena* genome permits growth of *Anabaena* dependent on lower concentrations of fructose (5 mM; Ungerer *et al.*, 2008). Hence, *Anabaena* has the metabolic capability to use fructose as a carbon and energy source but lacks a high affinity transporter for this sugar. On the other hand, *Anabaena* has been recently reported to grow mixotrophically using a number of carbon sources, including some sugars (fructose, glucose, maltose and sucrose), amino acids (glutamate, glutamine and proline) and other simple organic compounds (glycerol and pyruvate) (Malatinszky *et al.*, 2017). ABC transporters for amino acids (Pernil *et al.*, 2015) and a TRAP transporter that can take up pyruvate

(Pernil *et al.*, 2010) are known to be expressed in *Anabaena*, but transporters that mediate the uptake of sugars are less known. In this study, we addressed the identification of further components of the ABC transporters that mediate esculin uptake and the possible role of those transporters in sugar assimilation as well as in other aspects of the physiology of *Anabaena*.

Results

Identification and inactivation of further components of glucoside transporters

ABC uptake transporters typically comprise one periplasmic solute-binding protein (SBP), two integral membrane proteins [transmembrane domains (TMD)] and two nucleotide-binding domains (NBD) that hydrolyze ATP in the cytoplasm (Cui and Davidson, 2011). We were interested in the identification of transporter partners of GlsC (NBD) and GlsP (TMD). The genome of *Anabaena* contains 12 ORFs that encode proteins that are most similar to components of ABC uptake transporters for sugars (Supporting Information Table S1). These genes are spread in the *Anabaena* genome precluding the possibility of predicting their association in specific ABC transport complexes. Orthologs of *glsC* have no neighbors encoding ABC transporter components in any of the cyanobacterial genomes whose sequence is available (https://img.jgi.doe.gov/cgi-bin/m/main.cgi). Orthologs of *glsP* are however frequently accompanied by another ABC TMD-encoding gene in the genomes of heterocyst-forming cyanobacteria (Supporting Information Fig. S1). The *Anabaena* gene most similar to this gene is *alr2532*. In some heterocyst-forming and non-heterocyst-forming cyanobacteria, as well as in some other bacteria, a gene encoding a periplasmic SBP is clustered together with those two TMD-encoding genes (Supporting Information Fig. S1). The *Anabaena* gene most similar to this gene is *all1916*. We therefore constructed *Anabaena* mutants bearing inactivated versions of *all1916* or *alr2532*. No gene encoding an ABC transporter NBD is however clustered together with these genes in any available cyanobacterial genomic sequence. Because in *Anabaena* there is only one gene other than *glsC* that encodes a predicted ABC sugar transporter NBD protein, *all1823* (Supporting Information Table S1), we constructed an *Anabaena* mutant of this gene as well.

The genes were inactivated by insertion of pCSL145, a plasmid that cannot replicate in *Anabaena* and bears the *npt* gene encoding neomycin/kanamycin phosphotransferase. Internal fragments of each of the genes were inserted in pCSL145 to serve as platforms for integration into the *Anabaena* chromosome by homologous recombination, the constructs were transferred to

Table 1. Esculin uptake in *Anabaena* and some mutant strains.

| | | | Esculin uptake (nmol [mg chlorophyll *a*]$^{-1}$ min^{-1}) | | | |
| | | | BG11 | | BG11$_0$ | |
Strain	Genotype	Product of the mutated gene	Mean $\pm$ SEM (*n*)	% of WT (*p*)	Mean $\pm$ SEM (*n*)	% of WT (*p*)
PCC 7120	Wild type (WT)		0.159 $\pm$ 0.010 (30)		0.282 $\pm$ 0.018 (24)	
CSMN17	*all1823*::pCSL145	NBD (GlsD)	0.037 $\pm$ 0.010 (5)	23.3% (< 0.001)	0.020 $\pm$ 0.007 (5)	7.1% (< 0.001)
CSMN18	*all1916*::pCSL145	SBP (GlsR)	0.091 $\pm$ 0.010 (5)	57.2% (0.013)	0.134 $\pm$ 0.012 (5)	53.9% (0.003)
CSMN19	*alr2532*::pCSL145	TMD (GlsQ)	0.143 $\pm$ 0.023 (6)	89.9% (0.536)	0.132 $\pm$ 0.016 (5)	46.8% (0.001)

Filaments grown in BG11 medium (in the presence of 5 μg neomycin sulfate [Nm] ml^{-1} for the mutants) were washed and resuspended in BG11 or BG11$_0$ (BG11 medium lacking NaNO$_3$) media without Nm and incubated for 18 h under culture conditions. Filaments were then resuspended in the same media supplemented with 10 mM HEPES-NaOH (pH 7) and used in assays of uptake of 100 μM esculin as described in the Supporting Information. Data are mean and SEM of the results from the indicated number of assays performed with independent cultures. Significance of the difference between each mutant and the wild type was assessed by the Student's *t*-test; *p* is indicated in each case. NBD, nucleotide-binding domain; SBP, substrate-binding protein; TMD, transmembrane domain.

Anabaena by conjugation, and exconjugants were selected as neomycin-resistant clones (Supporting Information Fig. S2). Clones that were homozygous for chromosomes containing the inactivated construct were identified by PCR analysis and named CSMN17 (*all1823*::pCSL145), CSMN18 (*all1916*::pCSL145) and CSMN19 (*alr2532*::pCSL145).

To investigate the possible role of the inactivated proteins in glucoside transport, uptake of esculin was studied with filaments of wild-type *Anabaena* and the three mutants grown in BG11 medium (containing nitrate) or grown in BG11 medium and incubated for 18 h in BG11$_0$ medium (lacking any source of combined nitrogen). Strain CSMN17 showed a low esculin uptake activity in either BG11 or BG11$_0$ medium, strain CSMN18 showed about half of the wild-type esculin uptake activity in either medium, and strain CSMN19 was affected in esculin uptake in BG11$_0$ medium but not significantly in BG11 medium (Table 1). Thus, the three genes encode components of transporters that participate in glucoside uptake. We name All1823 as GlsD (NBD), All1916 as GlsR (periplasmic SBP) and Alr2532 as GlsQ (TMD).

Sugar-stimulated growth

We then investigated whether the ABC esculin transporters identified in this work and those described previously (Nieves-Morión *et al.*, 2017b) could mediate a growth response to sugars. Attempts of growth tests in the dark or in the light in the presence of 10 μM DCMU with sugars gave inconsistent results, and growth tests in shaken cultures failed to show any positive effect of sucrose. However, 100 mM sucrose, fructose or glucose stimulated phototrophic growth of *Anabaena* on plates, specifically in BG11$_0$ medium (Fig. 1). We then tested the effect of the three sugars, added at 50 mM, on growth in standing liquid cultures (in microtiter plates) in the light. Sucrose, fructose and glucose significantly

increased the yield of *Anabaena* in both BG11 and BG11$_0$ media (Student's *t*-test $p \leq 0.011$; see WT in Supporting Information Table S2A) suggesting mixotrophic growth. Fructose and glucose stimulated growth more than sucrose (Supporting Information Table S2 and Fig. 2). In contrast, maltose had only a marginal positive effect on the growth of *Anabaena* (not shown).

Sucrose-stimulated growth in BG11 and BG11$_0$ media was drastically hampered by inactivation of the NBD proteins GlsC and GlsD, and it was impaired by inactivation of the TMD proteins GlsP and GlsQ and of the SBP protein GlsR (Fig. 2; see whole set of data in Supporting Information Table S2). Fructose- and glucose-stimulated growth was also impaired in all the mutants, and the effect of the inactivation of *glsC* on glucose-stimulated growth was especially significant. These results show
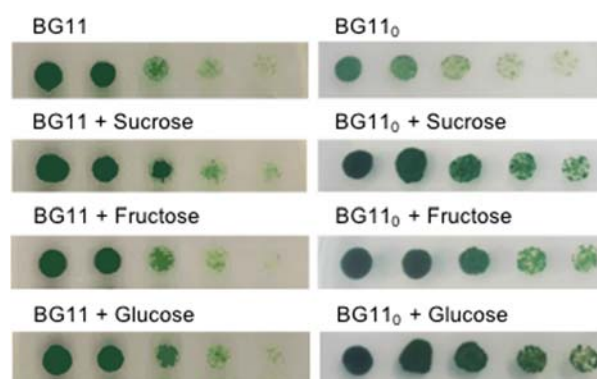
Fig. 1. Growth of *Anabaena* on solid BG11 or BG11$_0$ medium. Media were solidified with 1% Bacto agar and supplemented with 10 mM TES-NaOH (pH 7.5) buffer and, when indicated, 100 mM sucrose, fructose or glucose. Filaments grown in BG11 medium were collected, washed with BG11$_0$ medium and spotted on plates as shown (successively diluted spots contained 10, 5, 2.5, 1.25 and 0.625 ng chlorophyll *a*). The plates were incubated for 6 days (BG11 medium) or 10 days (BG11$_0$ medium) at 30°C in the light (ca. 25 μmol photons m^{-2} s^{-1}) in an air atmosphere and photographed.
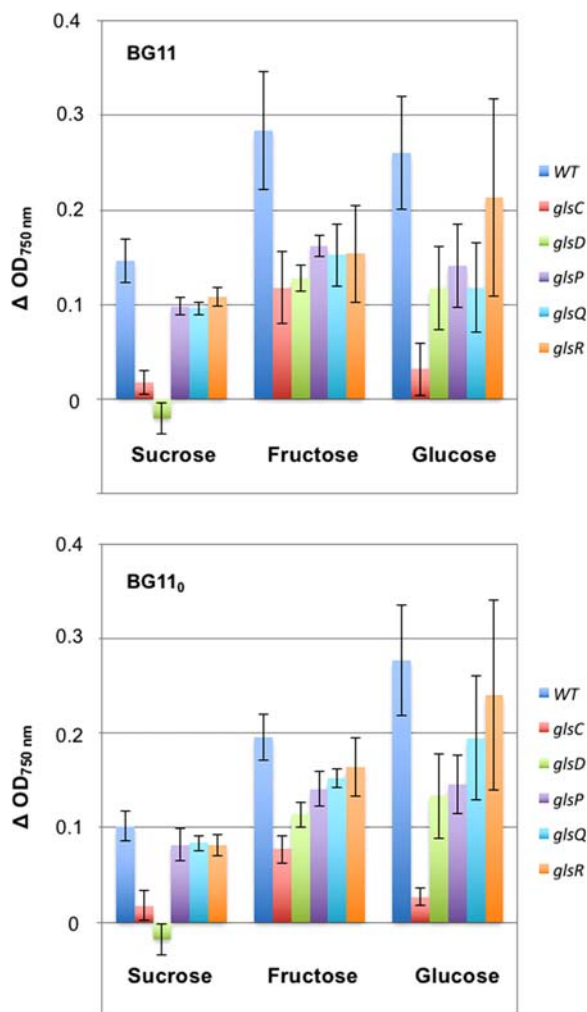
Fig. 2. Sugar-stimulated growth in *Anabaena* and some ABC gluco-side uptake transporter mutants.
The increase in growth yield in standing liquid cultures (top, BG11 media; bottom, $BG11_0$ media) in response to the addition of 50 mM of the indicated sugar (i.e., $OD_{750\ nm}$ with sugar less $OD_{750\ nm}$ without sugar) is presented as the mean and SEM. See Supporting Information Table S2 for the complete set of data.

that the identified ABC uptake transporter components mediate a positive growth response of *Anabaena* to sucrose, fructose and glucose.

Whereas direct uptake of radiolabeled sucrose (Nicolaisen *et al.*, 2009b; López-Igual *et al.*, 2012) and fructose (Stebegg *et al.*, 2012) has been previously shown for *Anabaena*, to the best of our knowledge uptake of glucose has not been reported. We therefore tested uptake of [^{14}C]glucose in filaments grown in BG11 medium and filaments incubated for 18 h in $BG11_0$ medium. *Anabaena* filaments could take up glucose, at higher levels after incubation in $BG11_0$ medium, but they did so significantly only at relatively high sugar concentrations indicating a very low affinity for the sugar (Supporting Information Fig. S3).

Analysis of septal junction function

Inactivation of *glsC* and *glsP* in *Anabaena* impairs diazotrophic growth likely because of effects on the septal junctions (Nieves-Morión *et al.*, 2017b). We tested growth of the *glsD*, *glsQ* and *glsR* mutants in liquid and solid BG11 or $BG11_0$ medium. Growth was not significantly impaired in any of the mutants in the liquid media (Supporting Information Table S2A, no sugar added). In contrast, whereas none of the mutants showed a deficit in growth on solid BG11 medium, the *glsR* and *glsQ* mutants were found to be impaired in growth on solid $BG11_0$ medium (Fig. 3).

Septal junctions mediate intercellular molecular transfer that can be studied by Fluorescence Recovery After Photobleaching (FRAP) analysis with fluorescent markers including calcein and 5-carboxyfluorescein (5-CF) (Mullineaux *et al.*, 2008; Merino-Puerto *et al.*, 2011). Intercellular transfer of these markers, quantified as the recovery constant *R*, was tested in the *glsD*, *glsQ* and *glsR* mutants. Whereas the *glsQ* mutant showed *R* values that were consistently lower than the wild-type figures for both calcein and 5-CF, the *glsD* and *glsR* mutants were impaired in calcein transfer but not in 5-CF transfer (Table 2). Hence, the *glsQ* mutant appears to be the most affected in intercellular transfer of fluorescence markers.
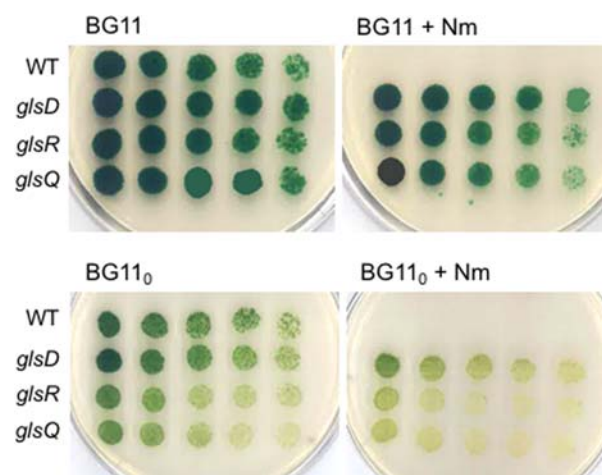
Fig. 3. Growth of strains CSMN17 (*glsD*::pCSL145), CSMN18 (*glsR*::pCSL145) and CSMN19 (*glsQ*::pCSL145) on solid BG11 or $BG11_0$ medium.
Filaments grown in BG11 medium (in the presence of Nm for the mutants) were collected, washed with $BG11_0$ medium and spotted on plates as shown (successively diluted spots contained 10, 5, 2.5, 1.25 and 0.625 ng chlorophyll *a*). The plates were incubated for 8 days (BG11 medium) or 14 days ($BG11_0$ medium) and photographed. The growth medium in the left panels was not supplemented with Nm to allow comparison with wild-type *Anabaena* (WT). Addition of Nm (right panels) inhibited growth of the wild type as expected.

Table 2. Transfer of calcein and 5-CF between nitrate-grown vegetative cells in *Anabaena* and ABC glucoside transporter mutant strains

Strain (mutated genes)	Calcein transfer (R, s^{-1})		5-CF transfer (R, s^{-1})	
	Mean $\pm$ SEM (n)	% of WT (p)	Mean $\pm$ SEM (n)	% of WT (p)
PCC 7120 (WT)	0.068 $\pm$ 0.006 (64)		0.090 $\pm$ 0.004 (160)	
CSMN17 (*glsD*)	0.047 $\pm$ 0.007 (34)	69% (0.029)	0.110 $\pm$ 0.005 (33)	122% (0.015)
CSMN18 (*glsR*)	0.040 $\pm$ 0.006 (32)	59% (0.004)	0.085 $\pm$ 0.011 (25)	94% (0.651)
CSMN19 (*glsQ*)	0.029 $\pm$ 0.011 (22)	43% (0.002)	0.064 $\pm$ 0.006 (44)	71% (0.001)

Filaments of the wild type and the indicated mutants grown in BG11 medium (with Nm for the mutants) and incubated in BG11 medium without Nm for 18–24 h were used in FRAP analysis as described in Suppl. Experimental procedures. Data (R, recovery constant) are the mean and SEM of the results obtained with the indicated number of filaments (n) subjected to FRAP analysis. Filaments from eight cultures of the WT or three cultures from each mutant were used for calcein, and filaments from 12 cultures of the WT or two cultures from each mutant were used for 5-CF. Student's t test (mutant vs. wild type) p is indicated in each case.

Localization of SepJ and protein–protein interactions

Specific glucoside transporters have been found to influence septal junctions by either affecting localization of the septal protein SepJ or by possible protein–protein interactions with SepJ (Nieves-Morión *et al.*, 2017b). We investigated the subcellular localization of SepJ in the mutants generated in this work by immunofluorescence analysis performed with antibodies raised against the coiled-coil domain of SepJ (Ramos-León *et al.*, 2015). SepJ was found localized at the intercellular septa of filaments of the *glsD*, *glsQ* and *glsR* mutants in a similar way as in the wild type (Supporting Information Fig. S4).

To investigate possible interactions of GlsD and GlsQ with SepJ and to assess whether some of the identified components of ABC transporters could be partners in

Fig. 4. Bacterial two-hybrid analysis of interactions between Gls proteins and between Gls proteins and SepJ. Interactions of T25- and T18-fusion proteins produced in *E. coli* were measured as β-galactosidase activity in liquid cultures. The protein fused to the N- or the C-terminus of T18 or T25 is indicated in each case (N-termius, protein-T18 or protein-T25; C-terminus, T18-protein or T25-protein). Data are mean and SEM of the activity with the indicated pair of fusion proteins less the activity of the T25/T18 negative control. Only interactions that were significant at $p < 0.05$ are shown. See Supporting Information Table S3 for the complete set of data.

specific transporters, we performed Bacterial Adenylate Cyclase Two Hybrid analysis (BACTH). In this analysis, adenylate cyclase activity is reconstituted from two fragments, T25 and T18, of adenylate cyclase from *Bordetella pertussis* brought together by interacting proteins fused to each of those fragments (Karimova *et al.*, 1998). Reconstituted adenylate cyclase in *Escherichia coli* produces cAMP that promotes induction of *lacZ* encoding β-galactosidase. Because cAMP has to be produced in the cytoplasm, the periplasmic SBP GlsR could not be included in this analysis. T25 and T18 fusions to GlsC and GlsP have been described previously (Nieves-Morión *et al.*, 2017b). We have now constructed N-terminal and C-terminal fusions of both T25 and T18 to each of the newly identified proteins GlsD and GlsQ. GlsD is a cytoplasmic protein and GlsQ is an integral membrane protein with its N- and C-termini predicted to be cytoplasmic. Of the tested combinations, GlsD interacting with itself produced high levels of β-galactosidase activity indicating self-interaction (Fig. 4; see complete set of data in Supporting Information Table S3). Previous work showed self-interaction also for GlsC (Nieves-Morión *et al.*, 2017b; included in Fig. 4 for comparison). Interestingly, GlsD interacted also with GlsC. Additionally, GlsD was found to interact with GlsP, GlsC with GlsQ and GlsP with GlsQ. Although these latter interactions were relatively weak, it should be noted that they were statistically significant (see Supporting Information Table S3). Finally, GlsQ was found to interact with SepJ, resembling the GlsP-SepJ interaction described previously (Nieves-Morión *et al.*, 2017b; included in Fig. 4 for comparison). This interaction may constitute the basis for the requirement of GlsQ for full intercellular molecular transfer and diazotrophic growth on plates.

Discussion

Results in this work indicate that GlsD (NBD) has a quantitatively important role in esculin uptake and in sucrose-stimulated growth in *Anabaena*, suggesting that

6   *M. Nieves-Morión and E. Flores*

GlsD is an essential component of transporters involved in the uptake of sucrose. Our results additionally show that GlsC (NBD) is also needed to assimilate sucrose, suggesting that GlsC and GlsD work together in the ABC glucoside uptake complexes of *Anabaena*. Consistently, GlsC and GlsD were observed to interact in BACTH analysis. Nonetheless, each of these proteins is also able to interact with itself suggesting that they can act as homodimers in some ABC transporter complexes. A transporter containing specifically GlsC appears to be especially relevant for glucose uptake. NBD proteins serving different TMD complexes in ABC transporters – the so-called multitask ABC ATPases – are well known, and classical examples are MalK and similar proteins that energize di- and oligo-saccharide uptake in several bacteria (Schlösser *et al.*, 1997; Webb *et al.*, 2008; Ferreira and de Sá-Nogueira, 2010).

The GlsP and GlsQ TMDs are also needed for full esculin uptake and sugar-stimulated growth, they interact with each other in BACTH analysis, and the genes encoding their orthologs are clustered together in the genomes of many heterocyst-forming cyanobacteria. These observations together suggest that GlsP and GlsQ are partners in ABC transporter complexes. The periplasmic SBP GlsR is also needed for full esculin uptake and sugar-stimulated growth, and a gene encoding a GlsR ortholog is clustered together with genes encoding GlsP and GlsQ orthologs in the genomes of some cyanobacteria. Therefore, GlsR may be a partner of GlsP and GlsQ. On the other hand, because the *glsP*, *glsQ* and *glsR* mutants still show substantial activity of esculin uptake and sucrose, fructose- and glucose-stimulated growth, additional SBPs and TMDs should be involved in the uptake of these sugars.

The 12 possible components of ABC sugar uptake transporters encoded in the *Anabaena* genome (Supporting Information Table S1) belong to the Transporter Classification Database (TCDB) family 3.A.1.1 (Saier, 2000; for the most recent discussion of the TCDB see Saier *et al.*, 2016), which transport disaccharides and other complex saccharides and for which the MalEFGK transporter of *E. coli* (MalE, SBP; MalF and MalG, TMDs; MalK, NBD) is a well-known representative (Nikaido, 1994). The predicted *Anabaena* proteins are four periplasmic SBP, six TMDs (three most similar to MalF and three to MalG) and two NBDs (Supporting Information Table S1). These data together with our results discussed above suggest the presence in *Anabaena* of at least three ABC glucoside transporters, one of which may be constituted by GlsR (SBP), GlsP-GlsQ (TMDs) and GlsC-GlsD (NBDs). The membrane complex of this transporter may use additional SBP(s), for which there is precedent in ABC transporters

(Davidson *et al.*, 2008), and the NBD proteins appear to be shared by the three glucoside transporters as discussed earlier.

The Gls proteins have a role not only in sucrose-stimulated growth but also in fructose- and glucose-stimulated growth. These results indicate that fructose and glucose can be incorporated into *Anabaena* at least in part by the ABC glucoside uptake transporters. Transport of fructose and glucose appears to take place, however, with low affinity. Thus, our results of direct uptake of [^{14}C]glucose by *Anabaena* permit to estimate a relatively high K_s of at least 20 mM, and the analysis of uptake of [^{14}C]fructose reported by Stebegg and colleagues (2012) also suggest low affinity. In contrast, the K_s of *Anabaena* for sucrose (determined in fragmented filaments) is 4.9 μM (Nicolaisen *et al.*, 2009b) and for esculin 150 μM (in BG11 medium) or 119 μM (in BG11$_0$ medium) (Nieves-Morión *et al.*, 2017b). Hence, *Anabaena* expresses high-affinity cytoplasmic membrane transporters for sucrose but not for fructose or glucose (see also Ungerer *et al.*, 2008). Indeed, no ORF evidently encoding a fructose or glucose transporter is found in the *Anabaena* genome. Why, then, is growth stimulated more by fructose or glucose than by sucrose? We have previously reported that *Anabaena* appears to lack any sucrose porin (Nicolaisen *et al.*, 2009b), but the *Anabaena* genome contains genes encoding homologs to porin OprB (Nicolaisen *et al.*, 2009a). OprB porins mediate the movement through the outer membrane of glucose and other monosaccharides (Wylie and Worobec, 1995; van den Berg, 2012), and an OprB-like porin in *N. punctiforme* is involved in glucose and fructose uptake (Ekman *et al.*, 2013). Facilitated movement through the outer membrane may be a key factor to permit assimilation of the sugars by *Anabaena*. Once in the periplasm, fructose and glucose can be transported into the cytoplasm, albeit with low affinity, by cytoplasmic membrane glucoside transporters. In contrast, sucrose hardly passes the outer membrane, but the sucrose molecules that reach the periplasm can be transported into the cytoplasm with high affinity. Sugar concentrations in freshwater and terrestrial environments are normally in the μM range, but there are reports of up to 4.5 mM (Hobbie and Hobbie, 2013), implying that the *Anabaena* sugar transporters might be useful in such environments.

The ABC transporter Gls appears to be needed also for normal function of septal junctions in the *Anabaena* filament. As mentioned earlier, GlsC (NBD) is required for normal subcellular localization of SepJ and septal maturation (Nieves-Morión *et al.*, 2017b). The NBD protein GlsD studied here is however not needed for SepJ localization indicating that this is a specific role of GlsC likely acting independently of GlsD. On the other hand,

inactivation of GlsQ (TMD) has an effect similar to that of inactivation of GlsP (TMD) on the intercellular transfer of calcein and 5-CF (compare to data in Nieves-Morión *et al.*, 2017b). The requirement of the ABC glucoside transporter Gls for the normal function of the septal junctions could be based on protein-protein interactions between the TMD subunits and SepJ (as shown by BACTH analysis), and it can account, at least partly, for the growth defect of the mutants.

Our work has identified an ABC glucoside transporter (Gls) from *Anabaena* that can be probed with the fluorescent marker esculin and is involved in the uptake of sucrose, fructose and glucose. In addition to its influence on the septal junctions, a putative function of this transporter is to mediate sugar assimilation. It should be noted, however, that we have consistently observed sugar-stimulated growth of *Anabaena* mainly in standing liquid cultures. Different relationships of gases (O_2 and CO_2) in different incubation conditions (growth on a surface or in shaken or standing liquid cultures) may affect the growth response to sugars. The presence in the *Anabaena* genome of numerous genes encoding organic substrate transporters is consistent with the idea that microorganisms are prepared to take up extensively substrates that become available (Hobbie and Hobbie, 2013; Muñoz-Marín *et al.*, 2013). Whereas the wide distribution of cyanobacteria in our planet is likely based on their photoautotrophic lifestyle, the capability of mixotrophic growth could enhance fitness in many ecological niches.

Conflicts of interest

The authors have no conflicts of interest to declare.

References

Bottomley, P.J, and van Baalen, C. (1978) Dark hexose metabolism by photoautotrophically and heterotrophically grown cells of the blue-green alga (Cyanobacterium) *Nostoc* sp. strain Mac. *J Bacteriol* **135**: 888–894.

Cui, J., and Davidson, A.L. (2011) ABC solute importers in bacteria. *Essays Biochem* **50**: 85–99.

Cumino, A.C., Marcozzi, C., Barreiro, R., and Salerno, G.L. (2007) Carbon cycling in *Anabaena* sp. PCC 7120. Sucrose synthesis in the heterocysts and possible role in nitrogen fixation. *Plant Physiol* **143**: 1385–1397.

Curatti, L., Flores, E., and Salerno, G. (2002) Sucrose is involved in the diazotrophic metabolism of the heterocyst-forming cyanobacterium *Anabaena* sp. *FEBS Lett* **513**: 175–178.

Davidson, A.L., Dassa, E., Orelle, C., and Chen, J. (2008) Structure, function, and evolution of bacterial ATP-binding cassette systems. *Microbiol Mol Biol Rev* **72**: 317–364.

Ekman, M., Picossi, S., Campbell, E.L., Meeks, J.C, and Flores, E. (2013) A *Nostoc punctiforme* sugar transporter necessary to establish a cyanobacterium-plant symbiosis. *Plant Physiol* **161**: 1984–1992.

Ferreira, M.J., and de Sá-Nogueira, I. (2010) A multitask ATPase serving different ABC-type sugar importers in *Bacillus subtilis*. *J Bacteriol* **192**: 5312–5318.

Flores, E., and Herrero, A. (2010) Compartmentalized function through cell differentiation in filamentous cyanobacteria. *Nat Rev Microbiol* **8**: 39–50.

Flores, E., Herrero, A., Forchhammer, K., and Maldener, I. (2016) Septal junctions in filamentous heterocyst-forming cyanobacteria. *Trends Microbiol* **24**: 79–82.

Gora, P.J., Reinders, A., and Ward, J.M. (2012) A novel fluorescent assay for sucrose transporters. *Plant Methods* **8**: 13.

Herrero, A., Stavans, J., and Flores, E. (2016) The multicellular nature of filamentous heterocyst-forming cyanobacteria. *FEMS Microbiol Rev* **40**: 831–854.

Hobbie, J.E, and Hobbie, E.A. (2013) Microbes in nature are limited by carbon and energy: the starving-survival lifestyle in soil and consequences for estimating microbial rates. *Front Microbiol* **4**: 324.

Jüttner, F. (1983) ^{14}C-labeled metabolites in heterocysts and vegetative cells of *Anabaena cylindrica* filaments and their presumptive function as transport vehicles of organic carbon and nitrogen. *J Bacteriol* **155**: 628–633.

Karimova, G., Pidoux, J., Ullmann, A., and Ladant, D. (1998) A bacterial two-hybrid system based on a reconstituted signal transduction pathway. *Proc Natl Acad Sci USA* **95**: 5752–5756.

López-Igual, R., Flores, E., and Herrero, A. (2010) Inactivation of a heterocyst-specific invertase indicates a principal role of sucrose catabolism in the heterocysts of *Anabaena* sp. *J Bacteriol* **192**: 5526–5533.

López-Igual, R., Lechno-Yossef, S., Fan, Q., Herrero, A., Flores, E., and Wolk, C.P. (2012) A major facilitator superfamily protein, HepP, is involved in formation of the heterocyst envelope polysaccharide in the cyanobacterium *Anabaena* sp. strain PCC 7120. *J Bacteriol* **194**: 4677–4687.

Malatinszky, D., Steuer, R., and Jones, P.R. (2017) A comprehensively curated genome-scale two-cell model for the heterocystous cyanobacterium *Anabaena* sp. PCC 7120. *Plant Physiol* **173**: 509–523.

Merino-Puerto, V., Schwarz, H., Maldener, I., Mariscal, V., Mullineaux, C.W., Herrero, A., and Flores, E. (2011) FraC/FraD-dependent intercellular molecular exchange in the filaments of a heterocyst-forming cyanobacterium, *Anabaena* sp. *Mol Microbiol* **82**: 87–98.

8 *M. Nieves-Morión and E. Flores*

Mullineaux, C.W., Mariscal, V., Nenninger, A., Khanum, H., Herrero, A., Flores, E., and Adams, D.G. (2008) Mechanism of intercellular molecular exchange in heterocyst-forming cyanobacteria. *EMBO J* **27**: 1299–1308.

Muñoz-Marín, Mdel C., Luque, I., Zubkov, M.V., Hill, P.G., Díez, J., and García-Fernández, J.M. (2013) *Prochlorococcus* can use the Pro1404 transporter to take up glucose at nanomolar concentrations in the Atlantic Ocean. *Proc Natl Acad Sci USA* **110**: 8597–8602.

Nikaido, H. (1994) Maltose transport system of *Escherichia coli*: an ABC-type transporter. *FEBS Lett* **346**: 55–58.

Nicolaisen, K., Hahn, A., and Schleiff, E. (2009a) The cell wall in heterocyst formation by Anabaena sp. PCC 7120. *J Basic Microbiol* **49**: 5–24.

Nicolaisen, N., Mariscal, V., Bredemeier, R., Pernil, R., Moslavac, S., López-Igual, R. *et al.* (2009b) The outer membrane of a heterocyst-forming cyanobacterium is a permeability barrier for uptake of metabolites that are exchanged between cells. *Mol Microbiol* **74**: 58–70.

Nieves-Morión, M., Mullineaux, C.W, and Flores, E. (2017a) Molecular diffusion through cyanobacterial septal junctions. *mBio* **8**: e01756–e01716.

Nieves-Morión, M., Lechno-Yossef, S., López-Igual, R., Frías, J.E., Mariscal, V., Nürnberg, D.J. *et al.* (2017b) Specific glucoside transporters influence septal structure and function in the filamentous, heterocyst-forming cyanobacterium *Anabaena* sp. strain PCC 7120. *J Bacteriol* **199**: e00876–e00816.

Nürnberg, D.J., Mariscal, V., Bornikoel, J., Nieves-Morión, M., Krauß, N., Herrero, A. *et al.* (2015) Intercellular diffusion of a fluorescent sucrose analog via the septal junctions in a filamentous cyanobacterium. *mBio* **6**: e02109.

Pernil, R., Herrero, A., and Flores, E. (2010) A TRAP transporter for pyruvate and other monocarboxylate 2-oxoacids in the cyanobacterium *Anabaena* sp. strain PCC 7120. *J Bacteriol* **192**: 6089–6092.

Pernil, R., Picossi, S., Herrero, A., Flores, E., and Mariscal, V. (2015) Amino acid transporters and release of hydrophobic amino acids in the heterocyst-forming cyanobacterium *Anabaena* sp. strain PCC 7120. *Life (Basel)* **5**: 1282–1300.

Ramos-León, F., Mariscal, V., Frías, J.E., Flores, E., and Herrero, A. (2015) Divisome-dependent subcellular localization of cell-cell joining protein SepJ in the filamentous cyanobacterium *Anabaena*. *Mol Microbiol* **96**: 566–580.

Rippka, R., Deruelles, J., Waterbury, J.B., Herdman, M., and Stanier, R.Y. (1979) Generic assignments, strain stories and properties of pure cultures of cyanobacteria. *J Gen Microbiol* **111**: 1–61.

Saier, M.H. Jr. (2000) Families of transmembrane sugar transport proteins. *Mol Microbiol* **35**: 699–710.

Saier, M.H., Jr., Reddy, V.S., Tsu, B.V., Ahmed, M.S., Li, C., and Moreno-Hagelsieb, G. (2016) The Transporter Classification Database (TCDB): recent advances. *Nucleic Acids Res* **44**: D372–D379.

Schlösser, A., Kampers, T., and Schrempf, H. (1997) The *Streptomyces* ATP-binding component MsiK assists in cellobiose and maltose transport. *J Bacteriol* **179**: 2092–2095.

Schmetterer, G.R. (1990) Sequence conservation among the glucose transporter from the cyanobacterium *Synechocystis* sp. PCC 6803 and mammalian glucose transporters. *Plant Mol Biol* **14**: 697–706.

Schmetterer, G., and Flores, E. (1988) Uptake of fructose by the cyanobacterium *Nostoc* sp. ATCC 29150. *Biochim Biophys Acta* **942**: 33–37.

Stebegg, R., Wurzinger, B., Mikulic, M., and Schmetterer, G. (2012) Chemoheterotrophic growth of the cyanobacterium *Anabaena* sp. strain PCC 7120 dependent on a functional cytochrome c oxidase. *J Bacteriol* **194**: 4601–4607.

Ungerer, J.L., Pratte, B.S, and Thiel, T. (2008) Regulation of fructose transport and its effect on fructose toxicity in *Anabaena* spp. *J Bacteriol* **190**: 8115–8125.

van den Berg, B. (2012) Structural basis for outer membrane sugar uptake in pseudomonads. *J Biol Chem* **287**: 41044–41052.

Vargas, W.A., Nishi, C.N., Giarrocco, L.E, and Salerno, G.L. (2011) Differential roles of alkaline/neutral invertases in *Nostoc* sp. PCC 7120: Inv -B isoform is essential for diazotrophic growth. *Planta* **233**: 153–162.

Webb, A.J., Homer, K.A, and Hosie, A.H. (2008) Two closely related ABC transporters in *Streptococcus mutans* are involved in disaccharide and/or oligosaccharide uptake. *J Bacteriol* **190**: 168–178.

Whitton, B.A., and Potts, M., Eds. (2000) *The Ecology of Cyanobacteria. Their Diversity in Time and Space*. Dordrecht, The Netherlands: Kluwer Academic Press.

Wilk, L., Strauss, M., Rudolf, M., Nicolaisen, K., Flores, E., Kühlbrandt, W., and Schleiff, E. (2011) Outer membrane continuity and septosome formation between vegetative cells in the filaments of *Anabaena* sp PCC 7120. *Cell Microbiol* **13**: 1744–1754.

Wolk, C.P. (1968) Movement of carbon from vegetative cells to heterocysts in *Anabaena cylindrica*. *J Bacteriol* **96**: 2138–2143.

Wolk, C.P, and Shaffer, P.W. (1976) Heterotrophic micro- and macrocultures of a nitrogen-fixing cyanobacterium. *Arch Microbiol* **110**: 145–147.

Wolk, C.P., Austin, S.M., Bortins, J., and Galonsky, A. (1974) Autoradiographic localization of ^{13}N after fixation of ^{13}N-labeled nitrogen gas by a heterocyst-forming blue-green alga. *J Cell Biol* **61**: 440–453.

Wylie, J.L, and Worobec, E.A. (1995) The OprB porin plays a central role in carbohydrate uptake in *Pseudomonas aeruginosa*. *J Bacteriol* **177**: 3021–3026.

Zhang, C.C., Durand, M.C., Jeanjean, R., and Joset, F. (1989) Molecular and genetical analysis of the fructose-glucose transport system in the cyanobacterium *Synechocystis* PCC6803. *Mol Microbiol* **3**: 1221–1229.

Supporting Information

Additional Supporting Information may be found in the online version of this article at the publisher's web-site:

Table S1. ORFs from the *Anabaena* genome predicted to encode components of ABC sugar uptake transporters.
Table S2. Sugar-stimulated growth in *Anabaena* and some ABC glucoside uptake transporter mutant strains.
Table S3. Bacterial two-hybrid analysis of protein–protein interactions.

Table S4. Oligodeoxynucleotide primers used in this work. Introduced restriction sites are underlined.

Fig. S1. Genomic region of *Anabaena* (*Nostoc*) sp. strain PCC 7120 ORF *all0261* (*glsP*) and some examples of genomic regions containing an *all0261* ortholog.

Fig. S2. Construction and verification of mutants of genes *glsD*, *glsR* and *glsQ* in *Anabaena*.

Fig. S3. Uptake rates of [^{14}C]glucose in wild-type *Anabaena*.

Fig. S4. Immunofluorescence localization of SepJ in wild-type *Anabaena* (WT) and *glsD* mutant CSMN17 (*all1823*::pCSL145), *glsR* mutant CSMN18 (*all1916*::pCSL145) and *glsQ* mutant CSMN19 (*alr2532*::pCSL145).

Supplementary experimental procedures

Strains and growth conditions

Anabaena sp. strain PCC 7120 (also known as *Nostoc* sp.) and derivative strains were grown in BG11 medium modified to contain ferric citrate instead of ferric ammonium citrate (Rippka *et al.*, 1979) or $BG11_0$ medium (BG11 further modified by omission of $NaNO_3$) at 30 ºC in the light (ca. 25 µmol photons m^{-2} s^{-1}), in shaken (100 r.p.m.) liquid cultures or in plates in medium solidified with 1 % Bacto agar. When indicated, BG11 or $BG11_0$ liquid medium was supplemented with 50 mM sucrose, fructose, glucose or maltose and 10 mM TES-NaOH buffer (pH 7.5), all sterilized by filtration, and production of biomass was determined as OD_{750nm} after 7 days of incubation without shaking. When appropriate, neomycin sulfate (Nm) was added to the cyanobacterial cultures at the following concentrations: 5 µg ml^{-1} (liquid cultures) or 30-40 µg ml^{-1} (solid media). Chlorophyll *a* content of cultures was determined by the method of Mackinney (1941).

     Escherichia coli strains were grown in LB medium, supplemented when appropriate with antibiotics at standard concentrations (Ausubel *et al.*, 2014). *E. coli* strain DH5α was used for plasmid constructions. This strain, bearing a conjugative plasmid, and strain HB101 bearing a methylase-encoding helper plasmid and one cargo plasmid were used for conjugation with *Anabaena* (Elhai *et al.*, 1997).

Construction of mutant strains

For inactivation of *all1823*, *all1916*, and *alr2532*, internal fragments of 738 bp, 708 bp and 564 bp, respectively, were amplified by PCR using primers all1823-1/all1823-2, all1916-1/all1916-2, alr2532-1/alr2532-2, respectively. All primers bore SacI sites in their 5' ends and are described in Table S4. Genomic DNA from *Anabaena* was used as a template. The amplified fragments were cloned into vector pSpark I producing pCSMN36, pCSMN37 and pCSMN38, and were transferred as SacI-fragments to SacI-digested pCSL145 (mobilizable plasmid containing cassette C.K1 [Nm^R]; Elhai and Wolk, 1988) producing pCSMN39, pCSMN40 and pCSMN41, which were verified by sequencing. These plasmids were transformed into *E. coli* HB101 [pRL623] and transferred to *Anabaena* by conjugation with selection for Nm^R. Clones that had incorporated pCSL145 by single recombination were selected for further study and named strain CSMN17, CSMN18 and CSMN19, respectively. The genetic structure of selected clones was studied by PCR to test recombination in the correct genomic location and test for segregation with the primer pairs indicated in Fig. S12.

Physiological parameters

To test uptake of esculin, *Anabaena* cultures grown in BG11 medium —with antibiotics for the mutants— were harvested by centrifugation, washed with BG11 or $BG11_0$ medium without antibiotics and incubated for 18 h in the same medium under culture conditions. Cells were harvested, washed and resuspended in growth medium supplemented with 10 mM HEPES-NaOH buffer (pH 7). Assays of uptake were started by addition of esculin hydrate (Sygma-Aldrich) at 100 µM, and cell suspensions were withdrawn and filtered. Cells on the filters were washed with 10 mM HEPES-NaOH buffer (pH 7) were resuspended in 2 ml of the same buffer. Fluorescence of the resulting cell suspension was measured in a Varian Cary Eclipse Fluorescence Spectrophotometer (excitation 360 ± 10 nm; emission 462 ± 10 nm). Esculin solutions in the same buffer were used as standards.

     For calcein and 5-CF transfer assays (FRAP analysis), calcein and 5-CF staining were performed as previously reported (Mullineaux *et al.*, 2008; Merino-Puerto *et al.*, 2011). Cell suspensions were spotted onto agar and placed in a temperature-controlled sample holder with a glass cover slip on top. All measurements were carried out at 30 °C. For both calcein and 5-

CF, cells were imaged with a Leica HCX Plan Apo 63X, 1.4-NA oil immersion objective attached to a Leica TCS SP5 confocal laser-scanning microscope with a 488-nm line argon laser as the excitation source. Fluorescent emission was monitored by collection across windows of 500 to 520 nm and a 150-μm pinhole. After an initial image was recorded, the bleach was carried out by an automated FRAP routine as previously reported (Mullineaux et $al.$, 2008). For FRAP data analysis, kinetics of transfer of the fluorescent tracer to a cell somewhere in the middle of a filament (i.e., with two cell junctions) was quantified. The recovery rate constant, R, was calculated from the formula $C_B = C_0 + C_R (1 - e^{-2Rt})$, where C_B is fluorescence in the bleached cell, C_0 is fluorescence immediately after the bleach and tending towards $(C_0 + C_R)$ after fluorescence recovery, t is time and R is the recovery rate constant due to transfer of the tracer from one neighbor cell (Nieves-Morion et $al.$, 2017).

For ^{14}C-labeled glucose uptake assays, filaments were grown in BG11 and BG11$_0$ media, harvested at room temperature, washed three times with BG11 or BG11$_0$ media and resuspended in the same media supplemented with 10 mM HEPES-NaOH (pH 7), to give a cell density corresponding to 10 μg chlorophyll a ml^{-1}. The assay was started by adding 0.2 ml of a sugar solution containing 10, 100 or 500 mM glucose and a small amount of [^{14}C]glucose (300 Ci mol^{-1}; American Radiolabeled Chemicals) to a 1.8-ml suspension. The filament suspensions were incubated at 30 ºC in the light (85 μmol m^{-2} s^{-1}), and 0.6-ml samples (taken at 20, 40 and 60 min) were filtered using 0.45-mm pore size Millipore HA filters. After washing with 10 mM HEPES-NaOH (pH 7) to remove excess labeled sugar, the filters were placed in a scintillation cocktail and their radioactivity was measured. Nonspecific retention of radioactivity was determined by using boiled cells.

Immunolocalization of SepJ

Cells from 1.5 ml of liquid cultures were collected by centrifugation, placed atop a poly-L-lysine-precoated microscope slide, and covered with a 45-μm-pore-size Millipore filter. The filter was removed and the slide was left to dry at room temperature, immersed in 70% ethanol at -20 ºC for 30 min, and dried for 15 min at room temperature. The cells were washed twice (2 min each time, room temperature) by covering the slide with PBS-T (Phosphate Buffered Saline supplemented with 0.05% Tween 20). Subsequently, the slides were treated with a blocking buffer (5% milk powder in PBS-T) for 15 min. Cells on the slides were then incubated for 90 min with anti-SepJ-CC antibodies (Mariscal et $al.$, 2011) diluted in blocking buffer (1:250), washed three times with PBS-T, incubated for 45 min in the dark with anti-rabbit antibody conjugated to FITC (1:500 dilution in PBS-T; Sigma), and washed three times with PBS-T. After dried, several drops of FluorSave (Calbiochem) were added atop, covered with a coverslip, and sealed with nail lacquer. Fluorescence was imaged using a Leica DM6000B fluorescence microscope and an ORCA-ER camera (Hamamatsu). Fluorescence was monitored using a FITC L5 filter (excitation, band-pass [BP] 480/40 filter; emission, BP 527/30 filter), and images were analyzed with ImageJ software (http://imagej.nih.gov/ij).

BACTH strain construction and assays

The possible interaction between different glucoside transporter components and between them and SepJ was tested using Bacterial Adenylate Cyclase Two Hybrid (BACTH) analysis. All tested genes were amplified using $Anabaena$ DNA as template. The following primers were used: all1823-5 and all1823-6 to amplify $glsD$, and alr2532-4 and alr2532-5 to amplify $glsQ$. Other constructs were previously described (Ramos-León et $al.$, 2015; Nieves-Morión et $al.$, 2017). The PCR products were transferred as XbaI- and KpnI-digested fragments to pUT18, pUT18C, pKNT25, and pKT25 (Battesti et $al.$, 2012), producing fusions to the 5' and 3' ends of the genes encoding the adenylate cyclase T18 and T25 fragments, respectively. The resulting plasmids (pCSMN59: *all1823*::pUT18; pCSMN60: *all1823*::pUT18C; pCSMN61: *all1823*::pKT25; pCSMN62: *all1823*::pKTN25; pCSMN63: *alr2532*::pUT18; pCSMN64: *alr2532*::pUT18C;

pCSMN65: *alr2532*::pKT25; pCSMN66: *alr2532*::pKTN25) were transformed into *E. coli* XL1-Blue for amplification. Isolated plasmids were cotransformed into *E. coli* BTH101 (cya-99). Transformants were plated onto LB medium containing selective antibiotics and 1% glucose. Efficiencies of interactions between different hybrid proteins were quantified in cells from liquid cultures by measuring β-galactosidase activity as previously described (Nieves-Morión *et al.*, 2017). The amount of *o*-nitrophenol produced from *o*-nitrophenol-β-galactoside (ONPG) was determined and referred to the amount of protein determined by a modified Lowry procedure (Bailey, 1967).

References

Ausubel, F.M., Brent, R., Kingston, R.E., Moore, D.D., Seidman, J.G., Smith, J.A., and Struhl, K. (2014) Current Protocols in Molecular Biology. New York: *Greene Publishing and Wiley-Interscience.*

Bailey, J.L. (1967) Techniques in protein chemistry, 2nd ed., p. 340. Elsevier, Amsterdam.

Battesti, A., and Bouveret, E. (2012) The bacterial two-hybrid system based on adenylate cyclase reconstitution in *Escherichia coli*. *Methods* **58:** 325-334.

Elhai, J., and Wolk, C.P. (1988) A versatile class of positive-selection vectors based on the nonviability of palindrome-containing plasmids that allows cloning into long polylinkers. *Gene* **68:** 119-138.

Elhai, J., Vepritskiy, A., Muro-Pastor, A.M., Flores, E., and Wolk, C.P. (1997) Reduction of conjugal transfer efficiency by three restriction activities of *Anabaena* sp. strain PCC 7120. *J Bacteriol* **179:** 1998-2005.

Mackinney, G. (1941) Absorption of light by chlorophyll solutions. *J Biol Chem* **140**: 315-322.

Mariscal, V., Herrero, A., Nenninger, A., Mullineaux, C.W., and Flores, E. (2011) Functional dissection of the three-domain SepJ protein joining the cells in cyanobacterial trichomes. *Mol Microbiol* **79:** 1077-1088.

Merino-Puerto, V., Schwarz, H., Maldener, I., Mariscal, V., Mullineaux, C.W., Herrero, A., and Flores, E. (2011) FraC/FraD-dependent intercellular molecular exchange in the filaments of a heterocyst-forming cyanobacterium, *Anabaena* sp. *Mol Microbiol* **82:** 87-98.

Mullineaux, C.W., Mariscal, V., Nenninger, A., Khanum, H., Herrero, A., Flores, E., and Adams, D.G. (2008) Mechanism of intercellular molecular exchange in heterocyst-forming cyanobacteria. *EMBO J* **27**: 1299-1308.

Nieves-Morión, M., Lechno-Yossef, S., López-Igual, R., Frías, J.E., Mariscal, V., Nürnberg, D.J., Mullineaux, C.W., Wolk, C.P., and Flores, E. (2017) Specific glucoside transporters influence septal structure and function in the filamentous, heterocyst-forming cyanobacterium *Anabaena* sp. strain PCC 7120. *J Bacteriol* **199:** e00876-16.

Ramos-León, F., Mariscal, V., Frías, J.E., Flores, E., and Herrero, A. (2015) Divisome-dependent subcellular localization of cell-cell joining protein SepJ in the filamentous cyanobacterium *Anabaena*. *Mol Microbiol* **96:** 566-580.

Rippka, R., Deruelles, J., Waterbury, J.B., Herdman, M., and Stanier, R.Y. (1979) Generic assignments, strain histories and properties of pure cultures of cyanobacteria. *J Gen Microbiol* **111:** 1-61.

Table S1. ORFs from the *Anabaena* genome predicted to encode components of ABC sugar uptake transporters.

ORF	Type of subunit	TCDB family	p	Substrate	Protein
all1027	SBP	3.A.1.1.40	10^{-64}	Chitobiose	
all1916	SBP	3.A.1.1.20	10^{-25}	Fructo-oligosaccharide	GlsR
alr2722	SBP	3.A.1.1.7	10^{-21}	Trehalose/maltose	
alr4277	SBP	3.A.1.1.20	10^{-32}	Fructo-oligosaccharide	
all0261	TMD^G	3.A.1.1.34	10^{-59}	Arabino-saccharide	GlsP
alr0738	TMD^F	3.A.1.1.20	10^{-61}	Fructo-oligosaccharide	
alr0789	TMD^F	3.A.1.1.4	10^{-55}	Lactose	
alr2532	TMD^F	3.A.1.1.20	10^{-60}	Fructo-oligosaccharide	GlsQ
all4824	TMD^G	3.A.1.1.34	10^{-53}	Arabino-saccharide	
all5282	TMD^G	3.A.1.1.41	10^{-51}	Trehalose/maltose/sucrose	
all1823	NBD	3.A.1.1.25	10^{-119}	Trehalose/maltose/sucrose	GlsD
alr4781	NBD	3.A.1.1.25	10^{-111}	Trehalose/maltose/sucrose	GlsC

The type of subunit (transmembrane domain, TMD; periplasmic solute-binding protein, SBP; nucleotide-binding protein or ATPase domain, NBD) and TCDB family (http://www.tcdb.org) to which the *Anabaena* ORF products are most similar, along with the expect probability (p) in the BLAST analysis, are indicated. The substrates that have been described for those transporter families are also shown. Note that all these transport proteins belong to the 3.A.1.1 family (The Carbohydrate Uptake Transporter-1 [CUT1] Family), for which a well-known representative is the malto-oligosaccharide MalEFGK transporter of *Escherichia coli* (MalE, SBP; MalF and MalG, TMDs; MalK, NBD). Among the indicated permeases encoded in the *Anabaena* genome, three are most similar to MalF and three to MalG (marked as superscripts). The right-hand column includes the names of the products of the genes that we have inactivated. Four additional ORFs in *Anabaena*, *alr5361, alr5362, alr5367* and *alr5368*, may encode a periplasmic SBP, an NBD and two TMDs, respectively, of an ABC nucleoside transporter.

Table S2. Sugar-stimulated growth in *Anabaena* and some ABC glucoside uptake transporter mutant strains.

A

Strain	Genotype	Prot.	OD$_{750nm}$							
			BG11 medium, sugar added:				BG11$_0$ medium, sugar added:			
			None	Sucrose	Fructose	Glucose	None	Sucrose	Fructose	Glucose
WT	Wild type (WT)		0.185 ± 0.020 (7)	0.330 ± 0.046 (6) [**0.011**]	0.471 ± 0.089 (5) [**0.004**]	0.449 ± 0.080 (6) [**0.005**]	0.173 ± 0.013 (7)	0.275 ± 0.012 (7) [**<0.001**]	0.372 ± 0.027 (6) [**<0.001**]	0.453 ± 0.069 (6) [**0.001**]
DR3912a	*alr4781::C.S3*	GlsC	0.123 ± 0.012 (5)	0.141 ± 0.019 (5) [0.442]	0.237 ± 0.048 (4) [**0.036**]	0.151 ± 0.039 (4) [0.479]	0.124 ± 0.012 (5)	0.142 ± 0.022 (5) [0.494]	0.197 ± 0.027 (4) [**0.031**]	0.147 ± 0.022 (4) [0.365]
CSMN17	*all1823::pCSL145*	GlsD	0.165 ± 0.029 (5)	0.144 ± 0.018 (5) [0.564]	0.297 ± 0.069 (4) [0.095]	0.286 ± 0.086 (4) [0.211]	0.159 ± 0.026 (5)	0.141 ± 0.013 (5) [0.548]	0.278 ± 0.039 (4) [**0.033**]	0.298 ± 0.074 (4) [0.093]
DR3915	*all0261::C.S3*	GlsP	0.198 ± 0.020 (5)	0.296 ± 0.013 (5) [**0.003**]	0.360 ± 0.035 (4) [0.127]	0.340 ± 0.064 (4) [0.060]	0.118 ± 0.010 (5)	0.200 ± 0.026 (5) [**0.020**]	0.264 ± 0.029 (4) [**0.001**]	0.269 ± 0.026 (4) [**0.001**]
CSMN19	*alr2532::pCSL145*	GlsQ	0.185 ± 0.020 (5)	0.263 ± 0.011 (4) [**0.017**]	0.318 ± 0.039 (3) [**0.014**]	0.307 ± 0.066 (4) [0.092]	0.150 ± 0.016 (5)	0.234 ± 0.017 (5) [**0.007**]	0.299 ± 0.012 (4) [**<0.001**]	0.341 ± 0.058 (4) [**0.010**]
CSMN18	*all1916::pCSL145*	GlsR	0.174 ± 0.021 (5)	0.269 ± 0.029 (4) [**0.031**]	0.315 ± 0.081 (3) [0.074]	0.391 ± 0.131 (4) [0.107]	0.158 ± 0.017 (5)	0.239 ± 0.012 (5) [**0.005**]	0.325 ± 0.043 (4) [**0.006**]	0.402 ± 0.116 (4) [0.052]

B

Strain	Genotype	Prot.	Δ OD$_{750nm}$ (sugar-no sugar)					
			BG11 medium, sugar added:			BG11$_0$ medium, sugar added:		
			Sucrose	Fructose	Glucose	Sucrose	Fructose	Glucose
WT	Wild type (WT)		0.147 ± 0.023 (6)	0.284 ± 0.062 (5)	0.260 ± 0.060 (6)	0.102 ± 0.016 (7)	0.196 ± 0.024 (6)	0.277 ± 0.058 (6)
DR3912a	*alr4781::C.S3*	GlsC	0.018 ± 0.012 (5) [**0.001**]	0.118 ± 0.038 (4) [0.072]	0.032 ± 0.028 (4) [**0.019**]	0.018 ± 0.016 (5) [**0.005**]	0.077 ± 0.014 (4) [**0.006**]	0.027 ± 0.009 (4) [**0.009**]
CSMN17	*all1823::pCSL145*	GlsD	-0.020 ± 0.014 (5) [**<0.001**]	0.128 ± 0.033 (4) [0.081]	0.117 ± 0.051 (4) [0.131]	-0.018 ± 0.017 (5) [**<0.001**]	0.114 ± 0.013 (4) [**0.034**]	0.134 ± 0.044 (4) [0.114]
DR3915	*all0261::C.S3*	GlsP	0.098 ± 0.009 (5) [0.105]	0.162 ± 0.011 (4) [0.130]	0.141 ± 0.044 (4) [0.187]	0.082 ± 0.017 (5) [0.425]	0.141 ± 0.018 (4) [0.142]	0.146 ± 0.031 (4) [0.127]
CSMN19	*alr2532::pCSL145*	GlsQ	0.096 ± 0.006 (4) [0.121]	0.152 ± 0.033 (3) [0.180]	0.118 ± 0.047 (4) [0.127]	0.084 ± 0.008 (5) [0.398]	0.153 ± 0.009 (4) [0.201]	0.195 ± 0.066 (4) [0.386]
CSMN18	*all1916::pCSL145*	GlsR	0.108 ± 0.010 (4) [0.231]	0.154 ± 0.052 (3) [0.204]	0.213 ± 0.104 (4) [0.683]	0.081 ± 0.011 (5) [0.352]	0.164 ± 0.031 (4) [0.438]	0.241 ± 0.100 (4) [0.743]

**Table S3.** Bacterial two-hybrid analysis of protein-protein interactions.

	T18	SepJ-T18	GlsC-T18	T18-GlsC	GlsP-T18	T18-GlsP	GlsD-T18	T18-GlsD	GlsQ-T18	T18-GlsQ
T25	12.49 ± 0.53 (21)	10.88 ± 0.43 (6)	13.01 ± 1.74 (4)	12.34 ± 0.40 (4)	12.11 ± 2.05 (4)	10.95 ± 1.68 (4)	13.14 ± 1.41 (3)	10.91 ± 1.11 (3)	10.08 ± 1.58 (2)	6.20 (1)
SepJ-T25	11.22 ± 2.04 (2)	80.12 ± 12.34 (9) [<0.001]	13.25 ± 1.30 (5) [0.951]	15.75 ± 6.53 (3) [0.494]	11.74 ± 1.65 (5) [0.394]	14.66 ± 1.06 (4) [0.298]	11.21 ± 1.47 (3) [0.404]	11.23 ± 1.77 (3) [0.423]	12.03 ± 1.84 (3) [0.778]	14.58 ± 3.43 (4) [0.266]
GlsC-T25	Nd	11.66 ± 0.81 (6) [0.221]	12.52 ± 1.66 (4) [0.695]	20.52 ± 2.45 (4) [0.003]	12.36 ± 0.55 (3) [0.587]	13.00 ± 3.30 (3) [0.944]	13.51 ± 1.13 (3) [0.498]	11.80 ± 1.33 (3) [0.647]	11.68 ± 1.79 (3) [0.604]	14.27 ± 1.83 (3) [0.263]
T25-GlsC	Nd	13.09 ± 1.25 (6) [0.963]	25.98 ± 2.73 (4) [<0.001]	15.93 ± 2.59 (6) [0.247]	12.72 ± 1.55 (4) [0.783]	12.79 ± 2.15 (3) [0.842]	11.74 ± 2.25 (3) [0.646]	12.32 ± 0.87 (3) [0.908]	12.03 ± 1.84 (3) [0.770]	9.20 ± 0.20 (2) [0.075]
GlsP-T25	Nd	14.34 ± 0.84 (7) [0.324]	12.32 ± 1.39 (5) [0.579]	14.19 ± 3.72 (4) [0.702]	12.16 ± 1.06 (4) [0.484]	11.64 ± 2.35 (3) [0.431]	11.84 ± 2.11 (3) [0.687]	10.96 ± 0.70 (3) [0.302]	9.30 ± 0.50 (2) [0.084]	9.21 ± 0.09 (2) [0.076]
T25-GlsP	Nd	29.12 ± 3.54 (7) [<0.001]	11.80 ± 1.02 (5) [0.314]	15.48 ± 4.14 (4) [0.435]	11.85 ± 0.32 (3) [0.376]	12.04 ± 3.52 (3) [0.638]	11.33 ± 2.31 (3) [0.480]	12.24 ± 1.74 (3) [0.872]	10.76 ± 0.47 (3) [0.241]	**16.59 ± 1.36 (4) [0.006]**
GlsD-T25	13.1 (1)	14.4 ± 1.51 (6) [0.136]	**16.9 ± 2.99 (4) [0.017]**	14.6 ± 1.29 (6) [0.090]	13.8 ± 1.22 (5) [0.309]	11.9 ± 0.68 (3) [0.710]	12.42 ± 1.20 (3) [0.961]	**26.90 ± 2.85 (3) [2.23 10⁻³]**	11.37 ± 3.17 (3) [0.528]	14.86 ± 1.84 (6) [0.097]
T25-GlsD	14.5 (1)	13.1 ± 0.87 (4) [0.639]	11.6 ± 0.50 (4) [0.472]	**16 ± 1.41 (4) [0.018]**	**15.9 ± 1.12 (5) [0.009]**	14 ± 0.58 (6) [0.171]	**49.69 ± 11.04 (3) [2.08 10⁻⁹]**	11.23 ± 1.17 (3) [0.4041]	10.60 ± 1.79 (3) [0.233]	10.80 ± 1.50 (2) [0.355]
GlsQ-T25	15.2 (1)	**17.4 ± 1.09 (4) [0.001]**	13.1 ± 0.87 (3) [0.687]	14.7 ± 1.94 (4) [0.141]	13.3 ± 1.28 (5) [0.514]	11.5 ± 0.17 (3) [0.516]	10.50 ± 1.17 (3) [0.191]	10.54 ± 1.72 (3) [0.217]	9.40 ± 1.40 (3) [0.051]	14.42 ± 1.07 (6) [0.104]
T25-GlsQ	8.8 (1)	12.5 ± 0.58 (4) [0.966]	11.9 ± 2.51 (3) [0.732]	**15.8 ± 0.92 (5) [0.009]**	**15.9 ± 2.48 (6) [0.042]**	14.1 ± 1.72 (3) [0.300]	10.98 ± 0.65 (3) [0.307]	11.32 ± 2.01 (3) [0.464]	10.10 ± 1.71 (3) [0.133]	14.78 ± 0.99 (4) [0.091]

Interactions of T25- and T18-fusion proteins produced in *E. coli* were measured as β-galactosidase activity in liquid cultures. Activity corresponds to nmol *o*-nitrophenol produced (mg protein)$^{-1}$ min^{-1}. The protein fused to the N- or the C-terminus of T18 or T25 is indicated in each case (N-terminus, protein-T18 or protein-T25; C-terminus, T18-protein or T25-protein). The mean and SEM of the results obtained with the indicated number of independent transformants (n) is presented. The difference between each fusion protein combination and the T18/T25 pair was assessed by the Student's *t* test; bold type denotes significant differences (* $p \leq 0.05$; ** $p \leq 0.01$). All other combinations gave activities not significantly different from the T25/T18 control. Nd, not determined. Italics, data from Nieves-Morión *et al.* (2017).

Table S4. Oligodeoxynucleotide primers used in this work. Introduced restriction sites are underlined.

Primer name	Sequence (5´ to 3´)
all1823-1	AGA<u>GAGCTC</u>GATGTGGCGATGGTGTTC
all1823-2	TAC<u>GAGCTC</u>ATCGGGTAAACTCACACG
all1823-3	TGGTAAATAACATCCCCGCAAGAG
all1823-4	GATGTAGACGCACGTTTCCACT
all1823-5	TC<u>TCTAGA</u>AAAAGTTCGTTTAGAAGATATAAA
all1823-6	AC<u>TGGTACC</u>TCCTGGGGTGATATTTTA
all1916-1	TC<u>TGAGCTC</u>TATATGGATGTGATCAAAACC
all1916-2	TT<u>CGAGCTC</u>ATGCTGTGATTGCTTACTCAT
all1916-3	ATCGCGATCGCCATTGTTG
all1916-4	GCATTCCGGCTTTACCTGTGA
all2532-1	ATC<u>GAGCTC</u>AGCTTGTTCGGATATGTATTCATG
alr2532-2	CTG<u>GAGCTC</u>TGCACCATCTAATTCTGC
alr2532-3	ACCATTTGATAAATCAGCAGCA
alr2532-4	GACTAAAC<u>TCTAGA</u>GTTGCGAATCAGAAGGT
alr2532-5	ATA<u>GGTACC</u>TCACCAGCAAAAACTCG
C.K1-2	GGGATCTCATGCTGGAGT
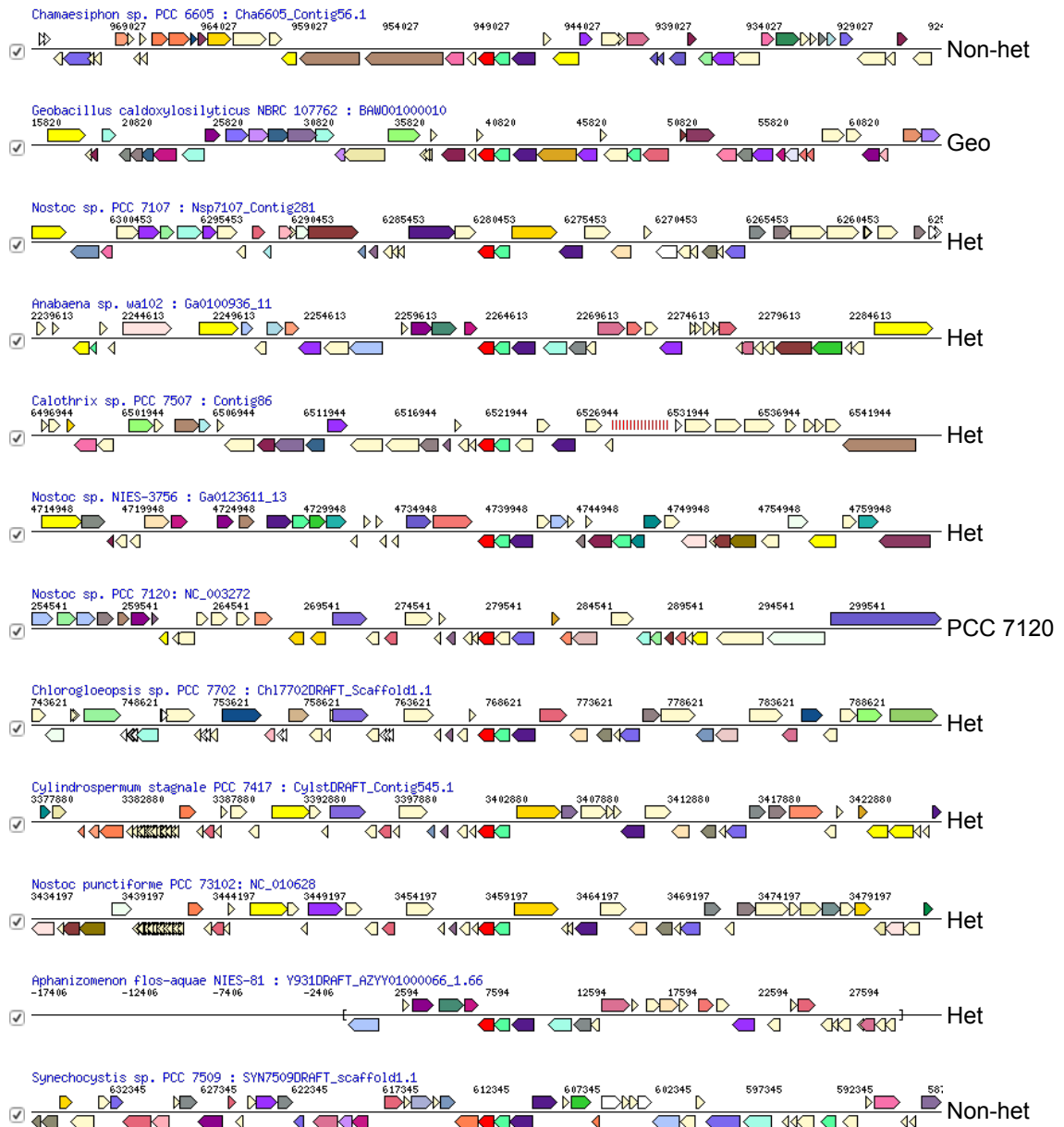
Figure S1. Genomic region of *Anabaena* (*Nostoc*) sp. strain PCC 7120 ORF *all0261* (*glsP*) and some examples of genomic regions containing an *all0261* orthologue. Whereas *all0261* is not accompanied by any ABC component-encoding gene, the *all0261* orthologues shown are accompanied by another TMD-encoding gene (colored green) or by TMD- and SBP-encoding genes (SBP gene colored dark purple). Het, heterocyst-forming cyanobacterium; Non-het, non-heterocyst-forming cyanobacterium. This gene cluster is also present in some bacteria other than cyanobacteria, and it is common in *Geobacillus* spp. (one strain shown [Geo]). Genomic regions retrieved from: https://img.jgi.doe.gov/cgi-bin/m/main.cgi.
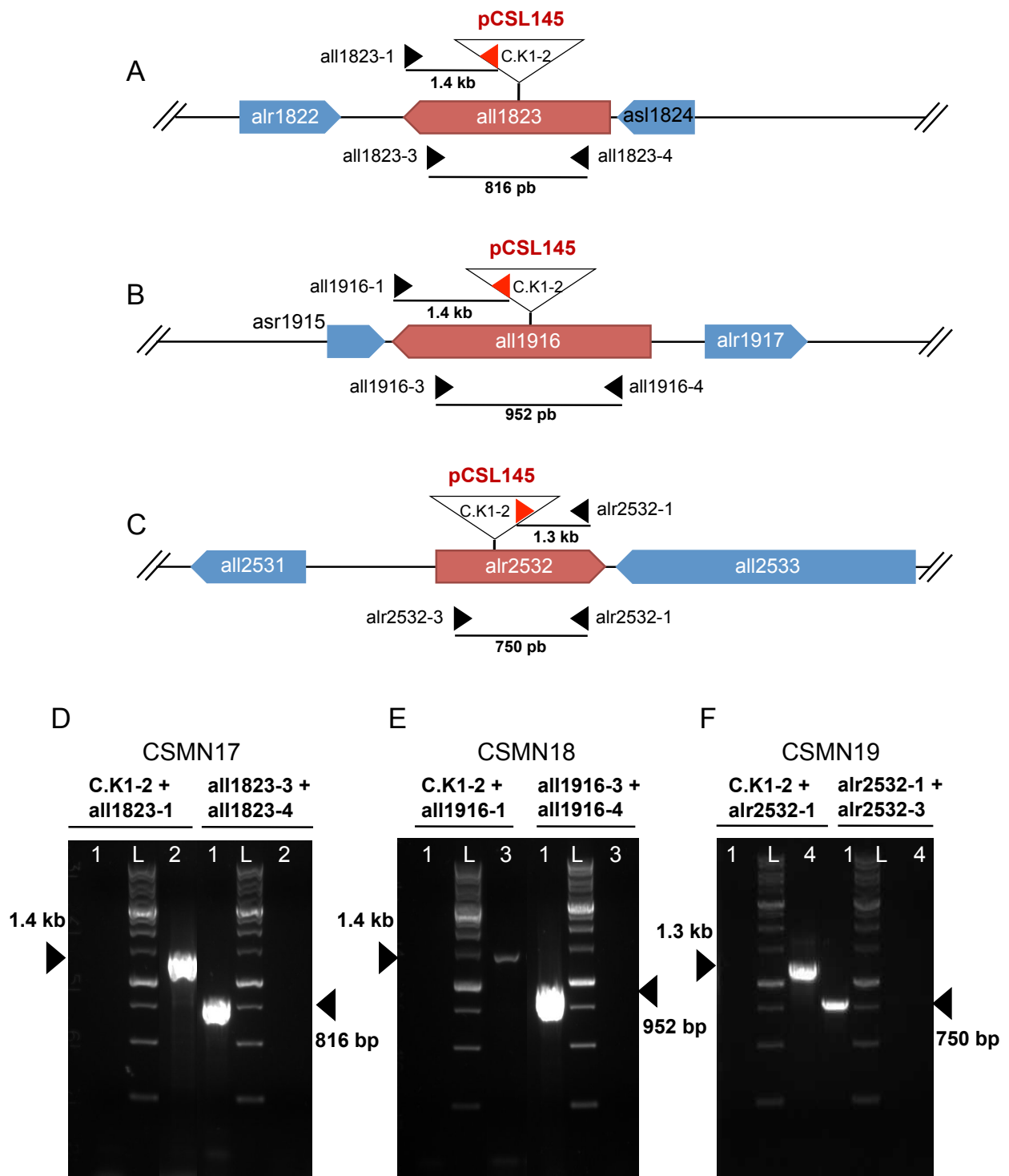
Figure S2. Construction and verification of mutants of genes *glsD*, *glsR* and *glsQ* in *Anabaena*. Schematic of the insertional mutation of genes (A) *all1823* (*glsD*), (B) *all1916* (*glsR*) and (C) *alr2532* (*glsQ*), with indication of their genomic regions, the inserted plasmid, and primers used in PCR analysis (black triangles, primers corresponding to the *Anabaena* genes; red triangle, primer corresponding to cassette C.K1 present in the inserted plasmid). (D, E, F) Verification of strains by colony PCR. L, 1-kb DNA ladder. Primer pairs are indicated on top. Templates: 1, wild-type DNA; 2, DNA from mutant CSMN17 (*glsD*; panel D); 3, DNA from mutant CSMN18 (*glsR*; panel E); 4, DNA from mutant CSMN19 (*glsQ;* panel F).
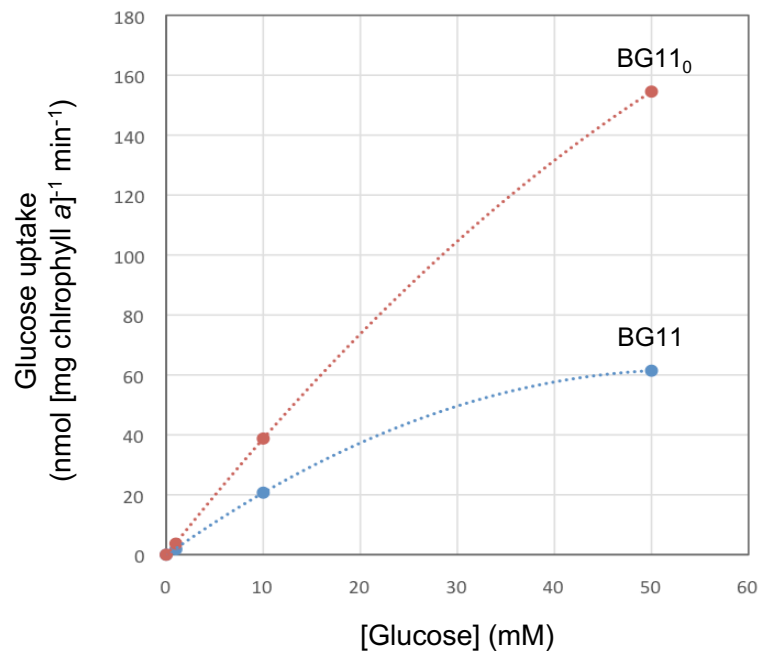
Figure S3. Uptake rates of [^{14}C]glucose in wild-type *Anabaena*. Filaments grown in BG11 medium or grown in BG11 medium and incubated for 18 h in BG11$_0$ medium were used in uptake assays with 1, 10 or 50 mM [^{14}C]glucose as described in Suppl. Experimental procedures.
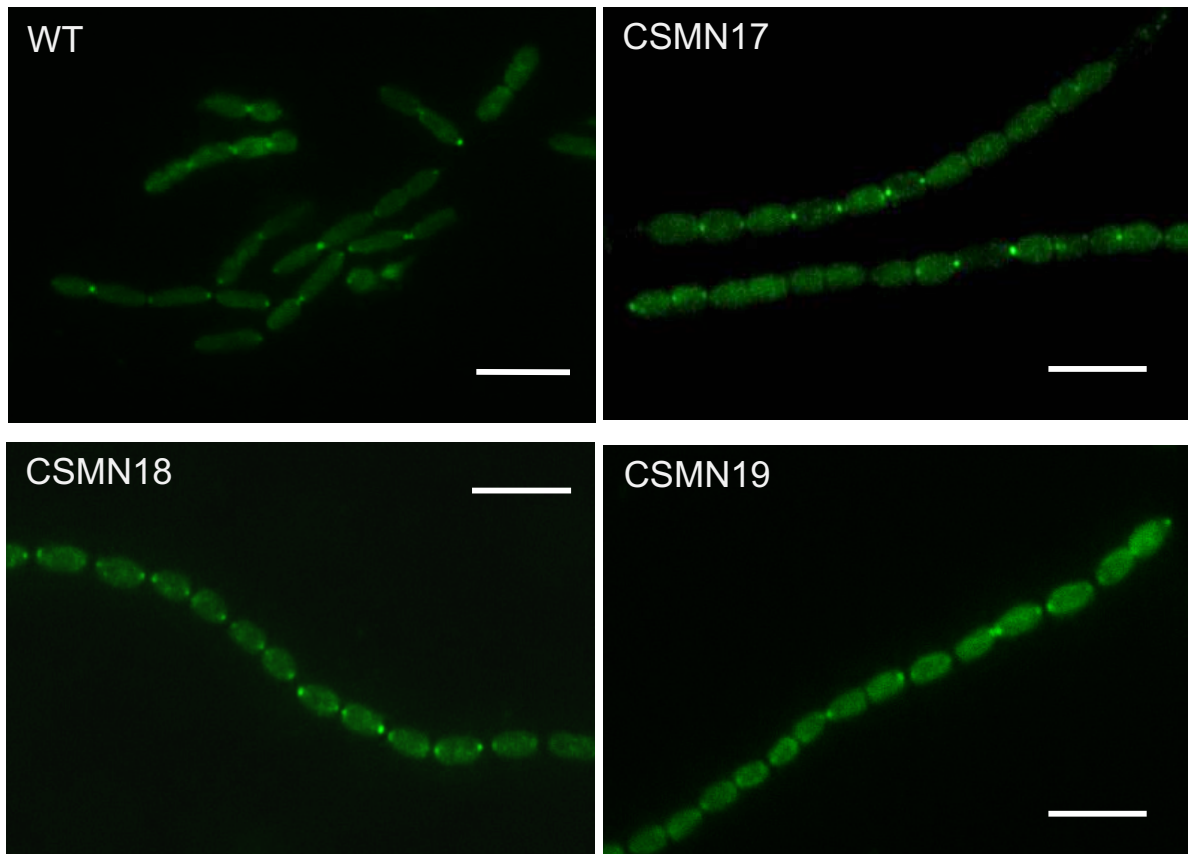
Figure S4. Immunofluorescence localization of SepJ in wild-type *Anabaena* (WT) and *glsD* mutant CSMN17 (*all1823*::pCSL145), *glsR* mutant CSMN18 (*all1916*::pCSL145) and *glsQ* mutant CSMN19 (*alr2532*::pCSL145). Filaments were grown in BG11 medium (with Nm for the mutants) and subjected to immunofluorescence analysis with anti-SepJ coiled coil antibodies. Antibody green fluorescence is shown. Brightness and contrast were adjusted to improve visibility. Size bars, 10 µm.

General Discussion

1.1. Molecular diffusion through cyanobacterial septal junctions

The structure and metabolism of heterocyst-forming cyanobacteria require a transfer of compounds —nutrients and regulatory factors— between the cells of the filament during both heterocyst differentiation and diazotrophic growth (Wolk et al., 1968, 1974, 1994; Yoon and Golden, 1998; Corrales-Guerrero et al., 2013). Two pathways have been discussed for this transfer, the continuous periplasmic space and possible direct intercellular connections (Mariscal et al., 2007; Mullineaux et al., 2008). To study the intercellular transfer of compounds in filamentous cyanobacteria, FRAP analysis was previously performed using two fluorescent markers, calcein and 5-carboxyfluorescein (5-CF) (Mullineaux et al., 2008; Mariscal et al., 2011; Merino-Puerto et al., 2011b). Calcein (622 Da) and 5-CF (376 Da) are compounds with no resemblance to any physiological substance in cyanobacteria. Hence, a usable fluorescent analogue of sucrose termed esculin (340 Da) has been used in this work to understand the possible transfer of sucrose from vegetative cells to heterocysts (see also Nürnberg et al., 2015). We have studied the temperature dependence of intercellular transfer of these fluorescent markers in the model heterocyst-forming cyanobacterium *Anabaena* sp. strain PCC 7120 (hereafter *Anabaena*). We found that the recovery rate constants in FRAP analysis are directly proportional to the absolute temperature (Q_{10} of about 1.035 in the physiological temperature range). This result shows that intercellular molecular transfer in the cyanobacterial filament has the physical properties of simple diffusion. Using our data, Kang et al. (2017) have performed a thermodynamic analysis and found that the activation energy (E_a) for the intercellular transfer of calcein, 5-CF and esculin is 6.1, 3.3 and 1.4 kJ/mol, respectively. Comparison of these figures to the E_a for facilitated diffusion, such as that of glucose by an MFS glucose transporter, 64 kJ/mol (Wille et al., 1996), strongly suggests simple diffusion for the intercellular transfer of fluorescent markers in *Anabaena*. Hence, our study is consistent with previous observations showing that the net movement of the fluorescent markers always takes place down the concentration gradient, and that its kinetics appears to be independent of direction (Mullineaux et al., 2008; Nürnberg et al., 2015). Because a periplasmic route would imply the activity of membrane transporters (i) between the cytoplasm of source cells and the periplasm and (ii) between the periplasm and the cytoplasm of target cells, and because the known amino acid transporters from *Anabaena* (Pernil et al., 2015) and the sugar transporters characterized in this work are active transporters, simple diffusion does not support a periplasmic pathway. Instead, simple diffusion suggests the involvement of direct connections between the cells in the filament.

The septal junctions that have been recently investigated in *Anabaena* are candidates for direct intercellular connections in the filament. As described in the Introduction, three proteins that are required for the formation of the septal junctions —SepJ on one hand and FraC and FraD on the other— are putative components of these structures (Herrero et al., 2016). These proteins, perhaps together with other yet unknown proteins, would form complexes accommodating conduits through which diffusion of small molecules (up to at least 622 Da, the size of calcein) would take place. Mediating simple diffusion, the cyanobacterial septal junctions are analogous to the connexons of the gap junctions of metazoans that also allow simple diffusion of

small molecules between adjacent cells. Diffusion through septal junctions is to be considered a novel mechanism of molecular transfer across membranes in bacteria, in addition to the common and well-known mechanisms of active transport and facilitated diffusion.

1.2. Glucoside transporters in *Anabaena*

In contrast to calcein and 5-CF that traverse cell membranes because they are sufficiently hydrophobic, esculin requires sucrose import systems to enter into the cytoplasm of *Anabaena* cells. Thus, the esculin uptake assay described in the Experimental Preamble shows that esculin is significantly taken up linearly for at least 70 min and retained in the cells, both in BG11 and $BG11_0$ medium, and studies of inhibition by different sugars (Chapter 2, Figure 3) indicated that esculin uptake is inhibited by sucrose and maltose. These results suggest that esculin is taken up in *Anabaena* by α-glucoside transporters and, hence, that it can be used as a fluorescent marker to probe such transporters. This is similar to previous studies in which uptake of esculin into yeast cells expressing higher-plant sucrose transporters was used to probe such transporters (Gora et al., 2012).

In this work, we have identified genes that encode components of ABC α-glucoside transporter(s) (*glsC*, *glsD*, *glsP*, *glsQ*, *glsR*) and an α-glucoside permease (*hepP*) that mediate esculin uptake in *Anabaena*. The genes encoding ABC transporter components identified and their products are summarized in Table 1.

Table 1. Components of ABC glucoside transporters from *Anabaena* that we have studied in this work.

ORF	Name of the gene	Product of the gene
all4781	*glsC*	Nucleotide-binding domain (NBD)
all1823	*glsD*	Nucleotide-binding domain (NBD)
all0261	*glsP*	Transmembrane domain (TMD)
alr2532	*glsQ*	Transmembrane domain (TMD)
all1916	*glsR*	Solute-binding protein (SBP)

We addressed the study of *glsC* and *glsP* because they are the possible *Anabaena* orthologues of *Anabaena variabilis* genes that encode putative components of carbohydrate uptake transporters specific for disaccharides and oligosaccharides that are highly expressed in heterocysts (Park et al., 2013). However, GlsC-GFP and GlsP-GFP fusions showed that in *Anabaena* these proteins are present in vegetative cells as well as in heterocysts (Chapter 2, Figure 4 and Figure S4). Additionally, they are evidently active in vegetative cells, since their inactivation affects esculin uptake in filaments grown in the presence of nitrate (Chapter 2, Table 1). Furthermore, a transcriptomic analysis of *Anabaena* has shown that these genes have a low expression that is not increased by nitrogen deprivation (Flaherty et al., 2011). On the other hand, the genes *glsD*, *glsQ* and *glsR* were identified as encoding possible transporter partners of GlsC and GlsP.

In the Transporter Classification Database (TCDB), there are two families of ABC-type Carbohydrate Uptake Transporters, CUT1 (family 3.A.1.1) and CUT2 (family 3.A.1.2) (Saier, 2000; Saier et al., 2016). The maltose transport system of *Escherichia coli* (MalEFGK$_2$: MalE, SBP; MalF and MalG, TMDs; and MalK, NBD), which mediates maltose and matodextrin uptake, is the best-known ABC transporter of the CUT1 family (Nikaido, 1994). Other than a possible CUT2 nucleoside transporter, the *Anabaena* genome encodes 12 possible components of sugar transporters that belong to the CUT1 family, including GlsC (*all8741*) and GlsP (*all0261*). As shown in Table S1, Chapter 3, the 12 components of CUT1 family transporters encoded in the *Anabaena* genome are four periplasmic SBP, six TMDs (three most similar to MalF and three to MalG) and two NBDs.

All the CUT1 family-encoding genes are located at different positions in the *Anabaena* genome precluding the possibility of predicting their association in specific ABC transport complexes. Additionally, orthologues of *glsC* (NBD) stand alone, unaccompanied by any ABC transporter-encoding gene, in the cyanobacteria whose genomic sequence is available (https://img.jgi.doe.gov/cgi-bin/m/main.cgi). In contrast, orthologues of *glsP* (TMD) are frequently accompanied by another ABC transporter TMD-encoding gene in the genomes of heterocyst-forming cyanobacteria (Chapter 3, Figure S1). An example is *Nostoc punctiforme* ORF Npun_R2793, and the *Anabaena* gene most similar to this *N. punctiforme* gene is *alr2532*, termed *glsQ* in our work. In a few heterocyst-forming cyanobacteria including *Chlorogloeopsis fritschii* PCC 6912, *Fischerella sp*. PCC 9605 and *Anabaena* sp. strain 90, and in other cyanobacteria such as *Chamaesiphon* sp. PCC 6605, *Synechocystis* sp. PCC 7509 and *Oscilliatoria acuminata* PCC 6304, a gene encoding a periplasmic SBP is clustered together with those two TMD-encoding genes. The *Anabaena* gene most similar to this gene encoding a periplasmic SBP is *all1916* (*glsR*). No gene encoding an ABC transporter NBD is however clustered together with these genes in any available cyanobacterial genomic sequence. However, we studied *all1823* (*glsD*) because it is the only gene in *Anabaena* (other than *glsC*) that encodes a predicted ABC sugar transporter NBD protein.

The effect of the inactivation of the *gls* genes on the uptake of esculin in *Anabaena* is summarized in Figure 1. All the mutants are affected in esculin uptake in either BG11 or BG11$_0$ medium, but inactivation of *glsD* (NBD) has a quantitatively more important effect than inactivation of any other gene. The five components of ABC transporters that we have studied are therefore involved in esculin uptake and are similar to components of CUT1 transporters for disaccharides or complex saccharides (Chapter 3, Table S1), which is consistent with their identification as components of α-glucoside transporters based on the inhibition of esculin uptake by sucrose and maltose (Chapter 2, Fig. 3).

Figure 1 also shows that inactivation of *hepP* impairs esculin uptake in filaments incubated under nitrogen deficiency. As we mentioned earlier, *hepP* (*all1711*) encodes an MFS protein that is involved in the production of the heterocyst-specific polysaccharide layer (López-Igual et al., 2012). Previous work has shown that HepP is present at higher levels in developing heterocysts (proheterocysts) and heterocysts than in vegetative cells, and that HepP could mediate sucrose uptake

specifically in (pro)heterocysts (López-Igual et al., 2012). We have found that the inactivation of *hepP* affects the uptake of esculin only in filaments that have been incubated in the absence of combined nitrogen, corroborating that (pro)heterocysts may take up esculin/sucrose with the concourse HepP. We found a decrease in the esculin uptake associated specifically with incubation in $BG11_0$ medium (i.e., uptake in $BG11_0$ medium less uptake in BG11 medium) with increasing pH beyond pH 6 (Chapter 1, Figure 2). Therefore, a transporter that acts under nitrogen deprivation (in $BG11_0$ medium) is dependent on the concentration of protons in the medium. The candidate for such transporter could be an MFS protein, which frequently act as secondary transporters that mediate symport with protons (Ayre, 2011), and in our case HepP, which may therefore function as a sucrose-H^+ or α-glucoside-H^+ symporter.
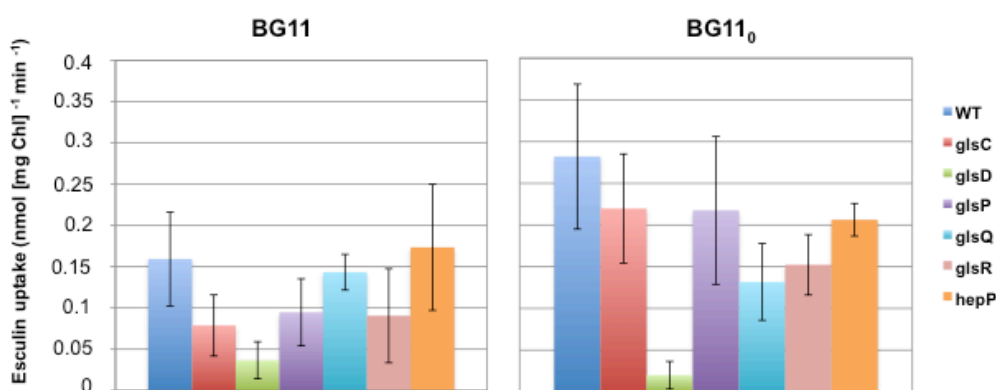
Figure 1. Esculin uptake of *Anabaena* and *Anabaena glsC*, *glsD*, *glsP*, *glsQ*, *glsR* and *hepP* mutants in BG11 or $BG11_0$ medium (data from Chapter 2, Table 1, and Chapter 3, Table 1).

Although *Anabaena* has been considered for a long time to be an obligatory photoautotroph, recent work has shown that it can grow heterotrophically using fructose at relatively high concentrations ($\geq$ 50 mM; Stebegg et al., 2012). We have now observed that phototrophic cultures of *Anabaena* (in liquid, standing media) gave higher yields in the presence of sucrose, fructose or glucose (each added at 50 mM concentration) than in their absence (Chapter 3, Fig. 2 and Table S2). Hence, *Anabaena* has a capability for mixotrophic growth that has not been generally appreciated previously.

To investigate whether the ABC glucoside transporter components identified in this work mediate the mixotrophic growth of *Anabaena* with sugars, we tested sugar-stimulated growth in the *glsC*, *glsD*, *glsP*, *glsQ* and *glsR* mutants (Chapter 3, Figure 2 and Table S2). We have not investigated the *hepP* mutant because the significant effect of its mutation on esculin uptake occurs in $BG11_0$ medium, and under this condition the *hepP* mutant shows a Fox⁻ phenotype making it not possible to study the sugar-stimulated growth. All the mutants were impaired in sugar-stimulated growth, but the effects were most significant in the *glsC* and *glsD* mutants with sucrose, and in the *glsC* mutant with glucose (Chapter 3, Fig. 2).

Our studies have shown that GlsD is very important for esculin uptake and sucrose-dependent growth, and that GlsC is also important for full esculin uptake and sucrose-dependent growth, suggesting that GlsD and GlsC could work together in the ABC sucrose uptake complexes of *Anabaena*. The interaction, albeit weak, of these NBD proteins in Bacterial Adenylate Cyclase Two-Hybrid (BACTH) analysis is consistent with this suggestion (Figure 2). Nonetheless, each of these proteins is also able to interact with itself suggesting that they can act as homodimers in some ABC transporter complexes. Indeed, GlsC is especially relevant for glucose uptake. Thus, this NBD appears to serve different ABC transporters and, therefore, may be defined as a multitask ATP-binding subunit. Classical examples of multitask ATP-binding subunits are MalK and similar proteins that energize di- and oligo-saccharide uptake in, e.g., *Streptomyces lividans* (Schlösser et al., 1997), *Streptococcus mutants* (Webb et al., 2008), *Bacillus subtilis* (Ferreira and de Sá-Nogueira, 2010), and *Corynebacterium alkanoly*ticum (Watanabe et al., 2015). Another multitask ATP-binding subunit is the BgtA protein of *Anabaena* that serves the basic amino acid transporter Bgt and the neutral amino acid transporter N-II (Pernil et al., 2008).
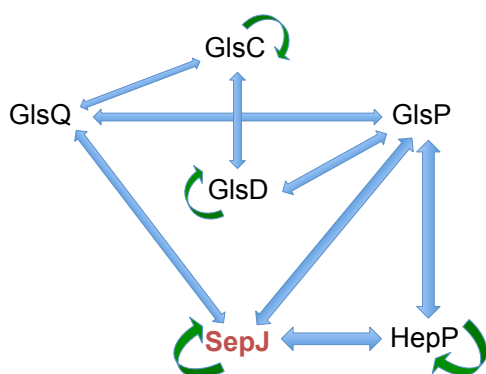
Figure 2. Schematic of protein-protein interactions in BACTH analysis between components of ABC glucoside transporters (GlsC, GlsD, GlsP, GlsQ), HepP and SepJ. Thickness of blue arrows reflects interaction strength as deduced from β-galactosidase activity levels. Interaction between SepJ and HepP is as strong as the self-interactions of SepJ and HepP. Drawn from data in Chapter 2, Table 5, and Chapter 3, Table S3.

The GlsP and GlsQ TMDs are also needed for full esculin uptake and sugar stimulated-growth. As mentioned above, the genes encoding the orthologues of GlsP and GlsQ are clustered together in the genome of many heterocyst-forming cyanobacteria. This information and our BACTH analysis, indicating that they interact with each other, suggest that GlsP and GlsQ are partners in ABC transporter complexes. Additionally, based on BACTH analysis, we suggest a preferential relation of GlsP with GlsD and of GlsQ with GlsC. On the other hand, the periplasmic SBP GlsR is also needed for full esculin uptake and sugar-stimulated growth. As mentioned before, a *glsR*-like gene is clustered together with *glsP*- and *glsQ*-like genes in the genomes of some cyanobacteria. Thus, GlsR may be a partner of GlsP and GlsQ. On the other hand, because the *glsP*, *glsQ* and *glsR* mutants have still substantial activity of esculin uptake and sugar-stimulated growth, additional SBPs and TMDs should be involved in the uptake of sugars.

The genomic information summarized above showing (i) the presence in *Anabaena* of CUT1-like proteins (four periplasmic SBPs; six TMDs [three MalF-like

and three MalG-like]; and two NBD proteins), and (ii) the clustering in some cyanobacterial genomes of some of these genes, together with our results with the *gls* mutants, suggest the presence in *Anabaena* of at least three ABC glucoside transporters, one of which may be constituted by GlsR (SBP), GlsP-GlsQ (TMDs) and GlsC-GlsD (NBDs). Because there are more SBP than putative membrane complexes, additional SBPs may be used by the membrane complex made of GlsP-GlsQ/GlsC-GlsD. Some ABC transporter membrane complexes that use more than one SBP are well known (Davidson et al., 2008). On the other hand, the NBD proteins appear to be shared by the three glucoside transporters as discussed above. Figure 3 shows a schematic of the proposed ABC glucoside transporters in *Anabaena* including a possible ascription of sugar substrates. The complex architecture of these systems, as well as possible indirect effects of inactivation of one gene on the expression or functionality of other components, may be the basis for the complex phenotypes observed. For example, it is possible that in the absence of one NBD protein such as GlsC or GlsD, the other available NBD protein substitutes, at least partly, for the mutated one (Webb et al., 2008).
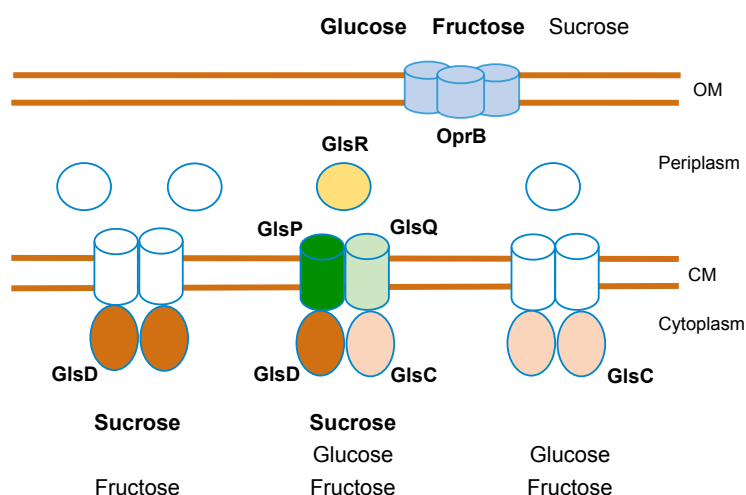
Figure 3. Possible set of ABC glucoside uptake transporters in *Anabaena*. Only two sugar transport-related NBD proteins are encoded in the *Anabaena* genome, suggesting that they are the only NBDs for these transporters, which is consistent with the strong phenotypic effect of inactivation of *glsC* and, especially, *glsD*. BACTH analysis shows GlsC-GlsD interactions and stronger GlsC and GlsD self-interactions, as well as GlsC-GlsQ and GlsD-GlsP interactions. Mutational analysis has shown that GlsC and GlsP contribute significantly to two different transporters (Chapter 2). BACTH and genomic analyses suggest that GlsP and GlsQ can interact, implying that they could be partners in a membrane complex, and gene clustering in a few cyanobacterial genomes suggests that GlsP, GlsQ and GlsR could be related. Because of the partial phenotypic effects of inactivation of *glsP*, *glsQ* and *glsR*, other unidentified permeases and periplasmic SBPs can be components of glucoside transporters in *Anabaena* (white figures; see possible candidates in Chapter 3, Table S1). In spite of complex phenotypes, the indicated substrate specificities are consistent with the sugar-stimulated growth phenotypes of the mutants. Thus, substantial fructose-stimulated growth is still observed in all the *gls* mutants, indicating the participation of systems other than that mutated in each mutant; inactivation of *glsC* has a much greater effect than inactivation of *glsD* on glucose-stimulated growth; and inactivation of *glsD* has a greater effect than inactivation of *glsC* on sucrose-stimulated growth. Additionally, inactivation of *glsP*, *glsQ* and, especially, *glsC* appear to have phenotypic effects related to the function of septal junctions that may affect growth. The OM porin OprB facilitates transport of fructose and glucose, and may also facilitate transport of sucrose at a lower level.

GlsC, GlsD, GlsP, GlsQ and GlsR appear to have a role not only in sucrose-stimulated growth but also in fructose- and glucose-stimulated growth (Chapter 3, Figure 2). Therefore, fructose and glucose, as well as sucrose, can be incorporated into *Anabaena* at least in part by the ABC glucoside uptake transporters (Figure 3). *Anabaena* expresses high-affinity cytoplasmic membrane transporters for sucrose (K_s for sucrose in fragmented filaments is 4.9 μM; Nicolaisen et al., 2009b) and for esculin (150 μM or 119 μM in BG11 and $BG11_0$ medium, respectively; Chapter 2), but not for fructose (Ungerer et al., 2008) or glucose. Our results of direct uptake of [^{14}C]glucose by *Anabaena* permit to estimate a relatively high K_s of at least 20 mM (Chapter 3, Figure S3), and the analysis of uptake of [^{14}C]fructose reported by Stebegg et al., (2012) showed low affinity as well. As we mentioned above, the *Anabaena* genome does not contain any ORF that encodes a fructose or glucose transporter, and neither a sucrose porin (Nicolaisen et al., 2009b). As described in the Introduction, the *Anabaena* genome contains, however, genes encoding homologs to porin OprB (Nicolaisen et al., 2009a) that mediate uptake of glucose and other monosaccharides (Wylie and Worobec, 1995). An OprB-like porin in *Nostoc punctiforme* is indeed involved in glucose and fructose uptake (Ekman et al., 2013). Interestingly, OprB from *Pseudomonas aeruginosa* also transports sucrose at low level (van den Berg, 2012). Therefore, the assimilation of sugars by *Anabaena* may be related to the presence of specific porins in the outer membrane that facilitate this process. Once in the periplasm, fructose and glucose can be transported into the cytoplasm with low affinity by the cytoplasmic membrane glucoside transporters. In contrast, sucrose hardly passes the outer membrane, but the sucrose molecules that reach the periplasm can be transported into the cytoplasm with high affinity.

From an environmental point of view, a variety of factors would influence the mixotrophic growth of a phototrophic cyanobacterium such as *Anabaena* that thrives in freshwater or soil environments. These include the availability of organic compounds, in this case sugars, that may support the growth, the ability of this organism to assimilate these compounds at concentrations which are found in nature, and the presence of other organisms including their interactions in the same environment (Smith, 1983). Interestingly, the sugar concentrations in freshwater and terrestrial environments are normally in the μM range up to 50 μM, but there are reports of up to 4.5 mM (Hobbie and Hobbie, 2013), suggesting that in similar conditions the *Anabaena* sugar transporters might be useful.

1.3. Influence of the glucoside transporters on the septal junctions

The weak Fox$^+$ phenotype found in the *glsC* and *glsP* mutants, which grow slowly without a source of combined nitrogen under oxic conditions and show low levels of nitrogenase activity, suggested the possibility of a limited transfer of sucrose from vegetative cells to heterocysts. Additionally, the *glsQ* and *glsR* mutants showed a deficit in diazotrophic growth on plates (Chapter 3, Fig. 3). We investigated whether the inactivation of *glsC*, *glsP* or *hepP* (which also results in a Fox$^-$ phenotype) affects intercellular molecular exchange tested with the fluorescent sucrose analog esculin. The *glsC*, *glsP*, and *hepP* mutants are impaired in the transfer of esculin between

vegetative cells but not from vegetative cells to heterocysts (Chapter 1, Table 3), suggesting that the encoded proteins are involved in sucrose transfer between vegetative cells, which might limit the amount of sucrose that reach the heterocysts. This would explain, in turn, the low nitrogenase activities observed in the *glsC* and *glsP* mutants. (The *hepP* mutant has low nitrogenase activity because it lacks the heterocyst polysaccharide layer as shown by López-Igual et al., 2012.) On the other hand, the transfer of esculin from vegetative cells to heterocysts was increased in the *hepP* mutant. HepP has been suggested to export saccharides from the heterocysts (López-Igual et al., 2012), and the inactivation of *hepP* might therefore block esculin export and, as a result, increase the concentration of esculin observed in the heterocysts. An alternative explanation for the increased transfer of esculin that is observed in the *hepP* mutant is that HepP somehow regulates septal junctions. In this scenario, septal junctions between vegetative cells and heterocysts could be more active in the absence of HepP than in its presence.

To test how specific the effect of the mutations on intercellular molecular exchange could be, transfer of calcein and 5-CF was tested between vegetative cells of *glsC*, *glsD*, *glsP*, *glsQ*, *glsR* and *hepP* mutants grown in BG11 medium. The inactivation of these genes impairs molecular transfer between vegetative cells in a different manner for calcein and 5-CF. The highest effect has been observed on the transfer of calcein (summarized in Figure 4), which is reminiscent of the effect of inactivation of *sepJ* (Merino-Puerto et al., 2011b; Mariscal et al., 2011; Nürnberg et al., 2015). These observations support the previous suggestion of the existence of two types of septal junction complexes in *Anabaena* (Merino-Puerto et al., 2011b), one related to SepJ (especially involved in calcein transfer) and another related to FraCD (especially involved in 5-CF transfer), and indicate a possible role of the glucoside transporters in the normal function of the SepJ-related septal junctions.
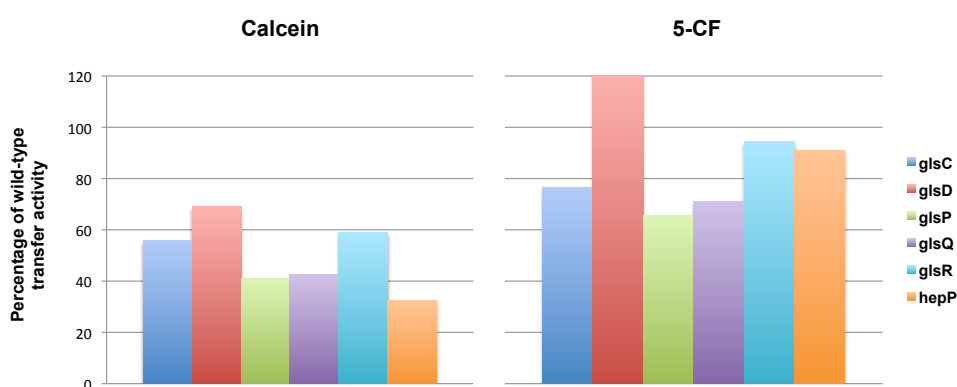
Figure 4. Percentage of wild-type intercellular transfer of calcein and 5-CF in each mutant tested, *glsC*, *glsD*, *glsP*, *glsQ*, *glsR* and *hepP* (data from Chapter 2, Table 4; Chapter 3, Table 2).

To investigate whether interactions between the glucoside transport proteins and SepJ are feasible, BACTH analysis was performed (summarized in Figure 2 above). This analysis showed that GlsP, GlsQ and, most strongly, HepP can interact with SepJ, whereas no interaction was observed between SepJ and GlsC or GlsD. Hence, GlsP, GlsQ and HepP may affect SepJ function by means of protein-protein interactions (Figure 5). Interestingly, inactivation of GlsQ and inactivation of GlsP (TMDs) have similar effects on the intercellular transfer of calcein and 5-CF and on diazotrophic growth (Chapter 2, Figure 5 and Chapter 3, Figure 3), which is consistent with their proposed contribution to the same ABC transporter (Figure 3). These observations suggest that the normal function of SepJ and, hence, of the SepJ-related septal junctions, requires their interaction with other cytoplasmic membrane proteins such as the GlsP-GlsQ complex and HepP (Figure 5). These interactions appear to be however complex as exemplified by HepP, which is required for maximal intercellular molecular exchange between vegetative cells but might negatively affect the transfer from vegetative cells to heterocysts as discussed above. Future research should explore whether the interaction between the identified membrane transporters and SepJ has a function on the structure or on the regulation of the septal junctions. If, as we suggest, the septal junctions accommodate conduits that mediate diffusion, we further hypothesize that they could be regulated by gating. Finally, it should be noted that a functional dependence between SepJ and an ABC transporter for polar amino acids has also been described (Escudero et al., 2015), making a more general interaction between SepJ-related septal junctions and relevant metabolite transporters a possibility of great interest.
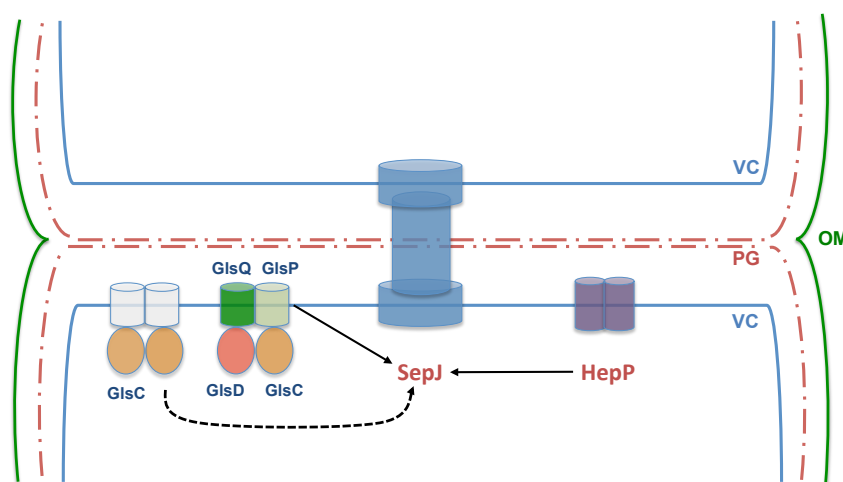
Figure 5. Schematic of suggested relationships between the identified glucoside transporters and the septal protein SepJ in the intercellular septa of *Anabaena* filaments. GlsC (NBD) is needed for the correct localization of SepJ (a discontinuous arrow indicates a possible indirect effect). GlsP, GlsQ (TMDs) and HepP (MFS) influence the function of SepJ-related septal junctions (continuous arrows indicate a direct interaction as shown by BACTH analysis). VC, vegetative cell; PG, peptidoglycan; OM, outer membrane. SepJ is represented as a large complex that likely involves SepJ multimers and possibly other proteins. HepP is represented as dimers.

We also found that the NBD protein GlsC is required for proper location of SepJ and maturation of the intercellular septa, the latter illustrated by the presence of a lower number of septal peptidoglycan nanopores in the *glsC* mutant than in the wild type. In a few cases, the neighboring genes of *glsC*-like proteins in cyanobacterial genomes are related to cell wall biosynthesis, including an N-acetylmuramoyl-L-alanine amidase-encoding gene in *Spirulina major* PCC 6313. As described in the Introduction, this type of proteins (AmiC proteins) are involved in the formation of the nanopores (Lehner et al., 2013). In addition, as deduced from the effect of inactivation of septal proteins on the number of nanopores, the correct function of the amidases requires the presence of septal proteins including SepJ (Nürnberg et al., 2015). The recent work of Bornikoel et al. (2017) suggests that SepJ and FraCD locate where nanopores will be built in the septal peptidoglycan, and direct AmiC proteins to digest the nanopores at those specific sites. In some bacteria, the activation of amidases that split the septal peptidoglycan during cell division and of endopeptidases that function in cell elongation need FtsE, the NBD of the ABC transporter-like FtsEX complex (Yang et al., 2011; Domínguez-Cuevas et al., 2013; Meisner et al., 2013; Bartual et al., 2014). Therefore, the multitask GlsC protein might participate in a complex that regulates amidases and localization of SepJ (Figure 5). The NBD protein GlsD is however not needed for SepJ localization indicating that this is a specific role of GlsC. Interestingly, compared to GlsD and other similar proteins, GlsC has two long insertions of unknown function in its amino acid sequence (Figure 6). It will be of interest to investigate in the future whether these insertions have a role in the interaction of GlsC with other proteins involved in SepJ localization and septal maturation.

In summary, by using the fluorescent sucrose analog esculin, we have identified glucoside transporters from *Anabaena* that are involved in several aspects of the biology of heterocyst-forming cyanobacteria. These glucoside transporters can have a role in the uptake of sucrose that may reach the periplasm of the filament either by leakage from the cells (Nicolaisen et al., 2009b; Herrero et al., 2016) or by uptake from the outer medium. In the latter case, the identified glucoside transporter(s) would be related to the capability of *Anabaena* for mixotrophic growth. Additionally, the glucoside transporters (or specific components of them) are required for the correct maturation and function of the septal junctions that join the cells in the filaments of heterocyst-forming cyanobacteria.

```
CLUSTAL multiple sequence alignment by MUSCLE (3.8)


Alr4781      MAQVVLENVYKSFPPRRGENVSSQTPSAKKTDAEPAGTVNVLRRINLTIPDGEFMVLVGP
All1823      MAKVRLEDIKRRF---------------------NNVTAIEEISFEIPDGEFWVLVGP
MSMX_BACSU   MAELRMEHIYKFY---------------------DQKEPAVDDFNLHIADKEFIVFVGP
MalK_ECOLI   MASVQLQNVTKAW---------------------GEVVVSKDINLDIHEGEFVVFVGP
AglK_RHIME   MTGLLLKDIRKSY---------------------GAVDVIHGIDLDIKEGEFVVFVGP
             *: : :: : . :                       . :.: * : ** *:***


Alr4781      SGCGKSTLLRLIAGLEVMTGGNIWVGDRLVNDLPPKERDIAMVFQNYALYPHMTVYDNIA
All1823      SGCGKSTILRTIAGLENATSGNLFIGDRLVNNIPARARDVAMVFQNYALYPHMTVAENIA
MSMX_BACSU   SGCGKSTTLRMVAGLEEISKGDFYIEGKRVNDVAPKDRDIAMVFQNYALYPHMTVYDNIA
MalK_ECOLI   SGCGKSTLLRMIAGLETITSGDLFIGEKRMNDTPPAERGVGMVFQSYALYPHLSVAENMS
AglK_RHIME   SGCGKSTLLRMIAGLEEITGGDMFIDGERVNDVPPSKRGIAMVFQSYALYPHMTVYDNMA
             ******* ** :**** : *:::: :*: .. *.:.****.******::* :*::


Alr4781      FGLRRRSGSEEHRDNHPSSPSQLPTWAENLLVGATRKLPKGLRYISDQEREVDEQVRSVA
All1823      FGLKMRKINPK-------------------------------------IVQERVVDVA
MSMX_BACSU   FGLKLRKMPKP-------------------------------------EIKKRVEEAA
MalK_ECOLI   FGLKLAGAKKE-------------------------------------VINQRVNQVA
AglK_RHIME   FGMRIARESKE-------------------------------------EIDRRVRGAA
             **:.                                            :. .* .*


Alr4781      HLLQIETLLHRLPKQLSGGQRQRVALGRAIARNPQVFLMDEPLSNLDAKLRAETRAQIVK
All1823      RSLSLDHLLDRKPKQLSGGQQQRVALGRAIAREPQVFLLDEPLSNLDAQLRDDTRAELKQ
MSMX_BACSU   KILGLEEYLHRKPKALSGGQRQRVALGRAIVRDAKVFLMDEPLSNLDAKLRVQMRAEIIK
MalK_ECOLI   EVLQLAHLLDRKPKALSGGQRQRVAIGRTLVAEPSVFLLDEPLSNLDAALRVQMRIEIAK
AglK_RHIME   DMLQLTPYLDRLPKALSGGQRQRVAIGRAICRNPKVFLFDEPLSNLDAALRVATRIEIAK
              * :    * * ** ****.****:**:: :..***:********* **   * :: .


Alr4781      LQRQLG--TTTIYVTHDQTEAMTMGDRIAIMNQGQIQQVASPLELYNHPANRFVAEFIGTP
All1823      LHQQLG--ITTIYVTHDQVEAMTLADKIVVLSGGRIQQIGEPQGIYARPANQMVATFLGNP
MSMX_BACSU   LHQRLQ--TTTIYVTHDQTEALTMATRIVVMKDGKIQQIGTPKDVYEFPENVFVGGFIGSP
MalK_ECOLI   LHKRLG--RTMIYVTHDQVEAMTLADKIVVLDAGRVAQVGKPLELYHYPADRFVAGFIGSP
AglK_RHIME   LSERMSDTTMIYVTHDQVEAMTLADRIVLSAGHIEQVGAPLELYERPANLFVARFIGSP
             *  .:   * *******.**:*:. .*.::. *.: *:. *  :*  * : :*. *:*.*


Alr4781      PMNFIPVEFHAPLLITHSQFRLTLPE---IWASVLQK--YDKQTLILGIRPEHLT---VS
All1823      PMNILPATYQLAGFDINGQL-LAIPA-----FLREKLQLRSAQRVNLGIRPEHIS---IN
MSMX_BACSU   AMNFFKGKLTDGLIKI-GSAALTVPEGK---MKVLREKGYIGKEVIFGIRPEDIHDELIV
MalK_ECOLI   KMNFLPVKVTATAIDQ-VQVELPMPNRQQVWLPVESRDVQVGANMSLGIRPEHLL-----
AglK_RHIME   AMNVIPATITATG----QQTAVSLAGGKSVTLDVPTNASENGKTASFGVRPEDLR-----
              **.:          . :.:.        :*:*** :


Alr4781      VPATKN----LPVQVDLVENLGNDSFINVVLTEAESRFSHTIKPLQVRVPSDRIINVSEQ
All1823      SDAINDQSSGLLVDVKLVEPLGRETLVRVSLPDST-------VLLSVQLSGNVRLHPGDR
MSMX_BACSU   VESYKNSS--IKAKINVAELLGSEIMIYSQI--DN-------QDFIARIDARLDIQSGDE
MalK_ECOLI   PSDIADVI--LEGEVQVVEQLGNETQIHIQIPSIR-------QNLVYRQNDVVLVEEGAT
AglK_RHIME   VTEADDFL--FEGTVSIVEALGEVTLLYIEGLVEN-------EPIIAKMPGIARVGRGDK
                 :    :   :.:.* **   :              :  .     : .


Alr4781      IWLSLTLDKIHFFDPD-TDLAIFPKN---
All1823      LSLQLDLNQLFIFDPQ-TGYKISPQD---
MSMX_BACSU   LTVAFDMNKGHFFDSE-TEVRIR------
MalK_ECOLI   FAIGLPPERCHLFREDGTACRRLHKEPGV
AglK_RHIME   VRFTADKAKLHLFDTNGQSYRA-------
             .  .    . .:*  :
```

Figure 6. Alignment of Alr4781 (GlsC) and Alr1823 (GlsD) with three highly similar proteins, MsmX from *Bacillus subtilis*, MalK from *Escherichia coli*, and AlgK from *Rhizobium meliloti*. Aligment was carried out at http://www.ebi.ac.uk/Tools/msa/muscle/ with default parameters. Note the long insertions in Alr4781 (GlsC) (brackets in garnet color).

Conclusions

Conclusions

1. The recovery rate constants determined by means of Fluorescent Recovery After Photobleaching (FRAP) with the fluorescent markers calcein, 5-carboxyfluorescein and esculin are directly proportional to the absolute temperature. Thus, the process of intercellular molecular exchange in filamentous cyanobacteria has the physical properties of simple diffusion.

2. The identified mechanism of simple diffusion for intercellular molecular exchange suggests that transfer through septal junctions is responsible for cell-cell communication in the cyanobacterial filament, because a periplasmic pathway would instead imply a role for active membrane transporters. Thus, cyanobacterial septal junctions are analogous to the connexons of the gap junctions of metazoans, which also mediate molecular transfer between cells by simple diffusion.

3. The esculin uptake assay developed in this work has permitted to identify components of an ABC-type glucoside transporter in *Anabaena* sp. strain PCC 7120. These components are GlsC and GlsD (nucleotide-binding domain proteins [NBDs]), GlsP and GlsQ (transmembrane domain [TMDs]), and GlsR (a periplasmic solute-binding protein [SBP]). HepP, a previously known Major Facilitator Superfamily (MFS) protein involved in the formation of the heterocyst-specific polysaccharide layer, is also a glucoside transporter acting specifically under diazotrophic conditions.

4. *Anabaena* appears indeed to express at least three ABC-type transporters for glucosides. The GlsR/GlsP-GlsQ/GlsC-GlsD transporter is one of them. This transporter could use periplasmic solute-binding proteins additional to GlsR and share the NBDs GlsC-GlsD with other transporters.

5. *Anabaena* can grow mixotrophically using sucrose, fructose or glucose. The identified ABC-type glucoside transporters are involved in the assimilation of these sugars, although fructose and glucose would be low-affinity (non-preferential) substrates.

6. Glucoside transporters influence the cyanobacterial septal junctions. Whereas GlsC (NBD protein) is required for a normal localization of SepJ and maturation of septal junctions, GlsQ-GlsP and HepP appear to influence the function of SepJ-related septal junctions through protein-protein interactions.

Resumen de la tesis

La aparición de organismos multicelulares supuso una de las mayores transiciones durante el curso de la evolución biológica temprana, habiendo surgido la multicelularidad de manera independiente en los tres dominios de la vida. Las cianobacterias son un amplio grupo monofilético de procariotas fotosintéticos con representantes unicelulares y multicelulares. Muchas cianobacterias filamentosas experimentan procesos de diferenciación celular dando lugar a células o grupos de células con funciones especializadas como son la fijación de nitrógeno, la supervivencia a condiciones adversas y la dispersión.

La cianobacteria formadora de heterocistos *Anabaena* sp. PCC 7120 representa un sistema modelo para estudiar la multicelularidad, la diferenciación celular y la fijación de nitrógeno. *Anabaena* crece formando cadenas de células, conocidas como tricomas o filamentos. En ausencia de una fuente de nitrógeno combinado, estos filamentos están formados por dos tipos celulares: células vegetativas que llevan a cabo la fotosíntesis oxigénica y heterocistos que fijan el nitrogeno atmosférico. Las células vegetativas transfieren carbono reducido a los heterocistos, y éstos transfieren nitrógeno a las células vegetativas. La transferencia intercelular de diferentes compuestos es un aspecto muy relevante de la biología de *Anabaena* que ha sido abordado en esta tesis. Dos vías distintas han sido consideradas para explicar la transferencia de nutrientes y reguladores entre las células del filamento durante la diferenciación de los heterocistos y el crecimiento diazotrófico en estas cianobacterias: una vía indirecta a través del periplasma del filamento y una directa a través de los complejos proteicos llamados "nexos septales" ("septal junctions"). La transferencia molecular intercelular en las cianobacterias filamentosas se ha estudiado con la técnica de análisis Fluorescent Recovery After Photobleaching (FRAP) usando diferentes marcadores fluorescentes: calceína, 5-carboxifluoresceína (5-CF) y esculina, que es un análogo a la sacarosa. En el Capítulo 1, analizamos la dependencia de la temperatura de la transferencia intercelular y concluimos que presenta propiedades de difusión simple. Esta observación es consistente con la presencia de nexos septales responsables de la comunicación intercelular. SepJ, FraC y FraD son proteínas septales identificadas como posibles componentes de los nexos septales, los cuales concluimos que permiten la transferencia intercelular de sustancias por difusión simple. Los nexos septales pueden ser considerados análogos a los conexones de las "gap junctions" de metazoos.

Como ha sido mencionado anteriormente, la esculina (análogo fluorescente de la sacarosa) se ha usado para estudiar la transferencia molecular intercelular. En el "Experimental Preamble", describimos un ensayo que puede ser usado para estudiar la incorporación de esculina a las células de *Anabaena*. Con este ensayo hemos definido que los transportadores que incorporan esculina en *Anabaena* son transportadores de α-glucósidos, ya que la incorporación de esculina es inhibida por α-glucósidos como la sacarosa y la maltosa. Los Capítulos 2 y 3 describen la identificación de componentes de transportadores de glucósidos del tipo ABC. Estos componentes son GlsC y GlsD ("nucleotide-binding domain proteins" [NBDs]), GlsP and GlsQ ("transmembrane domain proteins" [TMDs]), y GlsR ("solute-binding protein" [SBP]). Además, HepP, una proteína de la familia MFS, previamente

descrita, también contribuye a la incorporación de esculina especialmente en condiciones diazotróficas.

Anabaena ha sido considerada un organismo fototrófico estricto durante mucho tiempo. Sin embargo, aunque esta cianobacteria no tiene ningún gen que codifique de forma evidente un transportador de fructosa, trabajos recientes han indicado que puede crecer heterotróficamente con una concentración relativamente alta de fructosa (≥ 50 mM). En el Capítulo 3, describimos el crecimiento fototrófico estimulado por sacarosa, fructosa y glucosa en *Anabaena*, mostrando la capacidad de crecimiento mixotrófico de este organismo usando estos azúcares. Con objeto de averiguar si los componentes de los transportadores de glucósidos del tipo ABC que hemos identificado están relacionados con el crecimiento estimulado por azúcares, estudiamos el crecimiento mixotrófico en sus mutantes. Mientras que los mutantes *glsC* y *glsD* estaban drásticamente afectados en el crecimiento estimulado por sacarosa, los mutantes *glsP*, *glsQ* y *glsR* estaban afectados a menor nivel. Todos los mutantes también estaban afectados de alguna manera en el crecimiento estimulado por fructosa y glucosa, lo cual sugiere que estos azúcares pueden ser asimilados al menos en parte con el concurso de los transportador(es) de glucósidos. El genoma de *Anabaena* contiene 12 genes que codifican componentes de transportadores de glucósidos tipo ABC: cuatro SBPs, seis TMDs and dos NBDs. Esta información junto con nuestros resultados sugieren la presencia de al menos tres transportadores de glucósidos en *Anabaena*, uno de los cuales estaría formado por GlsR (SBP), GlsP-GlsQ (TMDs) y GlsC-GlsD (NBDs). Otras SBPs podrían contribuir al funcionamiento de este transportador, y las proteínas NBD (GlsC y GlsD) parecen ser compartidas por los tres transportadores como ocurre en otros sistemas ABC. El análisis llevado a cabo mediante Bacterial Adenylate Cyclase Two Hybrid (BACTH) ha mostrado interacciones proteína-proteína consistentes con el modelo propuesto.

El efecto de la inactivación de algunos de los genes *gls* en el crecimiento diazotrófico de *Anabaena* sugirió la posibilidad de una limitada transferencia de sacarosa a los heterocistos en algunos de estos mutantes. Los mutantes *glsC*, *glsP* y *hepP* estaban afectados en la transferencia intercelular de esculina, por lo que extendimos el estudio a la transferencia de calceína y 5-CF en todos los mutantes *gls*, así como al mutante *hepP*. Todos los mutantes ensayados estaban afectados, en particular, en la transferencia intercelular de calceína, lo cual recuerda al fenotipo de la mutación *sepJ*. Como ya hemos mencionado, SepJ es un posible componente de los nexos septales, y en este trabajo, mediante análisis BACTH, hemos visto que GlsP, GlsQ y HepP interaccionan con SepJ, lo cual sugiere que GlsP, GlsQ and HepP interaccionen con SepJ para un correcto funcionamiento de los nexos septales. Por otro lado, GlsC influye en la localización de SepJ y en el número de nanoporos formados en los discos septales de peptidoglicano. Estos resultados sugieren un papel específico de GlsC influyendo en la maduración de los nexos septales.

En conclusión, la cianobacteria formadora de heterocistos *Anabaena* sp. PCC 7120 expresa transportadores ABC de glucósidos que contribuyen a la asimilación de azúcares haciendo posible un crecimiento mixotrófico. Además, los transportadores de glucósidos estudiados influyen en la comunicación intercelular mediada por los nexos septales.

References

Anderson SL, McIntosh L. 1991. Light-activated heterotrophic growth of the cyanobacterium *Synechocystis* sp. strain PCC 6803: a blue-light-requiring process. J Bacteriol 73: 2761-2767.

Awai K, Wolk CP. 2007. Identification of the glycosyl transferase required for synthesis of the principal glycolipid characteristic of heterocysts of *Anabaena* sp. strain PCC 7120. FEMS Microbiol Lett 266: 98-102.

Ayre BG. 2011. Membrane-transport systems for sucrose in relation to whole-plant carbon partitioning. Mol Plant 4: 377-394.

Bagder MR, Hanson D, Price GD. 2002. Evolution and diversity of CO2 concentrating mechanisms in cyanobacteria. Funct Plant Biol 29: 161-173.

Bartual SG, Straume D, Stamsås GA, Muñoz IG, Alfonso C, Martínez-Ripoll M, Håvarstein LS, Hermoso JA. 2014. Structural basis of PcsB-mediated cell separation in *Streptococcus pneumoniae*. Nat Commun 5: 3842.

Bauer CC, Buikema WJ, Black K, Haselkorn R. 1995. A short-filament mutant of *Anabaena* sp. strain PCC 7120 that fragments in nitrogen-deficient medium. J Bacteriol 177: 1520-1526.

Baurain D, Brinkmann H, Petersen K, Rodriguez-Ezpeleta N, Stechmann A, Demoulin V, Roger AJ, Burger G, Lang BF, Philippe H. 2010. Phylogenomic Evidence for Separate Acquisition of Plastids in Cryptophytes, Haptophytes, and Stramenopiles. Molecular Biology and Evolution, 27, 1698-1709.

Berendt S, Lehner J, Zhang YV, Rasse TM, Forchhammer K, Maldener I. 2012. Cell wall amidase AmiC1 is required for cellular communication and heterocyst development in the cyanobacterium *Anabaena* PCC 7120 but not for filament integrity. J Bacteriol 194: 5218-27.

Bergman B, Gallon JR, Rai AN, Stal JL. 1997. N_2 fixation by non-heterocystous cyanobacteria. FEMS Microbiol Rev 19: 139-185.

Black TA, Wolk CP. 1994. Analysis of a Het[-] mutation in *Anabaena* sp. strain PCC 7120 implicates a secondary metabolite in the regulation of heterocyst spacing. J Bacteriol 176: 2282-2292.

Black TA, Cai Y, Wolk CP. 1993. Spatial expression and autoregulation of hetR, a gene involved in the control of heterocyst development in *Anabaena*. Mol Microbiol 9: 77-84.

Black K, Buikema WJ, Haselkorn R. 1995. The *hglK* gene is required for localization of heterocyst-specific glycolipids in the cyanobacterium *Anabaena* sp. strain PCC 7120. J Bacteriol 177: 6330-6448.

Blanco-Rivero A, Leganés F, Fernández-Valiente E, Calle P, Fernández-Piñas F. 2005. *mrpA*, a gene with roles to resistance to Na^+ and adaptation to alkaline pH in the cyanobacterium *Anabaena* sp. PCC7120. Microbiology 151: 1671–1682.

Bonner JT. 1998. The origins of multicellularity. Int Biol 1: 27-36.

Bonner JT. 2003. On the origin of differentiation. J Biosci 28: 523-428.

Bos MP, Robert V, Tommassen J. 2007. Biogenesis of the gram-negative bacterial outer membrane. Annu Rev Microbiol 61: 191-214.

Bornikoel J, Carrión A, Fan Q, Flores E, Forchhammer K, Mariscal V, Mullineaux CW, Perez R, Silber N, Wolk PC, Maldener I. 2017. Role of two amidases in septal junction and nanopore formation in the multicellular cyanobacterium Anabaena sp. PCC 7120. Front Cell Infect Microbiol 7: 386.

Bottomley PJ, Van Baalen C. 1978. Dark hexose metabolism by photoautotrophically and heterotrophically grown cells of the bluegreen alga (cyanobacterium) Nostoc sp Mac. J Bacteriol 135: 888–894.

Boussiba S, Dilling W, Gibson J. 1984. Methylammonium transport in *Anacystis nidulans* R-2. J Bacteriol 160: 204-210.

Buikema WJ, Haselkorn R. 1991. Characterization of a gene controlling heterocyst differentiation in the cyanobacterium *Anabaena* sp. PCC 7120. Genes Dev 5: 321-330.

Buikema WJ, Haselkorn R. 2001. Expression of the Anabaena *hetR* gene from a copper-regulated promoter leads to heterocyst differentiation under repressing conditions. Proc Natl Acad Sci 98: 2729-34.

Burnat M, Herrero A, Flores E. 2014. Compartmentalized cyanophycin metabolism in the diazotrophic filaments of a heterocyst-forming cyanobacterium. Proc Natl Acad Sci USA 111: 3823-3828.

Büttner FM, Faulhaber K, Forchhammer K, Maldener I, Stehle T. 2016. Enabling cell-cell communication via nanopore formation: structure, function and localization of the unique cell wall amidase AmicC2 of *Nostoc punctiforme*. FEBS J 283: 1336-1350.

Callahan SM, Buikema WJ. 2001. The role of HetN in maintenance of the heterocyst pattern in *Anabaena* sp. PCC 7120. Mol Microbiol 40: 941-950.

Cameron JC, Sutter M, Kerfeld CA. 2014. The Carboxysome: Function, Structure and Cellular Dynamics. In The Cell Biology of Cyanobacteria. Caister Academic Press (eds.) Enrique Flores and Antonia Herrero. pp 171-188.

Campbell EL, Cohen MF, Meeks JC. 1997. A polyketide-synthaselike gene is involved in the synthesis of heterocyst glycolipids in *Nostoc punctiforme* strain ATCC 29133. Arch Microbiol 167: 251–258.

Capone DG, Zehr JP, Paerl HW, Bergman B, Carpenter EJ. 1997. *Tricodesmium*, a globally significant marine cyanobacterium. Science. 276, 1221–1229.

Cardemil L, Wolk CP. 1979. The polysaccharides from heterocyst and spore envelopes of a blue-green alga. Structure of the basic repeating unit. J Biol Chem 254: 736-741.

Cardemil L, Wolk CP. 1981. Isolated heterocysts of Anabaena variabilis synthesize envelope polysaccharide. Biochim Biophys Acta 674: 265-276.

Carrol SB. 2001. Chance and necessity: the evolution of morphological complexity and diversity. Nature 409: 1102-1109.

Castenhols RW. 2001. Phylum BX, Cyanobacteria (Oxygenic Photosynthetic Bacteria). Bergey´s Manual of Systematic Bacteriology Vol. 1: The *Archaea* and the Deeply Branching and Phototrophic *Bacteria*. Springer New York, pp 473-599.

Chan CX, Gross J, Yoon HS, and Bhattacharya D. 2011. Plastid Origin and Evolution: New Models Provide Insights into Old Problems. Plant Physiol 155:1552-1560.

Claessen D, Rozen DE, Kuipers OP, Søgaard -Andersen L, van Wezel GP. 2014. Bacterial solutions to multicellularity: a tale of biofilms, filaments and fruiting bodies. Nat Rev Microbiol 88: 1093-1105.

Cooper GM. 2000. The Cell. A molecular approach. Boston University. Sunderland (MA): Sinauer Associates.

Corrales-Guerrero L, Mariscal V, Flores E, Herrero A. 2013. Functional dissection and evidence for intercellular transfer of the heterocyst-differentiation PatS morphogen. Mol Microbiol 88: 1093-105.

Corrales-Guerrero L, Mariscal V, Nürnberg DJ, Elhai J, Mullineaux CW, Flores E, Herrero A. 2014. Subcellular localization and clues for the function of the HetN factor influencing heterocyst distribution in Anabaena sp. strain PCC 7120. J Bacteriol 196: 3452.3460.

Cui J, Davidson AL. 2011. ABC solute importers in bacteria. Essays Biochem 50: 85-99.

Cumino A, Curatti L, Giarrocco L, Salerno GL. 2002. Sucrose metabolism: *Anabaena* sucrose-phosphate synthase and sucrose-phospate phosphatase define minimal function domains shuffled during evolution. FEBS Lett 517: 19-23.

Curatti L, Flores E, Salerno G. 2002. Sucrose is involved in the diazotrophic metabolism of the heterocyst-forming cyanobacterium *Anabaena* sp. FEBS Lett 513: 175-178.

Davidson AL, Dassa E, Orelle C, Chen J. 2008. Structure, function, and evolution of bacterial ATP-binding cassette systems. Microbiol Mol Biol Rev 72: 317-364.

Dismukes GC, Carrieri D, Bennette N, Ananyev GM, Posewitz MC. 2008. Aquatic phototrophs: efficient alternatives to land-based crops for biofuels. Curr. Opin. Biotechnol 19: 235-240.

Domínguez-Cuevas P, Porcelli I, Daniel RA, Errington J. 2013. Differentiated roles for MreB-actin isologues and autolytic enzymes in *Bacillus subtilis* morphogenesis. Mol Microbiol 89: 1084-1098.

Ehira S, Ohmori M. 2006. Nrra directly regulates expression of *hetR* during heterocyst differentiation in the cyanobacterium *Anabaena* sp. strain PCC 7120. J Bacteriol 188: 8520-8525.

Ekman M, Picossi S, Campbell EL, Meeks JC, Flores E. 2013. A *Nostoc punctiforme* sugar transporter necessary to establish a Cyanobacterium-plant symbiosis. Plant Physiol 161: 1984-1992.

Ermakova M, Battchikova N, Richaud P, Leino H, Kosourov D, Isojärvi J, Peltier G, Flores E, Cournac L, Allahverdiyeva Y, Aro EM. 2014. Heterocyst-specific flavodiion protein Flv3B enables oxic diazotrophic growth of the filamentous cyanobacterium *Anabaena* sp. PCC 7120. Proc Natl Acad Sci 111: 11205–11210.

Escudero L, Mariscal V, Flores E. 2015. Functional dependence between septal protein SepJ from Anabaena sp. strain PCC 7120 and an amino acid ABC-type uptake transporter. J Bacteriol 197: 2721-2730.

Fan Q, Huang G, Lechno-Yossef S, Wolk CP, Kaneko T, Tabata S. 2005. Clustered genes required for synthesis and deposition of envelope glycolipids in *Anabaena* sp. strain PCC 7120. Mol Microbiol 58: 227-243.

Fan Q, Lechno-Yossef S, Ehira S, Kaneko T, Ohmori M, Sato N, Tabata S, Wolk CP. 2006. Signal transduction genes required for heterocyst maturation in *Anabaena* sp. strain PCC 7120. J. Bacteriol. 188: 6688–6693.

Fay P. 1992. Oxygen relation of nitrogen fixation in cyanobacteria. Microbiol Rev 56: 340-373.

Feldmann EA, Ni S, Sahu ID, Mishler CH, Levengood JD, Kushnir Y, McCarrick RM, Lorigan GA, Tolbert BS, Callahan SM, Kennedy MA. 2012. Differential binding between PatS C-terminal peptide fragments and HetR from *Anabaena* sp. PCC 7120. Biochemistry 51: 2436-2442.

Ferreira MJ, Sá-Nogueira Id. 2010. A multitask ATPase serving different ABC-type sugar importers in Bacillus subtilis. J Bacteriol 192: 5312-5318.

Fiedler G, Arnold M, Hannus S, Maldener I. 1998. The DevBCA exporter is essential for envelope formation in heterocysts of the cyanobacterium *Anabaena* sp. strain PCC 7120. Mol Microbiol 27: 1193-1202.

Flaherty BL, Nieuwerburgh FV, Heas SR, Golden JW. 2011. Directional RNA deep sequencing sheds new light on the transcriptional response of *Anabaena* sp. strain PCC 7120 to combined-nitrogen deprivation. BMC Genomics 12: 332.

Flärdh K, Buttner MJ. 2009. Streptomyces morphogenetics: dissecting differentiation in a filamentous bacterium. Nat Rev Microbiol 7: 36-49.

Flores E, Herrero A. 2005. Nitrogen assimilation and nitrogen control in cyanobacteria. Biochem Soc Trans 33: 164-167.

Flores E, Herrero A. 2010. Compartmentalized function through cell differentiation in filamentous cyanobacteria. Nature Rev Microbiol 8: 39-50.

Flores E, Herrero A. 2014. The cyanobacteria: morphological diversity in a photoautotrophic lifestyle. Perspectives in Phycology 2: 63-72.

Flores E, Frías JE, Rubio LM, Herrero A. 2005. Photosynthetic nitrate assimilation in cyanobacteria. Photosynthesis Research 83: 117–133

Flores E, Herrero A, Wolk CP, Maldener I. 2006. Is the periplasm continuous in filamentous multicellular cyanobacteria? Trends Microbiol 14: 439-443.

Flores, E., Pernil, R., Muro-Pastor, A.M., Mariscal, V., Maldener, I., Lechno-Yossef, S., Fan, Q., Wolk, C.P., and Herrero, A. 2007. Septum-localized protein for filament integrity and diazotrophy in the heterocyst-forming cyanobacterium *Anabaena* sp. strain PCC 7120. J Bacteriol 189: 3884-3890.

Flores E, Muro-Pastor AM, Meeks JC. 2008. Gene transfer to cyanobacteria in the laboratory and in nature. In The Cyanobacteria: Molecular Biology Genomics and Evolution Caister Academic Press; Norfolk, UK. Herrero A, Flores E. (eds.) pp 45-57.

Flores E, Herrero A, Forchhammer K, Maldener I. 2016. Septal junctions in filamentous heterocyst-forming cyanobacteria. Trends Microbiol 24: 79-82.

Frías JE, Flores E, Herrero A. 1994. Requirement of the regulatory protein NtcA for the expression of nitrogen assimilation and heterocyst development genes in the cyanobacterium *Anabaena* sp. PCC 7120. Mol Microbiol 14: 823-32.

Giovanni S, Turner S, Olsen G, Barns S, Lane D, Pace N. 1988. Evolutionary Relationships among Cyanobacteria and Green Chloroplasts J Bacteriol 170: 3584-3592.

Giddings THJr, Staehelin LA. 1978. Plasma membrane architecture of *Anabaena cylindrica*: occurrence of microplasmodesmata and changes associated with heterocyst development and the cell cycle. Eur J Cell Biol 16: 235-249.

Golden JW, Yoon HS. 1998. Heterocyst formation in *Anabaena*. Curr Opin Microbiol 1: 623-629.

Gora PJ, Reinders A, Ward JM. 2012. A novel fluorescent assay for sucrose transporters. Plant Methods 8: 13.

Hahn A, Schleiff E. 2014. The cell envelope. In The Cell Biology of Cyanobacteria. Caister Academic Press; Norfolk, UK. Herrero A, Flores E. (eds.) pp 29-87.

Hahn A, Stevanovic M, Mirus O, Schleiff E. 2012. The TolC-like protein HgdD of the cyanobacterium Anabaena sp. PCC 7120 is involved in secondary metabolite export and antibiotic resistance. J Biol Chem 287: 41126-41138.

Heidrich C, Ursinus A, Berger J, Schwarz H, Höltje JV. 2002. Effects of multiple deletions of murein hydrolases on viability, septum cleavage, and sensitivity of large toxic molecules in *Escherichia coli*. J Bacteriol 184:6093-6099.

Herrero A, Muro-Pastor AM, Flores E. 2001. Nitrogen control in cyanobacteria. J Bacteriol 183: 411-425.

Herrero A, Stavans J, Flores E. 2016. The multicellular nature of filamentous heterocyst-forming cyanobacteria. FEMS Microbiol Rev 40: 831-854.

Herrero A, Muro-Pastor AM, Valladares A, Flores E. 2004. Cellular differentiation and the NtcA transcription factor in filamentous cyanobacteria. FEMS Microbiol Rev 28: 469-487.

Higa KC, Rajagopalan R, Risser DD, Rivers OS, Tom SK, Videau P, Callahan SM. 2012. The RGSGR amino acid motif of the intercellular signaling protein, HetN, is required for patterning of heterocyst in *Anabaena* sp. strain PCC 7120. Mol Microbiol 83: 682-693.

Higgins CF, Ames GF. 1981. Two periplasmic transport proteins which interact with a common membrane receptor show extensive homology: complete nucleotide sequences. Proc Natl Acad Sci USA 78: 6038– 6042.

Hobbie JE, Hobbie EA. 2013. Microbes in nature are limited by carbon and energy: the starving-survival lifestyle in soil and consequences for stimating microbial rates. Front Microbiol 4: 324.

Hoiczyk E, Hansel A. 2000. Cyanobacterial cell wall: news from an unusual prokaryotic envelope. J Bacteriol 182: 1191-1199.

Huang X, Dong Y, Zhao J. 2004. HetR homodimer is a DNA-binding protein required for heterocyst differentiation, and the DNA-binding activity is inhibited by PatS. Proc Natl Acad Sci USA 101: 4848-4853.

Huang G, Fan Q, Lechno-Yossef S, Wojciuch E, Wolk CP, Kaneko T, Tabata S. 2005. Clustered genes required for the synthesis of heterocyst envelope polysaccharide in *Anabaena* sp. strain PCC 7120. J Bacteriol 187: 1114-1123.

Jardetzky O. 1966. Simple allosteric model for membrane pumps. Nature 211: 969–970.

Jones KM, Haselkorn R. 2002. Newly identified cytochrome c oxidase operon in the nitrogen-fixing cyanobacterium *Anabaena* sp. strain PCC 7120 specifically induced in heterocysts. J Bacteriol 184: 2491-2499.

Jüttner F. 1983. ^{14}C-labeled metabolites in heterocysts and vegetative cells of Anabaena cylindrinca filaments and their presumptive function as transport vehicles of organic carbon and nitrogen. J Bacteriol 155: 628-633.

Kang J, Burten CN, Hong G. 2017. Thermodynamic basis of molecular diffusion through cyanobacterial septal junctions. mBio 8 (3): e00529-17.

Kaplan A, Reinhold L. 1999. CO2 concentrating mechanisms in photosynthetic microorganisms. Annu Rev Plant Physiol Plant Mol Biol 50: 539-570.

Khudyakov IY, Golden JW. 2004. Different functions of HetR, a master regulator of heterocyst differentiation in Anabaena sp. PCC 7120, can be separated by mutation. Proc Natl Acad Sci USA 101: 16040-16045.

Kim Y, Joachimiak G, Ye Z, Binkowski TA, Zhang R, Gornicki P, Callahan SM, Hess WR, Haselkorn R, Joachimiak A. 2011. Structure of transcription factor HetR required for heterocyst differentiation in cyanobacteria. Proc Natl Acad Sci USA 108: 10109-10114.

Knoll AH. 2008. Cyanobacteria and earth history. In The Cell Biology of Cyanobacteria. Caister Academic Press; Norfolk, UK. Herrero A, Flores E. (eds.) pp 1-19.

Kumar K, Mella-Herrera RA, Golden JW. 2010. Cyanobacterial heterocysts. Cold Spring Harb Perspect Biol 2: a000315.

Lang NJ, Fay P. 1971. The heterocyst of blue-green algae II. Details of ultrastructure. Proc Roy Soc Lond B 178: 193-203.

Lang NJ, Simon RD, Wolk CP. 1972. Correspondence of cyanophycin granules with structured granules in *Anabaena* cylindrical. Arch Mikrobiol 83: 313-320.

Lehner J, Zhang Y, Berendt S, Rasse TM, Forchhammer K, Maldener I. 2011. The morphogene AmiC2 is pivotal for multicellular development in the cyanobacterium *Nostoc punctiforme*. Mol Microbiol 79: 1655-1669.

Lehner J, Berendt S, Dörsam B, Pérez R, Forchhammer K, Maldener I. 2013. Prokaryotic multicellularity: a nanopore array for bacterial cell communication. FASEB J 27: 2293-2300.

Lechno-Yossef S, Fan Q, Ehira S, Sato N, Wolk CP. 2006. Mutations in four regulatory genes have interrelated effects on heterocyst maturation in Anabaena sp. strain PCC 7120. J Bacteriol 188: 7387-7395.

Lechno-Yossef S, Fan Q, Wojciuch E, Wolk CP. 2011. Identification of ten *Anabaena* sp. genes that under aerobic conditions are required for growth on dinitrogen but not for growth on fixed nitrogen. J Bacteriol 193: 3482-3489.

Li B, Huang X, Zhao J. 2002. Expression of *hetN* during heterocyst differentiation and its inhibition of *hetR* up-regulation in the cyanobacterium *Anabaena* sp. PCC 7120. FEBS Lett. 517: 87-91.

Locher KP. 2016. Mechanistic diversity in ATP-binding cassette (ABC) transporters. Nat Struct Mol Biol 23: 487-493.

López-Igual R, Flores E, Herrero A. 2010. Inactivation of a heterocyst-specific invertase indicates a principal role of sucrose catabolism in heterocysts of *Anabaena* sp. J Bacteriol 192: 5526–5533.

López-Igual R, Lechno-Yossef S, Fan Q, Herrero A, Flores E, Wolk CP. 2012. A major facilitator superfamily protein, HepP, is involved in formation of the heterocyst envelope polysaccharide in the cyanobacterium *Anabaena* sp. strain PCC 7120. J Bacteriol 194: 4677-4687.

Luque I, Flores E, Herrero A. 1994. Molecular mechanism for the operation of nitrogen control in cyanobacteria. EMBO J 13: 2862-2869.

Luque I, Forchhammer K. 2008. Nitrogen assimilation and C/N balance sensing. In The Cyanobacteria: Molecular Biology Genomics and Evolution Caister Academic Press; Norfolk, UK. Herrero A, Flores E. (eds.) pp 335-382.

Luque I, Vázquez-Bermúdez MF, Paz-Yepes J, Flores E, Herrero A. 2004. In vivo activity of the nitrogen control transcription factor NtcA is subjected to metabolic regulation in Synechococcus sp. strain PCC 7942. FEMS Microbiol Lett 1: 236: 47-52.

Maiden MCJ, Jones-Mortimer MC, Hendersen PJF. 1988. The cloning, DNA sequence, and overexpression of the gene araE coding for arabinose-proton symport in Escherichia coli K12. J Biol Chem 263: 8003–8010.

Malatinszky D, Steuer R, Jones PR. 2017. A comprehensively curated genome-scale two-cell model for the heterocystous cyanobacterium *Anabaena* sp. PCC 7120. Plant Physiol 173: 509-523.

Maldener I, Hannus S, Kammerer M. 2003. Description of five mutants of the cyanobacterium Anabaena sp strain PCC 7120 affected in heterocyst differentiation and identification of the transposon-tagged genes. FEMS Microbiol Lett 224: 205-213.

Maldener I, Summers ML, Sukenik A. 2014. Cellular differentiation in filamentous cyanobacteria. In Flores E, Herrero A (eds.), The biology of Cyanobacteria. Caister Academic Press, Norfolk, UK, pp 263-291.

Maloney PC. 1990. Microbes and membrane biology. FEMS Microbiol Rev 87: 91–102.

Maloney PC. 1992. The molecular and cell biology of anion transport by bacteria. Bioessays 14: 757–762.

Mariscal V. 2014. Cell-cell joining proteins in heterocyst-forming cyanobacteria. In The Cell Biology of Cyanobacteria. Caister Academic Press; Norfolk, UK. Herrero A, Flores E. (eds.) pp 293-304.

Mariscal V, Flores E. 2010. Multicellularity in a heterocyst-forming cyanobacterium: pathways for intercellular communication. Adv Exp Med Biol 675: 123-135.

Mariscal V, Herrero A, Flores E. 2007. Continuous periplasm in a filamentous heterocyst-forming cyanobacterium. Mol Microbiol 65: 1139-1145.

Mariscal V, Herrero A, Nenninger A, Mullineaux CW, Flores E. 2011. Functional dissection of the three-domain SepJ protein joining the cells in cyanobacterial trichomes. Mol Microbiol 79: 1077-1088.

Martín-Figueroa E, Navarro F, Florencio FJ. 2000. The GS-GOGAT pathway is not operative in the heterocysts. Cloning and expression of *glsF* gene from the cyanobacterium *Anabaena* sp. PCC 7120. FEBS Lett 476: 282-286.

Merino-Puerto V, Mariscal V, Mullineaux CW, Herrero A, Flores E. 2010. Fra proteins influencing filament integrity, diazotrophic and localization of septal protein SepJ in the heterocyst-forming cyanobacterium *Anabaena* sp. Mol Microbiol 75: 1159-1170.

Merino-Puerto V, Mariscal V, Schwarz H, Maldener I, Mullineaux CW, Herrero A, Flores E. 2011a. FraH is required for reorganization of intracellular membrane during heterocyst differentiation in *Anabaena* sp. strain PCC 7120. J Bacteriol 193: 6815-6823.

Merino-Puerto V, Schwarz H, Maldener I, Mariscal V, Mullineaux CW, Herrero A, Flores E. 2011b. FraC/FraD-dependent intercellular molecular exchange in the filaments of a heterocyst-formingcyanobacterium, *Anabaena* sp. 2011. Mol Microbiol 82: 87-98.

Meeks JC, Elhai J. 2002. Regulation of Cellular Differentiation in Filamentous Cyanobacteria in Free-Living and Plant-Associated Symbiotic Growth States. Microbiol Mol Biol Rev 66: 94-121.

Meisner J, Montero Llopis P, Sham LT, Garner E, Bernhardt TG, Rudner DZ. 2013. FtsEX is required for CwlO peptidoglycan hydrolase activity during cell wall elongation in *Bacillus subtilis*. Mol Microbiol 89: 1069-1083.

Mitchell, P. 1967. Proton-translocation phosphorylation in mitochondria, chloroplasts and bacteria: natural fuel cells and solar cells. Fed Proc 26: 1370–1379.

Montesinos ML, Muro-Pastor AM, Herrero A, Flores E. 1998. Ammonium/methylammonium permeases of a cyanobacterium. Identification and analysis of three nitrogen-regulated *amt* genes in *Synechocystis* sp. PCC 6803. J Biol Chem 273: 31463-31470.

Montoya JP, Holl CM, Zehr JP, Hansen A, Villareal TA, Capone DG. 2004. High rates of N_2 fixation by unicellular diazotrophs in the oligotrophic Pacific Ocean. Nature 430: 1027-1032.

Moslavac S, Bredemeier R, Mirus O, Granvogl B, Eichacker LA, Schleiff E. 2005. Proteomic analysis of the outer membrane of Anabaena sp. strain PCC 7120. J Proteome Res 4: 1330-1338.

Moslavac S, Nicolaisen K, Mirus O, Al Dehni F, Pernil R, Flores E, Maldener I, Schleiff E. 2007a. A TolC-like protein is required for heterocyst development in *Anabaena* sp. strain PCC 7120. J Bacteriol 189: 7887-7895.

Moslavac S, Reisinger V, Berg M, Mirus O, Voskya O, Plöscher M, Flores E, Eichacker LA, Schleiff E. 2007b. The proteome of the heterocyst cell wall in *Anabaena* sp. PCC 7120. Biol Chem 388: 823-829.

Mullineaux CW, Nürnberg DJ. 2014. Tracing the path of a prokaryotic paracrine signal. Mol Microbiol 94: 1208-1212.

Mullineaux CW, Mariscal V, Nenninger A, Khanum H, Herrero A, Flores E, Adams DG. 2008. Mechanism of intercellular molecular exchange in heterocyst-forming cyanobacteria. EMBO J 27: 1299-1308.

Muñoz-Marín Mdel C, Luque I, Zubkov MV, Hill PG, Diez J, García-Fernández JM. 2013. Prochlorococcus can use the Pro1404 transporter to take up glucose at nanomolar concentrations in the Atlantic Ocean. Proc Natl Acad Sci 110: 8597-602.

Muro-Pastor MI, Reyes JC, Florencio FJ. 2001. Cyanobacteria perceive nitrogen status by sensing intracellular 2-oxoglutarate levels. J Biol Chem 276: 38320-38328.

Muro-Pastor AM, Valladares A, Flores E, Herrero A. 2002. Mutual dependence of the expression of the cell differentiation regulatory protein HetR and the global nitrogen regulator NtcA during heterocyst development. Mol Microbiol 44: 1377-1385.

Nayar AS, Yamaura H, Rajagopalan R, Risser DD, Callahan SM. 2007. FraG is necessary for filament integrity and heterocyst maturation in the cyanobacterium *Anabaena* sp. strain PCC 7120. Microbiology 153: 601-607.

Nicolaisen K, Hahn A, Schleiff E. 2009a. The cell wall in heterocyst formation by *Anabaena* sp. PCC 7120. J Basic Microbiol 49: 5-24.

Nicolaisen K, Mariscal V, Bredemeier R, Pernil R, Moslavac S, López-Igual R, Maldener I, Herrero A, Schleiff E, Flores E. 2009b. The outer membrane is a heterocyst-forming cyanobacterium is a permeability barrier for uptake of metabolites that are exchanged between cells. Mol Microbiol 74: 58-70.

Nikaido H. 1994. Maltose transport system of Escherichia coli: an ABC-type transporter. FEBS Lett 346: 55-58.

Nikaido H. 2003. Molecular basis of bacterial outer membrane permeability revisited. Microbiol Mol Biol Rev 67: 593-656.

Ning D, Xu X. 2004. *alr0117*, a two-component histidine kinase gene, is involved in heterocyst development in *Anabaena* sp. PCC 7120. Microbiology 150: 447–453.

Novichkov PS, Omelchenko MV, Gelfand MS, Mironov AA, Wolf YI, Koonin EV. 2004. Genome-wide molecular clock and horizontal gene transfer in bacterial evolution. J Bacteriol 186: 6575-6585.

Nozaki H, Maruyama S, Matsuzaki M, Nakada T, Kato S, Misawa K. 2009. Phylogenetic positions of Glaucophyta, green plants (Archaeplastida) and Haptophyta (Chromalveolata) as deduced from slowly evolving nuclear genes. Molecular Phylogenetics and Evolution, 53, 872-880.

Nürnberg DJ, Mariscal V, Bornikoel J, Nieves-Morión M, Krauss N, Herrero A, Maldener I, Flores E, Mullineaux CW. 2015. Intercellular diffusion of a fluorescent sucrose analog via the septal junctions in a filamentous cyanobacterium. mBio 6(2): e02109.

Ochoa de Alda JA, Esteban R, Diago ML, Houmard J. 2014. The plastid ancestor originated among one of the major cyanobacterial lineages. Nat Commun. 5: 4937.

Olmedo-Verd E, Valladares A, Flores E, Herrero F, Muro-Pastor AM. 2008. Role of two NtcA-binding sites in the complex *ntcA* gene promoter of the heterocyst-forming cyanobacterium *Anabaena* sp. strain PCC 7120. J Bacteriol 190: 7584-7590.

Omairi-Nasser A, Haselkorn R, Austin J2[nd]. 2014. Visualization of channels connecting cells in filamentous nitrogen-fixing cyanobacteria. FASEB J 28: 3016-3022.

Omairi-Nasser A, Mariscal V, Austin JR 2nd, Haselkorn R. Requirement of Fra proteins for communication channels between cells in the filamentous nitrogen-fixing cyanobacterium *Anabaena* sp. PCC 7120. 2015. Proc Natl Acad Sci 112: E4458-4464.

Park JT, Raychaudhuri D, Li H, Normark S, Mengin-Lecreulx D. 1998. MppA, a periplasmic binding protein essential for import of the bacterial cell wall peptide L-alanyl-gamma-D-glutamyl-*meso*-diaminopimelate. J Bacteriol 180: 1215–1223.

Park JJ, Lechno-Yossef S, Wolk PC, Vieille C. 2013. Cell-specific gene expression in *Anabaena variabilis* grown phototrophically, myxotrophically, and heterotrophically. BMC Genomics 14: 759.

Pao SS, Paulsen IT, Saier MH Jr. 1998. Major facilitator superfamily. Microbiol Mol Biol Rev 62: 1-34.

Paulsen IT. 2016. http://www.membranetransport.org/index_v2_rc1.html

Paz-Yepes J, Herrero A, Flores E. 2007. The NtcA-regulated amtB gene is necessary for full methylammonium uptake activity in the cyanobacterium *Synechococcus elongates*. J Bacteriol 189: 7791-7798.

Paz-Yepes J, Merino-Puerto V, Herrero A, Flores E. The amt gene cluster of the heterocyst-forming cyanobacterium *Anabaena* sp. strain PCC 7120. 2008. J Bacteriol 190: 6534-6539.

Pernil R, Piccossi S, Mariscal V, Herrero A, Flores E. 2008. ABC-type amino acid uptake transporters Bgt and N-II of Anabaena sp. strain PCC 7120 share an ATPase subunit and are expressed in vegetative cells and heterocysts. Mol Microbiol 67: 1067-1080.

Pernil R, Herrero A, Flores E. 2010. Catabolic function of compartmentalized alanine dehydrogenase in the heterocyst-forming cyanobacterium *Anabaena* sp. strain PCC 7120. J Bacteriol 192: 5165-5172.

Pernil R, Picossi S, Herrero A, Flores E, Mariscal V. 2015. Amino acid transporters and release of hydrophobic amino acids in the heterocyst-forming cyanobacterium Anabaena sp. strain PCC 7120. Life (Basel) 5: 1282-1300.

Picossi S, Flores E, Ekman M. 2013. Diverse roles of the GlcP glucose permease in free-living and symbiotic cyanobacteria. Plant Signal Behav 8: e27416.

Picossi S, Valladares A, Flores E, Herrero A. 2004. Nitrogen-regulated genes for the metabolism of cyanophycin, a bacterial nitrogen reserve polymer: expression and mutational analysis of two cyanophycin synthetase and cyanophycinase gene clusters in heterocyst-forming cyanobacterium *Anabaena* sp. PCC 7120. J Biol Chem 279: 11582-11592.

Picossi S, Montesinos ML, Pernil R, Lichtlé C, Herrero A, Flores E. 2005. ABC-type neutral amino acid permease N-I is required for optimal diazotrophic growth and is repressed in the heterocysts of *Anabaena* sp. strain PCC 7120. Mol Microbiol 57: 1582-1592.

Picossi S, Flores E, Herrero A. 2014. ChIP analysis unravels an exceptionally wide distribution of DNA binding sites for the NtcA transcription factor in a heterocyst-forming cyanobacterium. BMC Genomics 15: 22.

Porchia AC, Salerno GL. 1996. Sucrose biosynthesis in a prokaryotic organism: Presence of two sucrose-phosphate synthases in *Anabaena* with remarkable differences compared with the plant enzymes. Proc Natl Acad Sci USA 93: 13600-13604.

Price GD, Badger MR, Woodger FJ, Long BM. 2008. Advances in understanding the cyanobacterial CO2-concentrating-mechanism (CCM): functional components, Ci transporters, diversity, genetic regulation and prospects for engineering into plants. J Exp Bot 59(7): 1441-1461.

Ramírez ME, Hebbar PB, Zhou R, Wolk CP, Curtis SE. 2005. *Anabaena* sp. strain PCC 7120 gene devH is required for síntesis of the heterocyst gycolipid layer. J Bacteriol 187: 2326-2331.

Ramos-León F, Mariscal V, Frías JE, Flores E, Herrero A. 2015. Divisomedependent subcellular localization of cell-cell joining protein SepJ in the filamentous cyanobacterium *Anabaena*. Mol Microbiol 96: 566 –580.

Ramos-León F, Mariscal V, Battchikova N, Aro EM, Flores E. 2017. Septal protein SepJ from the heterocyst-forming cyanobacterium Anabaena forms multimers and interacts with peptidoglycan. 2017. FEBS Open Bio 7: 1515-1526.

Rees DC, Johnson E, Lewinson O. 2009. ABC transporters: the power to change. Nat Rev Mol Cell Biol 10: 218-227.

Reinders A, Sun Y, Karvonen KL, Ward JM. 2012. Identification of amino acids important for substrate specificity in sucrose transporters using gene shuffling. J Biol Chem 287: 30296–30304.

Ren Q, Paulsen IT. 2005. Comparative analyses of fundamental differences in membrane transport capabilities in prokaryotes and eukaryotes. PLoS Comput Biol 1, e27.

Rice AJ, Park A, Pinkett HW. 2014. Diversity in ABC transporters: Type I, II and III. Crit Rev Biochem Mol Biol 49: 426-437.

Risser DD, Callahan SM. 2009. Genetic and cytological evidence that heterocyst patterning is regulated by inhibitor gradient that promote activator decay. Proc Natl Acad Sci USA 106: 19884-19888.

Rippka R. 1972. Photoheterotrophy and chemoheterotrophy among unicellular blue-green algae. Arch Microbiol 87: 93-98.

Rippka R, Waterbury JB. 1977. The synthesis of nitrogenase by non-heterocystous cyanobacteria. FEMS Microbiol Lett 2: 83-86.

Rippka R, Deruelles J, Waterbury JB, Herdman M, Stanier RY. 1979. Generic assigments, strain histories and properties of pure cultures of cyanobacteria. J Gen Micrbiol 111: 1-61.

Rubio LM, Ludden PW. 2008. Biosynthesis of the iron-molybdenum cofactor of nitrogenase. Annu Rev Microbiol 62: 93-111.

Rudolf M, Tetik N, Ramos-León F, Flinner N, Ngo G, Stevanovic M, Burnat M, Pernil R, Flores E, Schleiff E. 2015. The peptidoglycan-binding protein SjcF1 influences septal junction function and channel formation in the filamentous cyanobacterium *Anabaena*. MBio 6: e00376.

Russell RR, Aduse-Opoku J, Sutcliffe IC, Tao L, Ferretti JJ. 1992. A binding protein-dependent transport system in *Streptococcus mutans* responsible for multiple sugar metabolism. J Biol Chem 267: 4631- 4637.

Saier MH Jr. 2000. Families of transmembrane sugar transport proteins. Mol Microbiol 35: 699-710.

Saier MH Jr, Reddy VS, Tsu BV, Ahmed MS, Li C, Moreno-Hagelsieb G. 2016. The transporter classification database (TCDB): recent advances. Nucleic Acids Res 44(D1): D372-379.

Salerno GL, Currati L. 2003. Origin of sucrose metabolism in higher plants: when, how and why? Trends Plant Sci 8: 63-69.

Schilling N, Ehrnsperger K. 1985. Cellular differentiation of sucrose metabolism in *Anabaena variabilis* Z Naturforsh 40c: 776-779.

Schirrmeister BE, Gugger M, Donoghue PC. 2011. Cyanobacteria and the great oxidation event: evidence from genes and fossils. Paleontology 58: 769-785.

Schlösser A, Kampers T, Schrempf H. 1997. The Streptomyces ATP-binding component MsiK assists in cellobiose and maltose transport. J Bacteriol 179: 2092-2095.

Schmetterer GR. 1990. Sequence conservation among the glucose transporter from the cyanobacterium Synechocystis sp. PCC 6803 and mammalian glucose transporters. Plant Mol Biol 19904(5): 697-706.

Schmetterer GR, Flores E. 1988. Uptake of fructose by the cyanobacterium *Nostoc* sp. ATCC 29150. Biochimica et Biophysica Acta 942: 33-37.

Schneider D, Fuhrmann E, Scholz I, Hess WR, Graumann PL. 2007. Fluorescence staining of live cyanobacterial cells suggest non-stringent chromosomes segregation and absence of a connection between cytoplasmic and thylakoid membranes. BMC Cell Biol 8: 39.

Shapiro JA. 1988. Bacteria as multicellular organisms. Sci Am 256: 82:89.

Shi Y. 2013. Common folds and transport mechanisms of secondary active transporters. Annu Rev Biophys 42: 51–72.

Shih PM, Wu D, Latifi A, Axen SD, Fewer DP, Talla E, Calteau A, Cai F, Tandeau de Marsac N, Rippka R, Herdman M, Sivonen K, Coursin T, Laurent T, Goodwin L, Nolan M, Davenport KW, Han CS, Rubin EM, Eisen JA, Woyke T, Gugger M, Kerfeld CA. 2013. Improving the coverage of the cyanobacterial phylum using diversity-driven genome sequencing. Proc Natl Acad Sci USA 110: 1053-1058.

Sivitz AB, Reinders A, Johnson ME, Krentz AD, Grof CPL, Perrouz JM, Ward JM. 2007. Arabidopsis sucrose transporter AtSUC9. High-affinity transport activity, intragenic control of expression, and early flowering mutant phenotype. Plant Physiol 143: 188-198.

Smith AJ. 1983. Modes of cyanobacterial carbon metabolism. Ann Microbiol Paris 134: 93-113.

Stal LJ, Zehr JP. 2008. Cyanobacterial nitrogen fixation in the ocean: diversity, regulation and ecology. In The Cyanobacteria: Molecular Biology Genomics and Evolution Caister Academic Press; Norfolk, UK. Herrero A, Flores E. (eds.) pp 423-446.

Stanier RY, Cohen-Bazire G. 1977. Phototrophic prokaryotes: the cyanobacteria. Annu Rev Microbiol 31: 225-274.

Staron P, Forchhammer K, Maldener I. 2011. Novel ATP-driven pathway of glycolipid export involving TolC protein. 2011. J Biol Chem 286: 38202-38210.

Stebegg R, Wurzinger B, Mikulic M, Schmetterer G. 2012. Chemoheterotrophic growth of the Cyanobacterium Anabaena sp. strain PCC 7120 dependent on a functional cytochrome c oxidase. J Bacteriol 194: 4601-4607.

Sun L, Zeng X, Yan C, Sun X, Gong X, Rao Y, Yan N. 2012. Crystal structures of a bacterial homologue of glucose transporters GLUT1-4. Nature 490: 361-366.

Summers ML, Wallis JG, Campbell EL, Meeks JC. 1995. Genetic evidence of a major role for glucose-6-phosphate dehydrogenase in nitrogen fixation and dark growth of the cyanobacterium *Nostoc* sp. strain ATCC 29133. J Bacteriol 177: 6184–6194.

Tapia MI, Mourez M, Hofnung M, Dassa E. 1999. Structure-function study of MalF protein by random mutagenesis. J Bacteriol 181: 2267–2272.

Thomas J, Meeks JC, Wolk CP, Shaffer PW, Austin SM. 1977. Formation of glutamine from [^{13}N]ammonia, [^{13}N]dinitrogen, and [^{14}C]glutamate by heterocysts isolated from *Anabaena* cylindrica. J Bacteriol 129: 1545-1555.

Tomitani A, Knoll AH, Cavanaugh CM, Ohno T. 2006. The evolutionary diversification of cyanobacteria: Molecular–phylogenetic and paleontological perspectives. Proc Natl Acad Sci USA 103: 5442-5447.

Typas A, Banzhaf M, Gross CA, Vollmer W. 2011. From the regulation of peptidoglycan synthesis to bacterial growth and morphology. Nat Rev Microbiol 10: 123-136.

Ungerer JL, Pratte BS, Thiel T. 2008. Regulation of fructose transport and its effect on fructose toxicity in Anabaena spp. J Bacteriol 190: 8115-25.

van den Berg B. 2012. Structural basis for outer membrane sugar uptake in pseudomonads. J Biol Chem 287: 41044-41052.

van der Heide T, Poolman B. 2002. ABC transporters: one, two or four extracytoplasmic substrate-binding sites? EMBO Rep 3: 938–943.

Valladares A, Montesinos ML, Herrero A, Flores E. 2002. An ABC-type, high affinity urea permease identified in cyanobacteria. Mol Microbiol 43(3): 703-15.

Valladares A, Herrero A, Pils D, Schmetterer G, Flores E. 2003. Cytochrome *c* oxidase genes required for nitrogenase activity and diazotrophic growth in *Anabaena* sp. PCC 7120. Mol Microbiol 47: 1239-1249.

Valladares A, Maldener I, Muro-Pastor AM, Flores E, Herrero A. 2007. Heterocyst development and diazotrophic metabolism in terminal respiratory oxidase mutants of the cyanobacterium *Anabaena* sp. strain PCC 7120. J Bacteriol 189: 4425-4430.

Valladares A, Flores E, Herrero A. 2008. Transcription activation by NtcA and 2-oxoglutarate of three genes involved in heterocyst differentiation in the cyanobacterium *Anabaena* sp. strain PCC 7120. J Bacteriol 190: 6126-6133.

Valladares A, Rodríguez V, Camargo S, Martínez-Noël GMA, Herrero A, Luque I. 2011. Specific role of the cyanobacterial PipX factor in the heterocysts of *Anabaena* sp. strain PCC 7120. J Bacteriol 193: 1172-1182.

Valladares A, Flores E, Herrero A. 2016. The heterocyst differentiation transcriptional regulator HetR of the filamentous cyanobacterium *Anabaena* forms tetramers and can be regulated by phosphorylation. Mol Microbiol 99: 808-819.

Vargas WA, Nishi CN, Giarrocco LE, Salerno GL. 2011. Differential roles of alkaline/neutral invertases in *Nostoc* sp. PCC 7120: Inv-B isoform is essential for diazotrophic growth. Planta 233: 153-62.

Vázquez-Bermúdez MF, Herrero A, Flores E. 2002a. 2-Oxoglutarate increase the binding affinity of the NtcA (nitrogen control) transcription factor for the *Synechococcus glnA* promoter. FEBS Lett 512: 71-74.

Vázquez-Bermúdez MF, Paz-Yepes J, Herrero A, Flores E. 2002b. The NtcA-activated *amt1* gene encodes a permease required for uptake of low concentrations of ammonium in the cyanobacteria *Synechococcus* sp. PCC 7942. Microbiology 148: 861-9.

Vollmer W, Joris B, Charlier P, Foster S. 2008. Bacterial peptidoglycan (murein) hydrolases. FEMS Microbiol Rev 32: 259-286.

Wang Y, Lechno-Yossef S, Gong Y, Fan Q, Wolk CP, Xu X. 2007. Predicted glycosyl transferase genes located outside the HEP island are required for formation of heterocyst envelope polysaccharide in *Anabaena* sp. strain PCC 7120. J Bacteriol 189: 5372-5378.

Watanabe A, Hiraga K, Suda M, Yukawa H, Inui M. 2015. Functional characterization of Corynebacterium alkanolyticum in *Corynebacterium glutamicum*. Appl Environ Microbiol 81: 4173-4183.

Webb AJ, Home KA, Hosie AH. 2008. Two closely related ABC transporters in *Streptococcus mutans* are involved in disaccharide and/or oligosaccharide uptake. J Bacteriol 190: 168-178.

Whitton. 2000. Introduction to the cyanobacteria. In the Ecology of Cyanobacteria: Their Diversity In Time and Space. Kluwer Academic, Dordrecht, The Netherlands. Whitton BA, Potts M. (eds.) pp 1-11.

Wilcox M, Mitchison GJ, Smith RJ. 1973. Pattern formation in the blue-green algae, *Anabaena*. II. Controlled proheterocyst regression. J Cell Sci 13: 637-649.

Wilk L, Strauss M, Rudolf M, Nicolaisen K, Flores E, Kühlbrandt W, Schleiff E. 2011. Outer membrane continuity and septosome formation between vegetative cells in the filaments of *Anabaena* sp. PCC 7120. Cell Microbiol 13: 1744-1754.

Wilkens S. 2015. Structure and mechanism of ABC transporters. F1000 Prime Rep 7: 14.

Wille U, Seyfang A, Duszenko M. 1996. Glucose uptake occurs by facilitated diffusion in procyclic forms of *Trypanosoma brucei*. Eur J Biochem 236: 228-233.

Wolk CP. 1968. Movement of carbon from vegetative cells to heterocysts in *Anabaena cylindrica*. J Bacteriol 96: 2138–2143.

Wolk CP. 2000. Heterocyst formation in Anabaena. In Prokaryotic Development. ASMPress, Washington, DC. Brun YV, Shimkets LJ (eds.), pp 83-104.

Wolk P, Shaffer PW. 1976. Heterotrophic micro- and macrocultures of a nitrogen-fixing cyanobacterium. Archives of Microbiology 110(2-3), 145-147.

Wolk CP, Austin SM, Bortins J, Galonsky A. 1974. Autoradiographic localization of ^{13}N after fixation of ^{13}N-labeled nitrogen gas by a heterocyst-forming blue-green alga. J Cell Biol 61: 440–453.

Wolk CP, Thomas J, Shaffer PW, Austin SM, Galonsky A. 1976. Pathway of nitrogen metabolism after fixation of 13N-labeled nitrogen gas by the cyanobacterium, Anabaena cylindrical. J Biol Chem 251: 5027-34.

Wolk CP, Vonshak A., Kehoe P, Elhai J. 1984. Construction of shuttle vectors capable of conjugative transfer from *Escherichia coli* to nitrogen-fixing filamentous cyanobacteria. Proc. Natl. Acad. Sci. USA. 81: 1561–1565.

Wolk CP, Cai Y, Cardemil L, Flores E, Hohn B, Murry M, Schmetterer G, Schrautemeier B, Wilson R. 1988. Isolation and complementation of mutants of *Anabaena* sp. strain PCC 7120 unable to grow aerobically on dinitrogen. J Bacteriol 170: 1239-1244.

Wolk CP, Ernst A, Elhai J. 1994. Heterocyst metabolism and development. In The Molecular Biology of Cyanobacteria. Kluwer Academic Publishers, Holland. Bryan, D.A (ed.) pp 769-823.

Wylie JL, Worobec EA. 1995. The OprB porin plays a central role in carbohydrate uptake in *Pseudomonas aeruginosa*. J Bacteriol 177: 3021-3026.

Xiong W, Brune D, Vermaas WF. 2014. The δ-aminobutyric acid shunt contributes to closing the tricarboxylic acid cycle in *Synechocystis* sp. PCC 6803. Mol Microbiol 93: 786-796.

Xu X, Elhai J, Wolk CP. 2008. Transcriptional and developmental responses by *Anabaena* to deprivation of fixed nitrogen. In The Cyanobacteria: Molecular Biology Genomics and Evolution Caister Academic Press; Norfolk, UK. Herrero A, Flores E. (eds.) pp 383–422.

Yan N. 2015. Structural biology of the Major Facilitator Superfamily transporters. Annu Rev Biophys 44: 257-283.

Yang DC, Peters NT, Parzych KR, Uehara T, Markovsky M, Bernhardt TG. 2011. Proc Natl Acad Sci USA 108: E1052-1060.

Yoon HS, Golden JW. 1998. Heterocyst pattern formation controlled by a diffusible peptide. Science 282: 935-938.

Yoon H.S, Golden JW. 2001. PatS and products of nitrogen fixation control heterocyst pattern. J Bacteriol 183: 2605-2613.

Zimorski V, Ku C, Martin WF, Gould SB. 2014. Endosymbiotic theory for organelle origins. Curr Opin Microbiol 22: 38-48.

Zhang S, Bryant DA. 2011. The tricarboxylic acid cycle in cyanobacteria. Science 334: 1551-1553.

Zhang CC, Durand MC, Jeanjean R, Joset F. 1989. Molecular and genetical analysis of the fructose-glucose transport system in the cyanobacterium *Synechocystis* PCC 6803. Mol Microbiol 3: 1221-1229.

Zhang LC, Chen YF, Chen WL, Zhang CC. 2008. Existence of periplasmic barriers preventing green fluorescent protein diffusion from cell to cell in the cyanobacterium *Anabaena* sp. strain PCC 7120. Mol Microbiol 70: 814-823.

Zhang JY, Chen WL, Zhang CC. 2009. *hetR* and *patS*, two genes necessary for heterocyst pattern formation, are widespread in filamentous nonheterocyst-forming cyanobacteria. Microbiology 155: 1418-1426.

Zhang LC, Risoul V, Latifi A, Christie JM, Zhang CC. 2013. Exploring the size limit of protein diffusion through the periplasm in cyanobacterium *Anabaena* sp. PCC 7120 using the 13 kDa iLOV fluorescent protein. Res Microbiol 164: 710-717.

Zhang L, Zhou F, Wang S, Xu X. 2017. Processing of PatS, a morphogen precursor, in cell extracts of *Anabaena* sp. PCC 7120. FEBS Lett 591: 751-759.

Zheng Z, Omairi-Nasser A, Li X, Dong C, Lin Y, Haselkorn R, Zhao J. 2017. An amidase is required for proper intercellular communication in the filamentous cyanobacterium *Anabaena* sp. PCC 7120. Proc Natl Acad Sci USA 114: E1405-1412.

Zhou, R., and C. P. Wolk. 2003. A two-component system mediates developmental regulation of biosynthesis of a heterocyst polysaccharide. J Biol Chem 278: 19939–19946.

Zhu J, Jäger K, Black T, Zarka K, Koksharova O, Wolk CP. 2001. HcwA, an autolysin, is required for heterocyst maturation in *Anabaena* sp. strain PCC 7120. J Bacteriol 183: 6841-6851.

Zhu J, Kong R, Wolk CP. 1998. Regulation of *hepA* of *Anabaena* sp. strain PCC 7120 by elements 5 from the gene and by hepK. J Bacteriol 180: 4233–4242.

Zusman DR, Scott AE, Yang Z, Kirby JR. 2007. Chemosensory pathways, motility and development in *Myxococcus xanthus*. Nat Rev Microbiol 5: 862-72.